COPPE
Instituto Alberto Luiz Coimbra de Pós-Graduação e Pesquisa de Engenharia
UFRJ

MODELING PLASTIC PYROLYSIS: FROM LUMPED APPROACHES TO DETAILED MECHANISTIC AND VOLATILIZATION MODELS

Laura Pires da Mata Costa

Tese de Doutorado apresentada ao Programa de Pós-graduação em Engenharia Química, COPPE, da Universidade Federal do Rio de Janeiro, como parte dos requisitos necessários à obtenção do título de Doutor em Engenharia Química.

Orientadores: José Carlos Costa da Silva Pinto
Amanda Lemette Teixeira Brandão

Rio de Janeiro
Outubro de 2025

MODELING PLASTIC PYROLYSIS: FROM LUMPED APPROACHES TO DETAILED MECHANISTIC AND VOLATILIZATION MODELS

Laura Pires da Mata Costa

TESE SUBMETIDA AO CORPO DOCENTE DO INSTITUTO ALBERTO LUIZ COIMBRA DE PÓS-GRADUAÇÃO E PESQUISA DE ENGENHARIA DA UNIVERSIDADE FEDERAL DO RIO DE JANEIRO COMO PARTE DOS REQUISITOS NECESSÁRIOS PARA A OBTENÇÃO DO GRAU DE DOUTOR EM CIÊNCIAS EM ENGENHARIA QUÍMICA.

Orientadores: José Carlos Costa da Silva Pinto
Amanda Lemette Teixeira Brandão

Aprovada por: Prof. Márcio Nele de Souza
Prof. Fábio Pereira dos Santos
Prof. Márcio Luis Lyra Paredes

RIO DE JANEIRO, RJ – BRASIL
OUTUBRO DE 2025

Pires da Mata Costa, Laura

Modeling Plastic Pyrolysis: From Lumped Approaches to Detailed Mechanistic and Volatilization Models/Laura Pires da Mata Costa. – Rio de Janeiro: UFRJ/COPPE, 2025.

XXIII, 200 p.: il.; 29, 7cm.

Orientadores: José Carlos Costa da Silva Pinto

Amanda Lemette Teixeira Brandão

Tese (doutorado) – UFRJ/COPPE/Programa de Engenharia Química, 2025.

Referências Bibliográficas: p. 143 – 196.

1. Plastics. 2. Chemical recycling. 3. Kinetic modeling. I. Costa da Silva Pinto, José Carlos *et al.* II. Universidade Federal do Rio de Janeiro, COPPE, Programa de Engenharia Química. III. Título.

À Nilza

Resumo da Tese apresentada à COPPE/UFRJ como parte dos requisitos necessários para a obtenção do grau de Doutor em Ciências (D.Sc.)

MODELAGEM DA PIRÓLISE DE PLÁSTICOS: DE ABORDAGENS AGRUPADAS A MODELOS MECANÍSTICOS DETALHADOS E DE VOLATILIZAÇÃO

Laura Pires da Mata Costa

Outubro/2025

Orientadores: José Carlos Costa da Silva Pinto
Amanda Lemette Teixeira Brandão

Programa: Engenharia Química

A pirólise tem se destacado como uma tecnologia promissora para a reciclagem química de plásticos, complementando as rotas mecânicas. Ao converter plásticos pós-consumo em gases e óleo de pirólise, essa tecnologia possibilita a reintegração do material à cadeia produtiva, gerando produtos de qualidade comparável ao plástico virgem.

Para aprimorar a predição e a otimização do processo, este trabalho propõe duas abordagens cinéticas: um modelo simplificado ("lump") e um modelo mecanístico. O modelo simplificado descreve de forma eficiente os principais produtos e tempos de reação, enquanto o modelo mecanístico oferece uma representação fenomenológica detalhada da pirólise sob diferentes condições.

Poliestireno e polietileno foram selecionados como estudos de caso, e simulações de Monte Carlo cinético foram utilizadas para o modelamento mecanístico. A validação experimental com dados obtidos em micropirolisadores minimizou limitações associadas à transferência de calor e massa. Considerando que a pirólise ocorre na fase líquida, com volatilização das espécies mais leves, o modelo cinético foi acoplado a um modelo de volatilização baseado no equilíbrio termodinâmico entre as fases, utilizando as equações de estado de Peng–Robinson e PC-SAFT. Essa abordagem amplia a aplicação das simulações de Monte Carlo cinético para reatores multifásicos, e inova ao predizer a distribuição de produtos da pirólise baseado nas condições da reação.

Por fim, uma revisão crítica de estudos de Avaliação do Ciclo de Vida (ACV) sobre a pirólise de plásticos revelou lacunas relacionadas ao desempenho e à escala dos

processos, à variabilidade das matérias-primas e ao escopo geográfico, destacando a necessidade de uma integração mais abrangente entre modelos de processo e ACV.

Este trabalho representa um avanço na modelagem preditiva da reciclagem química por pirólise. A integração dos modelos validados com outros polímeros pós-consumo permitirá representar composições de resíduos mais diversas, com o objetivo final de otimizar a pirólise como uma tecnologia sustentável de implementação em escala global.

Abstract of Thesis presented to COPPE/UFRJ as a partial fulfillment of the requirements for the degree of Doctor of Science (D.Sc.)

MODELING PLASTIC PYROLYSIS: FROM LUMPED APPROACHES TO DETAILED MECHANISTIC AND VOLATILIZATION MODELS

Laura Pires da Mata Costa

October/2025

Advisors: José Carlos Costa da Silva Pinto
Amanda Lemette Teixeira Brandão

Department: Chemical Engineering

Pyrolysis has emerged as a promising technology for the chemical recycling of plastics, complementing mechanical routes. By converting post-consumer plastics into gases and pyrolysis oil, it enables material reintegration into the production chain, yielding products comparable to virgin plastic.

To improve process prediction and optimization, this work proposes two kinetic approaches: a simplified "lumped" model and a mechanistic one. The lumped model efficiently describes major products and reaction times, whereas the mechanistic model offers a detailed, phenomenological representation of pyrolysis under various conditions.

Polystyrene and polyethylene were selected as case studies, and kinetic Monte Carlo simulations were used for mechanistic modeling. Experimental validation with micro-pyrolyzer data minimized heat and mass transfer limitations. Considering that pyrolysis occurs in the liquid phase with volatilization of lighter species, the kinetic model was coupled with a thermodynamic equilibrium volatilization model using Peng–Robinson and PC-SAFT equations of state. This approach broadens the application of kinetic Monte Carlo simulations to multiphase reactors and innovates by predicting the pyrolysis product distribution based on reaction conditions.

Finally, a critical review of life cycle assessment (LCA) studies on plastic pyrolysis revealed gaps related to process performance and scale, feedstock variability, and geographic scope, emphasizing the need for more comprehensive LCA integration with process models.

This work represents a step further toward predictive modeling of chemical recycling by pyrolysis. Integrating the validated models with other post-consumer

polymers will allow the representation of more diverse waste compositions, with the ultimate goal of optimizing pyrolysis as a sustainable technology that can be implemented worldwide.

Contents

List of Figures

List of Tables

List of Abbreviations

P_C	Critical pressure, p. 111
T_C	Critical temperature, p. 111
ADP-fossil	Abiotic Resource Depletion – Fossil Fuels, p. 137
AP	Acidification Potential, p. 137
ASTM	American Society for Testing and Materials, p. 5
BHET	Bis(2-hydroxyethyl) terephthalate, p. 16
BR	Polybutadiene, p. 40
BTX	Benzene, Toluene, and Xylene, p. 21
CAPEX	Capital expenditure, p. 15
CCP	Climate Change Potential, p. 137
CC	Climate Change, p. 137
CED	Cumulative Energy Demand, p. 137
CO_{2e}	Carbon dioxide equivalents, p. 10
DEG	Diethylene glycol, p. 16
DMT	N,N-Dimethyltryptamine, p. 16
EG	Ethylene glycol, p. 16
EOL	End-of-life, p. 138
EPR	Extended Producer Responsibility, p. 4
EP	Eutrophication Potential, p. 137
ET	Terrestrial Eutrophication, p. 137

EoS	Equations of state, p. 99
FAETP	Freshwater Aquatic Ecotoxicity Potential, p. 137
FCC	Fluid catalytic cracking, p. 25
FETP	Freshwater Ecotoxicity, p. 137
FID	Flame ionization detector, p. 101
FRE	Fossil Resources Scarcity, p. 137
FR	Friedman method, p. 33
FWO	Flynn–Wall–Ozawa method, p. 33
GC-GC	Two-dimensional gas chromatography system, p. 100
GHG	Greenhouse gases, p. 47
GPC	Gel Permeation Chromatography, p. 100
GWP100	Global Warming Potential (100 years), p. 137
GW	Global Warming, p. 137
HDPE	High-density polyethylene, p. 10
HOFP	Photochemical Ozone Formation, Human Health, p. 137
HT	Human Toxicity, p. 137
HVCs	High-value chemicals, p. 137
IRP	Ionizing Radiation, p. 137
KAS	Kissinger-Akahira-Sunose, p. 33
LCA	Life cycle assessment, p. 18
LCI	Life Cycle Inventory, p. 137
LCO	Life cycle optimization, p. 49
LDPE	Low-density polyethylene, p. 10
LLDPE	Linear low-density polyethylene, p. 10
LOP	Land Use, p. 137

LPG	Liquefied petroleum gas, p. 21
MCDM	Multi-criteria decision-making, p. 49
MD	Metal Depletion, p. 137
METP	Marine Ecotoxicity Potential, p. 137
ME	Marine Ecotoxicity, p. 137
MFR	Molar response factor, p. 101
MF	Match factor, p. 101
MOO	Multi-objective optimization, p. 49
MSW	Municipal solid waste, p. 3
MWD	Molecular weight distribution, p. 40
MW	Molecular weight, p. 40
MeAN	Polymethacrylonitrile, p. 40
MoM	Method of Moments, p. 99
ODP	Ozone Depletion, p. 137
OPEX	Operating Expense, p. 27
PA6	Nylon 6, p. 10
PAN	Polyacrylonitrile, p. 40
PBE	Population balance equations, p. 40
PC-SAFT	Perturbed Chain Statistical Associating Fluid Theory, p. 102
PET	Polyethylene terephthalate, p. 10
PE	Polyethylene, p. 10
PG	Propylene glycol, p. 16
PIB	Polyisobutene, p. 40
PMFP	Particulate Matter Formation Potential, p. 137
PMMA	Poly(methyl methacrylate), p. 40

POFP	Photochemical Ozone Formation Potential, p. 137
POP	Photochemical Oxidation Potential, p. 137
PP	Polypropylene, p. 10
PR	Peng-Robinson, p. 111
PS	Polystyrene, p. 16
PTFE	Polytetrafluoroethylene, p. 40
PU	Polyurethane, p. 16
PVC	Polyvinyl chloride, p. 10
PVF	Polyvinyl fluoride, p. 40
RR	Rachford-Rice, p. 109
S-LCA	Social life cycle assessments, p. 138
SOP	Mineral Resource Scarcity, p. 137
STR	Stirred-tank reactor, p. 26
TAP	Terrestrial Acidification Potential, p. 137
TA	Terrestrial Acidification, p. 137
TCD	Thermal conductivity detectors, p. 100
TCR	Thermo-catalytic reforming, p. 26
TETP	Terrestrial Ecotoxicity Potential, p. 137
TGA	Thermogravimetric analyzer , p. 33
TPA	Terephthalic acid, p. 16
TPD	Tons per day, p. 26
TPE	Thermoplastic elastomers, p. 10
TRL	Technology readiness level, p. 16
ToF-MS	Time-of-Flight Mass Spectrometry, p. 101
VLE	Vapor-liquid equilibrium, p. 97

WC	Water Consumption, p. 137
$\frac{\varepsilon}{k}$	Segment dispersion energy, p. 112
ω	Acentric factor, p. 111
σ	Segment diameter, p. 112
m	Segment number, p. 112
kMC	Kinetic Monte Carlo, p. 80

Chapter 1

Introduction

Plastic consumption and its applications have become so widespread that imagining a world without them is nearly impossible. Our modern lifestyles have been shaped by their versatility, and many technologies owe their existence to the unique physical and chemical properties of plastics. In this text, the term *plastic* is used according to common usage, referring broadly to polymer-based materials, rather than any specific type.

The history of plastics began in the early 20th century with the invention of Bakelite, one of the first synthetic plastic-like materials. However, its widespread adoption and rapid expansion did not take off until after World War II [29]. Since then, plastics have become essential in many applications such as automotive, electronics, and technical textiles, offering durability, low cost, lower product weight, chemical resistance, ease of manufacturing and processing, safety and hygiene (e.g., food-safe applications), low permeability to gases and liquids, and design flexibility [30].

However, at the same time, plastics have also been widely adopted for disposable products like bags, packaging, and cups, bringing unprecedented convenience to daily life. This culture of disposability was celebrated in the 1955 *Life* magazine *Throwaway Living* (Figure 1.1) with the line: *'Oh Joy, Oh Bliss! Disposable products are an innovative way to make life easier'*. Plastics are produced, used (often only once), and then discarded, moving directly from consumption to landfill. This model has given rise to the prevalence of single-use plastics and reinforced a linear economic approach. While disposability is essential for healthcare services, the convenience and massive consumption of plastics in everyday activities have come at a significant environmental cost [31]. Figure 1.2 [29] presents the average useful life of various plastic items. The ones with the shortest life cycles are the ones most consumed, with the largest share of plastics demand (40 % of European plastics demand [32]).

Figure 1.1: Artistic representation illustrating the concept of "throwaway living" as promoted in mid-20th century consumer culture [31, 33, 34]. Photo by Peter Stackpole - The LIFE Picture Collection [34].

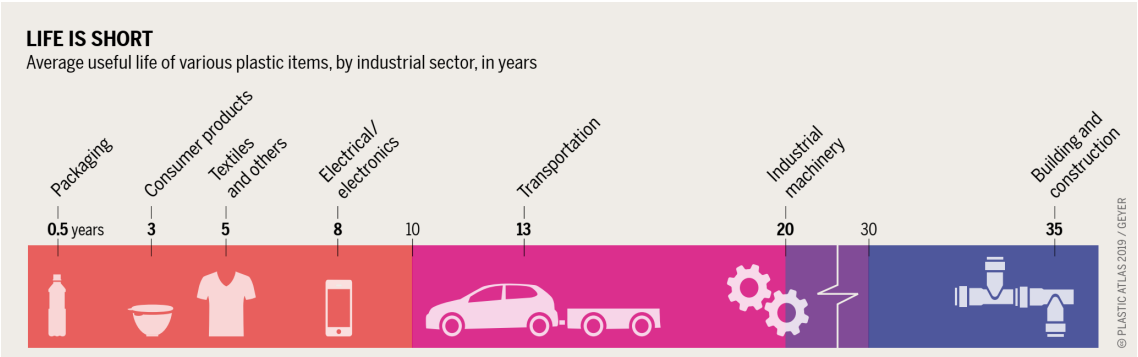

Figure 1.2: Average useful life (in years) of plastic products across different industrial sectors [1]. PLASTIC ATLAS| Appenzeller/Hecher/SackCC-BY-4.0.

As a result, the share of plastics in the municipal solid waste (MSW) corresponds to 16.8 wt % in Brazil (2020 data) [35], which corresponds to approximately 64 kg of plastics per capita (considering 382 kg of MSW generated per capita) [36]. In the European Union, this number is of 36.13 kg per capita (2022 data) [37]. In

the United States, 221 kg of plastic waste is generated per capita (2019 data) [38], or 12.20 % (35.7 million tons) of total MSW generated (2018 data) [39]. Among the many types of plastics consumed and discarded, only 9 % have been recycled [29, 40]. Per region, this number corresponds to 20.6 % in Brazil [41], 12.4% [40] in Europe, and only 5-9 % [39, 40] in the US. These figures highlight the global challenge of plastic waste management, with low recycling rates persisting despite high per capita consumption across all regions.

It is often said that the problem with plastic lies in its resistance to degradation. However, this very durability, which results from the strong carbon–carbon bonds in its hydrocarbon-based monomer units (such as ethylene, propylene, and styrene), is also one of its greatest advantages. No one would want a television that degrades during a movie, a keyboard that crumbles in use, or plastic bags that tear while carrying food, whether conventional or reusable "ecobags" [42]. The core issue is not the plastic itself, but the economic model in which it is embedded - a system that encourages limitless extraction of natural resources while neglecting reuse and recycling. Our current way of living exemplifies a metabolic rift - a disconnection between human systems and ecological cycles [43, 44]. Plastics now pose a major socio-environmental challenge, driven by a throwaway culture, planned obsolescence, inadequate recycling infrastructure, lack of corporate accountability for waste, and insufficient municipal waste management.

In response to the escalating plastic waste crisis, the number of academic groups and institutions studying its environmental and societal impacts has steadily grown. But it is undeniable that a significant surge in global awareness occurred in 2017, when China implemented a ban on the import of non-industrial plastic waste, forcing middle- and high-income countries to confront their own waste management challenges directly [45, 46]. This policy shift, combined with increasingly negative media coverage of plastic pollution, catalyzed a wave of research focused on post-consumer plastic. Figure 1.4 shows the number of documents indexed in the Scopus database containing the keywords "plastic waste" and/or "plastic pollution" (accessed January 20, 2025). The data clearly indicate a sharp increase in scientific publications following the 2017 ban, highlighting its impact on research trends.

Current research explores various aspects of the plastic issue, including environmental and human health impacts, bioplastics, biodegradation, functionalization, additives, microplastic release and implications, novel material design, reverse logistics, plastic separation technologies, life cycle assessments, the effects of plastic reduction policies, taxation measures (e.g., the European Green Deal), and recycling technologies [47–57].

At the same time, growing environmental concerns and global policy shifts have led to stricter legislation aimed at increasing plastic recycling rates. Companies are

being compelled to adopt recycling technologies not only to enhance their public image, but also in response to Extended Producer Responsibility (EPR) policies. These policies transfer the financial and operational burden of waste collection and recycling from local governments to producers [30].

However, many of the solutions proposed by policymakers and industry fall short of addressing the root cause: the excessive consumption of plastic. These approaches often prioritize improved waste management and recycling, while giving limited attention to strategies that promote material substitution or encourage behavioral change to reduce consumption. As illustrated in Figure 1.3, the circular economy framework has gained prominence as an alternative to linear production and disposal models, aiming to minimize waste by keeping plastic materials in use for longer. While this model offers potential for reducing environmental impact, critics argue that, in practice, it may sustain existing consumption patterns, with efforts typically advancing only when profitable or enforced through policy measures.

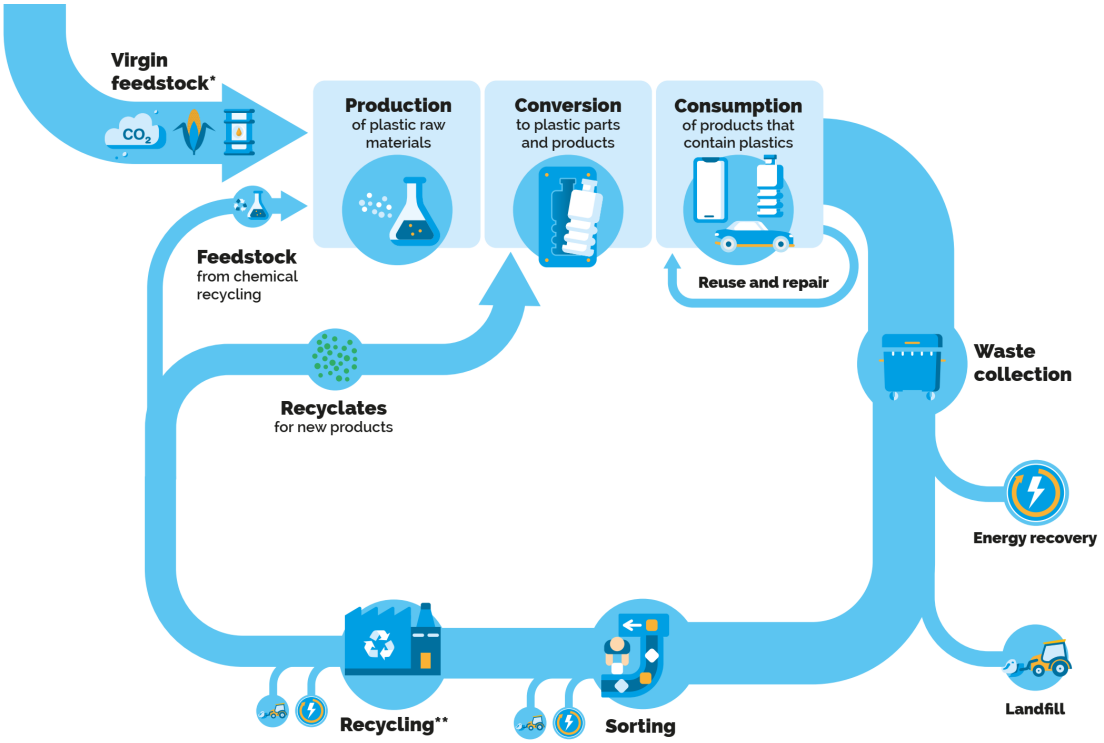

Figure 1.3: Schematic representation of the circular economy framework applied to plastics. Plastics Europe [2].

Nevertheless, addressing the plastic waste crisis remains imperative. Among the various strategies for managing post-consumer plastic waste, recycling occupies a central role due to its potential to reintroduce materials into the production cycle, reduce reliance on virgin feedstocks, and stop plastics from entering natural ecosys-

tems. However, it is not a comprehensive solution. Achieving complete recyclability is constrained by several technical and economic barriers, including limited infrastructure, particularly in low- and middle-income regions. Furthermore, much of the current developed recycling technology is subject to patent restrictions, limiting widespread implementation.

Despite these challenges, recycling remains the most widely promoted strategy and will be the focus of the following discussion. An alternative approach involves biodegradable plastics, which may offer advantages in specific applications [52]. However, their broader adoption is limited by distinct mechanical and chemical properties that often fail to meet the performance demands of conventional plastics, as well as economic barriers and inadequate disposal infrastructure [52]. Further research is needed to address these barriers.

According to the American Society for Testing and Materials (ASTM) D5033 , recycling can be categorized into four main types [3]:

- Primary recycling: the mechanical reprocessing of uncontaminated scrap materials into products of equivalent quality;
- Secondary recycling: the mechanical reprocessing of used materials into products with lower performance requirements;
- Tertiary recycling: the chemical recovery of valuable constituents such as monomers or additives;
- Quaternary recycling: destruction of the material into energy through incineration.

Among these, tertiary recycling, more commonly referred to as chemical recycling, is gaining attention for its ability to handle contaminated or mixed plastic waste streams more effectively than mechanical methods. It enables the recovery of the original building blocks of plastic materials by breaking down polymers into monomers or other useful chemicals.[1] [30, 58].

As a result, this approach has become a rapidly growing area of research and development [59]. Although some companies have begun operating commercial-scale facilities, the technology still faces significant obstacles, including optimizing product recovery efficiency, improving process economics, and minimizing environmental impacts [22]. Ongoing innovations in this field span a wide range of areas, including reactor design, catalyst development and delivery, processing atmospheres, solvent systems, feedstock pre-treatment, and downstream separation techniques.

[1]Unlike mechanical recycling, which reprocesses plastics through physical means, chemical recycling involves the depolymerization of plastic via molecular bond cleavage. This can be accomplished through thermochemical processes such as pyrolysis, hydropyrolysis, and gasification, or through solvolysis techniques [22].

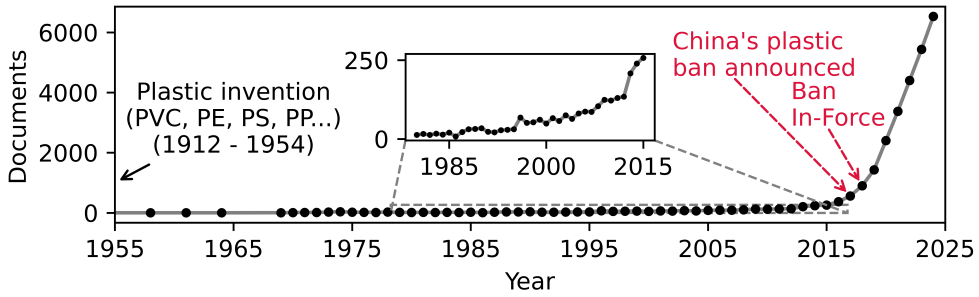

Figure 1.4: Number of scientific publications with the keywords "plastic waste" and/or "plastic pollution".

Despite significant research into chemical recycling, the fundamental mechanistic understanding of plastic thermal degradation remains relatively limited. Experimental data on degradation pathways are often inconsistent and scarce, largely because of the wide variability in reaction conditions. This lack of standardized data slows down the development of reliable models, making reactor design and process optimization challenging.

Moreover, modeling plastic waste mixtures introduces another layer of difficulty, as each polymer exhibits distinct thermal degradation kinetics. Additionally, the depolymerization of commonly used packaging polymers such as polyethylene (PE), polypropylene (PP), and polystyrene (PS) results in broad product distributions, generating not only monomers but also a wide spectrum of hydrocarbons with varying chain lengths, which also vary according to the reaction conditions. Therefore, accurate modeling requires detailed studies of the degradation behavior of individual polymers before any synergistic effects can be meaningfully assessed in mixed-material systems.

Nevertheless, the development and validation of mechanistic models under a range of polymer types and operating conditions remain essential. Such models provide valuable insights that directly inform experimental design, reactor engineering, process optimization, life cycle assessments, and safety analyses. Ultimately, a deeper mechanistic understanding constitutes a key factor in evaluating the true technical potential and limitations of chemical recycling technologies.

In this context, the present research aims to develop phenomenological models capable of quantitatively representing the degradation of polymers and the formation of pyrolysis products, focusing primarily on polyethylene and polystyrene. In order to do that, this document is organized as follows: Chapter 2 presents a bibliometric review of chemical recycling of plastics and existing models for polymer degradation, offering context and identifying gaps in the current literature. Chapter 3 introduces a lumped kinetic model applied to both thermal and catalytic pyrolysis, demonstrating its utility for rapid process understanding and optimization.

Chapter 4 investigates the degradation mechanism of polystyrene through the development and validation of a mechanistic kinetic Monte Carlo model. In Chapter 5, the focus shifts to polyethylene pyrolysis, where the importance of volatilization is addressed through the integration of kinetic and thermodynamic models, including vapor-liquid equilibrium calculations. Finally, Chapter 6 critically examines life cycle assessment (LCA) studies related to plastic pyrolysis, identifying common limitations and proposing improvements based on the validated kinetic models developed throughout this work.

Chapter 2

Bibliographic Review

Understanding the plastic life cycle is crucial for determining recyclability and addressing the challenges of plastic recycling. While plastic synthesis is well understood, the composition of additives is often undocumented, and tracking plastics after they leave the chemical industry is difficult. Therefore, it is necessary to begin with the plastic lifecycle before examining the recycling process in detail.

Plastics originate in refineries. Although the use of renewable feedstocks (e.g., sugarcane, corn) is increasing, most plastics are still derived from fossil resources [30, 60, 61]. For polyolefins, the monomers ethene and propene polymerize into polyethylene and polypropylene, respectively. The strong carbon-carbon covalent bonds that hold these polyolefins together contribute to their durability - lasting for decades, even centuries - but also make them difficult to break down and recycle [62]. After polymerization, the plastics are extruded before shipping to the manufacturers. At this stage, additives are introduced to improve the performance of the material [63].

During subsequent conversion into final products, a larger quantity of additives is introduced, not only to enhance the functional properties of the materials but also to increase their consumer appeal. Colorants, fillers, flame retardants, plasticizers, lubricants, and stabilizers are examples. However, they also contribute to significant challenges to recycling processes, mainly due to the presence of heteroatoms [64].

While additives pose a significant challenge to plastic recycling, certain applications also require plastics to be used in multilayered structures (e.g., snack packaging) or multicomponent products (e.g., electronic motherboards), adding another complexity layer. To address these challenges, initiatives such as Design for Recycling promote strategies that minimize problematic additives and reduce the use of multilayer packaging [65, 66].

At this stage, plastic converters often reuse production scraps through re-extrusion, the simplest form of recycling, also referred to as primary recycling [59, 67, 68]. Figure 2.1 illustrates the available recycling options. However, this

method is applicable primarily to thermoplastics[1] and typically requires exceptionally clean plastic scraps [62]. Nonetheless, re-extrusion can still be performed even when certain additives have already been incorporated.

The plastic recycling complexity is further amplified once the materials leave factories and are used by consumers. Over time, they will likely mix with other plastic types and materials such as paper, metals, and biomass. To enable recycling, these mixed waste streams must be collected, sorted, and separated at dedicated facilities [59].

Mechanical recycling is always the preferred choice due to its lower carbon footprint. However, this process is generally limited to pure and uncontaminated monomaterial streams to preserve plastic properties. Thus, as the plastics are always mixed, compared to primary recycling, additional steps are required, including polymer waste separation and sorting (e.g., metal removal via magnets or eddy current separators, classification using near-infrared (NIR) spectrometers), grinding/milling, washing, drying, and reprocessing. Despite these efforts, contamination from additives, poor sorting efficiency, and polymer degradation during the product lifespan significantly reduce the quality of recycled plastic[2]. As a result, the process generates a stream of mixed materials that cannot be separated, whereas, for the materials that could be isolated, these mechanically recycled plastics often fail to meet the quality standards required for high-value applications, leading to downcycling [22, 30, 64, 65, 67, 68, 79].

For example, PET bottles are commonly mechanically recycled, but to maintain quality for food-grade applications, advanced purification steps are required, such as Superclean, Flake-to-Resin, and Bottle-to-Bottle technologies [80, 81]. The latter, as an example, includes, at the end of the mechanical recycling process, a polycondensation reactor where the PET resin is submitted at 270 °C for at least 15 hours as a simultaneous decontamination and repolymerization step [80, 81]. Furthermore, for the bottles to be sold as new bottles with the same properties and appearance, a stream of fresh monomer must be pumped (configuring an open-loop, or cascade, recycling) or, otherwise, the PET bottle becomes darker and more brittle over time, limiting their reuse in these high-value applications [60]. Only recently, mechanical recycling rates for other packaging materials are increasing, such as high-density polyethylene from milk bottles, which also requires a certified food-grade procedure [59, 82, 83].

[1]Thermoplastics can be repeatedly heated and reshaped, though their mechanical properties degrade over time. In contrast, thermosets, such as cross-linked rubber (e.g., tires), undergo irreversible curing reactions, preventing remolding [3].

[2]During thermo-mechanical processing, shear degradation can cause chain scission, generating free radicals that alter polymer properties. For instance, LDPE may undergo cross-linking, while HDPE, polypropylene (which is particularly susceptible to oxidation), PET, and polystyrene experience molecular weight reduction due to disproportionation reactions [69–78].

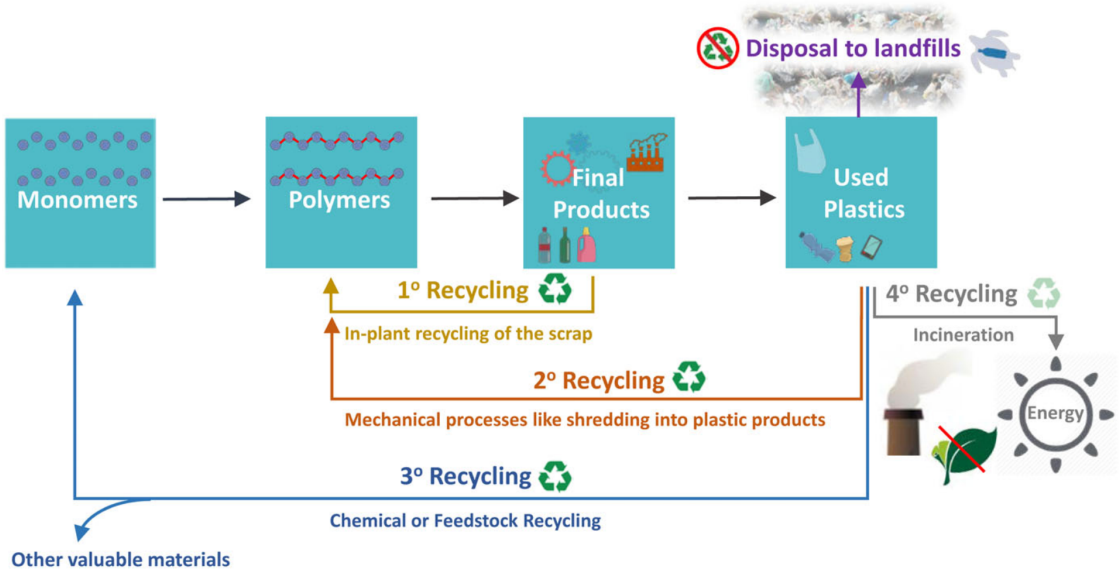

Figure 2.1: Types of plastic waste recycling [3]. © 2018 Society of Chemical Industry.

Incineration, the least circular option, burns plastics to recover energy [81]. While it can process mixed and contaminated plastics effectively, it does not align with circular economy principles as it is no longer reusable once the plastic is incinerated. Additionally, air pollution, high energy costs, and the availability of more sustainable recycling alternatives make incineration a last resort option [3, 29, 30, 58, 59, 69, 81, 84]. Unfortunately, due to the circularity overlook, between 1950 and 2015, about 8300 million tonnes (Mt) of virgin plastics were produced across the globe, generating approximately 6300 Mt of plastic wastes, of which around 9% have been recycled, 12% incinerated, and 79% accumulated in landfills [29]. In Europe, the amount of plastic incinerated to post-consumer plastic waste is over 30 % [68].

If plastics are to be truly recycled back into materials of the same quality as the original, chemical recycling is the best approach. Chemical recycling breaks down polymers into their fundamental building blocks using an energy source (heat or microwaves), chemical agents, or even microorganisms [3] [3, 62]. While this method requires significant energy input, it is an alternative to challenges faced by the other recycling methodologies:

- It can process a broader range of plastic types, including cross-linked polymers [84].

[3]The use of microorganisms to break polymer chains in the presence of air and water is also considered as chemical recycling, but as the technology involves biological aspects beyond the technical challenges of other chemical recycling technologies, they will not be further discussed. Instead, good reviews are available elsewhere [62, 85–91]

- It is more tolerant to impurities than mechanical recycling (see Figure 2.2) and does not require extensive pre-processing procedures [92].
- It produces monomers that can be re-polymerized into high-quality virgin plastics, recirculating the carbon in contrast to incineration [93].

Although chemical recycling holds great promise for closing the plastic cycle, it still requires further technical advancements to enhance efficiency and reduce environmental impacts. The following sections will explore why pyrolysis, a chemical recycling method that degrades plastics under high temperatures in an inert atmosphere, is emerging as one of the most viable solutions for recycling polyolefins and polystyrene. We will also discuss the factors influencing its performance, challenges, the mechanisms behind thermal degradation, and the life cycle assessments comparing chemical recycling with other technologies.

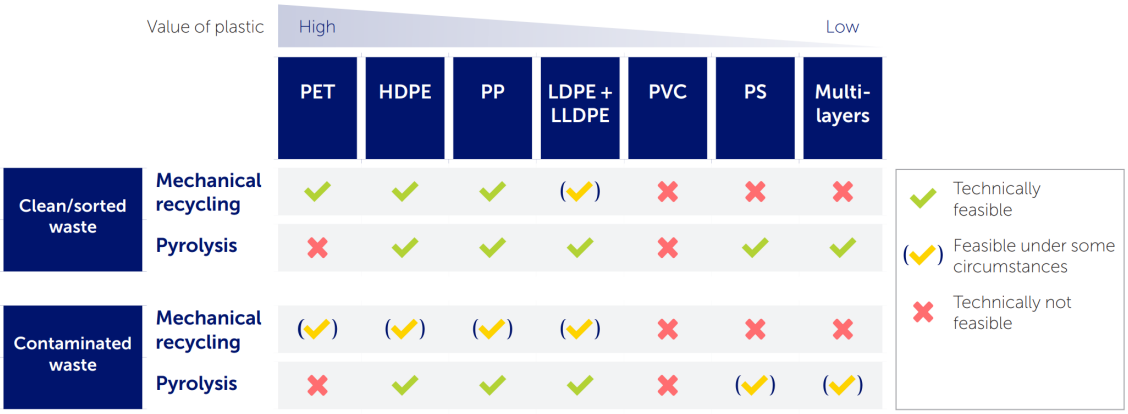

Figure 2.2: Comparison of feedstock tolerance between mechanical recycling and pyrolysis (a chemical recycling technology) [4][47].© 2020 The Pew Charitable Trusts

2.1 Plastics Chemical Recycling

The type of waste and respective degree of contamination constitute key factors in determining the appropriate treatment method for plastic recycling [94]. A widely recognized advantage of chemical recycling over other recycling technologies is its ability to process 100% of plastic materials, even when contaminated. The resulting

[4]The Pew Charitable Trusts and SYSTEMIQ define contamination as the presence of non-plastic waste (e.g., organics) or impurities such as inks, additives, and mixed polymers. Additionally, polymers containing oxygen or nitrogen are considered impurities in pyrolysis, as their presence can lead to the formation of CO_2 or NO_2, significantly reducing yield. However, PET is best suited for chemolysis, another chemical recycling technology discussed in Section 2.1. PVC, on the other hand, can be processed via pyrolysis if a pre-treatment step is applied beforehand, as detailed in Section 2.2.9.

chemical products can be repurposed to synthesize new polymers or used in other applications.

Chemical recycling breaks down polymers through two primary methods: chemolysis, which uses solvents to cleave specific chemical bonds in the polymer backbone, and thermolysis, which uses thermal energy to break these bonds. The choice of method depends on the specific polymer being recycled. The following subsections discuss each technology and its subclassifications as summarized in Table 2.2. However, since thermolysis remains the only viable method for processing large quantities of polyolefins (PE and PP) and polystyrene, the discussion will focus exclusively on thermolysis in further sections.

Chemolysis

Chemolysis (or solvolysis) is a targeted depolymerization process that breaks down certain plastics - specifically condensation polymers - into mixtures of monomers and short-chain oligomers. Condensation polymers contain heteroatoms in their backbone due to ether, amide, carbamate (urethane), or ester linkages. Examples include polyesters (e.g., PET, polycarbonates, poly(butylene terephthalate)), polyamides (e.g., nylons, PA6), polyurethanes, and ether-based polymers (e.g., epoxy resins) [3, 22, 58].

Chemolysis processes are categorized based on the chemical linkages targeted and the reagents used to cleave them. This classification includes hydrolysis, alcoholysis (glycolysis and methanolysis), phosphorolysis, ammonolysis, and aminolysis [22, 60]. For example, Figure 2.3 illustrates PET recycling through methanolysis, hydrolysis, and glycolysis [60]. [5] These processes, depending on the feedstock and solvent combination, are already being used in large industrial-scale transformation sites.

For PET, companies including Eastman (glycolysis and methanolysis) [95], BP (BP Infinia, hydrolysis) [96], Loop Industries (methanolysis) [97], and Indorama (glycolysis) [98] are investing in solvolysis for plastic recycling. These processes often have additional processing steps beyond solvent addition, such as a decolorization step required when PET is dyed (e.g., green flakes), to improve process efficiency [69]. For PA, Aquafil has developed the proprietary ECONYL® Regenerated Nylon technology, which depolymerizes Nylon 6 into caprolactam, its monomeric building block [99].

However, solvolysis becomes less efficient when applied to mixed plastic waste, as it requires more solvent and cannot tolerate high levels of organic, inorganic,

[5] Polyolefins (PE, PP) lack reactive groups, making them resistant to chemolysis [62]. However, solvent-assisted recycling is being explored using supercritical fluids (e.g., water, alcohols) or ionic liquids, as solvents can lower reaction temperatures, reduce viscosity and contamination, and improve product quality, though thermolysis remains the primary degradation mechanism. Despite these benefits, these methods are still at low Technology Readiness Levels (TRL) [22].

or biological contamination. While it enables the recycling of PET, PA, and other degraded condensation polymers that are no longer suitable for mechanical recycling - or reduces the need for fresh make-up material - it does not fully address plastic pollution. The main challenges remain associated with polyolefins, polystyrene, poly(vinyl chloride), and high contamination levels.

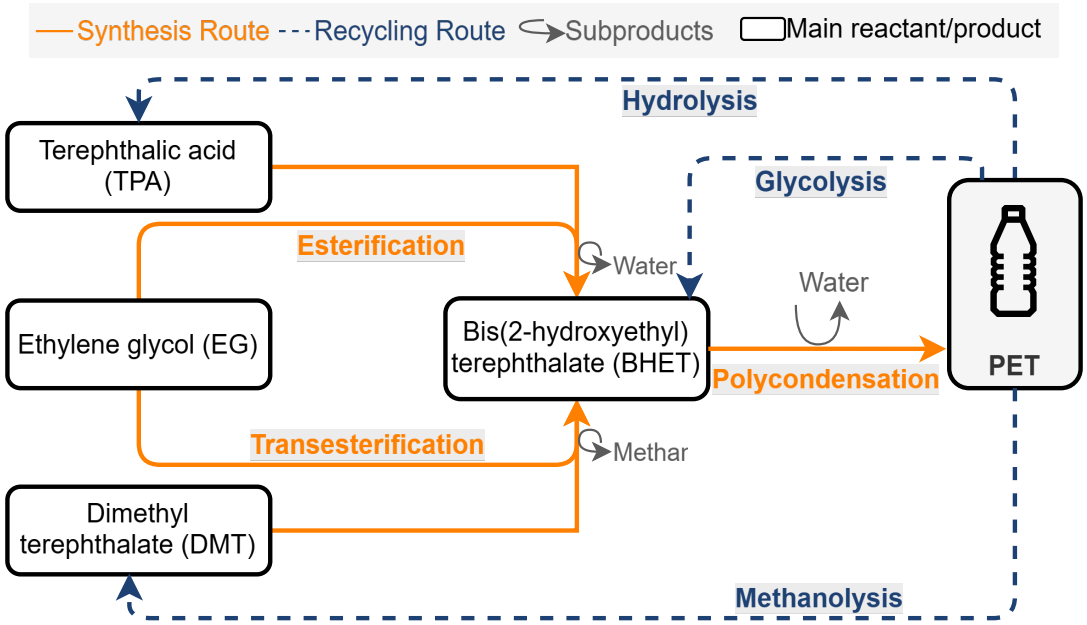

Figure 2.3: PET recycling via chemolysis.

Thermochemical processes

Unlike solvent-based methods, thermochemical processes can handle mixed plastic waste and tolerate contamination from organic, inorganic, and biological residues [62]. This flexibility makes them particularly suitable for recycling complex waste streams. This advantage stems from the simplicity of the process, which primarily involves applying sufficient energy to break chemical bonds along the polymer backbone, generating smaller molecules. Thus, the thermochemical processes are collectively known as thermolysis (*thermo* = heat; *-lysis* = decomposition), including pyrolysis and gasification as the most technologically advanced methods.

Pyrolysis is a relatively simple yet highly versatile process conducted at high temperatures (400–700 °C) in an inert, oxygen-free environment [81]. The operating conditions and feedstock composition directly influence the distribution of pyrolysis products, which include *oil (distillates), gases, and char*. The oil and gas fractions are particularly valuable as feedstocks for new plastics [3, 100]. As discussed in Section 2.2, several parameters influence product yields, but temperature is the most critical.

A major challenge in plastic recycling via pyrolysis is its significant carbon diox-

ide equivalents (CO_{2e}) emissions, primarily due to the high heat demand (higher than 400 °C). This carbon footprint is a key factor in the economic and environmental competitiveness of recycled plastics compared to virgin plastics, so that electrification of pyrolysis reactors (Section 2.2.8) can be a crucial step in mitigating emissions [101]. Beyond conventional electrified reactors, this transition has also stimulated interest in alternative pyrolysis technologies, such as plasma and microwave pyrolysis.

To enhance efficiency and product selectivity, plasma pyrolysis operates at extremely high temperatures (higher than 1000 °C) using plasma energy, leading to high syngas and monomer yields. For example, polypropylene pyrolysis in an inductively coupled plasma system achieved a 73 wt% propylene yield [102]. However, despite its efficiency, plasma pyrolysis faces major challenges, including high energy consumption, undesirable side reactions, and significant capital and operational costs, limiting its large-scale viability [103, 104].

Microwave-assisted pyrolysis offers an alternative by suggesting better heat transfer through microwave-absorbent dielectric materials (e.g., carbon, silicon carbide) as the main advantage [104], which is particularly interesting because of the usually low thermal conductivity of plastics, as further discussed in Section 2.2. However, its efficiency depends on the dielectric properties of the plastic waste, which can vary significantly, leading to challenges such as hot spot formation [22]. Companies like Pyrowave are actively developing this technology.

Despite their potential, plasma and microwave pyrolysis will not be explored further in this thesis. These technologies primarily address heat transfer and temperature control, aspects that can also be optimized through innovative reactor designs. More importantly, they do not fundamentally alter the pyrolysis process. Therefore, the same degradation mechanisms apply, and the influence of process conditions on pyrolysis products, as well as the overall results, remain valid.

Another advanced thermolysis method is gasification [92], which, unlike pyrolysis, does not require an inert atmosphere, instead using gasifying agents such as steam, air, oxygen, carbon dioxide, or their mixtures. Operating at higher temperatures (700–1000 °C), it primarily produces syngas (a mixture of hydrogen, carbon monoxide, and carbon dioxide) through key reactions like the water-gas shift reaction, the Boudouard reaction, and oxidation reactions [81]. The resulting syngas can be used as a chemical platform for synthesizing valuable products, including olefins via the Fischer–Tropsch process [92]. The Akzo and Laubag process or the Chalmers DFB system are examples of large-scale plastic gasification projects.

However, gasification also poses important challenges. One significant issue is the formation of dioxins and tars (high molecular weight condensable hydrocarbons, primarily aromatic compounds, including benzene up to multiple ring aro-

matic compounds and other oxygen-containing hydrocarbons). Tar concentrations in the product gas can range from 0.1% to 10%, causing severe operational problems such as the deactivation of sulfur removal systems, erosion of compressors, clogging of heat exchangers and filters, and damage to gas turbines and engines [105, 106]. Therefore, additional physical and chemical treatments are required to remove these impurities [94, 106].

Additionally, gasification generally results in higher CO_{2e} emissions than pyrolysis due to its higher heat and energy requirements [107]. Economic considerations also play a key role in choosing between the two technologies. As shown in Table 2.1, gasification typically requires higher capital expenditure (CAPEX) compared to pyrolysis. This cost difference makes pyrolysis more suitable for decentralized deployment as, due to reduced cost and simpler technology, more units can be constructed, offering both logistical and economic advantages over centralized gasification facilities. Transporting plastic waste is costly because of its low bulk density, contamination, and high moisture content. Therefore, decentralized pyrolysis facilities are increasingly being viewed as a viable solution, as they reduce transportation costs, support local economies, and reduce environmental impacts, as noted by CHAUDHARI *et al.* (2024) [108].

Furthermore, pyrolysis tends to be more profitable, particularly when the goal is to produce new plastics, because it generates liquid products similar to naphtha or diesel, which are valuable feedstocks for polymer production. In contrast, gasification breaks most carbon–carbon bonds, resulting primarily in syngas and light molecules rather than liquids [109]. Nevertheless, integrating pyrolysis and gasification in a sequential process may optimize product yields, depending on the desired end use [92].

Hydrocracking is another alternative to pyrolysis and gasification, particularly for increasing paraffin yields [118]. This process produces a product with a composition similar to naphtha, making it suitable as feedstock for traditional steam crackers. Unlike pyrolysis, hydrocracking operates at slightly lower temperatures (300–450 °C) but under high pressures (20–150 bar). It employs an in-situ bifunctional catalyst, consisting of an acidic support impregnated with metal, to facilitate two key reactions:

- Cracking and isomerization, driven by an acidic support such as amorphous oxides (e.g., silica-alumina), crystalline zeolites (e.g., HZSM-5), strong solid acids (e.g., sulfated zirconia), or a combination of these materials [118].

- Hydrogenation and dehydrogenation, catalyzed by metals such as noble metals (e.g., palladium or platinum) or non-noble metals (e.g., molybdenum, tungsten, cobalt, or nickel) [104, 118].

Table 2.1: Capital investment estimates for gasification and pyrolysis technologies. Values for the same technology may not be directly comparable due to differences in reactor configurations and the use of catalysts (in the case of catalytic pyrolysis).

Technology	**Cap. (kt/yr)**	**CapEx (M$)**	**M$/t/d**	**Reference**
Pyrolysis	1.0	0.5	0.199	[110]
	1.9	1.1	0.220	[110]
	13.0	6.0	0.168	[111]
	16.0	6.0	0.137	[112]
	25.0	39.3	0.574	[109]
	40.0	28.0	0.256	[113]
	65.0	70.0	0.393	[114]
	80.0	16.0	0.073	[115]
Gasification	3.1	3.8	0.455	[110]
	25.0	35.7	0.521	[109]
	79.0	111.0	0.513	[116]
	655.0	980.0	0.546	[117]

Despite its advantages, hydrocracking faces challenges, primarily the high cost of hydrogen and the risk of catalyst poisoning due to fluctuations in feedstock composition. To mitigate these issues, hydrocracking is often employed as the second stage in a two-step process, following pyrolysis. This sequential approach reduces catalyst deactivation while increasing paraffin yields. Additionally, the presence of hydrogen facilitates the removal of heteroatoms of gas/liquid pyrolysis products such as chlorine, which is commonly found in waste plastics and is associated with corrosion concerns [118].

To reduce hydrogen costs while still maximizing contaminant removal, thermal liquefaction has emerged as a promising alternative [59, 119, 120]. This process utilizes supercritical water, serving as a solvent and a reactant. Although still in the early stages of technological development, the oil composition from the HDPE hydrothermal process at 425 °C was similar to that observed in pyrolysis. However, an increase to 450 °C led to higher amounts of aromatics [121].

These considerations highlight that pyrolysis remains one of the most robust technologies for recycling thermoplastics. Moreover, other processes, such as gasification and hydrocracking, often benefit from incorporating pyrolysis as an initial stage. Also, thermal liquefaction optimization requires a solid knowledge of pyrolysis, reinforcing its central role in advanced plastic recycling strategies. Thus, Section 2.2 provides a deeper discussion on pyrolysis, examining how feedstock characteristics, process conditions, catalyst use, and reactor configurations influence product distribution. The chemical mechanisms governing plastic pyrolysis will be addressed in Section 2.3, followed by an assessment of pyrolysis LCAs in Section 2.4.

Table 2.2: Plastic chemical recycling technologies.

Technology	Process	Description	T (°C)	P (atm)	Polymer (Products)	TRL	References
Solvolysis	Methanolysis	Methanol	180 - 280	20 - 40	PET (DMT and EG, mixtured with 11 - 12% MHET)	Commercial (PET)	[22, 62, 122]
	Hydrolysis	NaOH, KOH (alkaline); H_2SO_4, HNO_3, H_3PO_4 (acid); steam (neutral)	70 - 300	10 - 40	PET (EG and TPA)	Pilot Plant (PET); Commercial (Nylon 6)	[22, 62, 122]
	Glycolysis	Catalyzed (zinc acetate) transesterification reactions with EG, DEG or PG	180 - 240	1 - 6	PET (BHET and oligomers)	Commercial (PET, PU)	[22, 60, 62, 69, 83, 122]
Thermolysis	Pyrolysis	Decomposition in an inert atmosphere	400 - 700	Vacuum - 10	Polyolefins; PS; PET; PVC, etc. (hydrocarbons)	Pilot scale	[81]
	Hydrocracking	Hydrogen-assisted catalytic cracking	300 - 500	20 - 150	Polyolefins, PET, PVC, PS (hydrocarbons, ↑ H/C)	Bench	[81, 104, 118]
	Gasification	Partial oxidation (air, vapor, or oxygen gas)	700 - 1500	1 - 2	PE, PS, PVC, biomass (syngas, CH_4, light hydrocarbons)	Commercial	[81, 92, 94, 123, 124]
	Thermal liquefaction	Degradation in supercritical water	375 - 450	220	Polyolefins, PET (hydrocarbons, ↑ H/C)	Bench	[119–121]

2.2 Pyrolysis

Pyrolysis, as previously introduced, is a thermal process that operates in an inert atmosphere (typically nitrogen) to break down large molecules. It is considered one of the most promising plastic recycling technologies due to its ability to handle mixed and contaminated plastic waste streams, obtaining valuable chemicals.

Some argue, however, that recycling plastic through pyrolysis contradicts the principles of a circular economy since the resulting product is a mixture of chemicals typically linked to fuel production rather than material recovery [59]. While some studies focused on pyrolysis oil as an alternative fuel, this represents the least sustainable pathway and is not the only option. Research efforts are increasingly focusing on refining pyrolysis processes to produce naphtha or monomers, which can be directly reintegrated into new plastic production. Furthermore, life cycle assessments (LCAs) indicate that pyrolysis-based recycling has a lower environmental impact compared to virgin petrochemicals when considering that the use of "virgin" naphtha is avoided (see Section 2.4) [125].

The pursuit of more selective product yields, lower contaminant levels, reduced environmental impact, and improved profitability has driven rapid advancements in pyrolysis technology in recent years. While plastic pyrolysis has already achieved a high degree of implementation due to its inherent advantages, ongoing research continues to refine and optimize the process. This is largely due to the many variables and reactor configurations that influence its efficiency and outcomes. This section examines these factors in detail and discusses how they affect the distribution of pyrolysis products.

For readers interested in a deeper exploration of this field, numerous high-quality review articles have been published in recent years. These works underscore the significance and potential of pyrolysis as a method for recycling post-consumer plastic waste, especially when compared to other end-of-life technologies [22, 25, 60, 67, 69, 94, 103, 104, 122, 126–147].

2.2.1 Feedstock

Pyrolysis offers greater flexibility in handling waste compared to chemolysis or mechanical recycling, but its efficiency and profitability depend on feedstock composition and quality [104, 148]. Studies have shown that heteroatoms and functional groups in the feedstock will likely be transferred to the lighter fractions of the products. Thus, a well-characterized feed can help predict and optimize the product distribution, but in commercial settings, variability and contamination make this challenging [92].

Feedstock impurities include both additives and organic residues, which can

volatilize and/or lead to byproducts that cause fouling, corrosion, and catalyst deactivation (e.g., HCl, nitrogenates, benzoic acid) [92]. To improve pyrolysis product quality for applications like steam cracking [58, 149], research focuses on sorting and pre-treatment methods, that albeit can be costly or increase the environmental impact, can be one of the key solutions to the production of more pure pyrolysis products.

Optical sorting (e.g., near-infrared spectroscopy, NIR) can remove heteroatom-containing plastics like PET, PA, and PVC, as well as unreactive polymers like PS [6] [150], while pre-treatment (e.g., hot washing, degassing) helps minimize contaminants. A more detailed discussion is present in the subsequent section (Section 2.2.9). Additionally, post-treatment strategies, such as hot filters, membranes, and hydrocracking, may further refine pyrolysis products [151, 152]. In general, further research is needed to understand the source and the impact of contaminants in post-consumer plastics and develop efficient removal strategies [63, 149].

Beyond the contamination, co-pyrolysis of plastics (with or without biomass) can create synergies affecting product distribution and reaction rates. Studies that have explored these effects [153–156] have shown that the products from binary plastic mixtures cannot be predicted by a simple linear combination of the results obtained for the individual plastics. These synergies arise from differences in radical stabilities and hydrogen availability, which shift the balance between statistical and non-statistical products (see Section 2.3). Therefore, to accurately capture these effects, models for each individual feedstock must first be developed and validated before being integrated.

2.2.2 Temperature

Cleaving (or cracking) carbon–carbon bonds requires an energy input: heat! The term pyrolysis originates from the Greek words *pur* = fire; *luo* = loosen [7]. From this definition alone, it is evident that temperature is the most critical parameter in pyrolysis: it governs both the rate of thermal decomposition and the reaction pathways [100].

The temperature required for pyrolysis depends on the thermodynamics of the material. Each post-consumer plastic requires a specific amount of heat to initiate bond cleavage (activation energy) (see Section 2.3), which can be determined through thermogravimetric analysis. In general, polystyrene begins to degrade at around 300 °C, while polyolefins require temperatures above 350 °C [100, 157]. This

[6] These plastics can be recycled separately (e.g., PET via solvolysis), or their presence may require post-processing like hydrogenation or distillation.

[7] Although "fire" implies the presence of oxygen, pyrolysis occurs in an inert atmosphere. Thus, the term thermolysis is often considered more precise [100].

explains the relatively high energy demand associated with thermochemical recycling technologies [8]. However, commercial applications rarely operate at these onset temperatures due to slow reaction kinetics

Since pyrolysis is a multi-phase process, temperature also dictates the volatilization of pyrolysis products via thermodynamic equilibrium and diffusion. Moreover, temperature strongly influences the pyrolysis product distribution across all plastic types. Polymer degradation involves multiple simultaneous reactions, some random, others leading to selective formation of low-molecular-weight products. Variations in temperature can significantly shift reaction pathways, altering the ratio of random to selective reactions. Several research groups have extensively investigated the impact of temperature on pyrolysis yields and product distribution [157–179].

At high temperatures (above 600 °C), pyrolysis favors the formation of aromatics and smaller molecules, increasing gas and naphtha yields. However, these results are also influenced by residence time as the high reaction rates at elevated temperatures make some secondary reactions nearly unavoidable even with short residence times. Nevertheless, besides leading to the production of more desirable products, high temperatures also impose higher financial and environmental costs [131, 157, 158], and technical challenges related to heating the plastic as will be discussed in the next section. Section 2.2.5 continues the discussion on residence time, and more thermodynamic and kinetic aspects will be explored in detail in Section 2.3.

2.2.3 Heating rate

In plastic pyrolysis, as the temperature is the key parameter, the heating rate is also highly important in industrial process design due to the inherent low thermal conductivity of plastics [180]. As plastic mass and particle size increase, heat conduction, rather than reaction kinetics, becomes the limiting factor, causing a significant portion of the pyrolysis (residence) time to be spent on heating and melting the sample. Table 2.3 highlights the critical role of particle size in heating rates and its influence on pyrolysis sub-classifications [24, 58]. However, these classifications may be outdated, as fast or flash pyrolysis can also occur at lower temperatures. Notably, for polypropylene and similar plastics, pyrolysis becomes conduction-limited even at film thicknesses (equivalent to particle size) above 15 µm. These heating limitations become even more pronounced in industrial settings, where reactor design and heating methods impose additional constraints.

At an industrial scale, the heating rate is inherently constrained by reactor engineering and thermal transfer mechanisms (e.g., electrical, microwave, LPG). In tank

[8] One approach to lowering this energy barrier is the use of catalysts mixed into the plastic feedstock (i.e., in situ catalysis). However, this method has several drawbacks, which will be discussed in Section 2.2.10.

pyrolysis, where heating occurs primarily via the reactor walls, long heating times are inevitable. Preheating plastics close to the pyrolysis temperature before feeding them into the reactor can improve process efficiency, enhance material homogenization during stirring, and mitigate particle size effects. Alternatively, using heat carrier materials or different reactor configurations (e.g., tube reactors, as discussed in Section 2.2.8) can optimize heat transfer.

Beyond affecting residence time, the heating rate directly influences product yields, particularly at high temperatures (greater than 500 °C). In lower temperature range (300–500 °C), more medium-to-heavy products are formed, the overall reaction rate is slower, and the heating rate has a minimal effect. Above 500 °C, gas and light oil yields increase, but with slow heating, some products may degrade and volatilize before reaching this temperature. PARKU *et al.* confirmed this at 600 °C, where fast heating rates led to significantly higher yields of light oil fractions (15 wt%) and permanent gases (5 wt%) compared to slow pyrolysis, at the expense of heavy oil fractions [181]. Additionally, faster heating accelerates volatilization, reducing gas residence time and minimizing byproduct formation, such as BTX [131, 160]. However, this effect is also influenced by the carrier gas flow rate.

	Conventional Pyrolysis	Fast Pyrolysis	Flash Pyrolysis
Operating temperature, °C	300 - 700	600 - 1000	500 - 800
Heating rate, °C/s	0.1 - 1	10 - 200	1000
Solid residence time, s	600 - 6000	0.5 - 5	< 1
Particle size, mm	5- 50	< 1	Dust

Table 2.3: Range of operating parameters for different pyrolysis processes [24].

2.2.4 Residence (reaction) time

The reactor residence time (or reaction/pyrolysis time) is intrinsically linked to the extent of conversion of the reactant and, therefore, is primarily governed by the heating rate and target pyrolysis temperature. Higher temperatures accelerate reaction kinetics, promoting volatile formation and reducing the required residence time. Conversely, at lower temperatures, longer reaction times are needed to achieve complete plastic conversion. For example, at 380 °C, 200 seconds proved insufficient to fully convert a PE/PP/PS mixture into light products, whereas at 400 °C, full conversion was achieved under 100 seconds [182].

However, inefficient heating can lead to temperature gradients and hot spots, causing excessive localized cracking and increasing the yield of naphthenes and

aromatics, as discussed in Section 2.2.3. This effect is particularly pronounced in bottom-heated reactors, where the pyrolysis temperature is reached at the bottom while the plastic remains unmelted in upper sections. As a result, the removal of light products is hindered, prolonging the residence time of both the plastic and pyrolysis products.

2.2.5 Gas residence time

The residence time of gaseous products is strongly influenced by reactor engineering, temperature, and carrier gas flow rate (types of carrier gas as discussed in the next section). It should not be confused with the plastic reaction time, as *"reaction times control the extent of conversion of the reactant, and the vapor residence time dictates the extent of secondary reactions"* [183].

These secondary reactions are often considered undesirable because they contribute to the formation of thermally stable compounds, such as naphthenes and aromatics. However, any further chemical transformation occurring in the gas phase is classified as a secondary reaction, many of which enhance light product yield [94, 100, 131, 158]. Based on this principle, the use of reflux has been proposed to reduce waxy product formation [184, 185]. The results have shown that, for virgin polyolefins, dimer formation remains minimal at short residence times, and a significant increase in naphthenes is only observed after prolonged gas residence times [184, 185]. In contrast, if the feedstock contains materials such as PS, PVC, PET, or biomass, naphthenes and aromatics appear even at low residence times due to the melt-phase pyrolysis degradation mechanism [186].

Gas residence time is also critical for ex-situ catalytic reactions, as it determines the contact time between the pyrolysis product stream and the catalyst. A discussion on catalysts and contact modes is available in Section 2.2.10. Therefore, optimizing residence time is critical in industrial process design to maximize the yield of high-value product fractions [180, 187].

2.2.6 Carrier gas

Pyrolysis occurs under an inert atmosphere, where the carrier gas flow rate plays a crucial role in controlling gas residence time, directly influencing product distribution [188]. Nitrogen is commonly used, but using a lighter carrier gas (e.g., helium $<$ nitrogen $<$ argon) reduces the gas residence time [189, 190].

Without a carrier gas, cracking within the reactor increases the yield of light fractions (e.g., gas yield) but may also promote undesirable side reactions. The same effect is observed when pyrolysis gas is recycled [132].

In some cases, reactive gases such as steam are introduced, though this process is often misclassified as pyrolysis. However, similar to hydrogenation [190], adding steam as a post-pyrolysis step can enhance olefin yields due to additional hydrogen availability [191].

In general, the choice of carrier gas depends on cost, process conditions, and desired products. In "stand-alone" pyrolysis units, the produced gas is typically burned to sustain the process, making it preferable to optimize gas yield without dilution. However, since paraffins and olefins are the most valuable products for plastic production, hydrogenation after pyrolysis may justify the use of carrier gas to optimize paraffin and olefin yields.

2.2.7 Pressure

Pressure is an important parameter in pyrolysis due to its influence on product volatilization, yet it remains relatively underexplored in the literature [94]. This is due to the usually high costs of pressurization and the low value of the feedstock and product streams, which should be regarded as commodities. Therefore, the use of pressurized vessels can compromise the economic feasibility of plastic waste pyrolysis processes.

In closed-batch reactors, increased pressure is linked to higher conversion rates at pyrolysis temperatures [164, 187, 192–195]. However, in semi-batch and continuous systems, pressure is strongly tied to phase transitions: lower pressures promote the removal of heavier products [196–198], whereas higher pressures hinder the release of high molecular weight compounds, leading to increased cracking and a greater yield of lighter products [199]. Consequently, at very high pressures, these additional reactions may also favor the formation of cyclic and aromatic compounds [200]. CHENG *et al.* (2020) demonstrated this effect by completely converting polyethylene into liquid and gas products at atmospheric and high pressure (greater than 28 bar) and between 385 - 485 °C in an autoclave reactor. At higher pressures, the olefin content was reduced in favor of an increased yield of isoparaffins, cyclic compounds, and aromatic products (Figure 2.4).

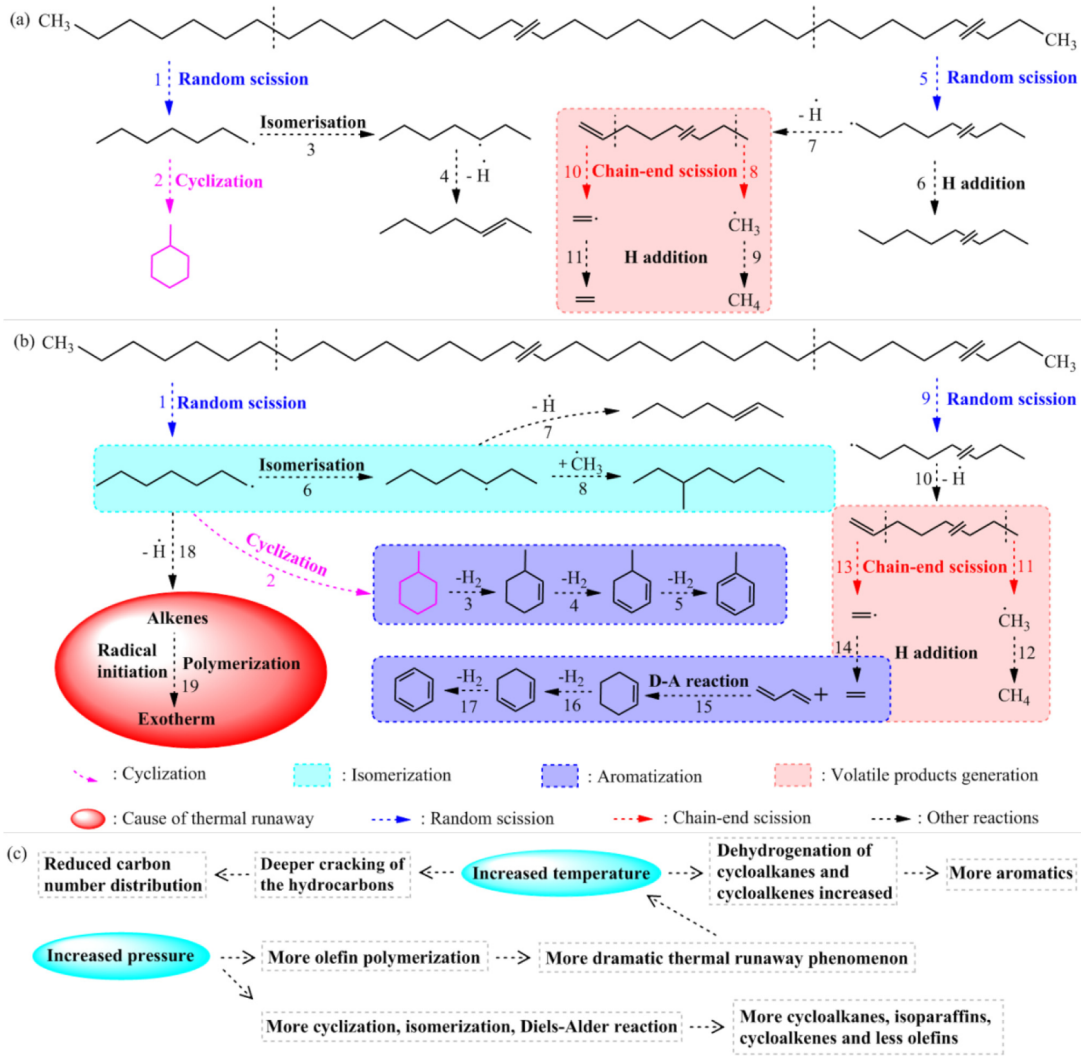

Figure 2.4: The proposed LDPE pyrolytic mechanism: (a) atmospheric-pressure pyrolysis pathways, (b) high-pressure pyrolysis pathways, and (c) the effect of temperature and pressure factors on the pyrolysis process [4]. Reprinted from Chemical Engineering Journal, Vol 385, CHENG *et al.*, Polyethylene high-pressure pyrolysis: Better product distribution and process mechanism analysis, 123866, Copyright (2020), with permission from Elsevier.

2.2.8 Reactors

As discussed in previous sections, process parameters (temperature and pressure), heating rate, and gas residence times are strongly correlated with pyrolysis yields and, most importantly, product distribution. As all of these aspects are tied to the reactor, as SCHEIRS e KAMINSKY (2006) states, the reactor type *determines mainly the quality of heat transfer, mixing, gas and liquid phase residence times, and the escape of primary products.*

Due to the usually high viscosity and low thermal conductivity of polymer melts, reactor design must ensure efficient feeding, mass and heat transfer, and solids re-

moval [92, 100]. For instance, reactors operating in fluidized regimes can pose significant operational challenges, such as bed material agglomeration, since plastics become viscous and sticky when heated [92]. Conversely, reactors with more uniform temperature profiles enable faster heating rates and better reaction control, as they promote consistent reaction rates throughout the reactor [22].

Historically, several reactor configurations have been explored for pyrolysis, each with characteristic competitive advantages and limitations. Below, the most frequent reactors used for plastic pyrolysis are listed, which are all either semi-batch (open removal of volatiles) or continuous:

- Fixed-bed reactor: Simple in design and easy to construct but suffers from poor temperature control, coke deposition, and batch operation constraints, making scale-up difficult [127, 131].

- Fluidized-bed reactor: Operates continuously, allows precise control over gas residence time and temperature, and ensures efficient heat and mass transfer. Therefore, a narrower and more predictable product distribution can be obtained. However, fluidized-bed reactors require high investment costs, complex design and operation, and careful control over the feedstock and particle size to prevent feeding issues. Poorly selected operating conditions can lead to bed defluidization and material attrition [25, 126, 127, 131, 132].

- (Conical) Spouted bed reactor: Similar to fluidized-bed reactors, this design reproduces some conditions found in fluid catalytic cracking (FCC) units but is subject to the same challenges as fluidized systems, including bed material attrition and defluidization [100, 131].

- Stirred tank reactor: Easy to construct and allows flexible residence times but may suffer from inefficient heat transfer, even when assisted by a stirrer, leading to thermal gradients and, possibly, secondary char formation. Additionally, these reactors require significant infrastructure and frequent maintenance, mainly to remove solid products [25, 126, 132]. To mitigate downtime, companies using this reactor type often operate multiple units in parallel, ensuring continuous operation while individual reactors undergo maintenance. A discussion on pre-heating and continuous feeding is included in the next section.

- Rotary kiln: A continuous tubular reactor, offering flexibility in terms of particle size, ease of construction, and scalability. However, its primary drawback is poor temperature control and long vapor residence times, which may reduce pyrolysis efficiency and lead to the formation of undesirable products [25, 127].

- Screw (or auger) reactor: A continuous tubular reactor equipped with a screw conveyor (see an example in Figure 2.5) in which, unlike other reactor types, are not limited by polymer viscosity and are well mixed as the screw physically displaces the plastic [100]. Optimization of the reactor length and control of the residence time via screw speed is needed to ensure complete conversion. This reactor is relatively easy to construct and scale up [25, 126, 127, 131, 132].

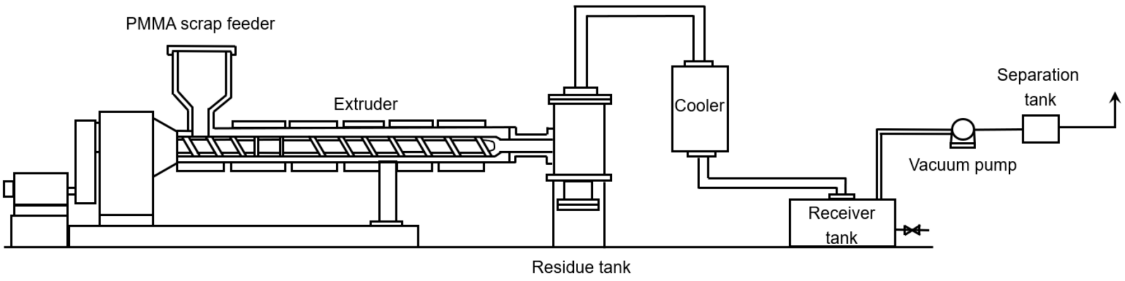

Figure 2.5: Screw pyrolysis reactor [5].

As highlighted in Section 2.2.2, temperature is the most critical parameter in plastic pyrolysis. Since different reactors exhibit varying heat and mass transfer performance, it follows that *different reactor designs lead to different product distributions*, a relationship confirmed by LOPEZ *et al.* (2017) [131], who reviewed product yields (gas, oil, waxes, and residue) from the thermal pyrolysis of polyolefins across different reactor types.

A summary of companies and their respective reactor technologies is presented by QURESHI *et al.* (2020) [25] (see Table 2.4). Further details on commercial facilities and a review of relevant patents are provided by DE MIRANDA (2024) [201].

Technology provider	**Capacity (TPD)**	**Reactor type**	**Location**	**Status**
VadXX	60	Rotary kiln	USA	Online
Nexus	50	Melting Vessel	USA	Online
Agilyx	10-50	Dual screw reactor	USA	Online
Recycling Technologies	20	Fluidized Bed	UK	Online
Plastic Energy	20	STR	Spain	Online
Susteen Technologies	12	Screw with recirculation	Germany	Online
PHJK	12-14	Rotary kiln	Finland	Online
Renewlogy	0.24 - 10	Rotary kiln	USA	Online
Pyrovac	1.2 - 12	STR	Canada	Online
Re-oil (OMV)	2.4	Melting vessel	Austria	Online
BP process	1	Fluidized bed	Germany	Dismantled
Pyrowave	0.1-0.2	Microwave catalytic (only PS)	Canada	Online

Table 2.4: Overview of pyrolysis technology providers and key process details. Adapted from [25]. Abbreviations: TPD = tons per day; STR = stirred-tank reactor; TCR = thermo-catalytic reforming.

2.2.9 Feeding system and pre-treatment

As discussed earlier, industrial-scale operations should ideally be continuous to accelerate processing. In the case of the stirred tank reactor, due to solid, and, when melted, viscous nature of plastic materials, an extruder is not only the ideal equipment to perform this task, but it is more efficient to heat the material than in an agitated tank, ultimately reducing operational expenditures (OPEX) and CO_{2e} emissions, and ensuring better homogeneity in the reactor [67, 132].

Moreover, as discussed in Section 2.2.1, additional sorting steps can significantly improve feedstock quality and, consequently, enhance the quality of pyrolysis products. However, these steps alone are insufficient for removing all impurities, particularly those with low water solubility or high boiling points. An additional strategy, as illustrated in Figures 2.6 and 2.7, is to remove non-plastic materials via degassing ports, while simultaneously heating the feed stream [202]. This approach helps to eliminate moisture, oxygenated, and chlorinated compounds [202]. This strategy is not limited to feeding extruders; it can also be effectively applied in rotary kilns and screw reactors.

Regarding chlorine removal, which is primarily linked to the presence of PVC and chlorinated additives, FUKUSHIMA *et al.* [203] (2010) achieved a 99.1% dechlorination efficiency by utilizing a feed screw operating at 350 °C to process a 15 kg/h PVP:PP mixture (50:50 wt%). Similarly, LEI *et al.* [204] (2018) obtained over 90% dechlorination efficiency by feeding plastic into a stirred tank pyrolysis reactor at 300 °C for over 30 minutes through a vented screw conveyor. Additionally, WANG *et al.* [205] (2021) achieved a 99.9% dechlorination efficiency using hydrothermal pretreatment (240 °C, 0.3 M NaOH). These findings indicate that incorporating a dechlorination step at temperatures exceeding 300 °C can effectively mitigate chlorine-related issues in the pyrolysis process. Furthermore, oxides such as calcium oxide can assist in halogen removal by binding with chlorine [206–208]. Thermal pre-treatment may also help in the removal of other heteroatoms present in additives, although further studies are necessary to confirm its effectiveness [63]. Additionally, depending on the extruder design, vent flooding (polymer escaping through the vent) may also occur; therefore, other modern equipment may be of interest.

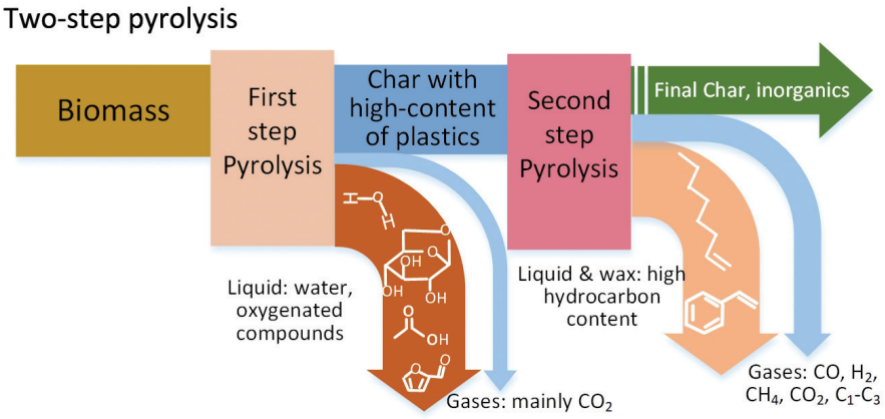

Figure 2.6: Step-wise biomass pyrolysis [6]. The first step typically occurs below 350 °C, and the second above 400 °C. Used with permission of Walter De Gruyter GmbH, Fractionation of biomass and plastic wastes to value-added products via stepwise pyrolysis: a state-of-art review, SHEN, 0, 1983; permission conveyed through Copyright Clearance Center, Inc.

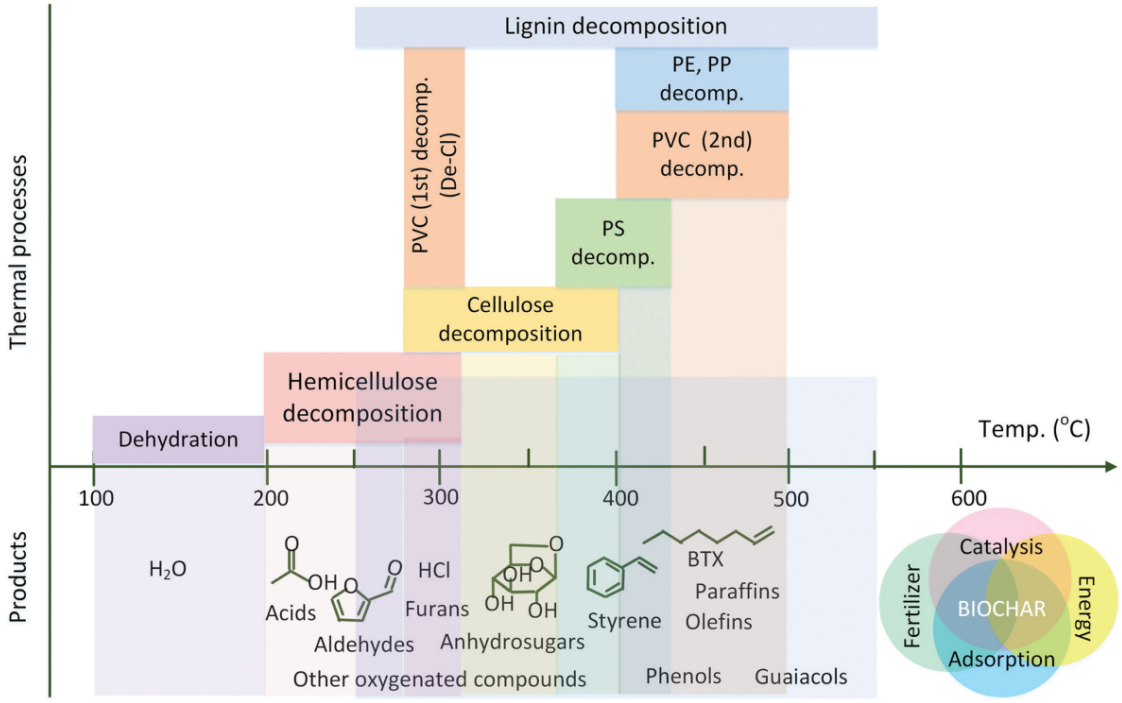

Figure 2.7: Thermal decomposition of materials as a function of temperature, and their products [6]. Used with permission of Walter De Gruyter GmbH, Fractionation of biomass and plastic wastes to value-added products via stepwise pyrolysis: a state-of-art review, SHEN, 0, 1983; permission conveyed through Copyright Clearance Center, Inc.

2.2.10 Catalysts

Catalysts are frequently employed to optimize product distribution and selectivity by influencing the degradation mechanism [59, 69, 83, 104]. The contact mode can

be in situ or ex-situ. In the case of the former, it requires either physical mixing with the polymer or a fluidized pyrolysis process, where the molten polymer interacts with catalyst particles [3, 26]. The main advantage is that the catalyst addition can also lower the reaction temperature. However, this approach promotes substantial coke formation, requiring frequent catalyst regeneration.

Thus, due to impurities in plastic waste, ex-situ catalytic pyrolysis is more common as some contaminants do not volatilize, although the contact time between pyrolysis products and the catalyst is crucial, as discussed in Section 2.2.5. In this case, the majority of gas-phase reactions are catalyzed by passing the reactant through, frequently, a packed bed of catalyst particles. Pyrolysis vapors can also undergo in-line reforming by introducing hydrogen or steam downstream of the pyrolysis reactor [104]. XUE *et al.* (2017) [209] investigated catalyst contact modes for PS, PVC, PP, and PE pyrolysis, suggesting the differences in in-situ and ex-situ catalytic pyrolysis mechanisms.

For both contact modes, various catalysts have been tested, differing in type, pore size, and acidity [59, 69]. Some were originally developed for polymerization but can also facilitate depolymerization by lowering the kinetic barrier for both processes to the same extent, as seen with Ziegler-Natta catalysts [83]. However, zeolites (HZSM-5, HY, Hβ, MCM-41, SBA-15, etc.) and clay remain the most extensively studied materials [26, 68, 83, 131, 210].

In general, catalysts enhance the yield of light compounds, particularly olefins, but they also promote the formation of naphthenes and aromatics, which can be undesirable in high concentrations (e.g., higher than 10 wt%). Thus, despite the improved selectivity [83], coke formation remains a major challenge, requiring strict feedstock control, which is not always feasible, especially when working with waste with high variability in plastic and contaminants composition [210]. OCHOA *et al.* (2020) [211] provides a comprehensive review of coke formation mechanisms and catalyst deactivation. Moreover, with an improved understanding of pyrolysis mechanisms and process parameters, maximizing the yield of desirable products is possible even without catalysts. These aspects will be further explored through the development and validation of kinetic mechanisms presented in this thesis.

2.3 Modeling plastic pyrolysis

Although plastic pyrolysis holds great promise for increasing recycling rates, most studies remain empirical. No robust, validated kinetic models exist for individual plastics, plastic mixtures, or waste across various operational conditions. Thermodynamic and transport models are also scarce. This lack of a comprehensive understanding hinders accurate product prediction, process optimization, reactor

design improvements, and the identification of process limitations.

The slow progress in model development is understandable, given the complex, multi-phase nature of pyrolysis. Obtaining accurate kinetic data is particularly challenging as studying kinetically controlled processes requires milligram-scale plastic samples, high heating rates, and rapid gas sweeping velocities. Without these conditions, kinetic effects become entangled with mass and heat transfer phenomena, further complicated by secondary reactions.

Nevertheless, various kinetic mechanisms have been proposed, each differing in its ability to predict product formation and its correlation with reactor and process parameters. This section examines these mechanisms, highlighting their predictive capabilities and limitations. There is no better way to introduce this discussion than with a statement from the 8th Chemical Sciences and Society Summit (CS3) (2020) [59]:

> "Over many decades, chemists have devoted a great deal of effort to developing the 'forward' reactions that turn monomers into polymers, but comparatively little research has gone into the 'back' reactions that break down these long chains into shorter molecules. This is an important new field for future development of methodologies, theories and processes."

This holds true for all the most common plastics: polyolefins, polystyrene, PET, and PVC. To the best of our knowledge, no mechanistic model has been validated across a wide range of temperatures and conditions, including the effects of pressure, carrier gas flow rate, synergy between different reactants, and gas-phase reactions. Some studies have varied the heating rate, but their analysis remains limited to global rate modeling rather than true mechanistic modeling.

To support the arguments presented, a literature review was conducted to identify studies on polymer degradation mechanisms, focusing primarily on polystyrene and polyolefins. The earliest works on the "Depolymerization of Long Chain Molecules" date back to the 1940s [212–214]. These initial statistical models were developed based on the assumption that all bonds have an equal probability of breaking, regardless of their position within the polymer chain or the polymer's molecular weight [212–217].

Later, Jellinek proposed that degradation begins specifically at weak links randomly distributed along the polymer chains, a concept later known as the weak link theory (e.g., in polystyrene, these weak links could be peroxide groups) [218, 219], also referred to as the "weak bond model" [220]. To validate this hypothesis, Jellinek investigated the influence of branches and inhibitors on degradation and calculated the activation energy for polystyrene and polyethylene in a vacuum [221–223]. Later, Madorsky recalculated the activation energy under vacuum conditions and corrected Jellinek's original values [224].

However, in the early 1950s, Simha, who had previously studied the statistical model [212, 216], and his co-workers expanded the idea of random scission inspired by the ethane cracking chain reaction mechanism proposed by RICE (1935) [225]. They stated that "*cracking is a chain process, characterized by at least an initiation, propagation, and termination and, very likely, also chain transfer*" [7]. This theory led to further investigation into the relevance of chain length and transfer reactions in determining the final molecular weight distribution [226–228]. Figure 2.8 shows the set of reactions considered by SIMHA *et al.* (1950).

Following Simha's contributions, many studies began utilizing gas chromatography and/or flame ionization detection to analyze pyrolysis products and formulate hypotheses regarding degradation mechanisms [229–241]. Despite these advancements, it was not until the 1990s and 2000s that more complex mechanistic models began to emerge, primarily developed by a few research groups. These models will be discussed in Section 2.3.1.

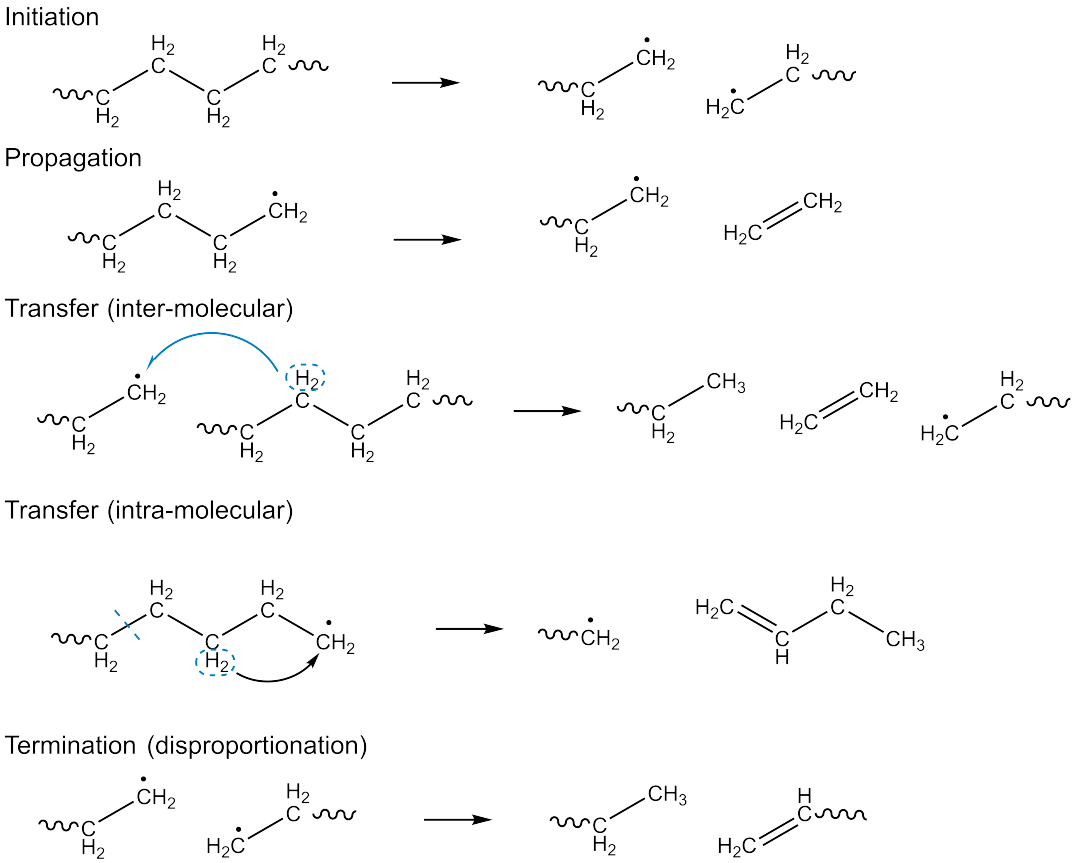

Figure 2.8: Set of reactions considered by Simha, using polyethylene as an example. Adapted from [7].

Building on these early investigations, the field has seen a growing number of kinetic studies over the past decades. However, as shown in Figure 2.9, their focus has gradually shifted. Earlier studies primarily aimed to elucidate chemical degradation

mechanisms (classified as 'mechanistic models'), whereas more recent research has largely concentrated on estimating overall kinetic constants (classified as 'empirical model').

The data in Figure 2.9 comes from a bibliographic review comprising 297 studies on polymer degradation. [9] In total, only 19% of these studies proposed and validated a detailed chemical mechanism, while the majority (75%) focused on estimating a global kinetic rate or a small set of rates. Additionally, as shown in Figure 2.10, 4% used molecular dynamics simulations, and 2% utilized empirical correlations to model pyrolysis in Aspen Plus and/or Aspen Hysys.

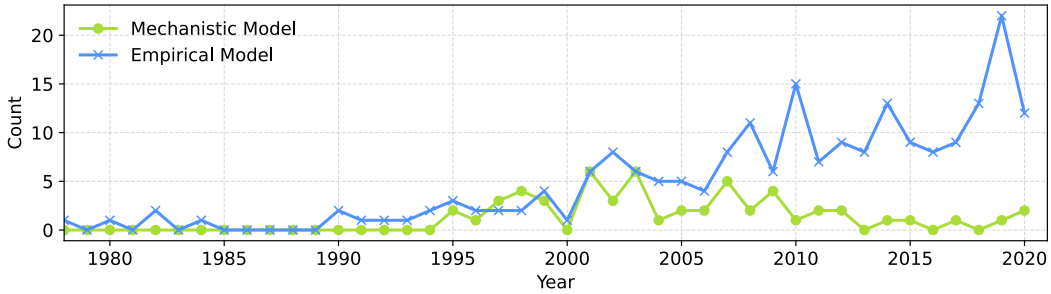

Figure 2.9: Temporal trend in the number of publications developing *mechanistic* and *empirical* polymer degradation models.

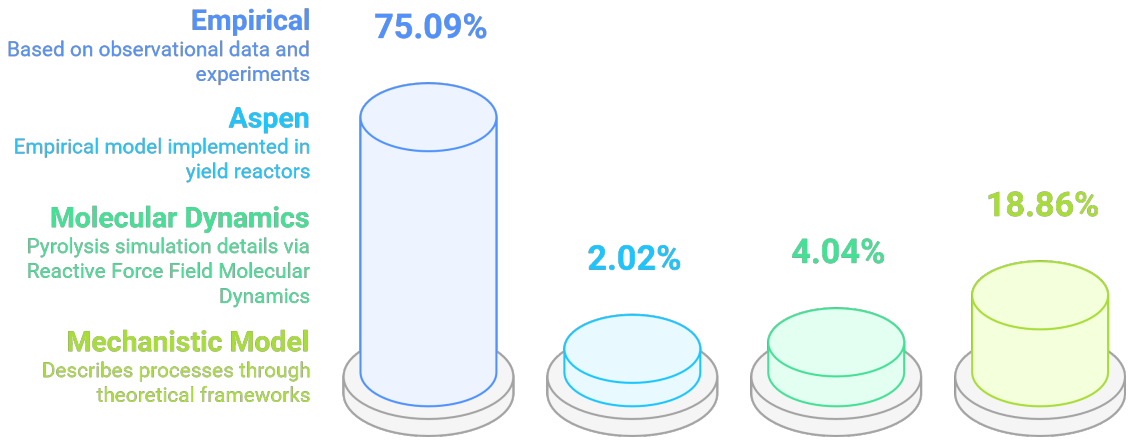

Figure 2.10: Bibliographic review of pyrolysis models.

Studies categorized as 'empirical' are equivalent to 'global models', which describe the degradation process using one or a small set of parameters. (These parameters are often referred to as kinetic constants, but they are not true kinetic constants, as they are applied to arbitrary reactions.). These models do not explicitly represent product formation, or when they do, the product distribution is

[9] This bibliographic review was conducted by the author. While it may not be exhaustive, it includes the majority of studies focusing on polyolefin or polystyrene degradation. Broader reviews may yield different statistics. Additionally, the review covers studies up to 2020, as recent trends remain consistent.

typically limited to a few lumped components. Most of these studies rely on dynamic or isothermal thermogravimetric analysis (TGA) to model sample weight loss or volatilization.

Dynamic TGA experiments involve heating the sample across a defined temperature range (typically 25–600 °C) at a predetermined rate (e.g., 5, 10, 12, 20, 25, or 50 °C/min). In contrast, isothermal experiments maintain the sample (typically up to 1 gram) at a constant temperature (usually between 400 and 500 °C) for a fixed duration [242]. In both cases, a purge gas (usually nitrogen or argon) is continuously supplied at a constant flow rate to remove gaseous pyrolysis products from the reaction zone [242].

The conversion, x, representing the reacted fraction at time t, is defined as:

$$x = \frac{w_0 - w_t}{w_0 - w_\infty} \tag{2.1}$$

where w_0 is the initial sample weight, w_t is the weight at time t, and w_∞ is the weight after complete pyrolysis.

The reaction rate is given by:

$$\frac{dx}{dt} = f(x)k(T) \tag{2.2}$$

where $f(x)$ is a function of x, and $k(T)$ is the kinetic constant, typically expressed using the Arrhenius equation:

$$k = k_0 \exp(-E_A/RT) \tag{2.3}$$

where k_0 (sometimes denoted as A) is the pre-exponential factor, E_A is the activation energy (J/mol), T is the temperature, and R is the gas constant [242].

Model-free methods such as the Flynn–Wall–Ozawa (FWO), Kissinger-Akahira-Sunose (KAS), and Friedman (FR) methods are commonly used for determining parameters [243–247]. Additionally, model-fitting methods, such as the Coats-Redfern and Criado approaches, apply algebraic expressions corresponding to common reaction mechanisms to determine the kinetic equation [243–247]. Most polymer degradation studies identified the mechanism as first-order, meaning the reaction rate follows $f(x) = (1 - x)$ [243, 244, 248–251]. However, this estimated rate is not the intrinsic as WESTERHOUT *et al.* (1997) noted:

> By using an apparatus such as a TGA in kinetic studies, the evaporation rate of products is determined and not the intrinsic chemical reaction rate, since not every broken bond leads to the evaporation of a product, only product fragments that are small enough to evaporate will actually evaporate and thus lead to a decrease of the polymer mass [252].

Another key limitation of using solely TGA data is that product yield is often not

measured [242]. Thus, lumping techniques are also often applied, especially when product yield is known, although it has also been applied to TGA data to assist in fitting the weight loss curve [253–261]. Lump models classify hydrocarbons into carbon-number/boiling point ranges (e.g., C_6–C_{11} and C_{12}–C_{24}) or chemical families (e.g., olefins, paraffins) [262], and define a set of reaction families and mass balances, instead of using an overall reaction rate (Equation 2.2).

While lumped models provide a better representation of pyrolysis (especially at small scales), they lack mechanistic detail, particularly with regard to fundamental reaction pathways [224]. As DENTE *et al.* emphasized:

> The reduction of intermediate products as well as the grouping of the reactions involved depends on the hypothesis assumed about the interactions between the propagation paths of the different initial radicals [262].

But, as the assumptions underlying kinetic modeling vary widely, as illustrated in Figure 2.11, the absence of a clear consensus among researchers highlights the challenge of achieving a universally applicable model. In practice, each lumped model is inherently tied to the specific dataset from which it was derived. Consequently, these models are better described as data-fitting tools rather than true kinetic representations, limiting their predictive capability outside the context in which they were developed.

Therefore, while lump models can provide insights into system-specific pyrolysis behavior, their applicability is limited beyond the studied reactor system. In Chapter 3, a lumped model is developed for catalytic ex-situ pyrolysis. The choice for a lumped model is justified because of the high system complexity (e.g., interplay of thermal and catalytic reactions) and variability (e.g., heterogeneous feedstock, catalyst screening). Despite its limitations, it is shown how the model parameters can be adapted with only a few experiments. Additionally, this model aids in determining the optimal catalyst-to-plastic mass ratio and the ideal vapor-catalyst contact time. Therefore, the model is useful when there are time constraints, such as in industrial environments when the process needs to be frequently adapted, catalyst screening is needed, and optimization is desirable.

Anyhow, comparing Simha's initial model (Figure 2.8) with lumped models, it becomes evident that, due to the high complexity of plastic degradation, researchers have opted for non-mechanistic models and have relied on simplifications that hinder an accurate representation of pyrolysis under varying conditions. The next section (Section 2.3.1) discusses mechanistic models for different plastics, offering insights into product distribution variations. However, even these models lack a comprehensive representation of critical factors such as heating, mixing, melt-phase kinetics, volatilization, mass transport, and gas-phase kinetics. Addressing these gaps remains a key research opportunity and a central motivation for this thesis.

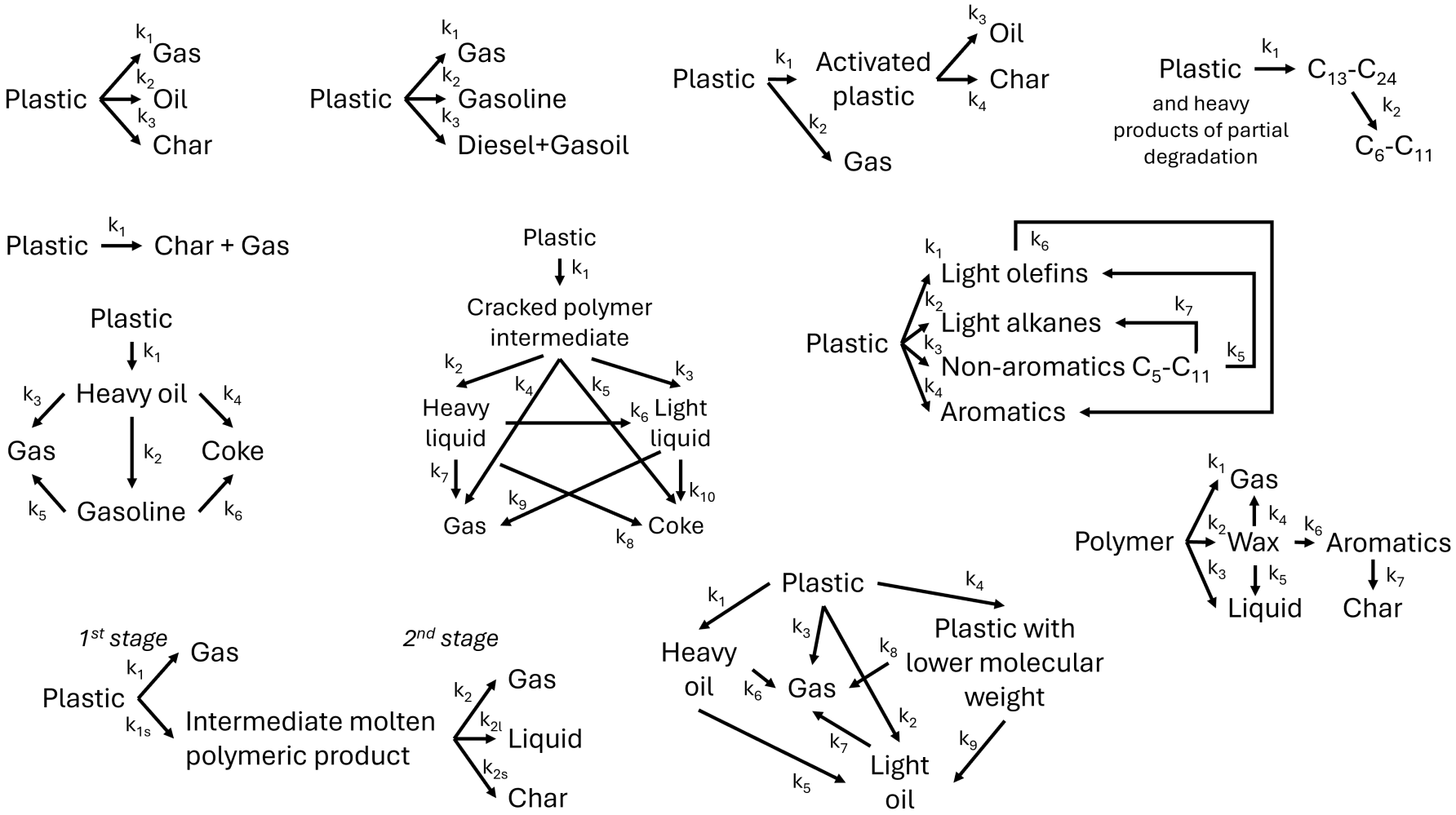

Figure 2.11: Examples of lumped kinetic models identified during the bibliographic review [8–19].

2.3.1 Mechanistic Models

In Section 2.2.1, it was discussed that predicting the composition of pyrolysis products is very challenging if the feedstock composition is not known. This occurs because the product distribution for each polymer is inherently linked to its degradation mechanism, which depends on factors such as radical stability, chain defects, degree of aromaticity, and the presence of halogens or other heteroatoms in the polymer structure. These aspects are crucial since thermal degradation is a radical-driven process.

Similar to polymerization, depolymerization consists of initiation, propagation, and termination steps. Initiation occurs primarily at random, breaking carbon-carbon bonds along the polymeric chain. In the previous section, the concept of weak-link theory was introduced [218–220], which suggests that the first bonds to break are not necessarily from the main polymer backbone but rather from branches, vinylene groups, catalysts, or inhibitor residues. However, these "weak links" are present in much lower concentrations than the total number of carbon bonds that must be cleaved, and their precise quantification is challenging due to variations in polymerization methodologies used by manufacturers [263]. Another type of initiation, known as end-chain scission, involves the degradation of polymer chain ends, forming allyl radicals. Termination occurs either by combination or disproportionation.

While both initiation and termination reactions influence the overall reaction rate, product distribution is primarily governed by reaction thermodynamics, radical stability, molecular structure, and steric hindrance. For instance, if the resulting radical is relatively stable, as in PS, degradation occurs predominantly via unzipping (also called end-chain β-scission), leading to high monomer yields. In contrast, PE degradation primarily produces unstable primary radicals, which rapidly undergo intra- or intermolecular hydrogen transfer to form more stable secondary or tertiary radicals rather than yield monomers. As a result, polyethylene pyrolysis generates a broad mixture of hydrocarbons with varying chain lengths.

Table 2.5 summarizes the predominant overall degradation pathways and their effects on monomer recovery. The reaction types can be described as follows:

- End-chain β-scission: the polymer degrades from the chain ends, successively yielding monomers;
- Random-chain scission: the polymer backbone breaks randomly, producing fragments of varying lengths;
- Chain-stripping: reactive side groups are eliminated from the polymer chain,

leading to the evolution of volatile degradation products and a polyene structure;

- Cross-linking: polymer chains form a network structure, which often occurs in thermosetting polymers when heated.

Table 2.5: Decomposition mechanisms and monomeric yields of main polymers. Adapted from BUEKENS e HUANG (1998) [26].

Polymer	**Decomposition Mechanism**	**Monomer Yield (wt%)**
Polymethylmethacrylate	End-chain β-scission	91–98
Polystyrene	End-chain β-scission	82–94
Polyethylene	Random-chain scission	2 - 10
Polypropylene	Random-chain scission	0 - 17
Polybutadiene	Random-chain scission	1
Polyethylene terephthalate	Random-chain scission + aromatization	2
Polyvinyl fluoride	Chain-stripping + aromatization	0

Compared to polyolefins and polystyrene, the degradation mechanisms of rubbers, polyethylene terephthalate (PET), and polyvinyl chloride (PVC) remain less well understood. In the case of PVC, degradation occurs in two steps: (i) dehydrochlorination via chain-stripping at approximately 300°C (see Section 2.2.9), and (ii) further conversion of the resulting polyene backbone, which primarily undergoes aromatization. However, these mechanisms have not been fully validated.

On the other hand, detailed mechanistic models for the pyrolysis of vinyl polymers, such as PS, PP, and PE, are well established. Figure 2.12 depicts the various typical reaction families for the pyrolysis of these polymers. Initiation and termination reactions are the initial three (chain fission, recombination, disproportionation, and end-chain fission). The remaining are the propagation reactions.

H-abstraction involves the cleavage of a C–H bond by hydrogen transfer to an abstracting radical. The abstracting radical and the product radical can be end-chain or mid-chain radicals. Mid-chain β-scission results in the bond cleavage in the β-position to the radical center, with the concomitant formation of a radical species and an unsaturated end. Radical addition (addition of a radical to a π-bond) competes effectively with the H-abstraction and end-chain β-scission reactions. End-chain β-scission (depropagation) is the main route to the formation of monomers. Intramolecular isomerizations (such as 1,x-shift, and x,x+n-shift) are essential for yielding oligomers, such as dimers and trimers. These reactions are primarily driven by how high the ring-strain energy of the cyclic transition state is. These reactions are further explored in chapters discussing the PS and PE degradation mechanisms. They are the main reactions considered by the studies from Politecnico di Milano, Broadbelt, and Poutsma, as later detailed in Section 2.3.1.

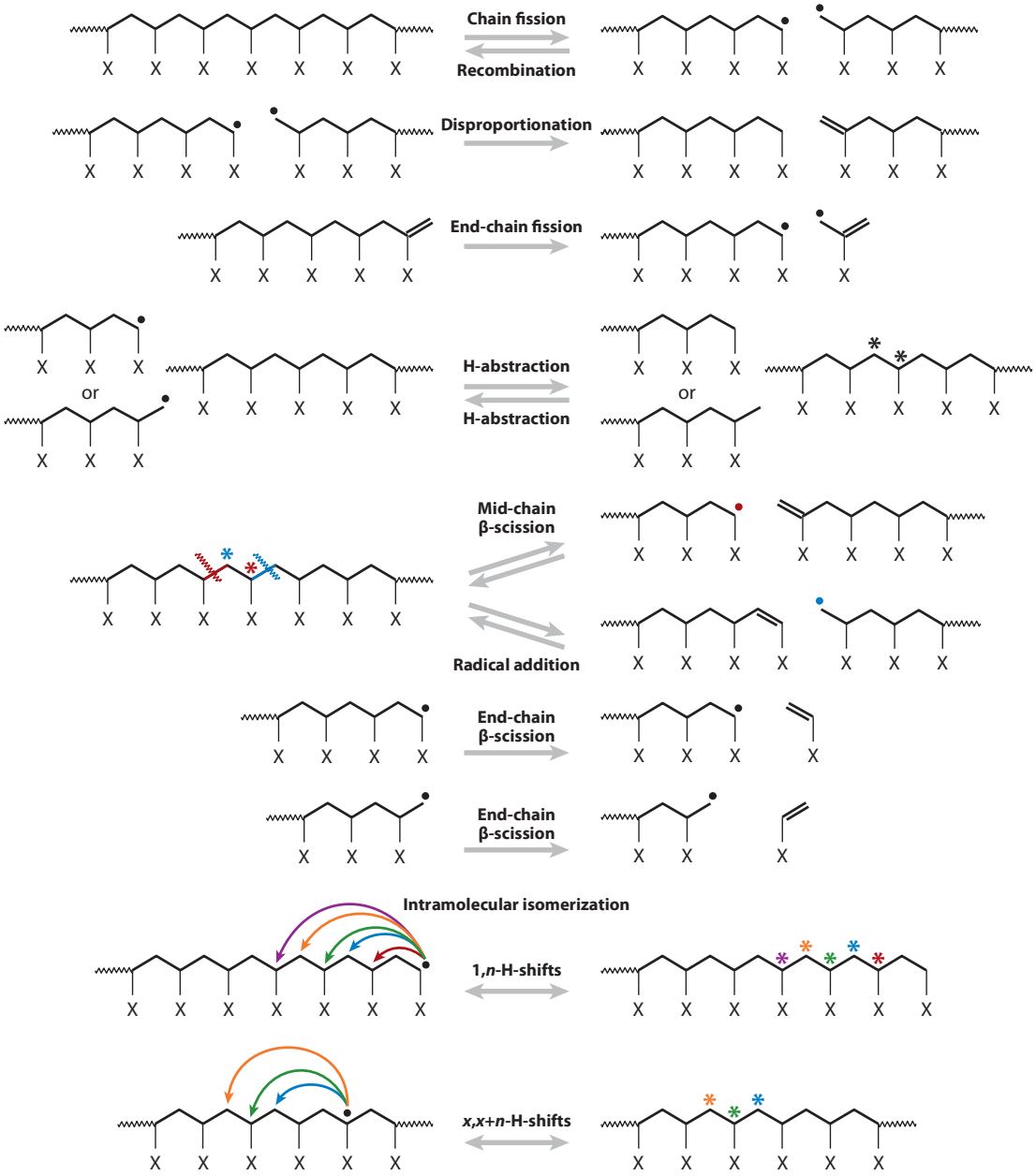

Figure 2.12: Various elementary reactions involved in the pyrolysis of vinyl polymers. X represents the substituent group; X = C_6H_5 for polystyrene, CH_3 for polypropylene, and H for polyethylene. The different possible radical sites are denoted by asterisks. [20]. Used with permission of Annual Reviews, Inc., from Unraveling reaction pathways and specifying reaction kinetics for complex systems, VINU e BROADBELT, 3, 1, 2010; permission conveyed through Copyright Clearance Center, Inc.

Beyond radical stability and molecular structure, reaction thermodynamics provides additional insight into monomer recovery potential. Polymerization is an exothermic process ($\Delta H < 0$) that must overcome the entropy loss ($\Delta S < 0$) associated with reduced monomer mobility [21, 264]. At the ceiling temperature (T_c), where $\Delta G = 0$ ($\Delta G = \Delta H - T\Delta S$), polymerization and depolymerization reach equilibrium (Figure 2.13)). Depolymerization in contrast is endothermic ($\Delta H > 0$) and entropically favorable ($\Delta S > 0$), requiring temperatures above T_c [21, 264].

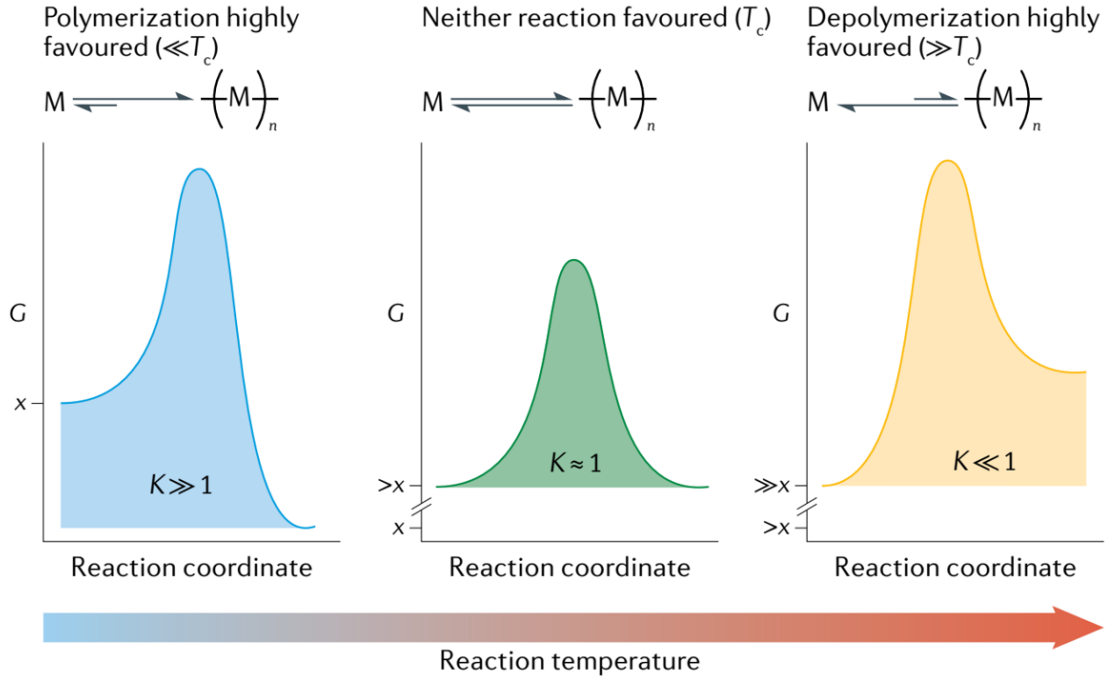

Figure 2.13: Conceptual model of polymerization energetics [21]. Plots of the Gibbs free energy (G) versus the reaction coordinate for polymerization (where M is the monomer) at three different reaction temperatures relative to the ceiling temperature (T_c). At temperatures T_c, the reaction equilibrium constant, K, lies far to the right, favoring polymerization. At T_c, neither reaction is favored. At temperatures T_c, K lies far to the left and depolymerization is favored. As the reaction temperature increases, so does the Gibbs free energy of the monomer, rising from x at low temperatures to x at high temperatures. Reproduced with permission from Springer Nature.

For highly exergonic polymerizations, such as PE and PP, depolymerization requires substantial energy input [21, 83]. Monomer recovery yields are low because chain-end unzipping (the direct reverse of chain-growth polymerization) demands a high energy input [83]. As a result, competing side reactions (e.g., H-abstraction), which require less energy, become dominant, further limiting monomer recovery [21, 265].

Figure 2.14 illustrates a conceptual reaction profile for a highly exergonic polymerization and its corresponding depolymerization pathways. While monomer re-

covery remains low for PE and PP due to their high polymerization enthalpies, increasing the reaction temperature can improve yields [265]. Additionally, compared to polyolefins, PS and PMMA exhibit less negative polymerization enthalpies, making their depolymerization more favorable [265].

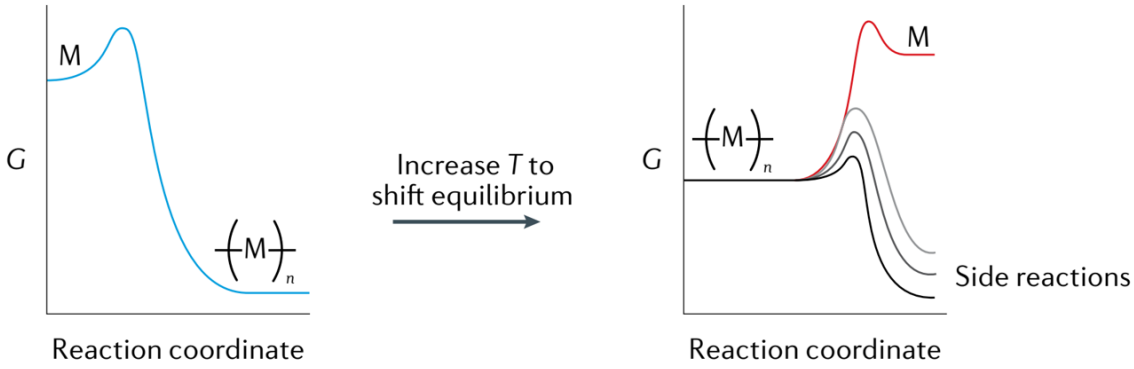

Figure 2.14: Conceptual reaction profiles for a highly exergonic polymerization reaction and its corresponding depolymerization reactions. M stands for monomer. In these cases, the standard change in the Gibbs free energy (ΔG_p^0) is too high for chemical recycling to monomer. Adapted from COATES e GETZLER (2020) [21]. Reproduced with permission from Springer Nature.

The development and validation of new mechanistic models

As briefly mentioned earlier in Section 2.3, the period from 1993 to the early 2000s saw the development of more complex mechanistic models by few key research groups:

- Benjamin J. McCoy and coworkers (University of California)
- Eliseo Ranzi, Giulia Bozzano, Mario Dente and Tiziano Faravelli (Politecnico di Milano)
- Linda J. Broadbelt (Northwestern University)
- Marvin L. Poutsma (Oak Ridge National Laboratory)

McCoy and Madras employed a relatively simple mechanistic model, primarily considering random scission, chain-end scission, and addition ("repolymerization"). They used continuous distribution kinetics based on population balance equations (PBEs). This allowed them to monitor the molecular weight distribution over time. However, their approach relied on lumped reactions, using global rate coefficients rather than predicting specific product yields. Table 2.6 summarizes McCoy's key publications on polymer degradation.

Table 2.6: McCoy's main works on plastic degradation.

Year	Authors	Title	Reference
1993	McCoy, B. J.	Continuous-Mixture Kinetics and Equilibrium for Reversible Oligomerization Reactions	[266]
1995	Wang, M., Smith, J. M., McCoy, B. J.	Continuous Kinetics for Thermal Degradation of Polymer in Solution	[267]
1995	Madras, G., Smith, J. M., McCoy, B. J.	Effect of Tetralin on the Degradation of Polymer in Solution	[268]
1996	McCoy, B. J.	Continuous kinetics of cracking reactions - Thermolysis and pyrolysis*	[269]
1996	Madras, G., Smith, J. M., McCoy, B. J.	Degradation of Poly(methyl methacrylate) in Solution	[270]
1997	Kodera, Y., McCoy, B. J.	Distribution kinetics of radical mechanisms - Reversible polymer decomposition	[271]
1997	Madras, G., Chung, G. Y., Smith, J. M., McCoy, B. J.	Molecular Weight Effect on the Dynamics of Polystyrene Degradation	[272]
1997	Madras, G., McCoy, B. J.	Degradation kinetics of polymers in solution - dynamics of molecular weight distributions*	[273]
1998	Madras, G., McCoy, B. J.	Effect of hydrogen donors on polymer degradation	[274]
1998	Madras, G., McCoy, B. J.	Time evolution to similarity solutions for polymer degradation	[275]
1998	Madras, G., McCoy, B. J.	Evolution to Similarity Solutions for Fragmentation and Aggregation	[276]
1998	Sezgi, N. A., Cha, W. S., Smith, J. M., McCoy, B. J.	Polyethylene Pyrolysis: Theory and Experiments for Molecular-Weight-Distribution Kinetics	[277]
1999	Madras, G., McCoy, B. J.	Distribution Kinetics for Polymer Mixture Degradation	[278]

Table 2.6 – McCoy's main works on plastic degradation (continued).

Year	Authors	Title	Reference
1999	McCoy, B. J.	Distribution Kinetics for Temperature-Programmed Pyrolysis*	[279]
2001	McCoy, B. J.	Polymer thermogravimetric analysis - effects of chain-end and reversible random scission	[280]
2001	McCoy, B. J.	Discrete and continuous models for polymerization and depolymerization	[281]
2001	Sterling, W. J., McCoy, B. J.	Distribution kinetics of thermolytic macromolecular reactions**	[282]
2002	Cha, W. S., Kim, S. B., McCoy, B. J.	Study of polystyrene degradation using continuous distribution kinetics in a bubbling reactor	[283]
2002	Kodera, Y., McCoy, B. J.	Distribution Kinetics of Polymer Thermogravimetric Analysis: A Model for Chain-End and Random Scission	[284]
2002	Madras, G., McCoy, B. J.	Numerical and Similarity Solutions for Reversible Population Balance Equations with Size-Dependent Rates	[285]
2003	Smagala, T. G., McCoy, B. J.	Mechanisms and Approximations in Macromolecular Reactions - Reversible Initiation, Chain Scission, and Hydrogen Abstraction	[286]

* stands for theoretical work, not comparing the modeling results with experimental data; ** stands for a review article.

In the early 2000s, Linda J. Broadbelt began publishing extensively on polymer degradation, focusing on complex mechanistic chemistry. Her work stands out as some of the most comprehensive in the field. Beyond studying pure plastics, she developed one of the few mechanistic models addressing the synergy between polystyrene and polypropylene degradation [156, 287]. However, these studies used data from closed-vial experiments to validate the model, which is an environment prone to secondary reactions and not representative of common pyrolysis reactors. Consequently, parameter estimation and model simplifications were necessary, limiting its direct applicability to other reactor configurations. Additionally, the kinetic model was simplified, not considering different reactivities in reactants/products.

Parallel to Broadbelt's contributions, Poutsma published highly detailed models, raising critical hypotheses about various chemical reactions and kinetic constants

proposed in earlier studies. Parameter estimation was rarely used and the different reactant/product reactivities were properly considered so that it could be possible to better define routes to pyrolysis products mechanistically. Despite not always drawing definitive conclusions, Poutsma's work remains foundational for understanding polymer degradation mechanisms. Tables 2.7 and 2.8 list key publications from both researchers.

Table 2.7: Poutsma's main works on plastic degradation.

Year	Authors	Title	Reference
2000	Poutsma, M. L.	Fundamental reactions of free radicals relevant to pyrolysis reactions*	[288]
2003	Poutsma, M. L.	Reexamination of the Pyrolysis of Polyethylene	[263]
2005	Poutsma, M. L.	Comparison of literature models for volatile product formation from the pyrolysis of polyisobutylene at mild conditions	[289]
2006	Poutsma, M. L.	Mechanistic analysis and thermochemical kinetic simulation of the pathways for volatile product formation from pyrolysis of PS, especially for the dimer	[290]
2007	Poutsma, M. L.	Mechanistic analysis and thermochemical kinetic simulation of the products from pyrolysis of poly(alpha-methylstyrene)	[291]
2009	Poutsma, M. L.	Further considerations of the sources of the volatiles from pyrolysis of polystyrene	[292]

* stands for theoretical work, not comparing the modeling results with experimental data.

Table 2.8: Broadbelt's main works on plastic degradation.

Year	Authors	Title	Reference
2001	Kruse, T. M., Woo, O. S., Broadbelt, L. J.	Detailed mechanistic modeling of polymer degradation - application to polystyrene	[293]

Table 2.8 – Broadbelt's main works on plastic degradation (continued).

Year	Authors	Title	Reference
2002	Kruse, T. M., Woo, O. S., Wong, H.-W., Khan, S. S., Broadbelt, L. J.	Mechanistic Modeling of Polymer Degradation - A Comprehensive Study of Polystyrene	[294]
2003	Kruse, T. M., Wong, H.-W., Broadbelt, L. J.	Modeling the Evolution of the Full Polystyrene Molecular Weight Distribution during Polystyrene Pyrolysis	[295]
2005	Kruse, T. M., Levine, S. E., Wong, H. W., Duoss, E., Lebovitz, A. H., Torkelson, J. M., Broadbelt, L. J.	Binary mixture pyrolysis of polypropylene and polystyrene - a modeling and experimental study	[287]
2008	Levine, S. E., Broadbelt, L. J.	Reaction pathways to dimer in polystyrene pyrolysis - A mechanistic modeling study	[296]
2009	Levine, S. E., Broadbelt, L. J.	Detailed mechanistic modeling of high-density polyethylene pyrolysis - Low molecular weight product evolution	[297]
2012	Vinu, R., Levine, S. E., Wang, L., Broadbelt, L. J.	Detailed mechanistic modeling of poly(styrene peroxide) pyrolysis using kinetic Monte Carlo simulation	[298]
2012	R. Vinu, Linda J. Broadbelt	Unraveling Reaction Pathways and Specifying Reaction Kinetics for Complex Systems**	[20]

** stands for a review article.

During the same period, Politecnico di Milano also contributed to the study of plastic degradation. Their models were less complex than those of Broadbelt and Poutsma as they focused on a new lump methodology for modeling degradation, which is further "delumped" to present specific yields. However, most of their validation relied on TGA experiments rather than comprehensive product yield analysis. Additionally, the simplifications in their approach limit the model's applicability to

a wider range of pyrolysis processes.

Table 2.9: Politecnico di Milano's main works on plastic degradation.

Year	Authors	Title	Reference
1997	Ranzi, E., Dente, M., Faravelli, T., Bozzano, G., Fabini, S., Nava, R., Cozzani, V., Tognotti, L.	Kinetic modeling of polyethylene and polypropylene thermal degradation	[299]
1999	Faravelli, T., Bozzano, G., Scassa, C., Perego, M., Fabini, S., Ranzi, E., Dente, M.	Gas product distribution from polyethylene pyrolysis	[300]
2001	Faravelli, T., Pinciroli, M., Pisano, F., Bozzano, G., Dente, M., Ranzi, E.	Thermal degradation of polystyrene	[23]
2001	Ranzi, E ; Dente, M ; Goldaniga, A ; Bozzano, G ; Faravelli, T	Lumping procedures in detailed kinetic modeling of gasification, pyrolysis, partial oxidation and combustion of hydrocarbon mixtures**	[301]
2003	Faravelli, T., Bozzano, G., Colombo, M., Ranzi, E., Dente, M.	Kinetic modeling of the thermal degradation of polyethylene and polystyrene mixtures	[302]
2003	Marongiu, A., Faravelli, T., Bozzano, G., Dente, M., Ranzi, R.	Thermal degradation of poly(vinyl chloride)	[303]
2004	Dente, M., Bozzano, G., Faravelli, T., Marongiu, A., Pierucci, S., Ranzi, E.	Kinetic Modelling of Pyrolysis Processes in Gas and Condensed Phase***	[304]
2007	Marongiu, A., Faravelli, T., Ranzi, E.	Detailed kinetic modeling of the thermal degradation of vinyl polymers	[262]

Table 2.9 – Politecnico di Milano's main works on plastic degradation (continued).

Year	Authors	Title	Reference
2007	Mehl, M., Marongiu, A., Faravelli, T., Bozzano, G., Dente, M., Ranzi, E.	A kinetic modeling study of the thermal degradation of halogenated polymers	[305]

** stand for a review article; *** stands for a book section in 'Chemical Engineering Kinetics', Advances in Chemical Engineering, 2007.

Several other research groups have also contributed to understanding the kinetic mechanism behind polymer degradation:

- José Francisco Mastral, César Berrueco, and Jesús Ceamanos (Universidad de Zaragoza, Spain) developed a model for high-density polyethylene (HDPE) pyrolysis in fluidized bed and free-fall reactors [306, 307]. Their approach, a sophisticated lumped model, categorized products into alkanes, olefins, diolefins, aromatic compounds, and radicals. While their model performed well in predicting HDPE pyrolysis product distributions, it could have been improved by incorporating additional kinetic steps, such as intra- and intermolecular hydrogen transfer.

- Ioana Pantano, Claudia Sarmoria, and Adriana Brandolin (Planta Piloto de Ingeniería Química, Argentina) studied polystyrene degradation in the presence of aluminum chloride ($AlCl_3$). Their mathematical model focused on the effect of Friedel-Crafts catalysts and cocatalysts on the molecular weight distribution of polystyrene [308–310].

More recently, new research efforts have revived interest in mechanistic modeling. As discussed in Section 2.3, in the last few years (2019–2020), two notable groups have integrated experimental data with mechanistic models:

- Professor Enrique Saldivar-Guerra (Centro de Investigación en Química Aplicada, Mexico) has long been involved in polymer research and recently expanded into plastic pyrolysis (thermal and catalytic). His recent modeling efforts include the degradation of polystyrene and HDPE in a plug-flow tubular reactor, both solved using the method of moments [311, 312].

- Professor Kevin Van Geem (Ghent University, Belgium) has extensive experience modeling cracking systems, including plastic pyrolysis. His recent work on PMMA, PS, and polystyrene peroxide degradation employs Monte Carlo techniques to predict specific product yields [313, 314].

Despite the progress made, the number of research groups dedicated to the mechanistic modeling of plastic pyrolysis remains low. This underscores the necessity of continued research and development in this area, including:

- Validation of kinetic models with experimental data in a wide range of conditions.
- A more detailed discussion of liquid-vapor equilibrium.
- Development of mechanistic models for complex plastic mixtures.
- Consideration of secondary reactions, especially in gas-phase.
- Consideration of heat and mass transfer effects, particularly in scale-up scenarios.

By addressing these challenges, future research can build upon previous efforts and contribute to a more comprehensive understanding of polymer degradation.

2.4 Life-cycle assessment

Life cycle assessment (LCA) is "*a systematic methodology to quantify the environmental burdens associated with a given product or service over its entire life cycle in terms of environmental effects on areas such as climate change, human health, biodiversity, and natural resources, among others*" [315]. It relies on mass and energy balances, applying data to specific technologies, locations, and timeframes. This process quantifies feedstock inputs, emissions, and waste streams (i.e., inventory flows) before converting them into environmental impact indicators.

Mechanical recycling is widely considered the most sustainable recycling option when plastics can be adequately separated [316–322]. However, as previously discussed, contamination and mixed plastic waste limit its feasibility [67, 69, 83], necessitating alternative end-of-life (EoL) treatments.

In contrast, incineration is the least favorable option due to its significant greenhouse gas (GHG) emissions [317, 323]. While it prevents plastic from entering landfills, its contribution to climate change outweighs this benefit [93, 318, 324]. Figure 2.15 illustrates the relative and absolute CO_2-equivalent emissions of different EoL treatment technologies for plastic waste [22].

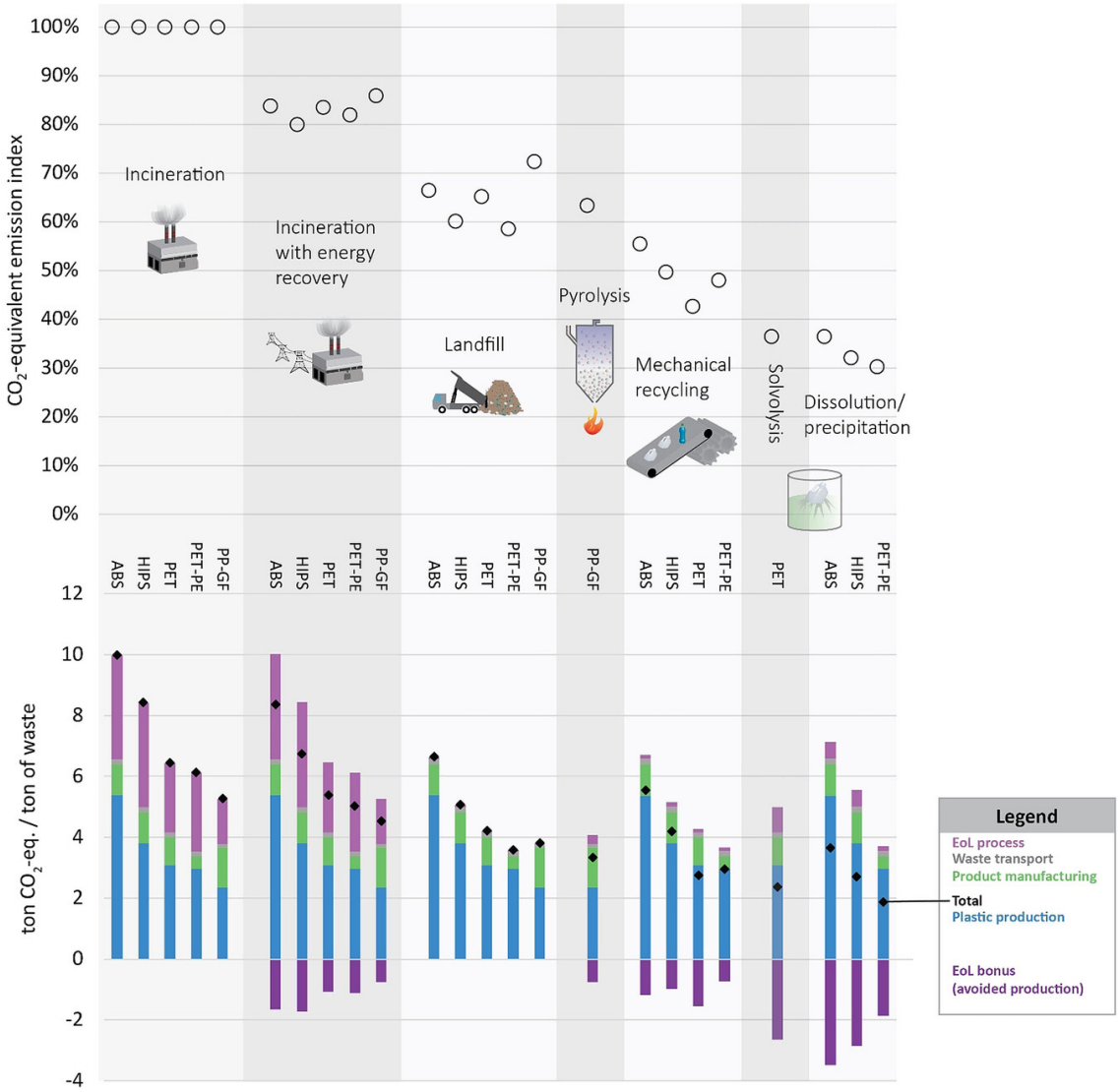

Figure 2.15: CO_{2e} emissions of various end-of-life treatment technologies for different plastic waste streams. Top: expressed as relative values indexed to incineration (set at 100%); Bottom: CO2*e* emissions broken down by life cycle stage (in tons CO_{2e}/ton of plastic waste). Source: VOLLMER *et al.* [22].

Compared to virgin plastic production, the key argument for pyrolysis having lower environmental impacts is the avoided production of virgin petrochemicals [317, 318, 321, 322, 325]. However, LCA studies on pyrolysis are often case-specific and lack adaptation to different plant configurations, feedstocks, and operational parameters (e.g., temperature, pressure, catalyst type, gas flow) [326]. ANTELAVA *et al.* highlighted these gaps, emphasizing the need for more comprehensive assessments.

Because plastic pyrolysis is an emerging technology, reported LCA results vary significantly due to the dependence on experimental setups and the scarcity of well-documented industrial data [327]. This variability can lead to inconsistencies and confusion, particularly for LCA practitioners unfamiliar with pyrolysis. Sensitivity

and uncertainty analyses should be incorporated to enhance study robustness, yet such assessments remain limited. Additionally, LCAs based on commercial data may suffer from conflicts of interest, potentially leading to biased conclusions and incomplete disclosure of process details [322, 323, 328]. Future LCAs should prioritize transparency and methodological rigor as more data becomes available.

Moreover, as MERY *et al.* suggests, "the use of LCA as a tool for eco-design requires a predictive and prospective LCI". However, currently, no LCA in chemical recycling benefits from detailed process modeling. Therefore, the Life Cycle Inventory (LCI), which compiles the data collected for all inputs and outputs related to the process's life cycle, often exhibits high variability, frequently overlooks optimal operating conditions, and, in some cases, relies on extrapolated lab-scale data. Therefore, integrating validated mathematical models of plastic degradation into LCA could improve the process analysis. For example, integrating LCA with life cycle optimization (LCO) frameworks, such as multi-objective optimization (MOO) and multi-criteria decision-making (MCDM), would enable a more holistic approach to the design of sustainable pyrolysis systems [315, 330].

Therefore, in general, to improve the reliability of pyrolysis LCAs, studies should enhance consistency and representativeness across temporal, geographical, and technological dimensions; and follow ISO 14040 standards to communicate assumptions and hypotheses effectively.

Nevertheless, these challenges are not unique to pyrolysis. Similar issues exist in other fields, such as water treatment, where traditional LCAs relies on averaged input-output data that may not capture real-world variability. The discussion on LCAs for plastic pyrolysis is expanded in Chapter 6.

2.5 State-of-the-art summary and research gaps

The literature reviewed in this chapter reveals the increasing interest in chemical recycling technologies, particularly pyrolysis, as a promising solution for processing plastic waste that is unsuitable for mechanical recycling. Among thermochemical routes, pyrolysis stands out for its ability to convert plastics into valuable chemical feedstocks. However, despite ongoing industrial and academic efforts, several technological and scientific challenges remain unsolved.

First, a significant gap persists in the mechanistic understanding of polymer degradation pathways, especially under diverse operating conditions. Experimental data in the literature are often limited or inconsistent, hindering the development of reliable models for process optimization and reactor design. Additionally, although various lumped kinetic models have been proposed, they typically rely on parameter fitting from specific datasets and lack generalizability across different systems and

feedstocks.

Mechanistic models, which provide first-principles insights into the degradation process, are still under development for most polymer types. Moreover, the integration of kinetic models with volatilization remains scarce, even though this coupling is essential for accurate prediction of product distributions in liquid-phase pyrolysis.

Another critical challenge is the incorporation of validated kinetic models into environmental assessments, such as life cycle analysis (LCA). The reviewed studies indicate that LCA models frequently rely on simplified process assumptions and generic databases, leading to inconsistent conclusions. There is a clear need for process-informed LCA frameworks that better reflect the actual behavior of pyrolysis systems.

This thesis addresses these challenges through a dual modeling strategy: the development of both lumped and mechanistic models for plastic pyrolysis. Using kinetic Monte Carlo simulations, the work provides detailed insights into the degradation mechanisms of polystyrene and polyethylene. Furthermore, it couples kinetic and thermodynamic models to account for volatilization phenomena, thereby enhancing predictive accuracy. Finally, it suggests that integrating mechanistic models into life cycle assessment frameworks could significantly improve the quality and relevance of future environmental analyses.

By bridging the gap between fundamental reaction mechanisms and practical process modeling, this research contributes to the advancement of more efficient, accurate, and environmentally relevant models for the chemical recycling of plastics.

Chapter 3

Modeling plastic pyrolysis using lumped models: non-catalytic and catalytic pyrolysis

This chapter is based on the article "A short-cut method for analysis of catalyst performances in pyrolytic reactor" published in the Journal of Analytical and Applied Pyrolysis in 2023 [331].

3.1 Introduction

Plastic pyrolysis can be modeled using different approaches, with mechanistic models being the most detailed and comprehensive. These models attempt to describe the complex chemical kinetics of pyrolysis by thoroughly accounting for each reaction step. However, developing mechanistic models for plastic pyrolysis is particularly challenging due to the heterogeneous nature of feedstocks and intricate reaction networks. Additionally, obtaining kinetically-controlled experimental data is only possible in micro-scale equipment due to complex effects such as mass and heat transfer limitations. These difficulties are even more pronounced when catalytic processes are involved, as the catalyst characteristics influence the reaction pathways, and the physical contact with the catalyst must be modeled. Moreover, the computational effort required for mechanistic modeling is substantial, making it time-consuming to develop and simulate.

Due to these challenges, lumped kinetic models offer a practical alternative when the primary objective is catalyst screening or optimizing macro-level aspects of the process, such as determining the optimal temperature, residence time, or catalyst-to-feedstock ratio. These models simplify the reaction network by grouping chemically similar species into "lumps" and modeling the reactions between these lumps rather

than tracking each individual species.

Lumped models have also been widely applied in the oil and gas industry, where, similar to plastic pyrolysis, feedstock composition variability, and fluctuating product demands necessitate fast process adjustments [301, 332–334]. The variability can represent a substantial cost burden for a refinery, and fast process modifications are required [332, 333].

To illustrate the application of a lumped kinetic model, this chapter uses as a case study the pyrolysis of high-density polyethylene (HDPE) as the feedstock and two different catalysts. The model aims to compare the catalysts performances and determine appropriate operational conditions to maximize desired product fractions. The specific process considered is an ex-situ catalytic process: thermal cracking of the plastic feedstock, followed by catalytic cracking of the resulting gaseous stream. This was chosen because two-stage processes are often employed due to reduced catalyst deactivation [137, 335, 336].

Using catalysts can enhance the reaction selectivity of plastic pyrolysis toward desired products, such as lighter hydrocarbons. The performance of a catalyst depends heavily on factors such as its pore size distribution, acidity, and surface area [21, 130]. Commonly used heterogeneous catalysts for plastic pyrolysis include zeolites (Y, USY, HZSM-5, Hβ), silica-alumina, alumina, FCC (Fluid Catalytic Cracking) catalysts, MCM-41, metal oxides, and molecular sieves [128, 130, 131, 137, 337].

Several lumped reaction networks have already been proposed to describe the process behavior and understand modifications of the activation energy when different catalysts are mixed with the feedstock. The studies were performed in a TGA [254–258, 338], fixed bed [11], fluidized bed reactor [175, 176, 339–342] or a semi-batch stirred reactor [343]. Others have studied two-stage pyrolysis in a fluidized reactor followed by an in-line fixed bed [16], and two-stage semi-batch reactor [17, 344]. These studies are summarized in Table 3.1.

However, previous lump models proposed for catalytic pyrolysis have primarily focused on understanding global kinetic models for pyrolysis, and there is a lack of efforts to develop and implement suitable procedures for designing reactors (thermal and/or catalytic), adapting actual operation procedures, and optimizing plastic pyrolytic reaction systems.

Thus, the focus of this study is the optimization of a two-stage pyrolysis process, considering both stages individually as well as the complete system. The two catalysts used for the experiments and model are a Zeolite Y (Cat_1) and another conventional petrochemical catalyst (Cat_2). The details of these catalysts are confidential. Nevertheless, even with simplified catalyst representations, the model provides a valuable tool for rapid catalyst screening and process optimization, enabling the identification of the optimal setup, including the ideal temperature, catalyst

mass, and residence time, resulting in the maximization of desired product yields. Moreover, the proposed approach is especially relevant for laboratory and industrial environments where complex models are impractical due to time constraints.

3.2 Theoretical Framework

The analyzed pyrolysis system has two steps, as shown in Figure 3.1. Plastic thermal pyrolysis occurs in the first reactor in the presence of a gas carrier (nitrogen), and the effluent gas is cracked further in the second catalytic fixed-bed reactor. The first reactor can be of any type, such as a drop tube reactor, as shown in the illustration, or a stirred reactor. As for the second reactor, including the heterogeneous step is optional, but it is utilized to achieve a product with a lower molar mass (such as reduced wax) or a modified composition (for example, increased aromatic content). Therefore, two-step configurations are commonly used in industrial plastic chemical recycling facilities. Details about each stage are given below, including the hypotheses and modeling equations employed for each step.

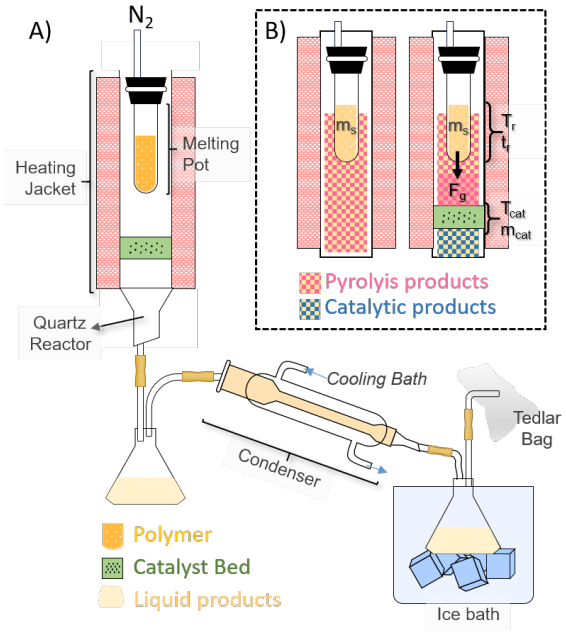

Figure 3.1: Two-stage pyrolysis unit: a) Schematic representation of the pyrolysis unit used for model validation; b) Pyrolysis and catalytic products (m_s: plastic mass; F_g: pyrolysis products flow rate; T_r: temperature of the first reactor; t_r: residence time of the first reactor; T_{cat}: temperature of the second, catalytic, reactor; m_{cat}: catalyst mass.

Table 3.1: Papers that applied lumping procedures to build kinetic models for plastics pyrolysis

Year	Authors	Article	Polymer	Catalyst	Reactor	
1994	Songip, A. R., Masuda, T., Kuwahara, H., Hashimoto, K.	Kinetic studies for catalytic cracking of heavy oil from waste plastics over REY zeolite	PE	REY	Fixed bed	[11]
1998	Lin, Y. H., Sharratt, P. N., Garforth, A. A., Dwyer, J.	Catalytic conversion of polyolefins to chemicals and fuels over various cracking catalysts	PE, PP	HZSM-5, HUSY, HMOR, SAHA, MCM-41	Fluidized bed	[339]
2001	Lin, Y.-H., Hwu, W.-H., Ger, M.-D., Yeh, T.-F., Dwyer, J.	A combined kinetic and mechanistic modelling of the catalytic degradation of polymers	PE, PP	HZSM-5, HUSY, Silica-alumina (SAHA)	Fluidized bed	[340]
2001	Marcilla, A., Gómez, A., Reyes-Labarta, J. A.	MCM-41 catalytic pyrolysis of ethylene–vinyl acetate copolymers: kinetic model	EVA	MCM-41	TGA	[254]
2002	Marcilla, A., Gómez, A., García, Á. N., Mar Olaya, M.	Kinetic study of the catalytic decomposition of different commercial polyethylenes over an MCM-41 catalyst	PE	MCM-41	TGA	[255]
2002	Cardona, S. C., Corma, A.	Kinetic study of the catalytic cracking of polypropylene in a semibatch stirred reactor	PP	USY, FCC	Semibatch Stirred	[343]
2003	Marcilla, A., Gómez, A., Reyes-Labarta, J. A., Giner, A., Hernández, F.	Kinetic study of polypropylene pyrolysis using ZSM-5 and an equilibrium fluid catalytic cracking catalyst	PP	ZSM-5, E-cat	TGA	[338]
2003	Marcilla, A., Gómez, A., Reyes-Labarta, J. A., Giner, A.	Catalytic pyrolysis of polypropylene using MCM-41: kinetic model	PP	MCM-41	TGA	[256]
2007	Marcilla, A., Gómez-Siurana, A., Valdés, F.	Catalytic cracking of low-density polyethylene over H-Beta and HZSM-5 zeolites: Influence of the external surface. Kinetic model	PE	H-Beta, HZSM-5	TGA	[257]

Table 3.1: Papers that applied lumping procedures to build kinetic models for plastics pyrolysis (continued)

Year	Authors	Article	Polymer	Catalyst	Reactor	
2008	Lin, Y. H., Yang, M. H.	Tertiary recycling of polyethylene waste by fluidised-bed reactions in the presence of various cracking catalysts	PE	HUSY, HZSM-5, HMOR, SAHA, MCM-41	Fluidized bed	[176]
2009	Lin, Y. H., Yang, M. H.	Kinetic and Mechanistic Modeling of Acid-Catalyzed Degradation of Polymers with Various Cracking Catalysts	PE, PP	HZSM-5, ECat-1, SAHA	TGA	[258]
2010	Wei, T.-T., Wu, K.-J., Lee, S.-L., Lin, Y.-H.	Chemical recycling of post-consumer polymer waste over fluidizing cracking catalysts for producing chemicals and hydrocarbon fuels	PE, PP	USY, ZSM-5, MOR, ASA, MCM-41	Fluidized bed	[175]
2010	Huang, W. C., Huang, M. S., Huang, C. F., Chen, C. C., Ou, K. L.	Thermochemical conversion of polymer wastes into hydrocarbon fuels over various fluidizing cracking catalysts	PE, PP, PS (mixture)	ZSM-5, MOR, USY, MCM-41, ASA	Fluidized bed	[342]
2010	Lin, Y. H., Yang, M. H., Wei, T. T., Hsu, C. T., Wu, K. J., Lee, S. L.	Acid-catalyzed conversion of chlorinated plastic waste into valuable hydrocarbons over post-use commercial FCC catalysts	PE, PP, PVC	FCC-R1, FCC-S1, HUSY, ZSM-5, SAHA	Fluidized bed	[341]
2014	Artetxe, M., Lopez, G., Amutio, M., Bilbao, J., Olazar, M.	Kinetic modelling of the cracking of HDPE pyrolysis volatiles on a HZSM-5 zeolite based catalyst	PE	HZSM-5	Two-stage: CSBR and in-line fixed bed	[16]
2018	Till, Z., Varga, T., Sója, J., Miskolczi, N., Chován, T.	Kinetic identification of plastic waste pyrolysis on zeolite-based catalysts	PE, PP, PVC, PET	HZSM-5, NiZSM-5, CuZSM-5, FeZSM-5, Ni/Mo-Al2O3	Two-step batch	[17]
2020	Till, Z., Varga, T., Sója, J., Miskolczi, N., Chován, T.	Structural assessment of lumped reaction networks with correlating parameters	PE, PP	ZSM-5	Two-step batch	[344]

In the first reactor, plastic (m_s) is fed and heated to the desired reaction temperature (T_R). In the case of polyolefins (polyethylene and polypropylene), due to the predominance of random chain scission reactions, chains with different carbon lengths are formed and start to volatilize. Although chains of different chemical natures can be produced (paraffin, isoparaffin, olefin, naphthenes, and aromatics), the chemical compounds in the liquid phase of the final product can be lumped into two different groups based on the boiling points: i) an oil phase that contains compounds with molecular sizes ranging from 5 up to 12 carbons (C5 - C12), and ii) a solid wax phase that contains compounds with molecular sizes with 13 carbons or more (C13+). Nonetheless, due to unzipping and hydrogen transfer [297], molecular species containing less than five carbons are also found in the pyrolysis products, such as ethane, ethene, propane, propene, butene, butadiene, among other less frequent chemical compounds. These transformations are illustrated in Scheme 3.1, which considers 3 phases: plastic, liquid, and gas. The liquid phase, however, can contain two distinct components: oil and wax. For this project, these lumps were considered with the aim of minimizing plastic consumption and reducing wax production, as discussed later. However, alternative lumps and compositions may be suggested based on specific research interests and available data.

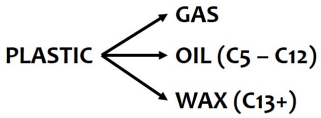

Scheme 3.1: Lumped-species considered in the first reactor.

Four mass balances for plastic, gas, oil, and wax can be considered as:

$$R_i = r_i * \Delta V = F_{i,out} - F_{i,in} \tag{3.1}$$

where R_i is the rate of mass generation of the lumped species inside the volume ΔV ($g \cdot s^{-1}$); r_i is the specific reaction rate ($g \cdot s^{-1} \cdot L^{-1}$); ΔV is the volume of the reactor (L); F_{in} and F_{out} are the mass flow rates at the inlet and outlet streams of the reactor ($g \cdot s^{-1}$). However, assuming that there are no recycling streams of the pyrolysis products, $F_{gas,in}$, $F_{oil,in}$, and $F_{wax,in}$ are all null. Besides, if the operation is performed in batch or semi-batch modes, it can be assumed that the flow rate of the outlet plastic stream is equal to $F_{s,out} = 0$. After taking these assumptions into account, the following approximations can be made:

$$R_s \simeq \frac{dM_s}{dt} \simeq \frac{M_s \cdot \varphi_s - M_a}{\Delta t} \tag{3.2}$$

$$R_l \simeq \frac{dM_l}{dt} \simeq \frac{M_a \cdot \varphi_o x_{o,l}}{\Delta t} \tag{3.3}$$

$$R_{l+} \simeq \frac{dM_{l+}}{dt} \simeq \frac{M_a \cdot \varphi_o x_{o,l+}}{\Delta t} \tag{3.4}$$

$$R_g \simeq \frac{dM_g}{dt} \simeq \frac{M_l \cdot \varphi_g \cdot 1}{\Delta t} \tag{3.5}$$

where M_a and M_s are respectively the initial and current mass of plastic sample (g); φ_i is the mass fraction of the ith phase produced by the plastic degradation; $x_{i,j}$ is the fraction of the component j in the analyzed phase i; and Δt is the reaction time (min).

As the main objective of plastic pyrolysis is the total degradation of plastic waste and the maximization of the obtained products, it is assumed that all plastic is degraded. Thus, to maximize the product yields, it is considered that the total plastic mass can be converted into products, and the ash (solid residue) content of the sample (due to the presence of contaminants and additives) is subtracted from the initial mass of plastics fed into the reactor. Therefore, the overall mass balance equation in the first reactor is considered as:

$$\begin{aligned} M_a - M_s &= M_g + M_l + M_{l+} \\ -R_s \Delta t &= R_g \Delta t + R_l \Delta t + R_{l+} \Delta t \\ -R_s &= R_g + R_l + R_{l+} \end{aligned}$$

As the mass rates of generation for the products are obtained experimentally, R_s can be easily obtained, and the reaction time required to convert all the plastic samples into the main products can be found. And, as R_i is affected by the reactor temperature, proper characterization of activation energies must be performed utilizing data obtained at different temperatures. Experimentally, it can be rather complicated to sample the effluent of the first reactor and determine the product composition between the two stages. For this reason, the reaction rates for the first stage should be obtained without adding a catalyst to the second stage.

It must be noted that the proposed model comprises very simple algebraic equations that can be applied to any pyrolysis system without product recycling and is independent of the reactor geometry, diffusion effects, or small fluctuations in feedstock composition. If experiments are performed to characterize the reaction rates, all these factors are somehow inserted into the effective reaction rates and apparent reaction rate constants, and activation energies. Despite that, and understanding

that these factors can prevent the fundamental interpretation of the obtained reaction rate constants, as shown below, the proposed model can help the preliminary design of operation conditions and comparison of catalyst performances based on a few experiments. Moreover, the proposed shortcut procedure can be easily adapted to represent different reaction systems and products due to the model's simplicity.

When a certain amount of catalyst mass (ΔW; g_{cat}) is added to the packed bed reactor, the products formed in the first reaction stage enter contact with the catalyst. If the catalyst is intended to reduce the average molar mass of the output stream, then it can be assumed that the wax is the main reactant at the surface of the catalyst particles, forming more gas, oil, and coke on the catalyst, as described in Scheme 3.2. Once again, the pathways may be adjusted to illustrate the preferred reaction system and end products, according to the needs of the analyst.

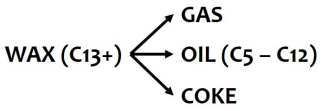

Scheme 3.2: Lumped-species considered in the second reactor.

The mass balance equations for each lumped species in the second stage can be proposed as performed previously:

$$R_i^{cat} = r_i^{cat} \Delta W = F_{i,out}^{cat} - F_{i,in}^{cat} \tag{3.6}$$

where R_i^{cat} is the rate of mass generation of the lumped species i by the total mass of catalyst ΔW ($g \cdot s^{-1}$); r_i^{cat} is the specific reaction rate ($g \cdot s^{-1} \cdot g_{cat}^{-1}$); F_{in}^{cat} and F_{out}^{cat} are the mass flow rates at the inlet and outlet streams of the second reactor ($g \cdot s^{-1}$).

It can be considered that the ideal scenario is when the wax is completely consumed, $F_{wax,out}^{cat} = 0$, by a certain amount of catalyst, $\Delta W = M_{cat}$. Thus, in the second reactor, the mass balance equation can be formulated as follows:

$$M_{l+} = M_g^{cat} + M_l^{cat} + M_{coke} \tag{3.7}$$

where M_i^{cat} is the produced mass of the lumped species i:

$$M_i^{cat} = M_s \cdot \varphi_i^{cat} x_{j,i}^{cat} \tag{3.8}$$

φ_i^{cat} is the mass fraction of the ith phase produced by the catalytic cracking of the gas stream produced in the first reactor; $x_{i,j}^{cat}$ is the fraction of the component j in the analyzed ith phase. According to Scheme 2, the present model considers 3 phases: coke, oil, and gas. According to the proposed model, the global mass balance of the

system is:

$$M_s = M_g + M_l + M_g^{cat} + M_l^{cat} + M_{coke} \tag{3.9}$$

So, if one determines the mass yields for pyrolysis experiments performed with the catalyst (M_g^{cat}, M_l^{cat}, M_{coke}); the rates of catalytic generation of the lumped-species by the mass of catalyst M_{cat} can be obtained with the help of the following approximation:

$$R_i^{int} \simeq \frac{d(M_i^{cat} - M_i)}{dt} \simeq \frac{M_i^{cat} - M_i}{\Delta t^{cat}} \tag{3.10}$$

where Δt^{cat} is the contact time of the wax with the catalyst:

$$\Delta t^{cat} \simeq t^{cat} \simeq \cdot \left(\frac{\phi \cdot M_{cat}}{(1-\phi)\rho_{cat}}\right) F_g^{-1} \tag{3.11}$$

ϕ corresponds to the porosity of the catalytic bed; ρ_{cat} is the catalyst density (g/cm^3); and F_g is the gas flowrate (cm^3/min) entering the catalytic bed, which is dependent on temperature T_{cat} (K), pressure P (atm), use of carrier gas, and the average molecular weights MW (g/mol) of the components that constitute gas, oil and wax fractions produced in the first stage. If the ideal gas behavior is assumed, given the high temperatures and low pressures (P = 1 atm):

$$F_G = \sum_{i=1}^{N} \frac{R_i}{MW_i} \frac{RT_{cat}}{P} \tag{3.12}$$

When the wax is completely converted into gas, oil, or coke, as described by Eq. 3.10, the following equation can be written:

$$R_{l+}^{int} \simeq \frac{M_{l+}^{cat} - M_{l+}}{t^{cat}} \simeq -\frac{M_{l+}}{t^{cat}} \tag{3.13}$$

And, thus, the catalyst mass needed to perform this job can be easily obtained.

$$M_{cat} = \frac{F_g(1-\phi)\rho_{cat} M_{l+}}{\phi R_{l+}^{int}} \tag{3.14}$$

As previously mentioned, depending on the available data and specific objectives of the investigation, other lumped species may be suggested. The current model does not take into account the impact of temperature changes or reduced catalytic activity resulting from the formation of coke. Nonetheless, given that the coke production is minimal, the model is still useful for determining how long it will take before a significant amount of coke builds up, and the need for catalytic material regeneration arises. Additionally, the model can also be adapted to consider a catalyst activity as a function of time [345].

3.3 Materials and Methods

For this study, high-density polyethylene (HDPE) was kindly donated by Braskem S.A. and was used as feedstock for illustrative purposes. A catalyst containing Zeolite Y (Cat_1) and another conventional catalyst (Cat_2) were used in the second stage for further cracking of pyrolysis products. The second catalyst is still in commercial development; therefore, details cannot be shared due to confidentiality. Moreover, this research paper aims not to suggest specific catalysts, but to validate an analysis tool to evaluate any catalytic performance.

The experiments were conducted in a lab-scale pyrolysis unit shown in Figure 3.1. The reaction system comprised a first drop tube quartz reactor (internal diameter of 3 cm and height of 23.5 cm) and a fixed bed reactor (internal diameter of 3 cm and height of 23.5 cm), which was aligned in series with the exhausting line of the first reactor and used to perform the catalytic treatment of the thermal pyrolysis product. When no catalyst is used, the total dimension of the reactor is 3 cm in internal diameter and 47 cm in height. The reactors were placed inside two independent cylindrical electrical furnaces, used to control the reaction temperature, and were isolated with glass wool. Two thermocouples ("A" and "B") were attached to the furnaces and used to provide temperature readings to the controller. A third thermocouple ("C") was connected to a datalogger (USB-501-TC-LCD Series, Measurement Computing Corporation) and placed inside the melting pot to record the heating profile with a sampling interval of 10 seconds. A heating coil surrounds the quartz reactor, preheating the nitrogen stream, which is used to maintain the reaction environment free of oxygen and drag the generated gases.

A cylindrical quartz melting pot (internal diameter of 2 cm and height of 12 cm) was used to place the polymer material inside the pyrolytic reactor. Before the start of the reaction, the melting pot was suspended by a wire above the furnace; after reaching the desired temperature, the melting pot was placed into the reactor to initiate the pyrolysis reaction. According to the third thermocouple inside the melting pot, the plastic average heating rate is 51 °C/min, as shown in Figure 3.2.

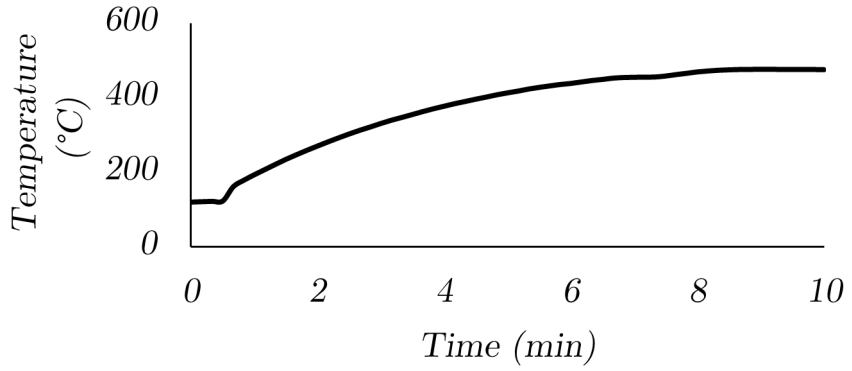

Figure 3.2: Plastic heating rate profile. Data were collected every 10 seconds.

In all cases, a fixed amount of 8 g of polymer was degraded at a pre-selected temperature (450, 500, or 550 °C) for 30 minutes. A fixed 1:1 catalyst/polymer mass ratio was employed when one of the catalysts was used. Three replicates were conducted at 500°C for both thermal pyrolysis and catalyst pyrolysis using Cat_1. The Cat_2 deviation was assumed to be equivalent to that of Cat_1. The nitrogen gas flow rate was kept constant in all analyzed trials (80 mL/min), although this operational variable can be easily manipulated to provide additional information about the effect of contact times on the product yields.

The selected conditions are commonly found in literature and commercial chemical plastic recycling facilities. Nevertheless, the analyst can adjust reaction temperatures, reaction times, and catalyst/polymer ratios to estimate the kinetic rate constants. This allows for greater flexibility and accuracy in the analysis. It must be emphasized that, according to the proposed short-cut analysis, only 6 reaction experiments (per combination of plastic with catalyst, and only other 3 if a new catalyst is used) are required to allow the preliminary estimation of reaction rate constants and activation energies and evaluate the effects of the operation conditions on the process responses, as described in Table 3.2.

The generated products were condensed with the help of an electrostatic precipitator after flowing through the catalyst bed, and the liquid fraction was stored in a glass flask. The liquid products were analyzed by GC–MS (GC Agilent G4513A; MS: Agilent 7890a/5975), using an HP5-MS column (19091S-433 model) with a split ratio of 1:10, under a continuous flow of He of 1 mL/min and the following temperature program: initial constant temperature of 40 °C for 5 min; heating rate of 5 °C/min until attainment of 270 °C; the final constant temperature of 270 °C for 1 min. The oil and wax amounts (M_l and M_{l+}) were calculated with the help of this GC-MS analysis. Noncondensable gases were collected with a homemade sampling Tedlar® bag and analyzed by gas chromatography. The final gas, liquid, and solid mass fractions were quantified by weighing and validated through mass

balance calculations.

Once catalytic reactions had ended, 1 g of the catalyst was weighed and burned in an oxidizing atmosphere to determine the amount of coke present. The calculation is based on Eq. 3.15, where m_{CatPy} is the catalyst mass after the two-stage pyrolysis reaction (darkened) and m_{CatReg} is the catalyst mass after regenerating the catalyst at 800 °C with quartz wool in a quartz reactor.

$$Coke(\%) = \frac{[m_{\text{CatPy}} - + m_{\text{CatReg}}]}{m_{\text{CatPy}}} \times 100\% \tag{3.15}$$

Table 3.2: Thermal and catalytic pyrolysis experiments considered for the short-cut analysis of the reaction performance. (Cat2 is a catalyst in commercial development, and its type cannot be shared due to confidentiality.)

Code	Polymer	Cat	Cat:P (wt %)	T (°C)	Time (min)
T_450°C	HDPE	-	-	450	30
T_500°C	HDPE	-	-	500	30
T_550°C	HDPE	-	-	550	30
C_1_450°C	HDPE	Y	1:1	450	30
C_1_500°C	HDPE	Y	1:1	500	30
C_1_550°C	HDPE	Y	1:1	550	30
C_2_450°C	HDPE	Cat2	1:1	450	30
C_2_500°C	HDPE	Cat2	1:1	500	30
C_2_550°C	HDPE	Cat2	1:1	550	30

3.4 Results

3.4.1 Experimental Results

In Tables 3.3 and 3.4 and Figures 3.3 and 3.4, comparative analyses between the performances of thermal pyrolysis and catalytic pyrolysis using a catalyst based on Zeolite-Y (Cat_1) and another conventional catalyst (Cat_2) are shown. The selected zeolite has been widely used for petrochemical processing, and Cat_2 is used to validate the methodology in Section 3.4.4. Experiments were performed at three different temperatures (450, 500, and 550 °C) for 30 min, using nitrogen as carrier gas at 80 cm^3/min. Thus, the thermal pyrolysis vapor residence time was between 1.5 and 1.7 min.

At 450 °C, the high amount of "solid" in both thermal and catalytic pyrolysis is explained by the low residence time (30 min) of the plastic inside the reaction

at the desired temperature. This information is important to calculate the reaction time needed to completely convert the plastic waste into products, as determined by Eq. 3.5 and shown in the following paragraphs. In addition, overall mass balance results were negligible between 500 and 550 °C and within the experimental error. Nonetheless, more olefins could be found at 550 °C as higher temperatures favor their formation. Higher temperatures also favor oil formation (< C13).

The catalytic results are consistent with other literature data: using the catalyst increases the fractions of light products in the output stream while simultaneously converting olefins mainly to aromatics [130, 334, 346, 347]. Additionally, based on the temperatures examined, it has been observed that the Y-zeolite catalyst produces more gas than Cat_2, while it simultaneously produces less oil. Although it may seem that Cat_2 is not as effective as Cat_1 due to its reduced cracking, for the goal of converting wax into lighter products, both catalysts have similar performance. This is further discussed in Section 3.4.4 as the proposed model eases the analysis of catalysis performances. Even so, higher temperatures favored coke formation, indicating more activity for both catalysts, and, although results for the PIONA fractions were highly similar for both temperatures (500 or 550 °C), more wax is obtained at 550 °C. This shows that the cracking ability decreases with coke evolution and promotes the formation of long carbon chain products as discussed by CHEN *et al.* [348] (2021).

3.4.2 Parameter Estimation

Based on the mass yields presented in Tables 3.3 and 3.4, the reaction rate parameters were estimated considering an "Arrhenius equation" (Eqs. 3.16 - 3.24). The estimation was done using the programming language Python 3.8, and the package Scipy [349], but any software that does regression could also be used.

$$R_g = 1.63\, exp(\frac{-3539.68}{T_R}) \tag{3.16}$$

$$R_l = 3.40\, exp(\frac{-4068.03}{T_R}) \tag{3.17}$$

$$R_{l+} = 267.94\, exp(\frac{-5889.43}{T_R}) \tag{3.18}$$

Table 3.3: Mass yields for thermal and catalytic pyrolyzes.

Code	Liquid (%)	Gas (%)	Solid (%)	Coke (%)
T_450°C	16.69 ± 1.74	3.23 ± 1.69	80.09 ± 0.22	-
T_500°C	89.30 ± 1.74	10.00 ± 1.69	0.7 ± 0.22	-
T_550°C	91.63 ± 1.74	8.37 ± 1.69	0.0 ± 0.22	-
C_1_450°C	12.74 ± 3.86	6.80 ± 3.73	78.01 ± 0.44	2.45 ± 1.17
C_1_500°C	41.45 ± 3.86	55.39 ± 3.73	0.43 ± 0.44	2.73 ± 1.17
C_1_550°C	31.62 ± 3.86	62.54 ± 3.73	0.0 ± 0.44	5.84 ± 1.17
C_2_450°C	16.50 ± 3.86	6.87 ± 3.73	74.32 ± 0.44	2.31 ± 1.17
C_2_500°C	53.19 ± 3.86	41.86 ± 3.73	0.14 ± 0.44	4.81 ± 1.17
C_2_550°C	62.94 ± 3.86	31.13 ± 3.73	0.0 ± 0.44	5.93 ± 1.17

Table 3.4: Products obtained in the liquid fraction by GC-MS (area %).

	T_-450°C	T_-500°C	T_-550°C	C_1_-500°C	C_1_-550°C	C_2_-500°C	C_2_-550°C
Paraffin	57.5	38.3	34.7	27.3	28.0	15.7	18.3
Isoparaffin	0.2	0.4	0.1	18.4	17.8	36.4	40.9
Olefin	36.1	54.5	61.7	1.0	2.0	1.5	2.3
Naphtene	2.4	5.7	2.4	4.2	3.2	3.7	3.5
Aromatic	0.3	0.1	0	48.0	47.7	42.6	34.8
Others	3.5	1.1	1.2	1.2	1.3	0.1	0.3
C1-C12	16.9	12.2	10.0	77.6	70.9	86.1	83.1
C13+	83.1	92.5	90.0	22.4	29.2	13.9	16.9

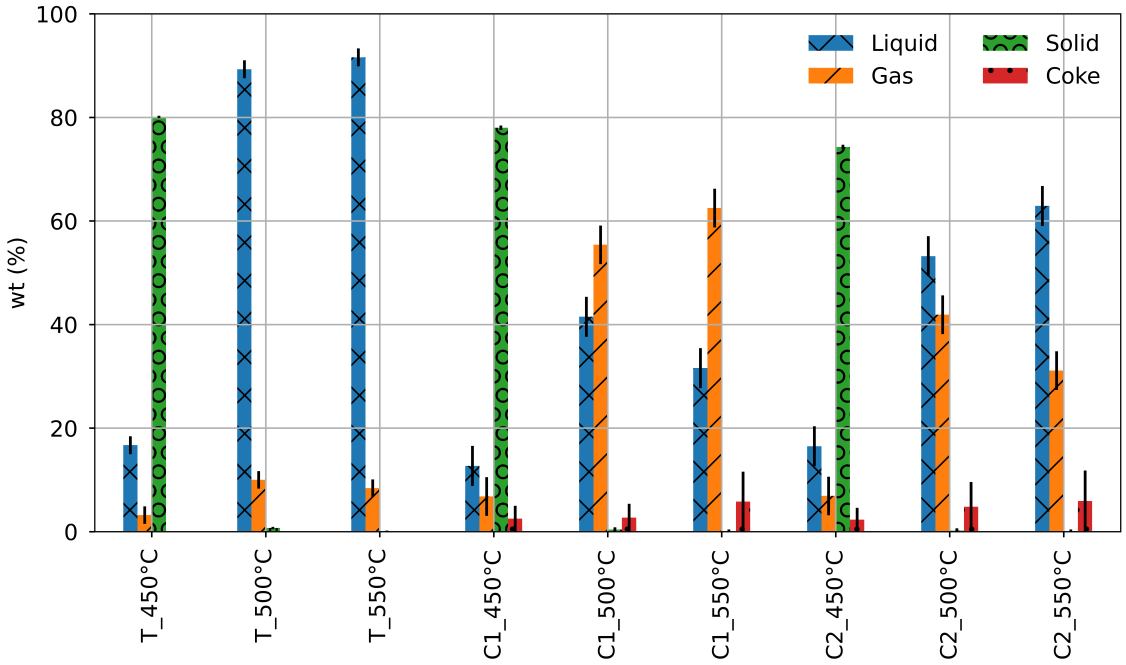

Figure 3.3: Mass yields for thermal and catalytic pyrolyzes.

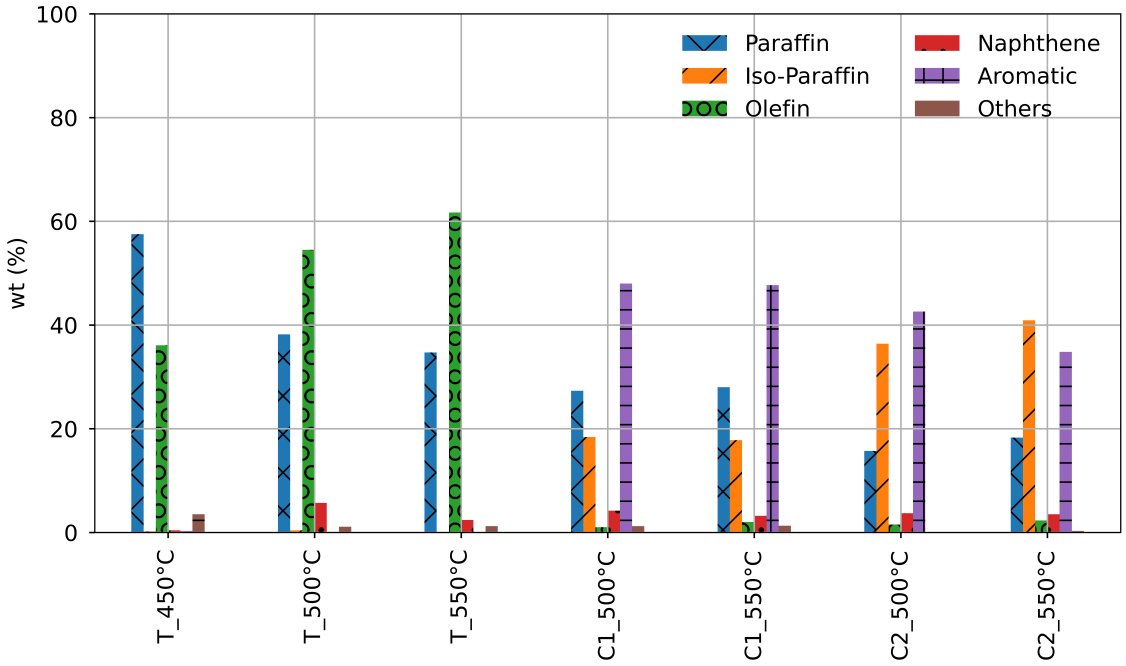

Figure 3.4: Products obtained in the liquid fraction by GC-MS (area %).

Similarly, the rate parameters can also be estimated for the catalytic reactions using the Zeolite Y in the form:

$$R_g^{cat} = 4.85\ 10^6\ exp(\frac{-7812.02}{T_{cat}}) \tag{3.19}$$

$$R_l^{cat} = 2.18\,10^3\,exp(\frac{-2514.08}{T_{cat}}) \tag{3.20}$$

$$R_{coke}^{cat} = 2.60\,10^5\,exp(\frac{-7303.64}{T_{cat}}) \tag{3.21}$$

One possible objective pursued by the analyst is to increase the light liquid (LIQ) fraction because this stream can be used as a steam cracker feed to manufacture monomers and new plastics (circular economy approach). However, the analysis can be adapted to consider the maximization of other product fractions. In addition, the zeolite selected here as an example, although the methodology is suitable for investigating any other catalyst, as shown in the next section.

In addition, the temperature employed (T_{cat}) in the second stage can be different from the one employed in the first stage (T_R). This is important as the catalytic activities are influenced by the catalyst bed temperatures [336].

3.4.3 Process Performance

Using the short-cut model and the set of estimated reaction rate expressions in the first pyrolysis stage, depending on T_R, different mass ratios of the gas, oil, or wax are obtained as shown in Figure 3.5. (Over 550 °C, the data is extrapolated. However, as higher temperatures are not used industrially, we only kept the data for illustrative purposes.) Although higher temperatures favor olefin formation, they also favor volatilization of higher molecular weight products, explaining the increase of waxes in the output stream. In addition, according to Eq. 3.5, different residence times are required to convert 100 % of the original plastic feed, as shown in Figure 3.5. For instance, at 450 °C, a temperature used industrially, a residence time of 73 minutes might be required to convert the plastic feed into products.

It must also be observed that depending on T_R, the flow rate and the composition of the products are changed, and, consequently, the flow rate of the feed stream of the catalyst bed is also changed (Eq. 3.12). So, as shown in Figure 3.6, lower temperatures will lead to the lowest flow rates, increasing the contact time of the products with the catalyst and lowering the mass of the catalyst needed to convert wax into lighter products. However, lower T_R values also produce more gas (Figure 3.5), which is less desirable.

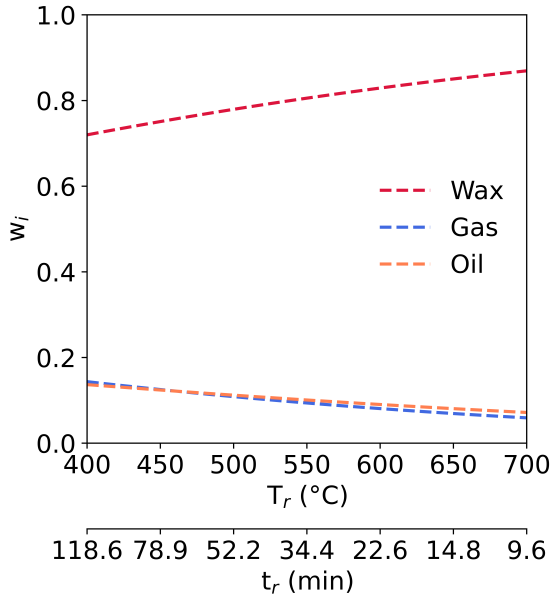

Figure 3.5: Product fractions (wt %) obtained in the pyrolysis reactor according to the temperature employed and the residence time required in the pyrolysis reactor to convert the plastic feed completely.

Additionally, for the catalyst bed, after calculation of rates of mass generation and feed flowrates for the desired values of T_R and T_{cat}, the mass of catalyst needed to crack all wax coming from the pyrolysis reactor can be determined with the help of Eq. 3.14. Figure 3.7 shows the catalyst-plastic ratio as a function of the selected temperatures. Due to high flow rates entering the catalyst bed at higher temperatures (Fig. 3.6), the catalyst/plastic ratio also becomes higher. In addition, once more, if less gas is also desired, lower temperatures will favour oil instead of gas formation. Figure 3.8 shows the mass ratios (overall mass balance) obtained after the catalyst bed with the catalyst/plastic ratio needed to convert the wax completely. Although the short-cut model does not account for the pressure drops through the catalyst bed and the catalyst decay, the catalyst efficiency can be monitored through the rate of coke formation. Pressure drop calculations can be easily added to the proposed short-cut procedure if the analyst desires.

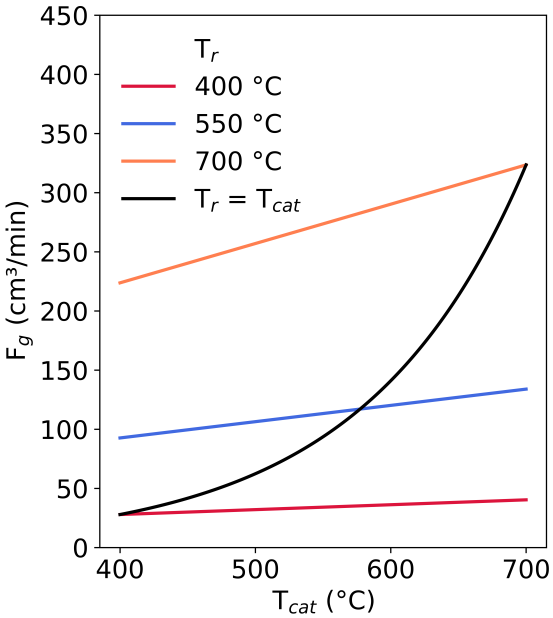

Figure 3.6: Flow rate of the products entering the catalytic reactor depending on the temperature employed.

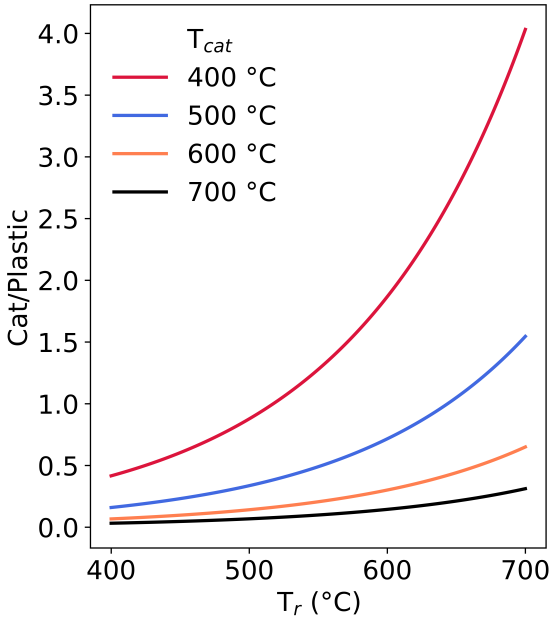

Figure 3.7: Catalyst-plastic ratio for complete wax conversion as function of the employed temperatures.

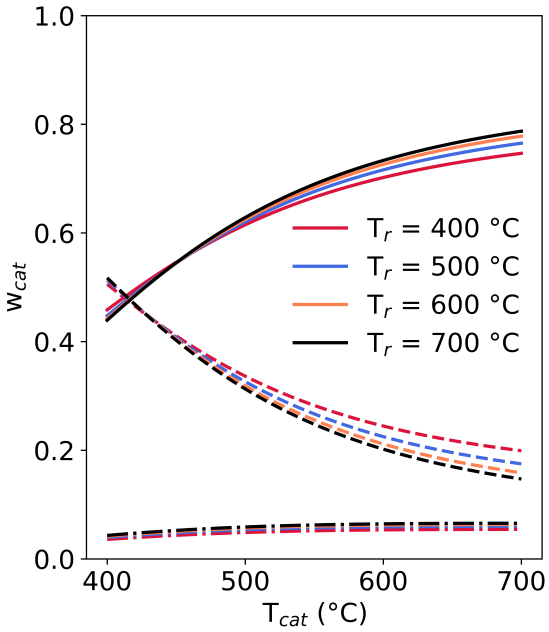

Figure 3.8: Mass ratios of the products in the output stream of the catalyst bed. −: Gas, −−: Oil, .−: Coke.

Finally, as a carrier gas may be used to assist the product removal from the pyrolysis reactor, further simulations were done considering using a carrier gas stream. For a nitrogen flow of 80 cm^3/s, Figures 3.9 and 3.10 show that the increase of the flowrate of carrier gas imposes the significant increase of the catalyst/plastic ratio for complete conversion of the wax fraction, given the shorter contact times of the flowing gas stream with the catalyst bed. However, with the increase of catalyst activity at higher T_{cat} values, the difference in catalyst/plastic ratio with/without nitrogen becomes lower but is still present.

One may wonder why in the simulations, the effect of carrier gas was not considered in the first reaction stage. In fact, in more rigorous simulations, this should be considered as a higher flux of carrier gas may decrease secondary reactions (mainly at lower T_R temperatures) and can also affect heat transfer efficiency [350]. However, for three different nitrogen flow rates investigated experimentally (60, 80, and 110 cm^3/s), only small changes were noticed in thermal pyrolysis products of HDPE (see in the Complementary Information). Broadly speaking, using a carrier gas commercially is undesirable due to its costs and reduction of contact times with the catalyst bed (as shown in Figure 3.10).

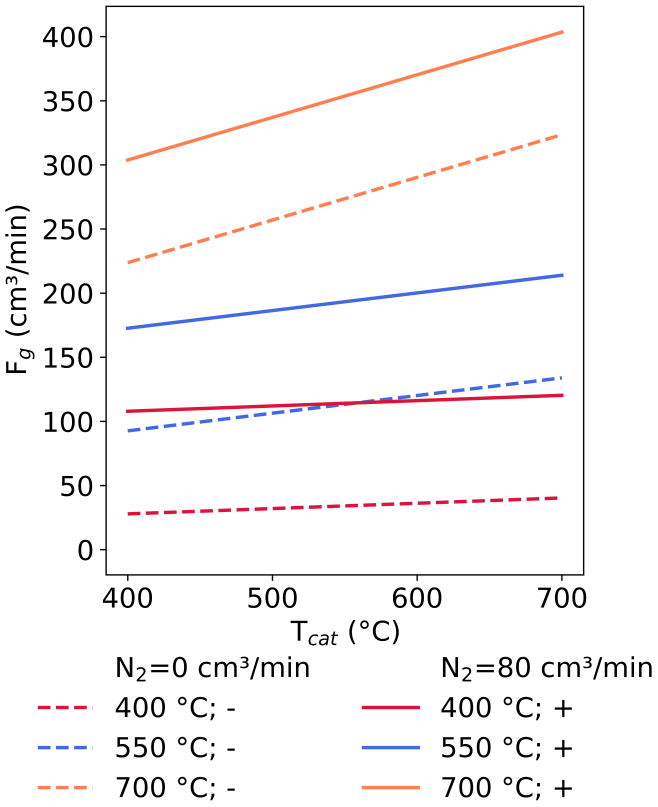

Figure 3.9: Dependence of flow rate with the temperature at the first reactor and the presence of additional carrier gas. (- means without nitrogen; + means presence of nitrogen.)

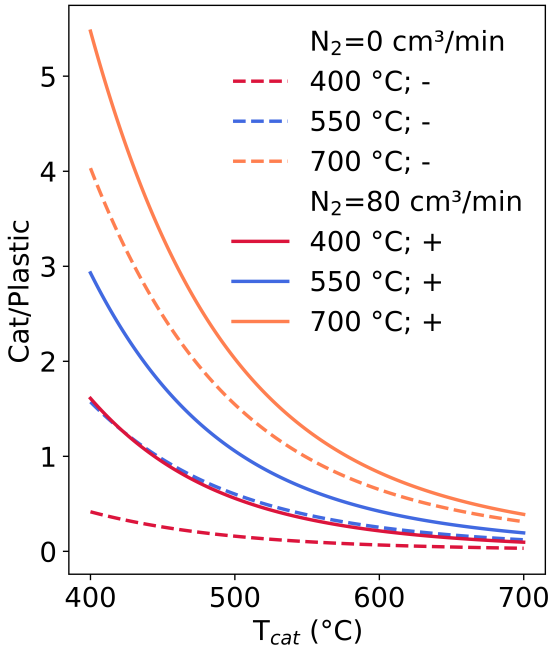

Figure 3.10: Dependence of the catalytic/plastic ratio with the temperature and the presence of additional carrier gas. (- means without nitrogen; + means presence of nitrogen.)

3.4.4 Validation

To validate the method, we applied the same procedure to another catalyst (Cat_2), and by only looking at Figure 3.3, one can notice that Cat_2 produces more oil and less gas, and also less wax. However, with the aid of the model, to achieve the goal of reducing the wax fraction, both catalysts have similar performance, requiring almost the same mass to convert the wax produced in the pyrolysis, first-stage reactor, as seen in Figure 3.11. Additionally, less catalyst is required at higher temperatures, and more oil is formed as reflected in the rate parameters for Cat_2 catalytic reactions:

$$R_g^{cat} = 5.387\ 10^4\ exp(\frac{-4735.39}{T_{cat}}) \tag{3.22}$$

$$R_l^{cat} = 6.48\ 10^5\ exp(\frac{-6355.07}{T_{cat}}) \tag{3.23}$$

$$R_{coke}^{cat} = 2.54\ 10^4\ exp(\frac{-5327.88}{T_{cat}}) \tag{3.24}$$

The lower kinetic rates compared to Zeolite Y (Cat_1) for the gaseous and coke reactions represent that more liquid product is formed. The mass ratios of the products in the output stream of the catalytic bed are shown in Figure 3.12. These straightforward performance comparisons show that the model is an important tool for catalysis screening, which can be time-demanding and misleading when many catalyzes are tested. Additionally, instead of only estimating kinetic parameters, as frequently reported in the plastic catalytic pyrolysis literature, the proposed 'short-cut' model can be used to set conditions (temperature, catalyst mass, and so on) to maximize desired products, and assist in the scale-up decision process.

3.5 Conclusion

A short-cut procedure was proposed to analyze plastic pyrolysis reactions using a few experiments and a straightforward mathematical model. To demonstrate this approach, high-density polyethylene (HDPE) pyrolysis was performed with and without a catalyst (zeolite Y or another conventional catalyst) at three temperatures: 450, 500, and 550 °C. The methodology combines mass balance characterization and GC-MS analysis of the liquid fraction to determine two key aspects: (1) the residence time required to fully convert the plastic feed into products at a specified temperature (T_R), and (2) the catalyst mass (expressed as a catalyst/plastic ratio) needed to convert all wax formed in the first stage into lighter products in the catalyst bed.

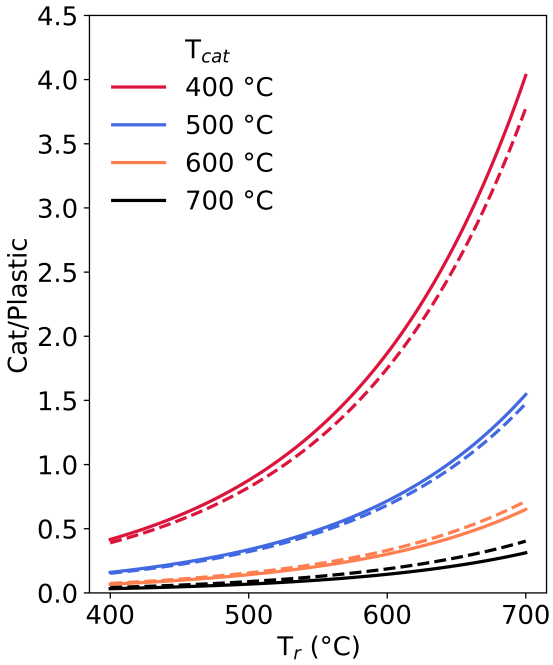

Figure 3.11: Comparison of the catalyst-plastic ratio for complete wax conversion between Cat_1: Zeolite Y (−), and Cat_2: another conventional catalyst (−−).

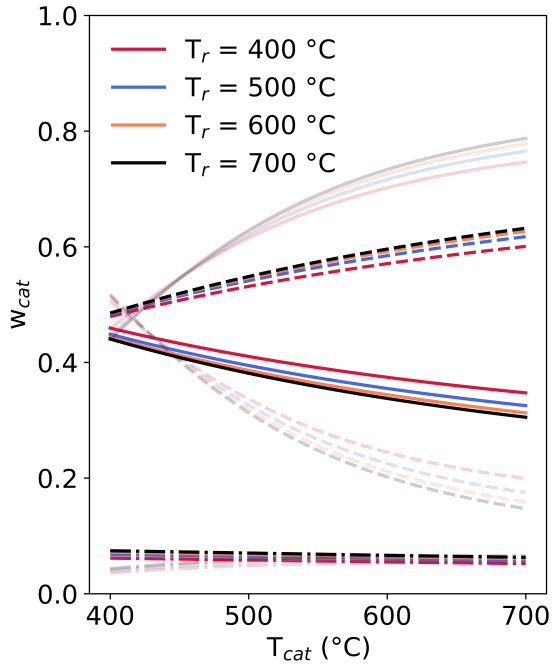

Figure 3.12: Comparison of the catalyst bed product's mass ratios according to the temperature and catalyst used: the blurred is the Zeolite Y, and the sharp lines are the conventional catalyst. −: Gas, −−: Oil, .−: Coke.

The model can be customized to account for different lump fractions and conditions, making it useful for comparing catalytic activities and evaluating catalysts based on criteria such as reducing coke formation and enhancing catalyst activity

with minimal gas production. Additionally, it provides a coke generation rate to monitor catalyst efficiency and usage.

While the procedure is straightforward, it requires adaptation for each system, considering factors like reactor design, catalyst type, heating rate, residence time, and other relevant conditions. Besides optimizing pyrolysis or packed-bed reactors, the approach is suitable for any experimental scale and offers a practical starting point for reactor scale-up. Furthermore, given the broad and continuously changing range of products produced during pyrolysis due to variations in solid waste composition, the simplicity and flexibility of the proposed methodology make it well-suited for systems that require quick adaptation.

However, it is important to note that this is a lumped model, which does not provide insights into the specific chemical reactions responsible for the products formed. If time is not a constraint, mechanistic models should be developed to accurately represent the process. These models must be validated using smaller reaction setups to avoid slow heating rate and mass transfer limitations (e.g., slow evaporation) that can influence the determination of kinetic parameters. Thus, the next chapter focuses on the development and validation of a mechanistic model for polystyrene as a case study.

Chapter 4

Polystyrene Pyrolysis: Mechanistic Modeling and Experimental Validation

This chapter is based on the article "Modeling of polystyrene degradation using kinetic Monte Carlo" published in the Journal of Analytical and Applied Pyrolysis in 2022 [351].

4.1 Introduction

Unlike empirical models, mechanistic models can capture the fundamental chemical pathways governing polymer degradation and product formation. This detailed representation allows for improved predictability of product yields and compositions across varying operating conditions, which is crucial for optimizing pyrolysis processes and designing efficient recycling technologies.

Nonetheless, the literature still lacks comprehensive investigations into the thermal degradation behavior of plastic materials. Besides the complex kinetics, it is also challenging to obtain kinetically-controlled data due to the low thermal conductivity and high viscosity of plastic materials, which often result in heat and mass transfer limitations. These limitations can hinder the accurate characterization of the intrinsic reaction kinetics, making mechanistic modeling particularly valuable for overcoming such experimental challenges. Such models are essential for isolating intrinsic kinetic parameters from confounding transport phenomena.

As a first case study, this chapter discusses polystyrene (PS) pyrolysis, including its degradation mechanism, primary products, and validation at different temperatures and scales. Polystyrene was chosen because its pyrolysis products are well-characterized and predominantly styrene. Moreover, polystyrene has a worldwide

production exceeding 3 Mton/year [352]. It is widely used in packaging, household appliances, consumer electronic products, building and construction (including foams, panels, and other applications), transportation, and medical items [352]. Consequently, appropriately recycling polystyrene waste presents a relevant technological and environmental challenge.

In this context, companies are developing technologies to recycle PS chemically, such as Agilyx, Pyrowave, PolyStyreneLoop, and Polystyvert [103]. These projects remain at a small or medium scale and are not adopted globally. This limitation is likely due to logistical issues, sorting challenges, lack of standardized procedures and quality guidelines for input materials, suboptimal operating conditions, and economic constraints. In addition, regulatory frameworks and market incentives for recycled polymers are still underdeveloped, further limiting widespread adoption. However, PS recycling research activities also need to be further improved as only a few mechanistic models have been studied [23, 290, 294]. Often, these studies used data not obtained under purely kinetic control, and the kinetic parameters are likely to encompass other effects such as slow heating rate or gas-phase reactions.

Therefore, in this work, the goal of revisiting the PS pyrolysis mechanism is to review the main mechanistic steps, the kinetic parameters, and the products formed according to the reaction scale. This analysis aims to identify knowledge gaps, improve model fidelity, and ultimately support designing more efficient and scalable chemical recycling technologies.

4.2 Methodology

4.2.1 Reaction Mechanism and Kinetic Parameters

The reaction mechanism of the thermal degradation of polystyrene (PS) is illustrated in Scheme 4.1, including the following reactions: R1: chain-fission (or 'random scission' or 'main chain homolysis'); R2: termination by recombination (or 'radical recombination'); R3: allyl chain scission (or 'specific chain scission', 'chain-end scission', or 'chain-end homolysis'); R4: hydrogen abstraction (or 'intermolecular abstraction'); R5: mid-chain β-scission; R6: radical addition; R7: unzipping (or 'end-chain β-scission or 'depropagation'); R8: hydrogen transfer (or 'backbitting', or 'alkyl radical isomerization'); and R9: termination by disproportionation. Four hydrogen abstraction steps (R8) are considered in the proposed PS degradation mechanism: 8a: 1,3-hydrogen abstraction; 8b: 1,5-hydrogen abstraction; 8c: 1,7-hydrogen abstraction; and 8d: 7,3-hydrogen abstraction. This model is inspired by discussions provided by FARAVELLI *et al.* (2001) [23], KRUSE *et al.* (2002) [294], and POUTSMA (2006) [290].

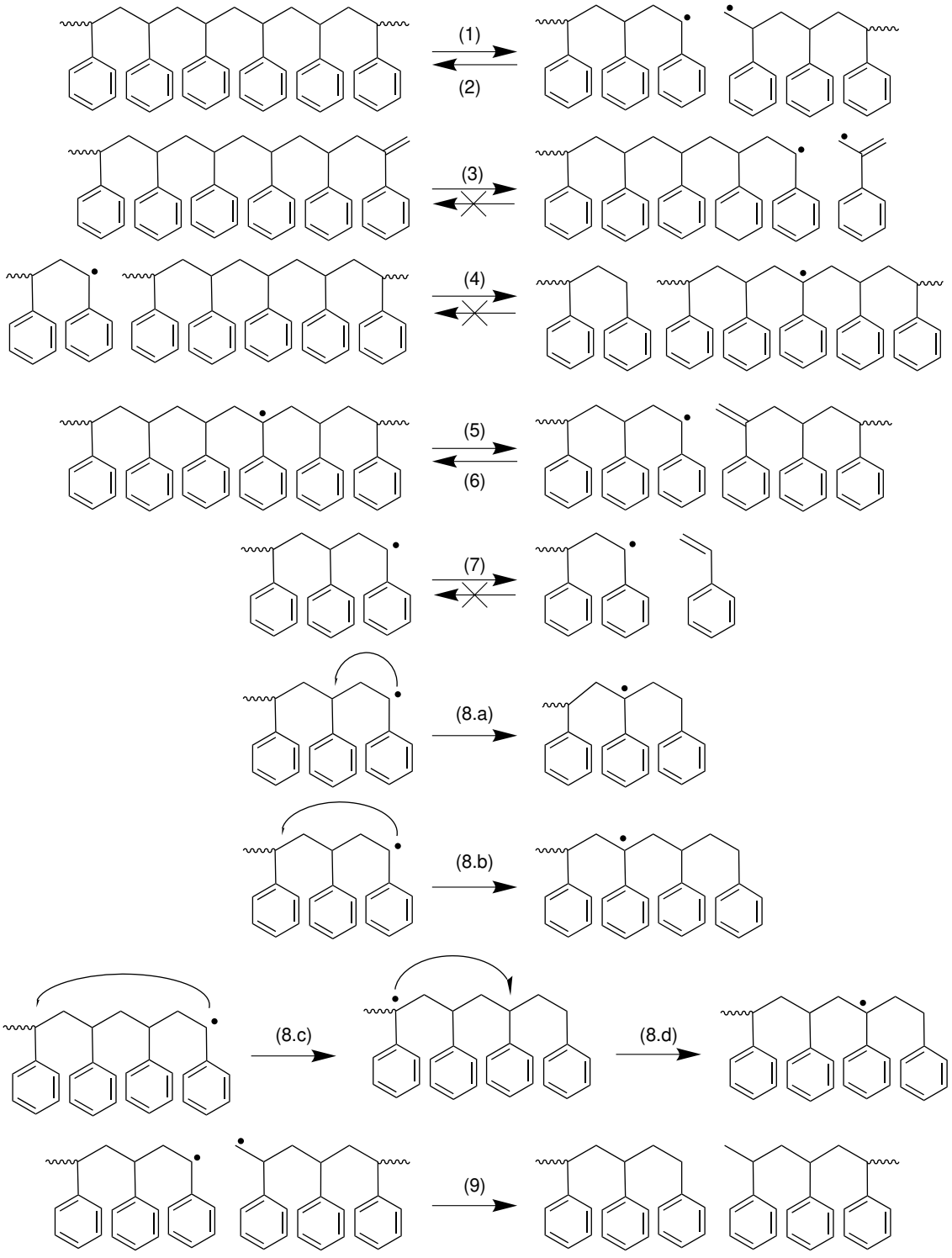

Scheme 4.1: The proposed polystyrene thermal degradation mechanism.

It is assumed that the thermal degradation of PS is initiated by reaction step R1, leading to a reduction in the average molecular weight, which creates radicals and promotes degradation. In this case, the MC reaction rate is proportional to the chain length, considering the number of styrene mer units within a molecule; thus, these two reactions occur more frequently. Furthermore, when selecting which dead

PS molecule will react, larger molecules are more likely to be chosen as they exist in greater abundance. The formed radicals are a *secondary benzyl radical* that is subject to benzylic resonance, *Rs*, and a *primary radical*, *Rp* [23].

Although it has been assumed that initial PS chains are saturated, other molecular configurations can be generated during the thermolytic process. Dead PS chains can present nine distinct chain end configurations, as shown in Figure 4.1. However, only three of these configurations are explicitly considered in the model, as described in the mechanism of Scheme 4.1. For example, the mid-chain β-scission reaction, R5, results in an unsaturated (primary or secondary carbon) chain end. In addition, as R3 can only take place in the presence of PS chains with unsaturated chain-end, forming a *secondary benzyl radical* and a resonantly stabilized *allyl benzene radical* (r_s), therefore, both PS saturated (alkane backbone type III) and unsaturated primary carbon chain ends (alkene backbone type I or dialkene backbone type II) are considered in the mechanism [23].

It is important to note that both living radicals *Rs* and *Rp* can undergo termination by combination (R2), forming dead PS chains. Besides, it is also considered that *secondary benzyl radical*, *Rs*, can either terminate (R2 or R9) or propagate (R4, R7, R8). Moreover, it is assumed that *primary radical*, *Rp*, can only terminate via R2 or R9 or react via R4 or R7.

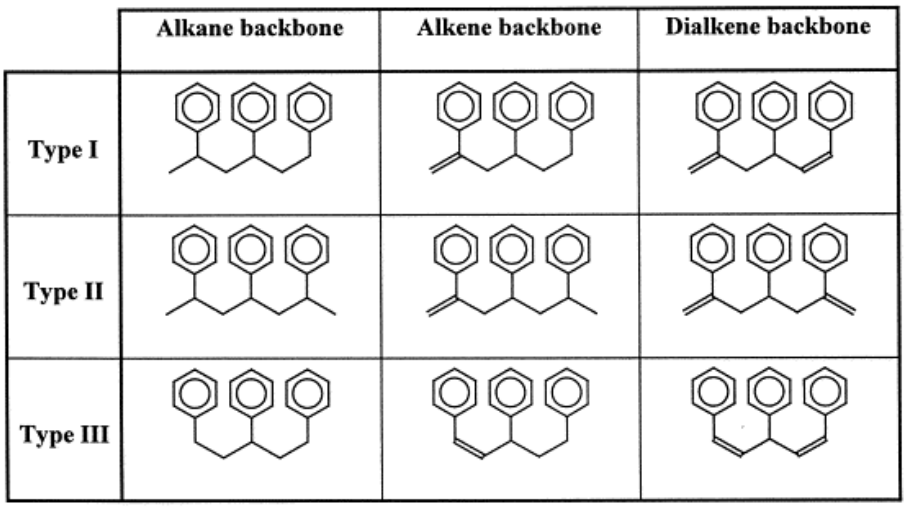

Figure 4.1: Families of chain configurations formed during thermal polystyrene degradation [23]. Only i) alkane backbone type III (saturated head ends), ii) alkene backbone type I (unsaturated tail end and saturated head end), and iii) dialkene backbone type II (both unsaturated tail ends) are considered in the model.
. Authorized from FARAVELLI *et al.* (2001) [23].

Reaction R4 occurs when R_s (or R_p) abstracts a hydrogen atom from a PS chain, generating a *tertiary benzylic radical*, R_m. R4 only occurs on tertiary carbons (mid-chain head radicals) due to the higher stability of the formed long-lived resonantly

stabilized benzylic radicals (the phenyl substituent provides resonance stabilization). Like R1, the MC reaction rate is proportional to the chain length, considering the number of styrene meres within a molecule. Additionally, bigger PS molecules are more likely to be chosen due to their higher weight fraction.

The R4 reverse reaction and the possibility of chain branching are not considered, given the stable characteristics of the tertiary radical and possible steric hindrance. Thus, Rm_i radicals can only undergo R5 midchain β-scission (scission of the C-C bond at β position) on either side of the midchain radical, forming a radical Rs and a dead unsaturated chain (it is now implicit that the unsaturated chain end is located in the primary carbon) [23].

The R5 reverse reaction, R6, only occurs in the presence of an unsaturated chain (as it does in R3) but returns a tertiary radical Rm_i. Additionally, the hydrogen transfer reactions R8 (also known as backbiting reaction) can occur and involve the *secondary benzyl radical*, forming a tertiary radical Rm_i in the 3rd, 5th, or 7th position (these specific mid-chain radicals formed from backbiting reactions are tracked separately from other midchain radicals). The first two mid-chain radicals can form a dimer or trimer through the R5 step, respectively, while some toluene and diphenylpropane can also be formed, but to a much lesser extent. It is still unclear if the active 7th radical position can allow the formation of a tetramer, but the 1,7 hydrogen shift reaction (R8.c) followed by the 7,3 hydrogen shift reaction (R8.d) may allow the dimer formation mechanism [292].

The end-chain β-scission reaction step, R7, is the most desired reaction, resulting in styrene. The formation of a monomer molecule and a shorter living radical polymer chain explains why this reaction step is usually known as 'depropagation' or 'unzipping'. The reverse reaction, which would be the polymerization, is not considered in the model because of existing thermodynamic constraints at usual thermolytic reaction conditions [21, 264].

Finally, termination by disproportionation (R9) of a *secondary benzyl radical* or a *primary radical* may also take place, forming two dead PS chains. Due to higher stability, the unsaturation is normally placed in the head, leading to the formation of a vinyl double bond.

As thermal degradation is a cracking process that takes place mainly in the condensed liquid phase and reaction products are released as volatiles, reactions in the gas phase are neglected, and it becomes necessary to distinguish the molecules that are present in the liquid phase from the ones that are present in the gaseous phase [23]. So, the final kinetic model contains 47 macro-reactions, 3 macroespecies, 6 radicalar macroespecies, 5 radicalar low molecular weight species, and 10 low molecular weight products, as described in Table 4.1.

Table 4.1: Summary of chemical components considered in the proposed polystyrene degradation model.

Component	Chemical Structure	Component	Chemical Structure
Alkane Dead PS Chain (PSs_n)	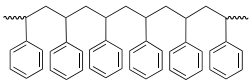	Secondary PS Radical (Rs_n)	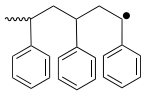
Alkene Dead PS Chain (PSu_n)	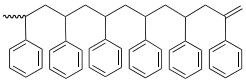	Primary PS Radical (Rp_n)	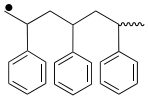
Dialkene Dead PS Chain ($PSuu_n$)	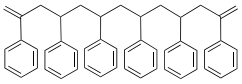	Mid-Chain PS Radical Rmn	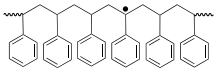
Styrene (Sty)	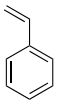	Allyl Benzene Radical ($aMSty_r$)	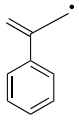
α-Methylstyrene (aMSty)	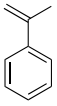	DPP Radical (DPP_r)	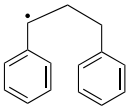
Ethylbenzene (EB)	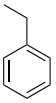	Ethylbenzene Radical (EB_r)	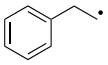
Dimer	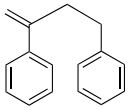	1,3 Mid-Chain PS Radical (MID_{13})	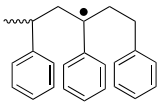
1,3-Diphenylpropane (DPP)	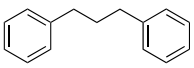	1,5 Mid-Chain PS Radical (MID_{15})	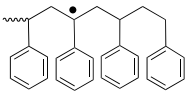
Trimer	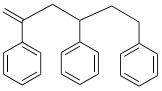	1,7 Mid-Chain PS Radical (MID_{17})	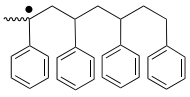
Toluene (Tol)		Benzyl Radical (Tol_r)	
Benzene		Styryl Radical ($Styrl_r$)	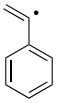
Tetramer	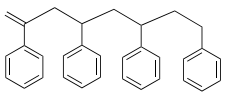		
Ethene			

The kinetic constants considered here are shown in Table 4.2. The kinetic constants were reported in other works [290, 292, 294, 296], based on the Evans-Polanyi relationship, Blowers-Masel relationship, or empirical estimation (case of the parameter k_{17}). Two kinetic constants for the primary radical R_p were considered: hydrogen abstractions ($k_{H,Rp}$), and depropagation ($k_{dp,Rp}$). These two kinetic constants were taken from POUTSMA (2006) [290]. A specific mid-chain β-scission rate constant was considered for small molecular weight radicals (<= 7 meres) (k_{bs0}), as reported by LEVINE e BROADBELT (2008) [296].

Table 4.2: Kinetic constants considered in the present model.

Reaction	Kinetic Constant	Ref.
R1: k_f	$2 * 10^{16.2} exp\left(\frac{-72.9}{RT}\right)$	[290]
R2: k_{tc}	$1.1 * 10^{11} exp\left(\frac{-2.3}{RT}\right)$	[294, 296]
R3: k_{fs}	$10^{15.6} exp\left(\frac{-61.7}{RT}\right)$	[290]
R4: k_H	$10^{8.1} exp\left(\frac{-15.85}{RT}\right)$	[290]
R4: $k_{H,Rp}$	$10^{8.0} exp\left(\frac{-14.35}{RT}\right)$	[290]
R5: k_{bs}	$10^{13.00} exp\left(\frac{-24.24}{RT}\right)$	[292]
R5: k_{bs0}	$10^{13.65} exp\left(\frac{-23.16}{RT}\right)$	[292]
R6: k_{ra}	$10^{8} exp\left(\frac{-6.94}{RT}\right)$	[292]
R7a: k_{dp}	$3.1 * 10^{12} exp\left(\frac{-23.9}{RT}\right)$	[296]
R7b: $k_{dp,Rp}$	$10^{12.9} exp\left(\frac{-24.9}{RT}\right)$	[290]
R8a: k_{13}	$10^{12.7} exp\left(\frac{-37.4}{RT}\right)$	[292]
R8b: k_{15}	$10^{9.75} exp\left(\frac{-16.28}{RT}\right)$	[292]
R8c: k_{17}	$0.1 * k_{15}$	[292]
R8d: k_{73}	$6.31 * 10^{9} exp\left(\frac{-16.6}{RT}\right)$	[292]
R9: k_{td}	$5.5 * 10^{9} exp\left(\frac{-2.3}{RT}\right)$	[296]

Frequency factor: s^{-1} or $l \cdot mol^{-1} \cdot s^{-1}$.
Activation energy: $kcal \cdot mol^{-1}$.

4.2.2 Kinetic Monte Carlo Model

Construction of the Initial PS MWD

It has been discussed that the relative yields of PS degradation products depend on the average molar mass and molecular structure of the sample, as well as on the conditions of degradation (temperature, atmosphere, heating rate, etc.) [353–356]. For example, SUGIMURA *et al.* (1981) [357] compared the performances of thermolytic degradations of conventional head-to-tail PS to head-to-head PS, and the obtained products were different in each case.

The radical nature of PS thermal degradation can lead to the formation of many

chain weak links that can trigger the PS degradation [23, 353, 358]. CASCAVAL *et al.* (1976) [359] compared the yields of the pyrolysis products of anionic, thermal, and azobisisobutyronitrile (AIBN) polymerized PS at 660 °C and differences were found when PS samples presented low average molar masses ($<$ 50,000 Da), being concluded that weak bonds can be more influential at lower temperatures.

It must be emphasized that the molar mass dependence is known to impact the overall kinetic rate of PS degradation [360, 361] mainly due to random chain scission (R1 as shown in Figure 4.1). This behavior also leads to deviations in product compositions as hydrogen abstraction (R4) is also dependent on chain size. However, some experimental studies indicate that significant differences in the pyrolysis product composition cannot be observed when the average molar masses of PS samples are above 10,000 Da (when polymerization has been initiated similarly) [354, 355].

Proper adaptive and corrective factors can force initiation through chain weak links, but this aspect of the technology falls beyond the main scope of the present work. This task would be even harder if additives and other constituents normally present in municipal solid wastes should be considered [353]. Therefore, for simplicity, it is initially assumed that PS chain ends contain the same chemical end groups; particularly, it has been assumed that only saturated PS chains are initially present. Moreover, the molecular weight distribution (MWD) of the initial PS sample was constructed using a Flory most probable distribution:

$$w_x = x(1-p)^2 p^{x-1} \tag{4.1}$$

considering the maximum degree of polymerization (x) as 6000; and the propagation probability (p) as 0.998. Then, the average molar masses ($\bar{M}_n$ and $\bar{M}_w$) can be calculated as:

$$\bar{M}_n = \frac{MW}{(1-p)} \tag{4.2}$$

$$\bar{M}_w = \frac{(1+p)MW}{(1-p)} \tag{4.3}$$

where MW is the molecular weight of the monomer. It is important to note that the use of the Flory distribution is not necessary if the full MWD of the polymer sample is available. In this particular case, is can be assumed that w_x is known and Equation (1) can be skipped. Due to molecular weight influence on kinetic rates and product distribution, for initial simulations and model validation, the maximum degree of polymerization (x) was selected to ensure that the product distribution would not be affected by this numerical hyperparameter.

The MWD was then approximated by a histogram and further converted to a number of molecules. Therefore, for each polymer length i, D_i molecules can be

found in the form:

$$D_i = \frac{V_c \rho_p N_a}{iMW} w_x \tag{4.4}$$

where N_a is the Avogadro number. Therefore, the total number of dead PS chains can be obtained as $\Sigma_{i=1}^{\infty} D_i$, with concentration given by $\Sigma_{i=1}^{\infty} D_i / V_c$, where V_c is the selected control volume, ρ_p is the polymer density, which is a function of the temperature.

The maximum degree of polymerization (x) defines the minimum sizes of vectors and matrices used to perform the Monte Carlo methodology. However, when termination by combination is considered, a size bigger than the initial value of x has to be implemented, as combination leads to chain growth. In this case, the maximum chain size was assumed to be equal to $2x$. From a numerical perspective, whenever chains of size larger than x (or $2x$) were generated, the size was truncated. Nevertheless, no significant differences were observed in simulations performed with maximum sizes higher than $2x$, showing a good approximation of the obtained length distribution.

4.2.3 The Kinetic Monte Carlo Algorithm

For each mechanistic step, an individual Monte Carlo (MC) reaction rate is assigned, R_j^{MC}, with j varying from 1 to the total number of mechanistic steps in the degradation mechanism. The MC reaction rates are defined with the help of microscopic rate constants, k^{MC},

$$R^{MC} = k^{MC} N_c \tag{4.5}$$

where N_c is the number of unique combinations between reactant molecules inside the control volume. The parameter N_c depends on the reaction order, reactants number, and whether or not the reactants are of the same type. Table 4.3 shows how to calculate MC reaction rates for unimolecular, bimolecular, and termolecular reactions.

Table 4.3: N_c combinations * [27, 28].

Initiation**	$N_c = e_f X_i$
Bimolecular reactions between different molecules	$N_c = X_i X_j$
Bimolecular reactions between equal molecules	$N_c = X_i(X_i - 1)/2$
Termination by combination between equal molecules	$N_c = X_i^2/4$
Termination by combination between different molecules	$N_c = X_i X_j/2$

* * X_i, X_j: Number of molecules of reactants i and j in the control volume.

** ** For random scission, $e_f = 2i$ is the number of bonds that can undergo scission within a polymer chain (two bonds per monomer unit). For *chain-end scission* (R3), there are 0, 1, or 2 breakable chains for alkane, alkene or dialkene macromolecules, respectively: $e_f = 0$ (alkane); $e_f = 1$ (alkene); $e_f = 2$ (dialkene).

The microscopic reaction rate constants k^{MC} are calculated from the macroscopic reaction rate constants k^{exp} as presented in Table 4.4.

Table 4.4: Conversion of macroscopic reaction rate constants into microscopic Monte Carlo rate constants [27].

Unimolecular reactions	$k^{MC} = k^{exp}$
Bimolecular reactions between different molecules	$k^{MC} = \dfrac{k^{exp}}{V N_A}$
Bimolecular reactions between equal molecules	$k^{MC} = \dfrac{2k^{exp}}{V N_A}$

The MC algorithm used here is the direct method as explained by BRANDÃO *et al.* (2016) [27]. The randomness takes place during the selection of the reaction step by generating, at each iteration, a random number following the uniform distribution in the interval [0,1) (r_1) and selecting the reaction with an index equal to k that will occur according to Eq. 4.6 and 4.7.

$$P_j = \frac{R_j^{MC}}{\sum_{k=1}^{n} R_k^{MC}} \tag{4.6}$$

$$\sum_{j=1}^{k-1} P_j \leq r_1 \leq \sum_{j=1}^{k} P_j \tag{4.7}$$

The iteration time-step (τ) can be calculated with the help of a second uniform distributed random number (r_2) as shown in Eq. 4.8. At the end of each iteration, the MC rates must be upgraded.

$$\tau = \frac{\ln(r_2^{-1})}{\sum_{k=1}^{n} R_j^{MC}} \tag{4.8}$$

4.2.4 Technical Details and Reaction Conditions

All simulations were executed on a Dell personal computer equipped with an Intel CPU (Intel Core i7-7700HQ CPU 2.80GHz) and 16 GB RAM and running under Windows 10 (Professional, 64 bit). The source code was written in Python programming language using Numba [362].

For all simulations, the stopping criterion was the attainment of a specified final time, which always led to the molar conversion of the initial carbon-carbon bonds above 90% on a molar basis. One typical simulation took an average simulation time of 3 ± 1 min for a control volume of 10^{-16} L (940160 molecules), which was used for all simulations after convergence testing. This computational time was only possible because of the accelerated convergence procedure implemented in Numba, as it will be shown.

The initial PS sample presented M_n of 52,000 g/mol, and M_w of 100,000 g/mol [354, 356, 357, 363]. The temperature was set at 500, 600 or 700 °C [354, 356, 357, 363].

4.3 Results and discussion

4.3.1 Model validation

To define a control volume (sample size), convergence testing was performed for every evaluated temperature, resulting in 10^{-16} L as an adequate V_c value for every temperature. Fig. 4.2a shows the molecular weight distribution distributions of the polymer residues calculated with distinct control volumes, indicating that the value of 10^{-16} L was sufficiently high to ensure accurate simulation results without stochastic noise. Fig. 4.2b also shows that the dynamic degradation for the selected control volume of 10^{-16} L can be followed accurately and without stochastic noise. Similar results were obtained at 600 and 700 °C.

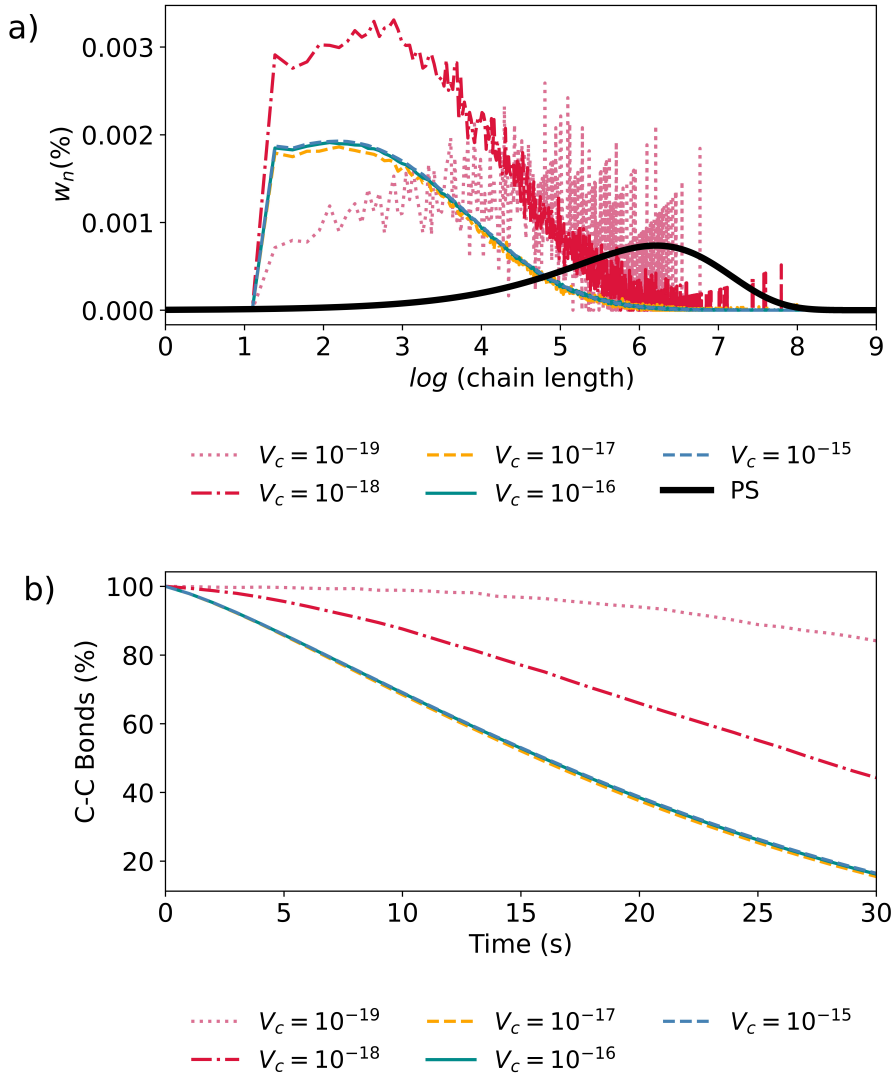

Figure 4.2: Effect of different control volumes on the simulation results: a) molecular weight distributions for polymer residues at 500 °C after 95% conversion and using different control volumes; b) evolution of the number of C-C bonds during the thermal PS degradation at 500 °C using different control volumes.

The residence time is a settable parameter and was initially set at 10 min to ensure the high conversion, although the complete conversion could be achieved at lower reaction times: 30 s (92.36 % of conversion), 1 s (92.57 % of conversion), and 0.03 s (100 % of conversion) at 500, 600, and 700 °C respectively. Experimentally, these extremely fast polymer degradation rates cannot be observed because of the limited heating rates (usually equal or smaller than 10 °C/min to achieve the desired temperature).

In addition, the effects of mass and heat transfer were not considered. For instance, DEAN *et al.* (1989) [364] showed that lower monomer/trimer ratios were obtained for larger samples due to the higher importance of mass and heat transfer constraints. These different yields may be associated with secondary reactions that

occur in the polymer melt, which become more probable when the residence time of primary products in the melt is increased by increasing the sample size [360, 365].

Similarly, using a carrier gas flow rate, the monomer can be swept more readily, reducing the rate of trimer formation (so that a higher monomer/trimer ratio can be obtained with a higher carrier gas flow rate). For this reason, the gas residence time was not considered in the present model. Additionally, the simulations considered that volatiles can be rapidly removed (including styrene, dimer, trimer, and other low molecular weight products) and that secondary reactions in the gas phase are negligible [358].

It is important to note that high conversions could be achieved with computational times of 3 ± 1 min using a control volume of 10^{-16} L (Table 4.5). This is an important reduction if compared with the computational time demanded by other kMC methodologies [147] and only made possible with the utilization of Numba's just-in-time function, which reduced all the simulation times by more than 99%. This methodology had been previously suggested by REGO e BRANDÃO (2020) [362] for a polymerization case study. Here, we proved that the use of this speedup method also opens up new possibilities for the use of kMC simulations to simulate depolymerization reactions without the major drawback of massive simulation times.

Table 4.5: Conversion and computational times needed to perform the simulations.

T (°C)	Depolymerization time (s)	C-C conversion reached (%)	Computational time without Numba (min)	Computational time with Numba (min)
500	36.6	99	1251	3.7
600	0.61	99	1313	3.1
700	0.022	99	1381	3.2

4.3.2 Experimental dataset and hypothesis

PS thermopyrolysis trials performed at 500, 600, and 700 °C were selected because the high temperatures favor styrene formation (as shown in modeling results), reduce the reaction time, and consequently allow for a reduction of economic and environmental costs. For temperatures above 700 °C, the product distribution changes in favor of lower molecular weight products such as hydrogen [366], carbon dioxide, ethylene, acetylene, benzene, and toluene [367]; simultaneously decreasing the percentage of styrene in the pyrolyzate. Thus, experimental data (weight percentage) were acquired for monomer, dimer, trimer, toluene, α-methyl styrene, and 1,3-diphenylpropane (DPP) at 500 - 700 °C.

The analyzed experimental datasets correspond to micropyrolyser-gas chromatography/mass spectrometry/flame ionization detector (Py-GC/MS/FID) data reported by BOUSTER *et al.* (1989), SUGIMURA *et al.* (1981), OHTANI *et al.* (1982), and NONOBE *et al.* (1995) [354, 356, 357, 363]. The PS sample sizes ranged from 0.02 - 1 g and presented M_n values in the range 30,000 - 860,000 g/mol. Micropyrolysis experiments were selected as references in order to minimize the importance of mass and heat transfer constraints in the melt and allow to neglect of gas phase effects. The average values and standard deviations for products obtained at distinct reaction temperatures and used for the model validation are shown in Table 4.6, as reported by the original references.

Table 4.6: Experimental product compositions used to validate the PS degradation model.%: average value; σ_i: standard deviation; *: it was considered equal to 5% of the average value.

	500 °C		600 °C		700 °C	
	%	σ_i	%	σ_i	%	σ_i
Toluene	0.8	0.1	0.75	0.04*	0.7	0.04*
Monomer	75.7	6.1	76.4	3.7	77.2	1.1
aMS	0.2	0.01	0.25	0.01*	0.4	0.1
Dimer	6.1	1.2	4.2	1.5	3.4	0.17*
DPP	7.4	6.1	0.6	0.1	1.4	0.3
Trimer	12.2	4.0	8.5	3.0	5.2	0.3

One must notice that, although PS pyrolysis may lead to dozens of final products, only six compounds are used for this initial validation, as supported by the experimental data available for this type of reactor. Heterogeneous results are common in pyrolysis experiments due to feed heterogeneity and different reaction types and reaction conditions (temperature, pressure, carrier gas, reaction time, gas residence time, and so on). However, as micropyrolysis experiments reduce the relevance of mass and heat transfer constraints, the reported experimental data are somewhat similar and appropriate for model validation.

According to SAWAGUCHI e SENO (1998) [361], the stationary concentration of R_s should be much higher than that of R_p because reactions with R_s consumption and R_s regeneration occur faster than chain scission reactions (R1) that lead to R_p. This can explain why products of a possible backbiting (R8) of R_p are scarcely formed. Moreover, as the radical stability decreases from $R_m > R_s > R_p$, this means that, when R_p is a reactant, the respective kinetic constant should be higher in module. Thus, while Broadbelt [296] considers a unique kinetic rate constant for a reaction step, independently of the reactant structure, Poutsma [290] takes

into account the individual molecular reactivity. Figure 4.3 shows that the concentration of R_s is indeed higher than for R_p as expected; and this behavior is seen independently of the Broadbelt/Poutsma kinetic constant considered.

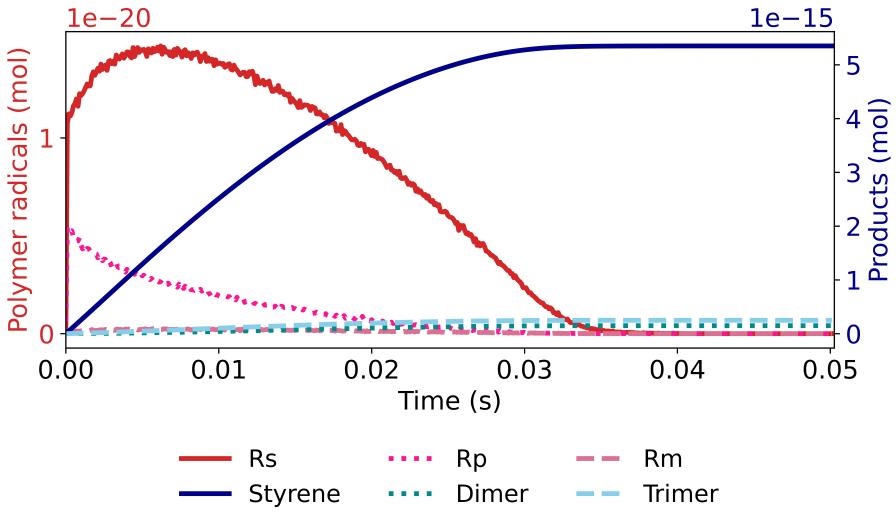

Figure 4.3: Evolution of concentrations of radicals R_m, R_s, and R_p and of monomer, dimer and trimer for degradation performed at 700 °C.

Indeed, POUTSMA (2006) [290], while studying the influence of reaction conditions on R_p reactions, concluded that R_p contribution to the overall kinetic rate and products was very low (see Section *5.3 Simulations for the T series* of POUTSMA (2006) for more details [290]). For instance, the author considered the inclusion of the unzipping step (R7) for R_p as well, but this did not affect the final amount of styrene nor the concentration of polymeric radicals during the degradation. During our simulations, even at higher temperatures than those tested by Poutsma, significant differences were not seen when the kinetic parameters of R_p were equal to those of R_s. Therefore, as the mechanistic model does not detect any special effect coming from R_p, at the current development stage of the proposed model, it may be unnecessary to discriminate R_p from R_s.

4.3.3 Influence of temperature

It is well known that random scission (R1) triggers thermal degradation (remembering that weak links are not being considered) and that the propagation of the depolymerization process takes place mainly via unzipping to monomer (R7) and intramolecular hydrogen transfer (R8), whose competition defines the relative yields of the volatile products [353, 357]. Figure 4.4 presents this competitive behavior for degradation performed at 500 °C. For any reasonable value of the reaction temperature, the number of dead PS chains increases at the beginning of the degradation

due to R1, starting to fall as the number of styrene molecules and other products increases.

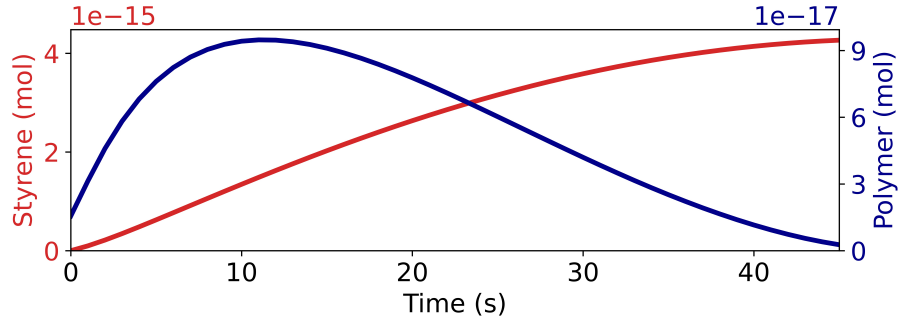

Figure 4.4: Evolution of numbers of dead PS chains and styrene molecules for degradation performed at 500 °C.

Simultaneously, the MWD decreases fast towards lower molecular weight species as shown in Figures 4.5 and 4.6. According to the initial Flory distribution, the PS sample had M_n = 52,074 g/mol and M_w = 104,045 g/mol, and, after 30 s, most of it was degraded. Similar behavior could be observed at every tested temperature.

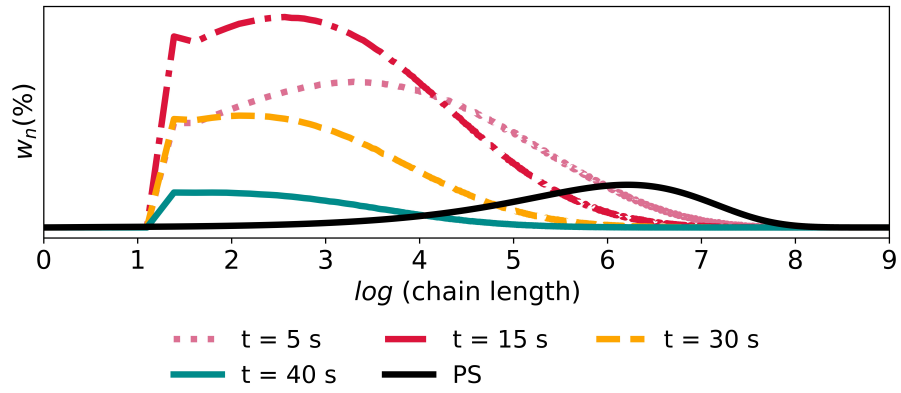

Figure 4.5: Evolution of the molecular weight distribution of the polymer residue during the degradation performed at 500 °C. n is the chain length.

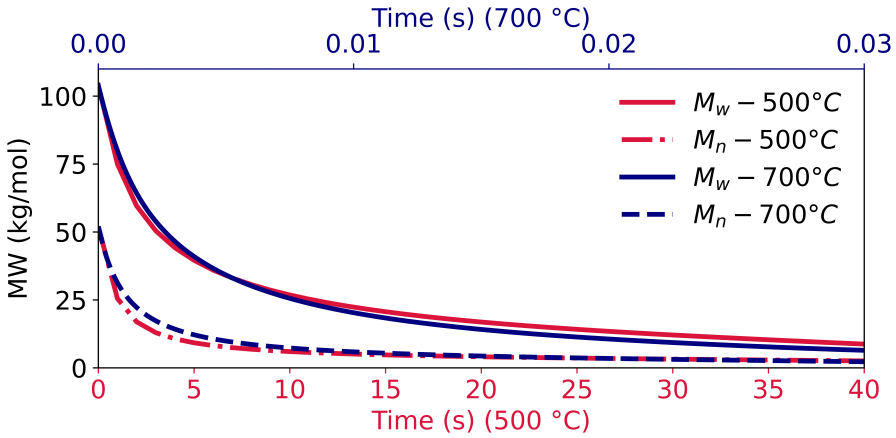

Figure 4.6: Evolution of average molecular weights of polymer residues for degradation performed at 500 and 700 °C.

Figures 4.7 to 4.9 show the carbon distribution for the PS degradation at 500, 600, and 700 °C. One must notice that styrene is predominantly formed at higher temperatures and oligomers at lower temperatures (Figure 4.10). This is explained by the higher activation energy for depropagation with respect to intramolecular hydrogen transfer [361]. Moreover, independently of the temperature, the trimer concentration reaches higher values than the dimer concentration due to forming a more stable quasi-six-membered cyclic structure in the transition state towards trimer [361]. Therefore, the proposed degradation model can represent the degradation products at 500 °C (considering the heterogeneity of the available experimental data), but diverges mainly for toluene at higher temperatures. This was somewhat expected as both Broadbelt or Poutsma did not report experiments at temperatures above 500 °C and did not consider the production of toluene.

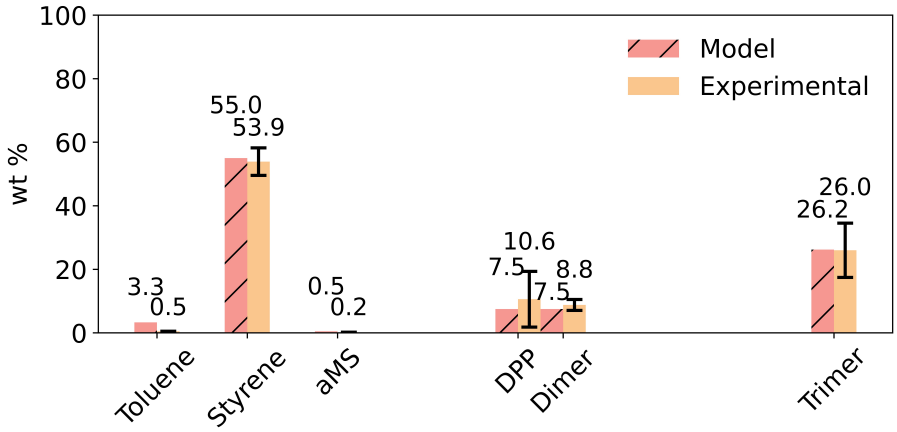

Figure 4.7: Product distribution for PS thermal degradation performed at 500 °C.

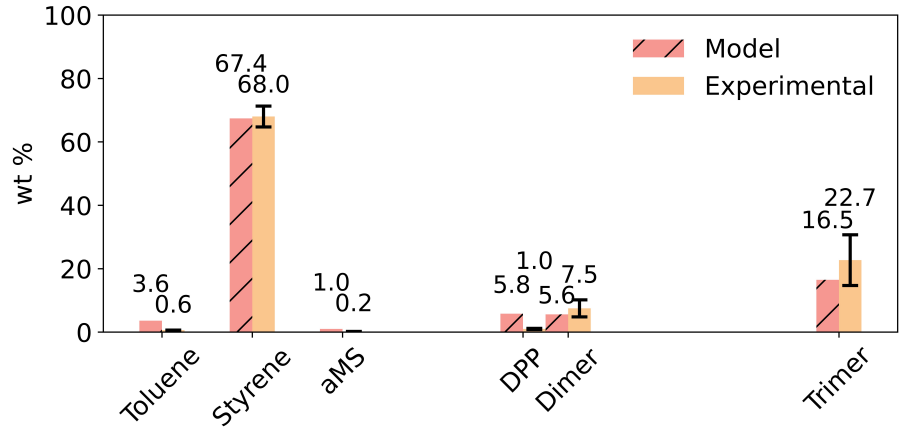

Figure 4.8: Product distribution for PS thermal degradation performed at 600 °C.

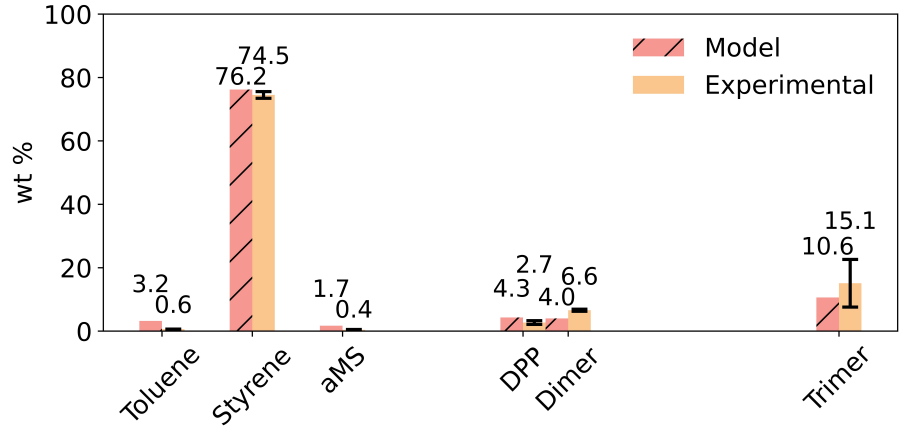

Figure 4.9: Product distribution for PS thermal degradation performed at 700 °C.

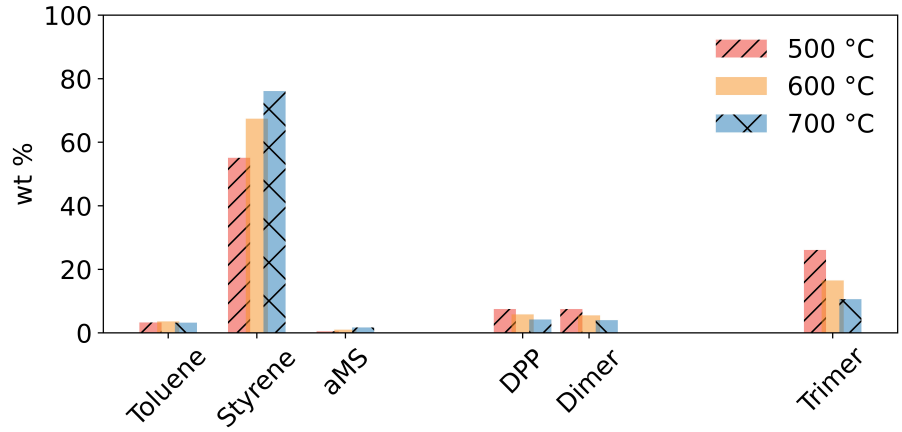

Figure 4.10: Product distribution for PS thermal degradation performed at different temperatures (500, 600 and 700 °C).

Thus, the kinetic constants for hydrogen transfer (R8), depropagation, and benzyl radical addition (toluene radical to 1,3 mid-chain radical) should be the main

parameters to be corrected at the higher temperatures (600 and 700 °C). Moreover, the formation of other products, such as tetramer or ethylbenzene, was not included in the model due to the lack of experimental data, as shown in Table 4.6. This makes it more difficult to confirm the model accuracy, as other light hydrocarbons may have been formed and not monitored. However, the mechanistic model has accurately represented PS degradation at the temperatures studied, mainly at 500 °C, which is the most probable temperature for industrial use. On the other hand, according both to the model and the available data, at higher temperatures, higher yields of styrene over other products can be obtained, indicating that the model can appropriately capture the increase of styrene yields with temperature, although adjustment of the activation energy is perhaps needed. However, as at any studied temperature, the pyrolysis time is very fast; the lower reaction time at 700 °C may not be beneficial due to the required sensible heat. To evaluate this, the whole pyrolysis system (including pre- or post-treatment) must be considered for the valuation of economic and environmental balances.

4.3.4 Mass transfer

The micropyrolyzer reduces the effects of mass and heat transfer, and these effects are often considered neglected, although they may still occur. However, when the reaction scale increases, significant modification of the product distribution may be seen, which can be attributed to these effects and, eventually, to extra reactions [368, 369]. Nevertheless, comments on the behavior and explanation of transfer effects have not yet been provided in the open literature.

For instance, if one considers that a certain amount of styrene can be formed within the polystyrene melt, as the styrene diffusivity is $9.52 \cdot 10^{-5}\, cm^2/s$ at 500 °C (extrapolated data from 270 °C) [370], it can take relatively long time for styrene molecules to reach the free evaporation surface. This mass transfer limitation may eventually allow the occurrence of several side reactions inside the melt, such as the spontaneous styrene thermal polymerization, that can be relatively favored at high temperatures [371].

Therefore, considering the kinetic rate constant for thermal initiation of $k_{dm} = 2.190 * 10^5 * exp(-27440/RT)$ $(L^2 mol^{-2} s^{-1})$ [372, 373] and the reactions presented in Scheme 4.2, if the whole C_{16} pool can be regarded as 'dimer' and the whole C_{24} pool can be regarded as 'trimer', one can notice that the effect of mass transfer reduces the amount of styrene in the output stream, increasing simultaneously the amounts of dimer and trimer and producing ethylbenzene as shown in Figure 4.11. Therefore, the occurrence of mass and heat transfer limitations can indeed cause significant modifications of the output stream compositions, an issue that has largely been

overlooked in the open literature and that can be extremely important for scaling up pyrolysis processes and reactors.

The mass transfer effect related to the constrained release of styrene molecules from the polystyrene melt was simulated through the partial removal of styrene molecules from the reaction environment (Sty/1, Sty/2, or Sty/4, respectively). In these cases, Sty/X means that a fraction 1/X of the available styrene molecules was kept inside the stochastic reaction environment. Therefore, Sty/1, Sty/2, and Sty/4 indicate that 100%, 50%, and 25% of the styrene molecules were kept inside the reaction volume, respectively. Although this can be regarded as a very simple numerical approach to describe the mass transfer constraint, this numerical procedure does allow one to observe how mass transfer constraints can affect the evolution of product compositions as the reaction evolves. Consequently, more dimer/trimer is produced when X increases, as the removal of styrene becomes more difficult. As a matter of fact, there is significant experimental scatter regarding the dimer and trimer contents in available experimental studies, which can be related to existing and poorly comprehended mass transfer limitations inside the reaction vessel.

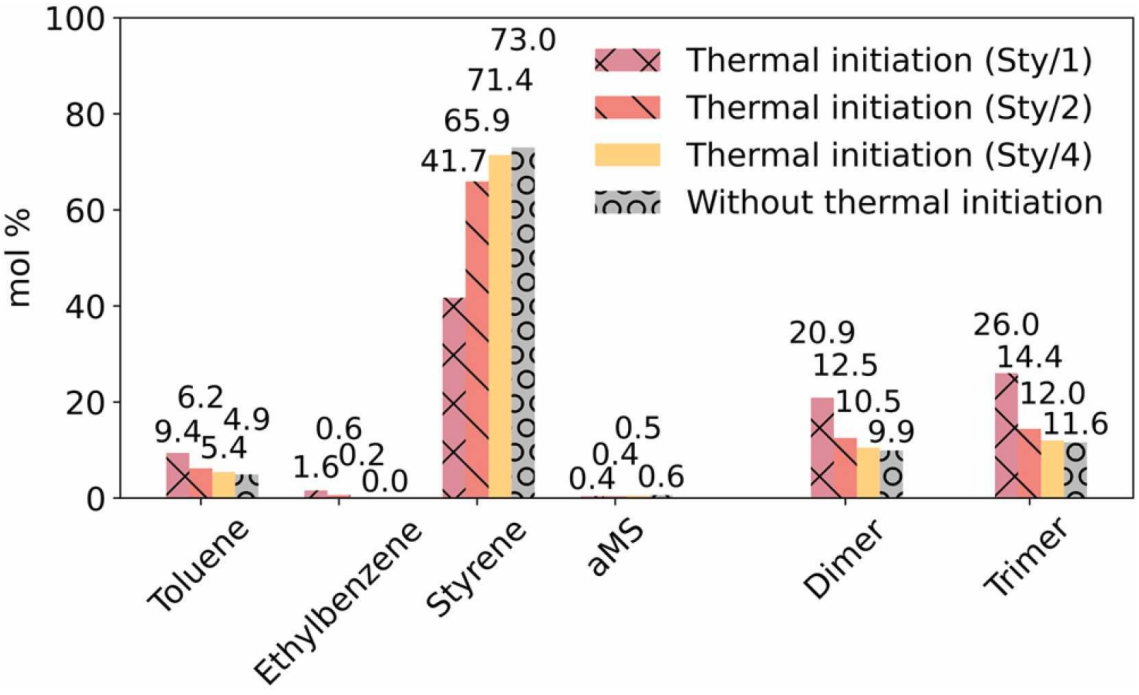

Figure 4.11: Product distribution for PS thermal degradation performed at 500 °C considering thermal initiation of styrene.

Therefore, although this can be regarded as a very simple example, it clearly shows that the kinetic mechanism should incorporate mass and heat transfer effects if real pyrolysis systems are to be modeled. As shown in Figure 4.11, it can be speculated that the scatter of experimental data published in the literature can be due to the incomparable heat and mass transfer effects (due to the different

reactor designs and polymer sample masses) in the different studies. Besides, Figure 4.11 strongly suggests that scaling-up of pyrolysis systems cannot be performed appropriately without carefully considering heat and mass transfer resistances.

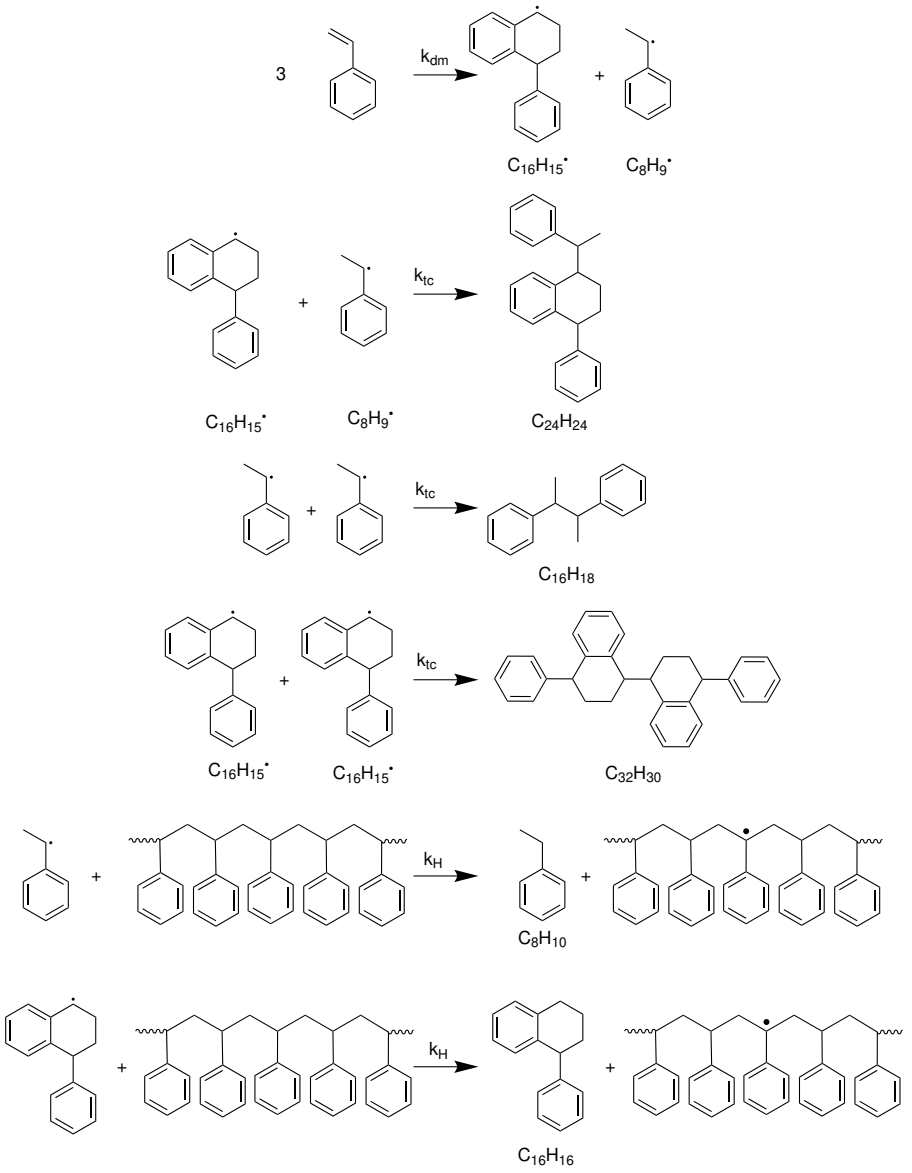

Scheme 4.2: Thermal initiation reactions proposed for polystyrene.

4.4 Conclusions

This work presented a detailed overview of polystyrene degradation modeling under an inert atmosphere (pyrolysis) and implemented a stochastic kinetic Monte Carlo (kMC) model to simulate the polystyrene pyrolysis reaction. For validation, the model was compared against experimental product distributions obtained from the literature (Py-GC/MS/FID). Across all analyzed temperatures, the model achieved very good agreement with experimental data without any parameter fitting. No-

tably, deviations were more significant for toluene and diphenylpropane at 600 °C. These discrepancies are not unexpected, given that most reported kinetic constants in the literature are derived from thermochemical balances performed at lower temperatures (300–500 °C).

To enable large-scale simulations, the model was successfully accelerated using Numba, reducing computation time by more than 99%. This performance boost allowed simulations to be run with a larger control volume ($10^{-16}L$), enhancing the statistical reliability of the results. The ability to efficiently simulate large systems opens promising avenues for applying stochastic methods to polymerization and degradation of high-molecular-weight polymers such as polystyrene and polyolefins. Furthermore, the model highlighted the sensitivity of product distributions to heat and mass transfer limitations, suggesting that such effects may play a critical role in the scale-up of pyrolysis processes, which is an aspect that has yet to be thoroughly addressed in the open literature.

Despite its strengths, the model has several limitations. It is mechanistic in nature and provides greater physical insight than lumped models; however, some relevant phenomena were not included. Gas-phase secondary reactions, which may become significant at high temperatures due to rapid conversion, were not considered. The formation of light gases such as ethylene, often associated with secondary reactions, was also excluded due to the scarcity of reliable experimental data. These simplifications were done because the literature often does not report the gas-phase residence time (or reactor dimensions).

Additionally, the reverse reaction of thermal styrene initiation was not incorporated, although it may influence the product distribution under the studied conditions. Moreover, product removal from the liquid phase was approximated based on boiling points, whereas a more accurate approach would involve modeling vapor-liquid equilibrium (VLE). Furthermore, key compounds like the styrene tetramer, which could serve as a validation point for VLE models, are frequently omitted in reported yields due to chromatographic limitations in detecting high-boiling-point species.

To address these limitations and better capture the complexity of pyrolysis product distributions, vapor-liquid equilibrium, and gas-phase reaction pathways were further incorporated into a subsequent polyethylene degradation model (Chapter 5). Given the broader range of products and higher propensity for gas formation in polyethylene pyrolysis, these additional mechanisms were essential to improving the accuracy and representativeness of the simulations. This extended framework also serves as a foundation for future studies aiming to model pyrolysis processes at larger scales and under industrial conditions.

Chapter 5

Polyethylene Pyrolysis: Mechanistic Modeling, Volatilization and Experimental Validation

This chapter is based on the article "High Density Polyethylene Thermal Pyrolysis: Kinetic and Volatilization Modeling" published in the Journal of Analytical and Applied Pyrolysis in 2025 [374].

5.1 Introduction

Understanding the degradation mechanisms of different plastics is essential for developing a versatile pyrolysis model that can handle a wide range of feedstocks. Given that post-consumer plastics are contaminated, the model must eventually be integrated with pyrolysis models for other materials to simulate real-world conditions accurately. As a step towards this goal, the pyrolysis of polystyrene was investigated in Chapter 4, whereas this chapter focuses on the pyrolysis of high-density polyethylene (HDPE), one of the most widely used polyolefins. HDPE is found in applications such as cosmetic packaging, bottles, household items, piping, and healthcare products, HDPE accounted for 12.2% of global plastic production in 2022, equivalent to 49 million tonnes [375].

Accurate prediction of pyrolysis products and process optimization requires a comprehensive understanding of not only feedstock properties and reaction kinetics but also thermodynamic and transport phenomena. Plastic pyrolysis involves a complex multiphase system, where the high viscosity and low thermal conductivity of polymers hinder efficient heat and mass transfer [376]. While this has been briefly addressed for polystyrene, polyethylene poses additional challenges due to its broad product distribution and the presence of heavier species with low volatilities. These

heavier compounds may remain in the melt during pyrolysis, making it essential to apply a vapor-liquid equilibrium (VLE) framework to capture their partitioning between the vapor and liquid phases.

Additionally, incorporating VLE is critical for accurately modeling product yields, transport behavior, and reaction pathways. Neglecting this aspect can lead to significant errors, including underestimated residence times and misrepresented intermediate concentrations. A simplified process visualization is shown in Figure 5.1. Additionally, products farther from the liquid-gas interface may escape as gas bubbles, driven by nucleation and growth processes [377], due to faster gas-phase diffusion and low solubility in the polymer [378]. Therefore, the residence time of the gases formed is not a fixed value but instead follows a distribution, which, in the case of semi-batch reactors, is time-dependent.

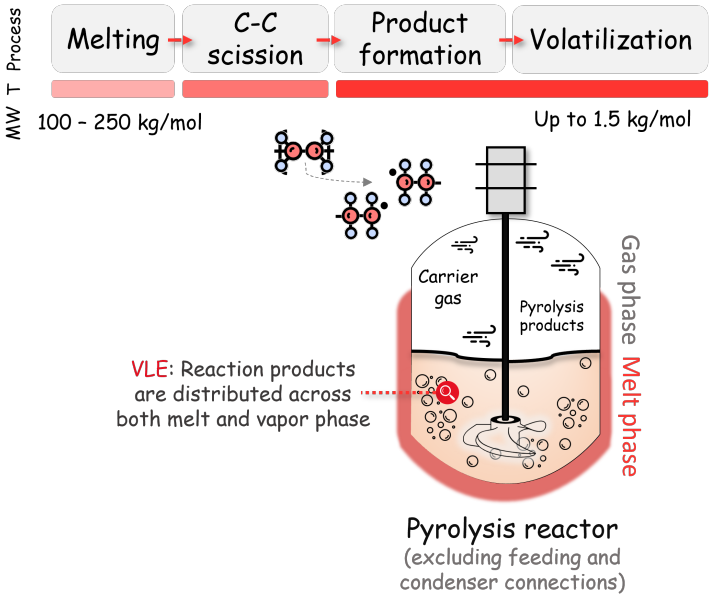

Figure 5.1: Different phenomena taking place in the pyrolysis of polyolefins in a semi-batch reactor.

Unfortunately, these complex phenomena are rarely addressed in the literature. Regarding the kinetics, experimental data often show high variability, likely because most measurements were not kinetically controlled due to factors such as sample size, operational method (e.g., closed-batch reactor), long residence times, and poor homogeneity [379]. Additionally, the lack of detailed reporting (e.g., molecular weight distributions, pressure, heating rate, or gas residence times) further complicates comparisons [380]. A more in-depth discussion on experimental data comparisons and parametric analyses for the pyrolysis of polyolefins and other plastics is available elsewhere [381–383].

While many models exist to represent polyethylene pyrolysis, they often focus on thermogravimetric data (TGA) or a simplified lumped product distribution (e.g.,

boiling point cuts – such as naphtha, diesel, and wax – or other measurable properties). TGA models often only represent the observed rate of mass loss, which lumps thermal, chemical and evaporation rates [263]. And empirical lumped models, although useful for specific optimizations (e.g., gas yield optimization), are also based on fitted parameters that are not transferable between reactors or feedstocks due to the influence of heat- and mass-transport effects and species volatility. Consequently, the empirical nature and simplifications result in a loss of information and limited applicability [384].

On the other hand, Poutsma (2003), Levine and Broadbelt (2009), and Popov and Knyazev (2015) focused on detailed mechanistic modeling of HDPE pyrolysis [263, 297, 378]. However, the available experimental data was either limited by the analytical techniques used or influenced by secondary effects (e.g., non-isothermal conditions or closed reactor systems). As a result, Poutsma's model comparisons with experimental data were constrained by data gaps and inconsistencies, while kinetic parameters were estimated to improve model fit in the other two studies. Consequently, no comprehensive, validated model applicable across various conditions could be established.

Regarding vaporization, existing studies rely on strong simplifications, such as arbitrary cutoffs for carbon numbers, assumptions of instantaneous removal for certain products [185, 226, 297, 385–388], or linear/polynomial expressions to represent the VLE as a function of the molecular weight of the products [277]. The lack of research on VLE for pyrolysis is likely a consequence of a poorly defined pyrolysis problem due to the system's complexity and the experimental challenges to isolate effects and quantify the full pyrolysis product distribution. However, the VLE is critical because vaporization changes the melt-phase composition, volume and properties, such as viscosity and average molecular weight, directly influencing the kinetics. Thus, failure to accurately couple kinetics and vaporization can lead to unreliable and unrepresentative modeling results under different pyrolysis conditions.

Recently, kMC pyrolysis models were developed for plastics other than HDPE, including polystyrene, poly(styrene peroxide), and poly(methyl methacrylate) [314, 351, 381, 389]. However, all these studies assume instantaneous volatilization of small oligomers, with the heaviest oligomer considered in this volatilization determined based on experimental data. Although the authors may have claimed that volatilization depends on pyrolysis temperature and product boiling points, this assumption is not always valid. For example, polystyrene trimer (2,4,6-triphenyl-1-hexene) has a boiling point of approximately 450°C, yet it volatilizes and is detected at pyrolysis temperatures below this threshold [390]. Moreover, other polystyrene pyrolysis studies have observed the volatilization of the polystyrene tetramer, which these models fail to account for [292, 363, 390]. Additionally, the models do not cap-

ture the influence of pressure and other process conditions [391], and most cannot be applied to different reaction setups since their kinetic parameters were estimated rather than derived from fundamental principles.

Similarly to the polystyrene study, to validate the polystyrene model, a micro-pyrolyzer setup was used for intrinsic kinetic measurements, which minimizes secondary heat- and mass-transfer effects due to its small sample mass, fast heating rate, and short gas residence time. This type of setup is considered among the best for obtaining intrinsic kinetics [162, 382, 392, 393]. A mechanistic-level modeling approach is proposed to model the pyrolysis process, providing a detailed representation by integrating fundamental knowledge of molecular structures and kinetic mechanisms. This approach is essential for developing models capable of handling diverse feedstocks and reactors without requiring re-calibration. The kinetic Monte Carlo (kMC) stochastic method was selected because it can accurately represent the complex composition of feedstock and products without relying on oversimplifications or theoretical distribution assumptions. Additionally, kMC is a robust alternative to population balance methods, which are challenging to solve for systems with highly complex species distributions. It also addresses the limitations of the method of moments (MoM), which often necessitates simplifications such as reduced kinetic models, omission of radical position tracking, quasi-steady-state approximations, or long-chain assumptions [300].

Aiming to represent the vaporization based on thermodynamic principles and well-established equations of state (EoS), it is proposed to integrate the kinetics with VLE, which is calculated according to the pyrolysis temperature, pressure, and melt composition. Additionally, despite the advantages of kMC, only a few studies have combined it with VLE to model multiphase reactors, such as the vacuum gas oil hydrocracking study by Alvarez-Majmutov *et al.,* which coupled flash calculations with the kMC algorithm [384, 394, 395]. In this case study, vaporization is similar to that occurring in plastic pyrolysis; however, a detailed methodology was not presented.

Therefore, a phenomenological model for HDPE pyrolysis is developed and validated based on elementary rate constants derived from small-molecule analogs (a first-principles-based model, or thermochemical kinetic approach). Previous works typically inferred kinetic constants by fitting them to experimental data. In addition, it is proposed a novel methodology that integrates kinetics with multicomponent phase equilibrium calculations. These calculations, based on thermodynamic principles and well-established equations of state (EoS), account for the influence of pyrolysis temperature, pressure, and melt composition. Prior studies failed to model volatilization phenomenologically, relying instead on strong simplifications (e.g., setting an arbitrary threshold of compounds that can volatilize to match ex-

perimental data). Consequently, as vaporization affects the melt-phase composition and volume, directly influencing the kinetics, unreliable and unrepresentative modeling results were obtained. Beyond its novelty for plastic pyrolysis, this methodology also extends the application of kMC to more complex reaction systems.

5.2 Materials and Methods

5.2.1 Thermal Pyrolysis Experiments

In the present work, a virgin HDPE sample was donated by DOW Chemical Co. (HDPE 25055E), with $\overline{M}_n$= 43.2 kg/mol and $\overline{M}_w$= 133.5 kg/mol, and was used for all the experiments. The GPC methodology is similar to previous works [381].

The pyrolysis experiments were performed by using a single-shot tandem micropyrolysis facility (Rx-3050 TR, Frontier Lab, Japan) coupled with a comprehensive two-dimensional gas chromatography system (GC-GC, Thermo Scientific TRACE Ultra) and a separate multicolumn GC dedicated for analysis of light gases (Thermo Scientific TRACE 1310) equipped with thermal conductivity detectors (TCD). A scheme representing the experimental unit is also available in Figure 5.2. The reader may also refer to other studies that employed the same micropyrolyzer facility for plastic pyrolysis for further details [381, 396–400].

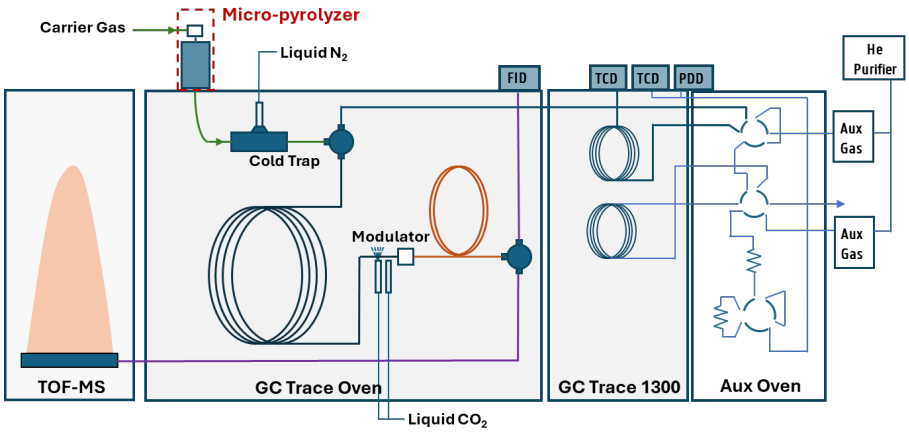

Figure 5.2: Experimental setup: micro-pyrolysis facility coupled with a comprehensive two-dimensional gas chromatography system and a separate multicolumn GC dedicated to the analysis of light gases equipped with thermal conductivity detectors.

The experiments were performed at 550, 600, and 650 °C, dropping 500-800 g of HDPE into the preheated pyrolysis furnace with a deactivated stainless steel sample cup (Eco-cup LF). The reactor was operated with a He flow rate of 50 mL/min and a pressure of 2.7 bar. According to the reactor dimensions (50 mm length, 2.5 mm diameter), the residence time of the volatiles is 0.3 s. These released volatiles

were then collected in a cryo-trap (MJT-1035E) cooled with liquid nitrogen for 5 minutes, and portions were simultaneously directed to the online analysis of pyrolysis products. The GC columns, an MXT-1 (Restek) (60 m, ID = 0.25 mm) non-polar and mid-polar BPX-50 column (2 m, ID = 0.15 mm), were held at -40 °C for 6 minutes, followed by heating to 350 °C with a rate of 3 °C/min.

Compound identification was performed with a BenchTOF-Select (Markes, United Kingdom) scanning m/z = 50–500 at 70 eV. To ensure accurate identification, the mass spectra of each compound was compared with those in the NIST library, using the match factor (MF) as the metric, cross-checked with Kovats indices [401, 402]. Compound quantification was performed with a flame ionization detector (FID), calibrated internally with iso-butane. Thus, based on the quantified iso-butane in each run, the product yields were calculated using the molar response factor (MRF) approach [403, 404]. A comprehensive discussion of the GC-GC analysis and the multicolumn GC setup is also available elsewhere [396, 405, 406], while the quantification procedure is described in references [396, 407–409].

Time-resolved experiments were also performed, enabling the qualitative characterization of the products in a temporal mode. HDPE was introduced into the heated zone of the first reactor maintained at 450 or 500 °C. The restriction column of the ToF-MS was connected directly to the GC injector to obtain the time-resolved profiles of all products eluting from the reactor.

5.2.2 Construction of the initial molecular weight distribution

The initial molecular weight distribution for the simulations is based on the GPC characterization. HDPE chain ends are assumed to contain the same chemical end groups; particularly, it has been assumed that only saturated HDPE chains are initially present. To compare the influence of the molecular weight distribution, artificial HDPE samples were constructed considering the Flory–Schulz distribution [410]:

$$w_x = x(1-p)^2 p^{x-1} \tag{5.1}$$

where w_x is the weight fraction, x is a vector from 1 to the maximum degree of polymerization, and p is the propagation probability. The chosen distributions have $\overline{M}_n$= 31.2 kg/mol and $\overline{M}_w$= 62.3 kg/mol, and $\overline{M}_n$= 140.3 kg/mol and $\overline{M}_w$= 280.5 kg/mol, respectively, according to Eqs. 5.2 and 5.3, where MW_M is the molecular weight of the monomer - ethylene in this case.

$$\overline{M}_n = \frac{MW_M}{(1-p)} \tag{5.2}$$

$$\overline{M}_w = \frac{(1+p)MW_M}{(1-p)} \tag{5.3}$$

The MWD was then converted to the number of carbon atoms (Figure 5.3), approximated by a histogram, and further converted to the number of molecules according to Eq. 5.4:

$$n_i \;=\; \frac{V_c\ \rho_P\ w_{x,i}\ N_A}{14i\ +\ 2}\ (molecules) \tag{5.4}$$

where i is the number of carbon atoms, V_C is the control volume of the kinetic Monte Carlo, ρ_P is the density of HDPE at the desired T (calculated with the Perturbed Chain Statistical Associating Fluid Theory, PC-SAFT EoS, details in Section 5.2.5) (notice that $V_c\ \rho_P$ is the initial mass of HDPE for the simulation), $w_{x,i}$ is the HDPE weight fraction of length i, N_A is the Avogadro number. Since the number of molecules in the kMC simulation must always be an integer, the histogram is rounded to the nearest integer.

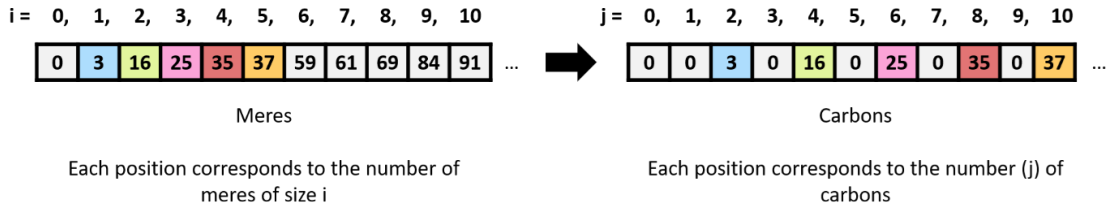

Figure 5.3: Example of conversion of meres to carbons.

5.2.3 Kinetic Model

The reactions considered for the HDPE pyrolysis model were considered of recursive nature and can be organized into a limited set of reactions families as shown in Scheme 5.1.

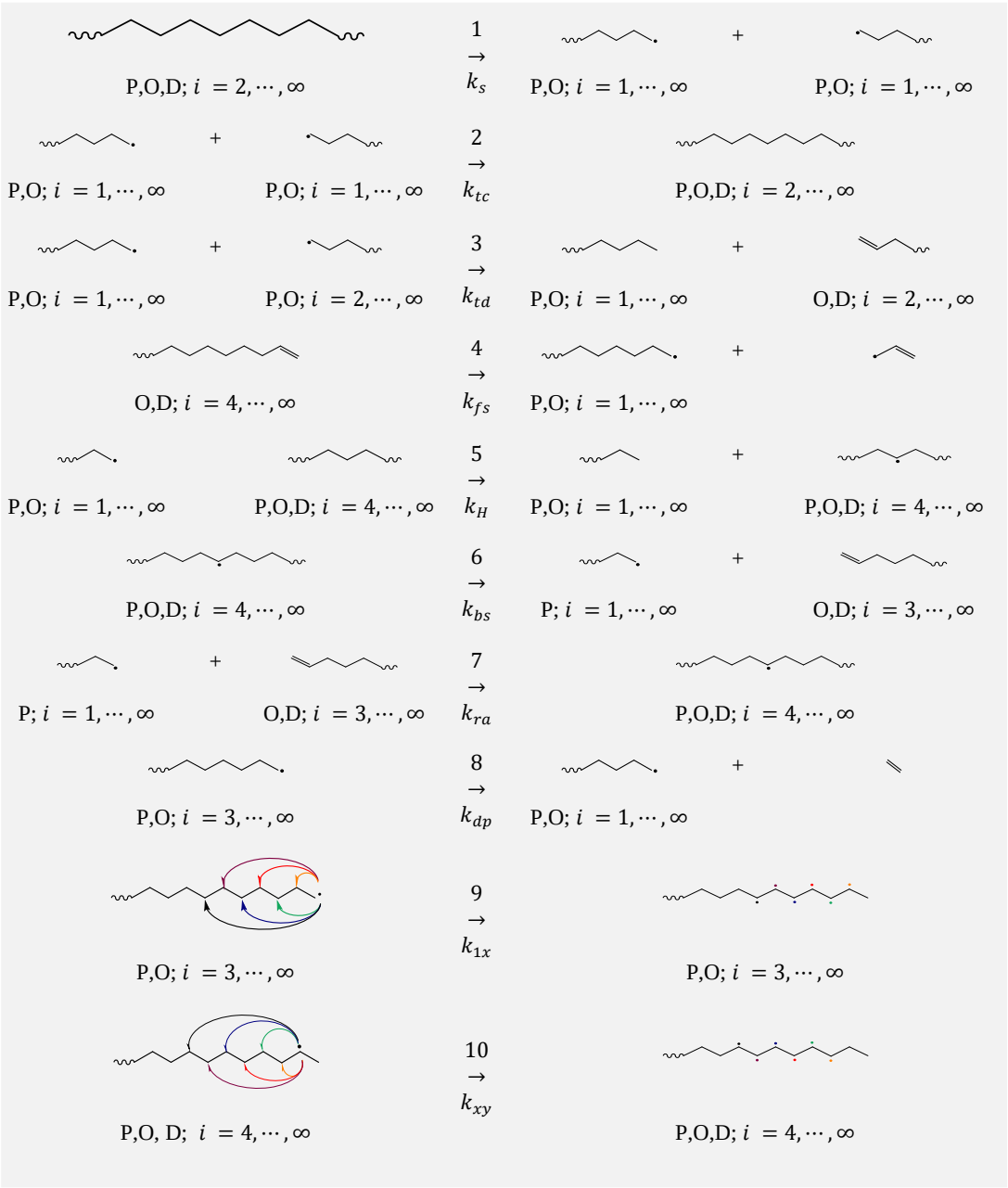

Scheme 5.1: Reaction families included in the HDPE pyrolysis model (P: paraffin, O: olefin, D: diolefin; i: chain length).

The reaction families considered are: mid-chain scission (1, k_s) ($P/O/D$ means it can be a paraffin – saturated compound, olefin – one unsaturation, or diolefin – two unsaturations; and i is the length – the reader may notice that the minimum i for olefins and diolefins are 2 and 3, respectively; and, therefore, the length considered for the compound just be adjusted accordingly); termination by combination (2, k_{tc}); termination by disproportionation (3, k_{td}); allyl bond fission (4, k_{fs}); hydrogen abstraction (5, k_H); mid-chain β-scission (6, k_{bs}); radical addition (7, k_{ra}); end-chain β-scission (or depropagation, or unzipping) (8, k_{dp}); 1-x hydrogen shift (backbiting) (9, k_{1x}) –x = 2 to 7 are considered in the proposed model, and y-x

intramolecular hydrogen shift (intra-backbiting) (10, $k_{bb,yx}$). Specific products of backbiting followed by mid-chain β-scission are shown in the Scheme 5.2.

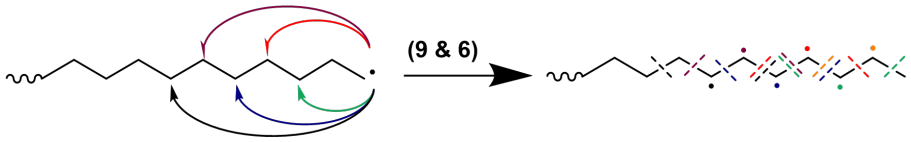

Scheme 5.2: Scission sites of mid-chain radicals formed mainly via backbiting reactions

The reaction families considered align with previously proposed kinetic mechanisms, such as those by Broadbelt and Poutsma [263, 297, 378]. However, prior studies typically fitted the kinetic parameters to experimental data, often using reactor configurations that were likely not kinetically controlled. Thus, the models did not distinguish between kinetic and transport effects and were unable to provide a detailed molecular weight distribution of the pyrolysis products.

Additionally, Scheme 5.1 presents only the main reactions, offering a simplified representation of the complete HDPE model. As model species, paraffins, olefins, diolefins, end-chain radicals, mid-chain radicals, and specific radicals such as methyl (lower stability) and allylic radicals (stabilized by resonance) radicals were tracked. Within each reaction family, different kinetic parameters were assigned depending on the species involved.

All reactions are assumed to be independent of chain length, and most are also independent of the presence of double bonds, except for allyl bond fission and radical addition. Additionally, the model includes the following considerations or exceptions:

- Vinyl (or vinylic) radicals are not considered;
- Intra-molecular hydrogen transfer: not allowed to occur after nine carbons about the chain end. This is considered because transferring the radical to farther away parts of the molecule is nearly equivalent to transferring it to any other chain of the same fraction of the population, which is already included in the model;
- The initial HDPE was considered to be linear. This assumption was also considered by Poutsma, who considered the same kinetic model for both HDPE and low-density polyethylene (LDPE) [263]. This likely occurs because branched radicals are easily cracked through a β-scission reaction to produce smaller hydrocarbon fragments.
- Branch formation was excluded since experimental data and previous studies [263, 393, 411] suggest that branched or vinylidene compounds form only in

minor amounts under the studied conditions. This is attributed to diffusional restrictions, weak branched positions, and the thermodynamic unfavourability of secondary radical addition to olefins at pyrolysis temperatures [263, 288, 412].

- Finally, as the dienes of the Diels-Alder (D-A) reaction in our case are mostly low-molecular-weight (e.g., butadiene), which mostly partitions to the gas phase, their reactions with dienophiles (ethylene or other small-molecule olefins) in the gas phase occurs to a minimal extent due to the very short gas-phase residence time of the micro-pyrolyzer. In the liquid phase, the chance of multiple unsaturation to be next to each other (dienes) is small for larger molecules. In addition, the larger molecules are not conformationally flexible for a D-A reaction to have any significance. Consequently, they contribute little to an overall molecular-weight-increasing effect compared to radical recombination. However, when gas phase residence time is long ($>$ seconds), D-A reactions may need to be considered in detailed models, which is the case for industrial-size reactors. We keep this question open for future studies.

Regarding the reaction rates, ongoing studies focus on properly adjusting the reaction rates for gas-phase reactions to account for their transition to the liquid phase, considering factors like steric hindrance and diffusion limitations. This is the case of termination by recombination (k_{tc}), which in the polymer melt is likely diffusion-limited, meaning the rate increases with time due to the reduction of average molecular weight. Kruse *et al.* (2002) considered the diffusion-limited recombination rate as inversely proportional to the length of the radical ($k_{tc,eff} = \frac{k_{tc}}{2}\left(\frac{1}{i^{\gamma}} + \frac{1}{j^{\gamma}}\right)$), where k_{tc} is the unhindered recombination term, i and j represent the chain lengths in monomer units of the terminating radicals, and γ represents the diffusion dependence on chain length ($\gamma = 1$ or 2, depending on the entanglement limit) [294]. This approach is known as the diffusion mean model.

Popov and Knyazev also aimed to account for the diffusion dependence on termination reactions by incorporating the influence of diffusion (k_{diff}) on the (unhindered) recombination term (k_{tc}) [378]. This methodology is very known in polymerization works [413]. The effective recombination rate is calculated as shown in Eq. 5.5:

$$k_{tc,eff} = \frac{1}{\frac{1}{k_{tc}} + \frac{1}{k_{diff}}} \tag{5.5}$$

The diffusion term is calculated by Smoluchowski's equation ($4\pi R_0 D$). However, Popov and Knyazev simplified this calculation by fixing the radius of interaction for termination (R_0) and the mutual diffusion coefficient between two terminating chains (D). As a result, this term is calculated based on the weight averaged molecular

weight and temperature, without considering the chain length of the terminating radicals: $k_{diff} = 6.02.10^{18}.\overline{M}_w{}^{-1.98} exp(-\frac{3127}{T})$ (L/mol/s).

However, considering the rate constant dependence on bulk viscosity, which itself depends on the average molecular weight of the polymer, may not yield an accurate rate constant because termination rates are inherently chain-length-dependent, with smaller molecules exhibiting higher mobility. Nevertheless, this approach was employed, but further studies are required to address this effect in depolymerization properly. Additionally, termination by disproportionation was also considered as 0.1 $k_{tc,eff}$ as suggested by earlier works [297].

For mid-chain scission (k_s), it is known that the cage effect has to be considered as the PE melt impedes the tumbling motions of separating fragments in C-C bond scission, which may result in a lower pre-exponential factor. Popov and Knyazev, fitted k_s to the experimental data [378]; Poutsma concluded that it is difficult to predict an 'efficiency' factor ($0 < f \leq 1$) [263], whereas other HDPE modeling works did not discuss the cage effect. In this study, different efficiency factors (i.e. altering k_s values) were studied and the results were compared to the calculated conversion from time-resolved experiments, with an efficiency factor of 0.01 closely correlating with the model prediction. This value is similar to the data-fitted value obtained by Popov and Knyazev, who used 0.015. This is further discussed in Section 5.3.3.

For backbiting (radical isomerization reactions), the rate is restricted in the melt because of resistance to internal rotations of large C-C segments. Nevertheless, most authors estimate these rates based on experimental data, use gas-phase rate constants or do not consider them at all [263]. For the present work, the backbiting reaction rates were obtained based on ab initio calculations by Van de Vijver *et al.* [414] and Destro *et al.* [415], and then adjusted to the melt phase using the software COSMOtherm (considering hexadecane as the solvent) [414, 416, 417]. However, parameter estimation also had to be used for the rates k_{15}, k_{16}, k_{y5}, k_{y6} up to a factor.

For all other reactions, literature data suggest that similar rate parameters can be applied for the gas phase [297]. The final kinetic parameters used in the simulations are listed in Table 5.1, excluding reaction degeneracies, which were incorporated into the radical reaction rates.

Table 5.1: Macroscopic reaction rate coefficients used for the simulations. Values are divided by the degeneracy.

Reaction Family	**Rate Constant**	A [s^{-1} or L mol^{-1} s^{-1}]	E_a [kcal/mol]	**Ref.**
Mid-chain scission	$k_{s,\mathrm{pp}}$	$1.27 \cdot 10^{17.4}$	86.30	[263]
	$k_{s,\mathrm{pCH_3}}$	$1.00 \cdot 10^{16.0}$	81.26	[418]

Continued on next page

Table 5.1: (continued)

Reaction Family	**Rate**	A [s^{-1} or L mol^{-1} s^{-1}]	E_a [kcal/mol]	**Ref.**
Allyl bond fission	k_{fs}	$3.75 \cdot 10^{19} \cdot T^{-1.13}$	76.20	[419]
Termination by combination	$k_{tc,\mathrm{pp}}$	$5.16 \cdot 10^{11.0} \cdot T^{-0.71}$	-1.92	[420]
	$k_{tc,\mathrm{pCH_3}}$	$4.89 \cdot 10^{11.0} \cdot T^{-0.5}$	-	[421]
	$k_{tc,\mathrm{CH_3CH_3}}$	$3.27 \cdot 10^{13.0} \cdot T^{-1.1}$	0.32	[422]
	$k_{tc,\mathrm{pC_3H_5}}$	$1.02 \cdot 10^{10.0}$	-0.13	[423]
	$k_{tc,\mathrm{CH_3C_3H_5}}$	$1.01 \cdot 10^{11.0} \cdot T^{-0.32}$	0.13	[423]
	$k_{tc,\mathrm{C_3H_5C_3H_5}}$	$1.02 \cdot 10^{10.0}$	-0.26	[423]
Hydrogen abstraction	$k_{H,\mathrm{pp}}$	$6.8 \cdot 10^{7.0}$	14.75	[263]
	$k_{H,\mathrm{ps}}$	$7.6 \cdot 10^{7.0}$	12.78	[263]
	$k_{H,\mathrm{sp}}$	$4.2 \cdot 10^{7.0}$	15.17	[263]
	$k_{H,\mathrm{ss}}$	$6.4 \cdot 10^{7.0}$	14.20	[263]
	$k_{H,\mathrm{CH_3p}}$	$3.0 \cdot 10^{-4.0} \cdot T^{3.65}$	7.15	[424]
	$k_{H,\mathrm{CH_3s}}$	$7.53 \cdot 10^{-4.0} \cdot T^{3.46}$	5.49	[424]
	$k_{H,\mathrm{C_3H_5p}}$	$7.84 \cdot 10^{-2.0} \cdot T^{3.3}$	19.85	[423]
	$k_{H,\mathrm{C_3H_5s}}$	$3.93 \cdot 10^{-2.0} \cdot T^{3.3}$	18.16	[423]
Mid-chain β-scission	$k_{bs,\mathrm{sp}}$	$4.47 \cdot 10^{11.0} \cdot T^{0.57}$	28.04	[378]
	$k_{bs,\mathrm{sCH_3}}$	$1.11 \cdot 10^{10.0} \cdot T^{1.02}$	31.07	[419]
Radical addition	$k_{ra,\mathrm{p}}$	$2.88 \cdot 10^{7.0}$	5.90	[297]
	$k_{ra,\mathrm{CH_3}}$	$17.61 \cdot T^{2.48}$	6.13	[425]
	$k_{ra,\mathrm{C_3H_5}}$	$1.31 \cdot T^{2.60}$	10.90	[426]
Depropagation	k_{dp}	$1.00 \cdot 10^{13.03}$	27.80	[263]
Backbiting	k_{12}	$1.02 \cdot 10^{13.0}$	39.06	[263, 414, 415]
	k_{21}	$2.22 \cdot 10^{4.0} \cdot T^{2.64}$	37.10	
	k_{13}	$2.57 \cdot 10^{12.0}$	38.98	
	k_{31}	$1.65 \cdot 10^{0} \cdot T^{3.48}$	34.80	
	k_{14}	$1.64 \cdot 10^{11.0}$	22.08	
	k_{41}	$2.71 \cdot 10^{10.0}$	23.70	
	k_{15}	$1.16 \cdot 10^{10.0}$	14.86	
	k_{51}	$4.70 \cdot 10^{1} \cdot T^{2.48}$	13.00	
	k_{16}	$2.76 \cdot 10^{9.0}$	13.69	
	k_{61}	$1.79 \cdot 10^{9.0}$	17.20	
	k_{x2}	$3.13 \cdot 10^{12.0}$	40.40	
	k_{x3}	$8.15 \cdot 10^{11.0}$	38.62	
	k_{x4}	$9.05 \cdot 10^{10.0}$	21.83	
	k_{x5}	$2.15 \cdot 10^{9.0}$	15.94	
	k_{x6}	$1.40 \cdot 10^{8.0}$	14.15	

Examples of the reaction degeneracies considered include: for k_H, it is multiplied by 2 for each intermediate carbon; for $k_{\beta s}$, it is also multiplied by 2 when two sets of products are possible; for k_{1x}, it is multiplied by 2; for k_s, it is multiplied by the total number of C-C bounds; for k_{fs}, it is multiplied by total number of double bounds; when it is a diolefin as a reactant for k_{ra}, it is multiplied by 2.

5.2.4 Kinetic Monte Carlo

Similar to a previous study for polystyrene degradation, the direct method has been used to simulate the HDPE degradation kinetics [351]. All the species characteristics (length, unsaturation, and position of the radical) are tracked at all times. Additionally, the reaction rates ($i = 1, ..., n$) are defined as $R_{i,kMC} = k_{i,kMC} N_{C,i}$,

where $k_{i,kMC}$ is the microscopic reaction rate calculated from the macroscopic reaction rate coefficients; and $N_{C,i}$ is the number of unique combinations between reactant molecules inside the control volume (V_C). The species and reaction rates are updated in an interactive procedure illustrated in Figure 5.4.

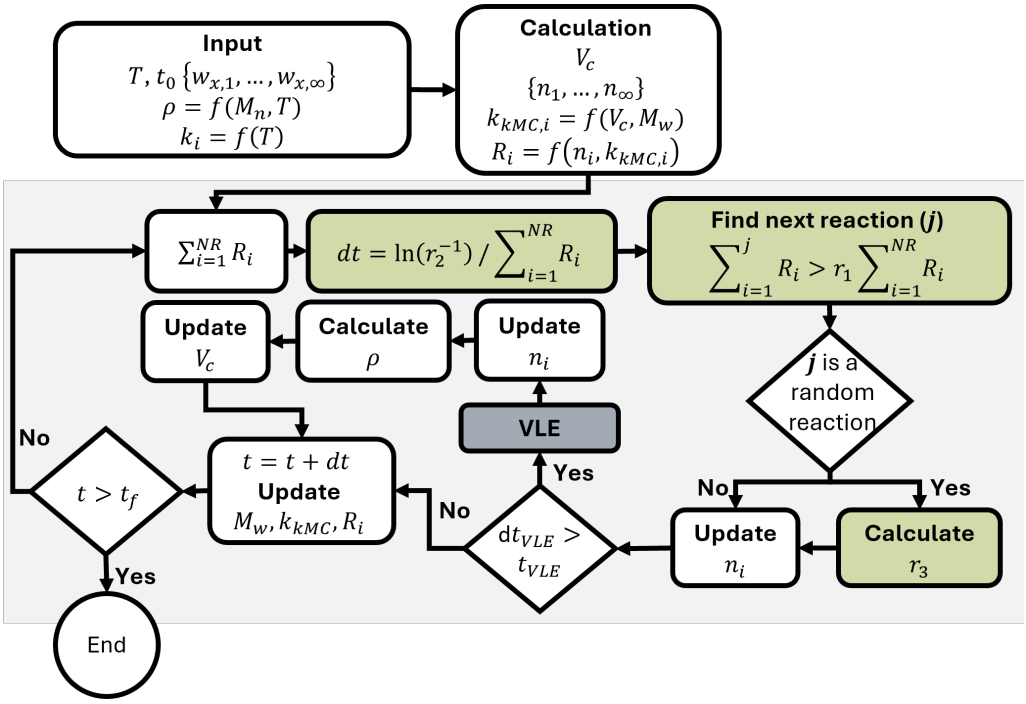

Figure 5.4: Algorithm for kinetic Monte Carlo simulations with thermodynamic equilibrium integration.

Before initiating the interactions, the initial plastic structure is defined based on either GPC data or a Flory-Schulz distribution, and the number of molecules in the control volume (V_c) is determined (see Section 5.2.2). This is the liquid phase at $t = 0$ s.

During the simulation, randomness is introduced in the selection of the reaction step (j) by generating a random number (r_1) from a uniform distribution in the interval $[0, 1)$ (Eq. 5.6). Additionally, the iteration time step (dt) is calculated using a second uniformly distributed random number (r_2) (Eq. 5.7). If the selected reaction involved a random mechanism (e.g., mid-chain scission, hydrogen transfer), a third random number (r_3) is used to select the specific reaction site, such as the carbon-carbon bond to be broken or hydrogen to be abstracted.

$$\sum_{i=1}^{j} P_i \geq r_1 \sum_{i=1}^{n} R_{i,kMC} \tag{5.6}$$

$$dt = \frac{\ln\left(r_2^{-1}\right)}{\sum_{i=1}^{n} R_{i,kMC}} \tag{5.7}$$

Once the reaction occurs, the system's species are updated. This melt-phase composition is sent to the VLE package, which determines the fraction of melt-phase species in equilibrium transition to the gas phase. The transferred species are no longer available for further reactions in the melt phase. As a result, the melt-phase composition is updated again, along with the volume. At the end of each iteration, the kMC reaction rates must be recalculated.

The VLE calculations, however, are not performed every kMC iteration but only at predefined intervals (dt_{VLE}), which corresponds to a certain number of interactions. The optimal frequency of the VLE calculations should be determined in advance and in parallel with the optimization of the control volume [351].

Importantly, the vapor-liquid equilibrium does not suggest that plastic pyrolysis is in equilibrium. The system is dynamic, and the volume, composition and time are updated every interaction as shown in Figure 5.4. As the reaction progresses, the composition at each dt can be used to calculate the bubble and dew temperatures. If the condition $T_{bubble} < T_{system} < T_{dew}$ holds, the distribution of pyrolysis products between the melt and vapor phases is determined by a flash calculation, solving the Rachford-Rice equation. This approach is widely used in dynamic systems to approximate phase behavior under evolving conditions, and more details are given in Section 5.2.5.

5.2.5 Vaporization

Plastic pyrolysis is a multi-phase and multi-component problem. In this study, polymer melting is not considered; the simulation begins at the set pyrolysis temperature without a heating curve, as the micro-pyrolyzer's heating rate is rapid (100 – 250 °C/s) [382]. Moreover, due to the small sample size, the reaction is approximated as isothermal. Thus, phase transition is only considered for the vaporization of pyrolysis products, which is done by considering a vapor-liquid equilibrium between the pyrolysis products in the polymer phase (i.e., liquid or melt phase) and the vapor phase.

The proposed methodology employs an iterative approach between the kMC and VLE calculations. The kMC procedure, shown in Figure 5.4, requires the initial plastic distribution and the kinetic parameters. kMC updates the concentration of the species, and this liquid-phase composition is sent to the VLE package, which calculates the liquid-vapor composition of the system (i.e., at the given T, P, and liquid component fraction). The VLE requires thermodynamic properties, which depend on the chosen equation of state and are described later in this section, and the conjunction kMC+VLE is represented as the "melt-phase kinetics" model box in Figure 5.5. Due to the use of carrier gas, the products are considered to be swept

out of the liquid phase rapidly, and the products in the vapor phase do not react further (unless gas-phase reactions are considered). The interactions repeat while $t < t_f$, or the conversion is below 100%.

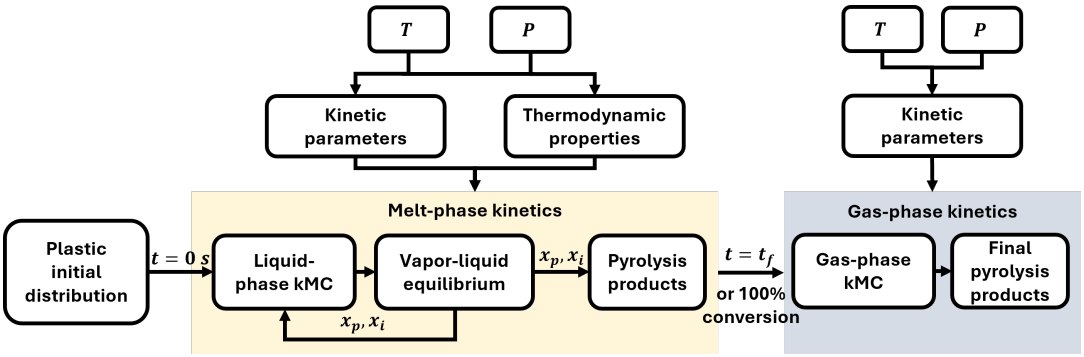

Figure 5.5: Representation of the proposed plastic pyrolysis model with VLE calculations.

Importantly, in the studied pyrolysis system, the carrier gas flow rapidly sweeps out the products to minimize secondary reactions. However, the equilibrium determines the fraction of species that volatilize at a given temperature and pressure, independent of the sweeping effect, as the VLE accounts for the thermodynamic partitioning of species between the melt and gas phases before they are removed. Thus, while the rapid removal in the micropyrolyzer reduces residence time in the gas phase, it does not alter the fundamental VLE considerations, which depend on species volatility and thermodynamic properties.

To solve the equilibrium calculation (considered isothermal and isobaric), the roots of a Rachford-Rice objective function have to be solved [427]. Because the problem includes compounds that are very light (e.g., naphtha compounds) and very heavy (the polymer distribution itself), four modified Rachford-Rice (RR) objective functions can be used:

$$\sum_{i=1}^{N_c}(y_i - x_i) = \sum_{i=1}^{N_c}\frac{z_i(K_i-1)}{1+\Psi(K_i-1)} = 0 \tag{5.8}$$

$$\sum_{i=1}^{N_c}(y_i - x_i) = \sum\frac{z_{g,i}}{\Psi} + \sum\frac{z_i(K_i-1)}{1+\Psi(K_i-1)} = 0 \tag{5.9}$$

$$\sum_{i=1}^{N_c}(y_i - x_i) = \sum\frac{z_i(K_i-1)}{1+\Psi(K_i-1)} - \sum\frac{z_p}{1-\Psi} = 0 \tag{5.10}$$

$$\sum_{i=1}^{N_c}(y_i - x_i) = \sum\frac{z_{g,i}}{\Psi} + \sum\frac{z_i(K_i-1)}{1+\Psi(K_i-1)} - \sum\frac{z_p}{1-\Psi} = 0 \tag{5.11}$$

where N_c are the total number of components; y_i is the component gas fraction

(y_i = number of mols of i in the gas phase/total mols in the gas phase); x_i is the component liquid fraction (x_i = number of mols of i in the liquid phase/total mols in the liquid phase); z_g: light compounds ($T > T_c$); z_p: polymer fraction; z_i: compounds in equilibrium; K_i is the equilibrium constant, or the component VLE partition coefficient ($K_i = \frac{y_i}{x_i} = \frac{\varphi_i^x}{\varphi_i^y}$); φ_i is the fugacity coefficient; and Ψ is the vapor/liquid fraction. Thus, z_i are the heavy pyrolysis products in the region of the thermodynamic equilibrium - i.e. may be volatilized or stay in the liquid phase, and, therefore, are distributed between the vapor and liquid phase according to the K_i value.

Eq. 5.8 (RR1) is the most frequently applied RR expression [185]. It assumes that all components are in equilibrium. However, when a mixture involves substances with asymmetric interactions such as very light gases and polymer in the case of pyrolysis, alternative RRs expressions are proposed for these situations.

Thus, Eq. 5.9 (RR2) do not include light compounds (z_g) in the equilibrium, and these z_g are considered to be instantaneously removed and do not influence the volatilization of the heavier pyrolysis products (z_i) ($T < T_c$). In both RR1 and RR2, the polymer (z_p) is not considered in the calculations.

Eq. 5.10 (RR3) modified RR1 by considering that, although the polymer (z_p) cannot volatilize due to its low partial pressure, it may still retain pyrolysis products, influencing their volatilization. Thus all the products (including the light volatile gases) are either in thermodynamic equilibrium or retained within the polymer melt.

Eq. 5.11 (RR4) includes both hypothesis considered for RR2 and RR3. Light compounds (z_g) are not in equilibrium and are not solubilized by the polymer due to the high temperature [378]. However, heavier pyrolysis products (z_i) ($T < T_c$) are in equilibrium and may be partially soluble in the polymer. The results obtained using these modified Rachford Rice equations (Eqs. 5.9 - 5.11) are compared in Section 5.3.2.

The fugacity coefficients are calculated using the Peng-Robinson (PR) EoS (Eq. 5.9) or PC-SAFT EoS (Eqs. 5.9 - 5.11) based on the following thermodynamic properties. For the PR EoS, the critical properties (T_C, P_C) and the acentric factor (ω) were obtained from NIST ThermoData Engine [428]. However, these values are not available for all compounds. In such cases, a regression was performed to estimate the missing values:

$$\omega_{P,i} = 0.0023\ MW_{P,i}\ + 0.1758 \tag{5.12}$$

$$T_{C_P,i}(K) = 200.72 \ln(MW_{P,i})\ - 373.3 \tag{5.13}$$

$$P_{C_P,i}\ (Pa)\ =\ 3E8\ {MW_{P,i}}^{-1} \tag{5.14}$$

$$\omega_{O,i} = 0.003\ MW_{O,i} + 0.0427 \tag{5.15}$$

$$T_{C_O,i}(K) = 210.2 \ln(MW_{O,i})\ -\ 422.27 \tag{5.16}$$

$$P_{C_O,i}\ (Pa)\ =\ 2E8\ {MW_{O,i}}^{-0.914} \tag{5.17}$$

where $MW_{P,i}$ and $MW_{O,i}$ are the molecular weight of paraffin and olefins, respectively, with i carbons. For diolefins, when the values are not tabulated, the same values as for olefins were used.

For the PC-SAFT EoS, the component's segment number (m), segment diameter (σ), and the segment dispersion energy parameter ($\frac{\varepsilon}{k}$) values were used when available in literature [429], or were determined using Nguyen-Huynh's group contribution approach [430, 431]. Nguyen-Huynh's calculated parameters were also compared with regressed values (linear correlation methodology) [429]. This approach has also been employed by Pàmies and Vega [432] or by Tihic *et al.* [433]:

$$m_{P,i} = 0.0249\ MW_{P,i} + 0.971 \tag{5.18}$$

$${\sigma_{P,i}}^3 m_{P,i} = 1.70\ MW_{P,i}\ +\ 23.27 \tag{5.19}$$

$$\left(\frac{\varepsilon}{k}\right)_{P,i} m_{P,i} = 6.55\ MW_{P,i}\ +\ 177.92 \tag{5.20}$$

$$m_{O,i} = 0.0247\ MW_{O,i} + 0.9173 \tag{5.21}$$

$${\sigma_{O,i}}^3 m_{O,i} = 1.7575\ MW_{O,i}\ +\ 11.983 \tag{5.22}$$

$$\left(\frac{\varepsilon}{k}\right)_{O,i} m_{O,i} = 6.9348\ MW_{O,i}\ +\ 119.25 \tag{5.23}$$

Similarly as for the PR parameters, when the values are not tabulated for diolefins, the same values as for olefins were used. For the polymer, it was considered the HDPE parameter suggested by Peters *et al.* [429]:

$$m_{HDPE} = 0.0263\ \overline{M}_w \tag{5.24}$$

$$\sigma_{HDPE} = 4.0226 \tag{5.25}$$

$$\left(\frac{\varepsilon}{k}\right)_{HDPE} = 253.16 \tag{5.26}$$

The units are m (dimensionless), σ(Å), $\frac{\varepsilon}{k}$ (K). As $m = f(\overline{M}_w)$, the value is updated at all interactions. The polymer was also considered as pseudocomponents (i.e. considering multiple HDPE compounds of different average molecular weights, instead of only one), but no significant difference was seen. For both EoS, the interaction coefficients between the components were maintained in zero.

5.3 Results and Discussion

5.3.1 Experimental results

Figure 5.6 displays the experimental mass fraction yields of the major products from HDPE pyrolysis, grouped by carbon number. Figure 5.6a shows the total yield of paraffins, olefins and diolefins, which are individually plotted in Figure 5.6b-c.

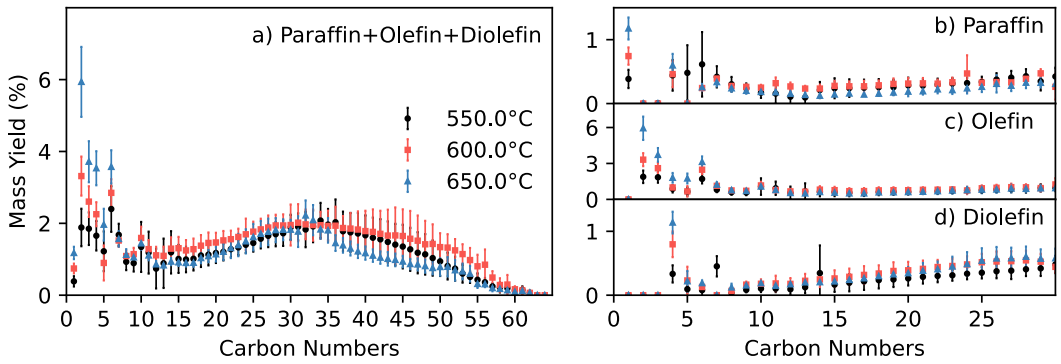

Figure 5.6: Experimental yields (wt%) of major HDPE pyrolysis products at 550, 600, and 650 °C, grouped by carbon number.

The term 'carbon number' refers to the number of atom carbons in a given molecule (e.g., C_1 corresponds to methane, C_2 includes ethane and ethylene, and C_3 includes propane, propylene and propadiene). The standard deviation was calculated based on five independent experiments at 550 °C, three at 600 °C, and 2 at 650 °C. Numerical values, including standard deviations,are provided in the Appendix. For the paraffin, olefin and diolefin lumped (Figure 5.6a), the average was determined as the sum of the individual hydrocarbon averages ($\mu_{POD} = \mu_P + \mu_O + \mu_D$), while the standard deviation was computed as the combined standard deviation ($\sigma_{POD} = \sqrt{\sigma_P^2 + \sigma_O^2 + \sigma_D^2}$).

One of the main contributions of this dataset is the detection and quantification of heavy molecules. Because the analysis was performed in-line, it avoided partitioning the products into gas and liquid fractions, preserving the yields of components with 5 to 8 carbon atoms. These components are often split between both fractions and partially lost in other setups. However, for the yield of paraffins, olefins and diolefins, individually plotted in Figure 5.6b-c the maximum carbon length was limited to 30 carbon atoms because hydrocarbon peaks overlap in the chromatogram for heavier molecules, making it not possible to distinguish them individually, only the total per carbon number is reported. A chromatogram for the HDPE pyrolysis at 600 °C is shown in Figure 5.7 and a zoomed-in view of the range covering of C_{28}-C_{32} paraffins and olefins is shown in Figure 5.8.

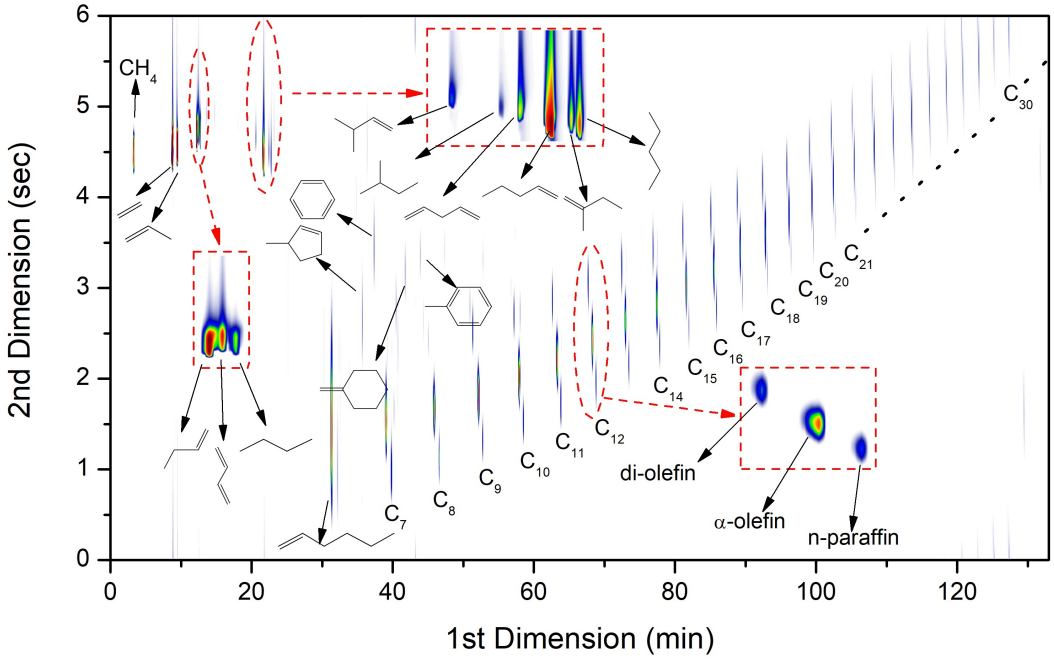

Figure 5.7: HDPE pyrolysis chromatogram at 600 °C.

Therefore, although the proposed model can predict a detailed distribution by hydrocarbon class and chain length, hydrocarbons above C_{30} are presented as lumped in the following sections to facilitate comparison with the experimental data. Additionally, iso-compounds, naphthenes or aromatics were not included in the lump as, at the temperatures studied, only 1.6 to 2.5 wt% of these compounds were obtained.

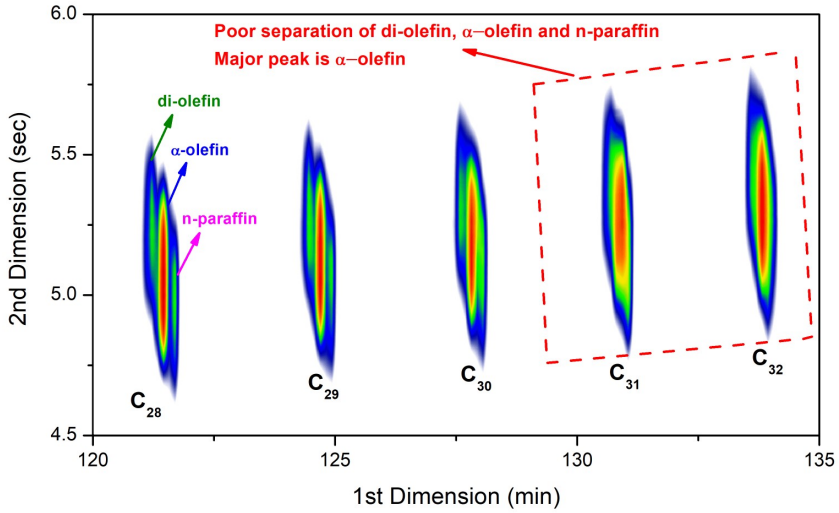

Figure 5.8: Zoomed chromatogram of C_{28}-C_{32} olefins and paraffins from HDPE pyrolysis chromatogram at 600 °C.

While several studies have investigated HDPE pyrolysis, only a few have used a micro-pyrolyzer reactor with online comprehensive gas chromatographic analysis of the products. The mass balances in these studies are often not closed and heavier products with more than 30 carbon atoms are not typically reported or measured, making direct comparisons challenging. Additionally, previous works often lack comprehensive quantification (such as results reported in "area %") or use reactor configurations and/or conditions that may promote additional gas-phase reactions due to prolonged gas-phase residence times [162, 382, 392, 393, 434]. For instance, Krishna *et al.* (2024) tested the pyrolysis at 480, 540, and 600 °C; but only a limited number of major products were quantified, with the maximum carbon number being 28 [382].

Additionally, as previously discussed, other reactor configurations or scaling-up processes may not operate under isothermal conditions or in the kinetic-controlled regime, which can make it more challenging to validate a kinetic model. In contrast, the micro-pyrolyzer reactor, with its small sample size and rapid reaction rates, offers a valuable tool for isolating kinetic effects from secondary mass and heat transfer influences, with minimal gas-phase reactions when an appropriate carrier gas flow rate is used. Validation of melt-phase kinetics is therefore recommended in this or similar systems. Following sections, the kMC+VLE model validation using the experimental data introduced here.

5.3.2 Thermodynamic equilibrium model

HDPE pyrolysis occurs in a liquid system composed by the melted plastic, which, as reaction progresses, also contains pyrolysis products. As discussed in Section

5.2.5, to represent this multicomponent phase equilibrium, the fugacity coefficients are calculated considering the PR or PC-SAFT EoS, considering three modified Rachford-Rice objective functions proposed according to the system's composition: light compounds (z_g, $T > T_c$) – considered to be gas (RR2 or RR4, Eq. 5.9 or Eq. 5.11, respectively), or partially soluble in the polymer melt (RR3, Eq. 5.10) -, compounds in equilibrium (z_i), and the polymer fraction (z_p).

Figure 5.9 illustrates the model's fit to the experimental results at 550 °C for the three proposed approaches: PR for RR2 (a PC-SAFT comparison for RR2 is shown in Figure 5.10) and PC-SAFT for RR3 and RR4.

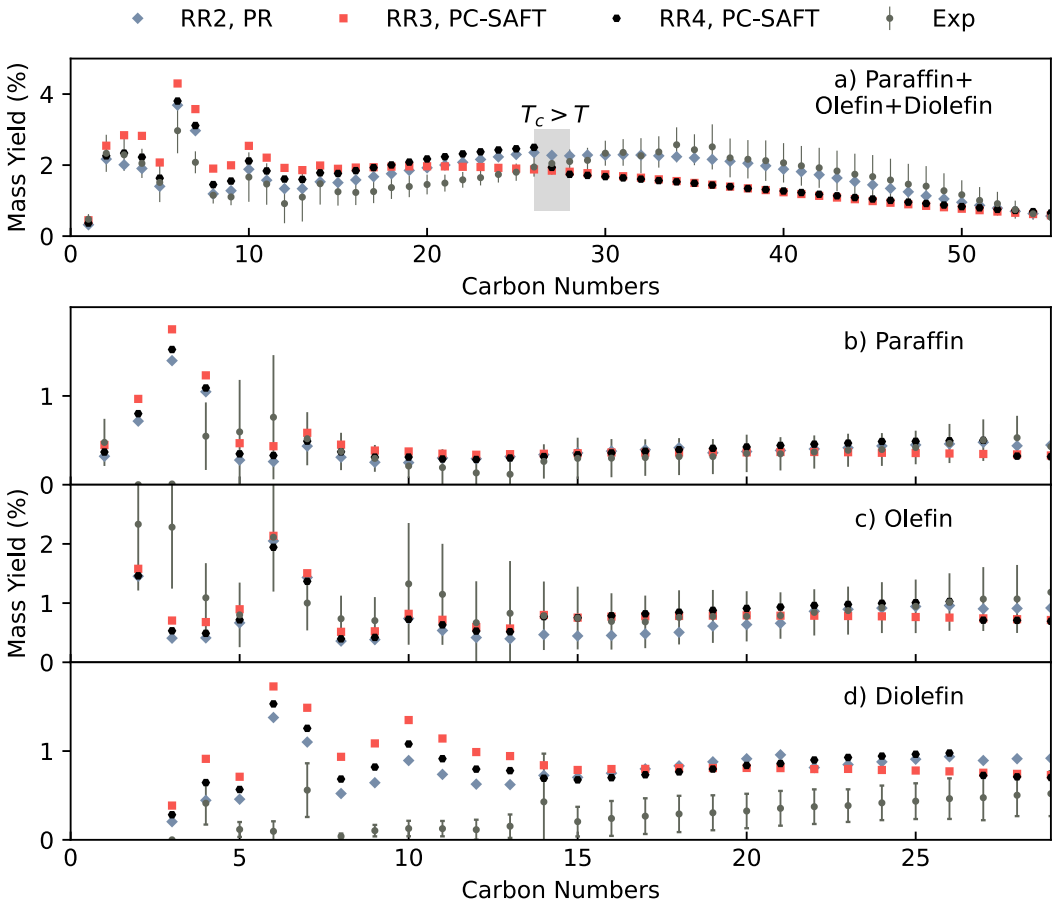

Figure 5.9: Model results for HDPE pyrolysis at 550 °C, comparing different modified Richford-Rice objective functions and equations of state (Peng Robinson, PR, and PC-SAFT). Experimental data are also included for reference.

The results illustrates that the choice of EoS and the thermodynamic parameters can significantly change the volatilization of pyrolysis products, light and heavy components, despite all cases employed the same reaction mechanisms and kinetic parameters. A discontinuity is apparent in the gray-highlighted region ($T_c > T$) only for RR2 and RR4. This is explained because noncondensable gases were considered to have negligible solubility and are not considered in equilibrium in the pyrolysis

condition for RR2 and RR4. Conversely, because there is no z_i/z_g distinction, a continuous behavior is seen for RR3 as it considers that the gases might be soluble in the polymer.

Overall, RR2 (PR) shows better agreement with experimental data compared to RR3 or RR4 (PC-SAFT), as incorporating the polymer-phase yield lower vapor/liquid fractions (Ψ) and resulted in reduced volatilization for the components in equilibrium. However, theoretically, RR3 and RR4 are the most correct representation of the system because the polymer is accounted for. Nevertheless, it may be that the EoS parameters need to be better estimated and adjusted, as discussed later in this section.

Figure 5.9 also shows that model captures the general mass yield trend for both the lump and the individual hydrocarbon types, particularly for paraffins and olefins. For diolefins, the model tends to overpredict the yield. This overprediction is also observed in the lump yield, particularly in the C_{15} – C_{26} range. A key experimental limitation is the mass closure at 550 °C, which averages approximately 76 %, leaving a portion of the products unaccounted for. This discrepancy is worth further investigation to better identify potential unmeasured species or losses [434]. Additionally, for C_2 and C_3 hydrocarbons, the experimental data lumped the products as olefins due to co-elution of ethane and propane with ethylene, propylene, and propadiene [400]. Addressing these uncertainties will be essential for refining the model and improving its predictive accuracy.

Moreover, although the C_6 and C_7 yield are overpredicted to the previously mentioned diolefins overprediction, these products are also correlated with the yield of C_3 and C_4, which, in contrast, show good agreement with the experimental data. This is because all of these products primarily result from backbiting reactions (1,5 and 1,6). In fact, in molar fraction, the yield of C_3 is very similar to that of C_6, and the same applies to the yields of C_4 and C_7.

In Figure 5.9, Nguyen Huynh's group-contribution PC-SAFT parameters were used [430, 431]. However, as these parameters lack validation for all pyrolysis products and conditions, alternative PC-SAFT parameter sets were explored, as shown in Figure 5.10. According to Peters *et al.* [70], the parameters σ(Å) and $\frac{\varepsilon}{k}$ (K) can be fixed of the length, only varying the segment number (m) (Eqs. 5.24 - 5.26). The parameters were also considered the same regardless if saturated/unsaturated. The results using these parameters are highly comparable to those obtained with Nguyen Huynh's parameters. In contrast, the model's outcome is different if the regressed values (Eqs. 5.18 - 5.23) [432, 433] are used.

When comparing the results of PC-SAFT and PR, both using RR2, the results are generally similar (Figure 5.10a). Particularly, the model fit improves for the C_{15} – C_{26} range when Nguyen Huynh's group-contribution PC-SAFT parameters are

used or σ and $\frac{\varepsilon}{k}$ are fixed. However, the fit worsens beyond C_{30} and it also predicts volatilization of heavier products, which could explain the remaining unquantified mass.

Regarding the different Rachford-Rice functions, it is not possible to affirm which is the best option. While RR3, which accounts the solubility of gases in the polymer, provides a more realistic system representation, it exhibits larger deviations from experimental data. This discrepancy could be attributed to the model's neglect of mass transfer effects, which can significantly influence volatilization. Furthermore, although PC-SAFT is theoretically well-suited for oligomers and polymers, there are uncertainties in its parameters, especially for heavier molecules and binary interaction parameters (k_{ij}), which were assumed to be zero as there is also not enough data in the literature to calculate or estimate these values. However, the assumption that k_{ij} values are zero may introduce significant deviations in the results obtained with RR3 and RR4.

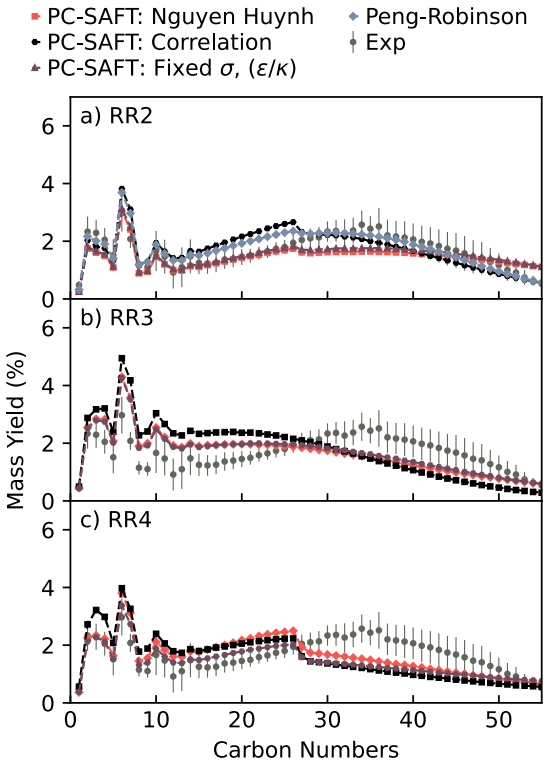

Figure 5.10: Comparison of three different parameter sets used for PC-SAFT EoS at 550 °C to calculate the modified Richard-Rice objective functions RR2, RR3, and RR4. Peng-Robinson's RR2 result is included for the sake of comparison.

On the other hand, while the widely-used PR EoS is not ideal for modeling asymmetric mixtures or systems with significant chain contribution effects, such oligomers, due to its neglect of molecular geometry and structure [435, 436], it generally yields better agreement with the experimental data (Figure 5.9) and faster

computational times compared to PC-SAFT [427]. The results may be improved by future studies that estimate interaction parameters for PR and may help reducing deviations caused by long-chain molecules. Nevertheless, although PC-SAFT also provided very satisfactory results using RR2, the subsequent sections present results based on the PR EoS using RR2.

Lastly, predicting the vaporization of pyrolysis products would not be feasible without the VLE calculation. As noted earlier, this topic is often oversimplified in the literature. This work introduces a promising methodology that can be further refined to optimize plastic pyrolysis and other petrochemical processes.

5.3.3 Model validation at different temperatures

The previous section presented the final product distribution results for HDPE pyrolysis at 550 °C. However, the model is also capable of tracking the melt-phase composition, including the distribution and average molecular weights ($\overline{M}_n$ and $\overline{M}_w$), as well as the product distribution and mass loss ("conversion") during the pyrolysis reaction. This section provides these additional details and includes the model validation at various temperatures.

Still, for HDPE pyrolysis at 550 °C, Figure 5.11a demonstrates the rapid volatilization of the entire product spectrum (C_1-C_{70}) during the initial stages of pyrolysis. Even at low conversions (e.g., 10% at 0.4 s), a significant distribution of products across the entire carbon number range is observed. The C_1-C_{10} products are primarily formed by backbiting reactions and their relative abundance within the total product range remains relatively constant throughout the reaction (17-19%). Heavier products result mainly from random reactions (e.g., intermolecular hydrogen abstraction), and the thermodynamic model represents the volatilization of these products according to the pyrolysis conditions and the melt-phase component.

As volatilization occurs, the average molecular weight decreases (or the conversion increases) very rapidly (Figure 5.11b). The conversion is calculated by considering the number of carbon-carbon bonds remaining in the melt phase relative to the initial plastic. Similar conversion values are obtained considering the mass remaining in the melt phase or the reduction in volume is considered. The $\overline{M}_w$ value increases slightly at high conversions due to volatilization of light products, while HDPE molecules of different sizes remain in the system. These molecules, although present in much lower amounts than at the beginning, remain in the system and continue to degrade, but at a slower rate as the overall reaction rate significantly decreases after 90% conversion.

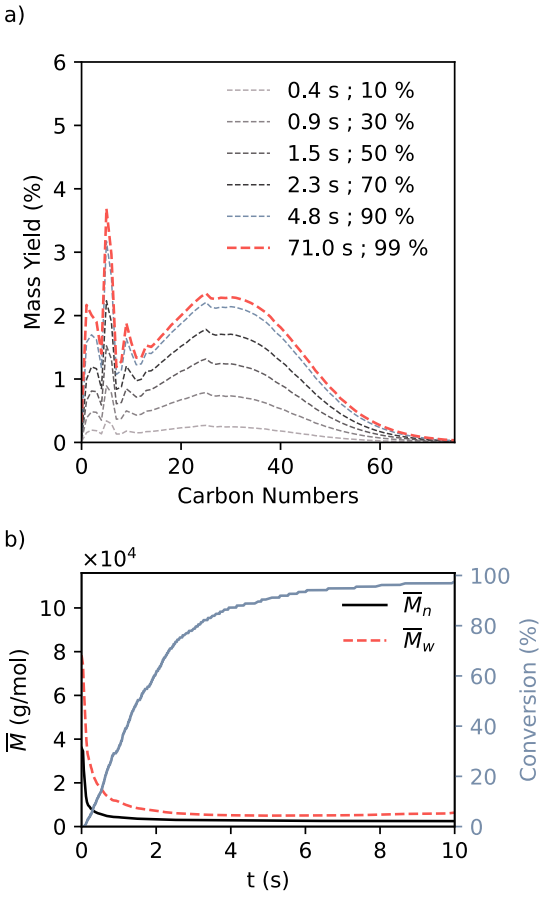

Figure 5.11: Modeled evolution of HDPE pyrolysis products at 550 °C: a) mass yield relative to the initial plastic mass; b) Average molecular weights and conversion rates.

Beyond product distribution, validating the reaction time is important. At 550°C, pyrolysis products can already be detected in less than 0.2 s [300]. Due to the rapid reaction time at this temperature, lower temperatures were chosen (450 °C and 500 °C) to conduct time-resolved experiments in the micro-pyrolyzer unit using an MS detector to quantify when volatiles were leaving the reactor.

As shown in Figure 5.12 the signal (continuous line) was normalized to the area under the curve, enabling conversion calculations at different time intervals (circles). These time-resolved results confirm that higher temperatures significantly reduce reaction time while the overall rate decreases over time. Similar trends have been reported in the literature: at 400 - 440 °C, initial pyrolysis products appear in under 5 minutes [378], while at 500 °C, they emerge in less than 10 seconds (0.16 minutes) [300].

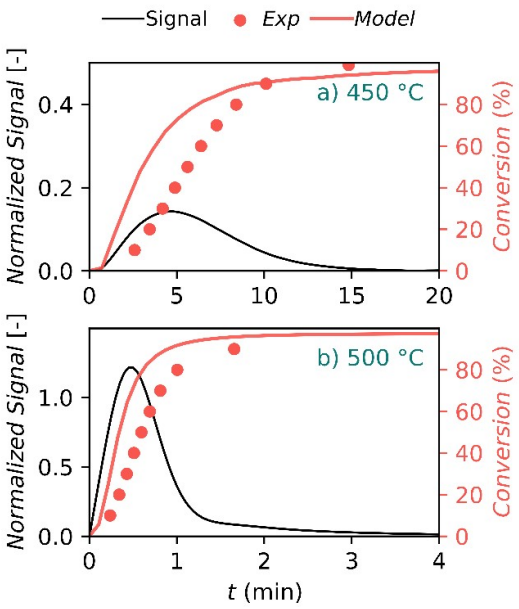

Figure 5.12: Conversion at 450 and 500 °C. Model results (-) versus experimental data: MS signal (-) (continuous line) and respective conversion (•).

The values, particularly at high conversions (> 80%), in Figure 5.12 have some uncertainly because the raw signal was adjusted according to a calculated baseline. However, despite this uncertainty, the conversion profiles obtained at both 450 and 500 °C are generally consistent with those reported in the literature [437–441].

Furthermore, Figure 5.12 demonstrates that the model accurately captures the pyrolysis progression both at 450 and 500 °C. This close agreement suggests that the kinetic model effectively represents not only the product distribution, but also conversion trends and the temperature dependency. It is important to note that the reaction times obtained from simulations do not account for heating rates, which are extremely high in the micro-pyrolyzer. However, for scale-up, heating rates must be considered, as plastics have low thermal conductivity.

At 450 °C and 500 °C, besides time-resolved experiments, product quantification was challenging. Nevertheless the time-resolved data provided valuable insights into the reaction dynamics. Further work will focus on product quantification and model validation at a broader range of temperatures. Later in this section, product distribution is also validated at 600 and 650°C.

When validating the pyrolysis time, it was observed that the conversion is strongly influenced by the rates of mid-chain scission (k_s), termination by combination (k_{tc}), and allyl bond fission (k_{fs}). This occurs because these reactions affect the radical concentration in the system (initiation and termination), whereas the others maintain a constant radical concentration (equivalent to propagation reactions). It is also known that mainly k_s and k_{tc} are influenced by diffusional effects, making

the direct use of gas-phase constants unrealistic. While previous mechanistic studies have proposed methods to account for these effects, a robust and reliable strategy remains uncertain.

The mid-chain scission rate constant (k_s) should be multiplied by an initiation efficiency factor (f), which accounts for the fraction of radicals that escape the cage where they are formed. This adjustment is necessary because, in a viscous polymer melt, the limited mobility of fragments restricts their diffusion away from scission sites, increasing the likelihood of recombination [442]. While smaller radicals are more likely to escape the cage than polymeric radicals, a single parameter is typically used for all chain lengths [443]. In our work, a cage-effect efficiency factor of $f = 0.01$ was adopted. As mentioned in Section 5.2.3, Popov reported a similar value (0.015). A comparison of system conversion with different f values is provided in Figure 5.13, demonstrating that higher f values mean faster overall rate.

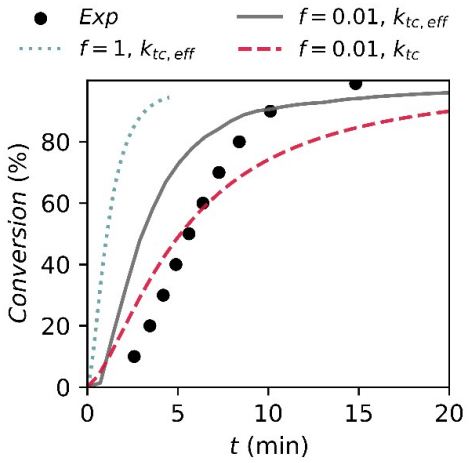

Figure 5.13: Conversion profiles at 450 °C: experimental (•) obtained from time-resolved experiments, and modeled conversion profiles for different initiation efficiencies (f) and k_{tc} ($k_{tc,eff}$ is diffusion limited, and k_{tc}).

Termination by combination is also known to be lower in the melt-phase than in the gas phase due to reduced radical mobility in the melt, which decreases the probability of radical encounters. As conversion progresses and molecular weight decreases, $k_{tc,eff}$ increases. It was also observed that incorporating the influence of diffusion (k_{diff}) (Eq. 5.5) results in an overall increase in the reaction rate. This effect can be attributed to the higher radical concentration: with less frequent recombination, more radicals remain active, accelerating the reaction. Consequently, propagation reactions, such as hydrogen abstraction followed by mid-chain scission, become more frequent. A comparison of system conversion without considering k_{diff} in shown in the Figure 5.13.

In practice, both k_s and $k_{tc,eff}$ are influenced by diffusion and equally challenging

to estimate, with their effects on reaction kinetics being interconnected. Thus, changes in $k_{tc,eff}$ considerations (such as the gel-effect considered by Kruse *et al.* (2002) [294]), may also impact the efficiency factor for k_s. Moreover, depending on the reactions considered, the estimation of the efficiency factor may require further refinement. For instance, if branching pathways were incorporated, it would likely need re-estimation to reflect overall kinetic changes. These uncertainties should be addressed in future works. Nevertheless, as shown in Figure 5.12, the time-evolution of the pyrolysis products were well represented at both 450 and 500 °C with the current approach.

Finally, multiple k_{fs} values were found in the literature. We compared the values of Power *et. al.*, Tsang, Mehl *et al.*, Zhou *et al.*, and Popov and Knyazev [378, 419, 444–446], which vary up to two orders of magnitude (see Table 5.2). The value that best matched the experimental data was the one of Power *et al.* as this rate was calculated for 500 – 1500 K and 0.01 – 1000 atm, it is more accurate for the conditions found in plastic pyrolysis than the values obtained for combustion (Mehl *et al.*, and Zhou *et al.*) or other systems. It was also tested if considering the initial polyethylene as olefins (instead of paraffins) would make a significant change, but the conversion times remained very similar.

Table 5.2: Comparison of different literature for allyl bond fission constants. R = 8.314 J mol^{-1} K^{-1}.

Reference	**Expression for k_{fs} (s^{-1})**	**k_{fs} (s) at 500 °C**	**$k_{fs}/k_{fs,\mathbf{Power}}$**
Power et al. [419]	$3.75 \cdot 10^{19} \cdot T^{-1.13} \cdot e^{-38347.3/T}$	5.89×10^{-6}	1
Tsang [444]	$10^{16} \cdot e^{-35900/T}$	6.83×10^{-5}	11.6
Westbrook [445]	$10^{16} \cdot e^{-297000/RT}$	8.61×10^{-5}	14.6
Curran [446]	$9.86 \cdot 10^{21} \cdot T^{-2.086} \cdot e^{-295000/RT}$	1.09×10^{-4}	18.6
Popov and Knyazev [378]	$2.02 \cdot 10^{14} \cdot e^{-38711/T}$	3.64×10^{-8}	0.01

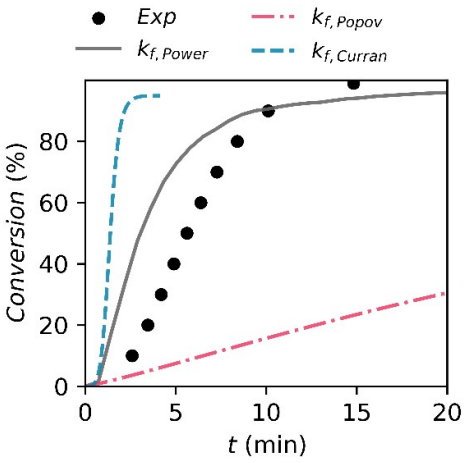

Figure 5.14: Time-resolved experiments at 450 °C: FID signal (-) (continuous line) and respective conversion (•). Modeled conversion profiles at 450 °C are also shown for different allyl bond fission constants.

With the defined reaction rates, Figure 5.15 compares the model predictions with micro-pyrolyzer experiments conducted at 600 and 650 °C. (Previous model results at 550 °C already considered these k_s, k_{tc} and k_{fs}) for the lumped products (Figure 5.15a and b) and individual hydrocarbon groups: paraffins, olefins or di-olefins (Figure 5.15: c-h). However, at these temperatures, even a volatile residence time as short as 0.3 s is sufficient for secondary gas-phase reactions, evidenced by the model's underprediction of light hydrocarbons (C_1–C_5). (The residence time is estimated based on reactor dimensions, considering the carrier gas flow rate and, if applicable, the volatilization of other products.)

Therefore, in this case, as illustrated in Figure 5.5, the melt-phase pyrolysis results serve as input for a gas-phase kinetic model, which includes the same reaction types as the melt-phase model and same kinetic parameters, except mid-chain scission and the backbiting rates, as described in Section 5.2.3. The gas-phase parameters are available in the Appendix.

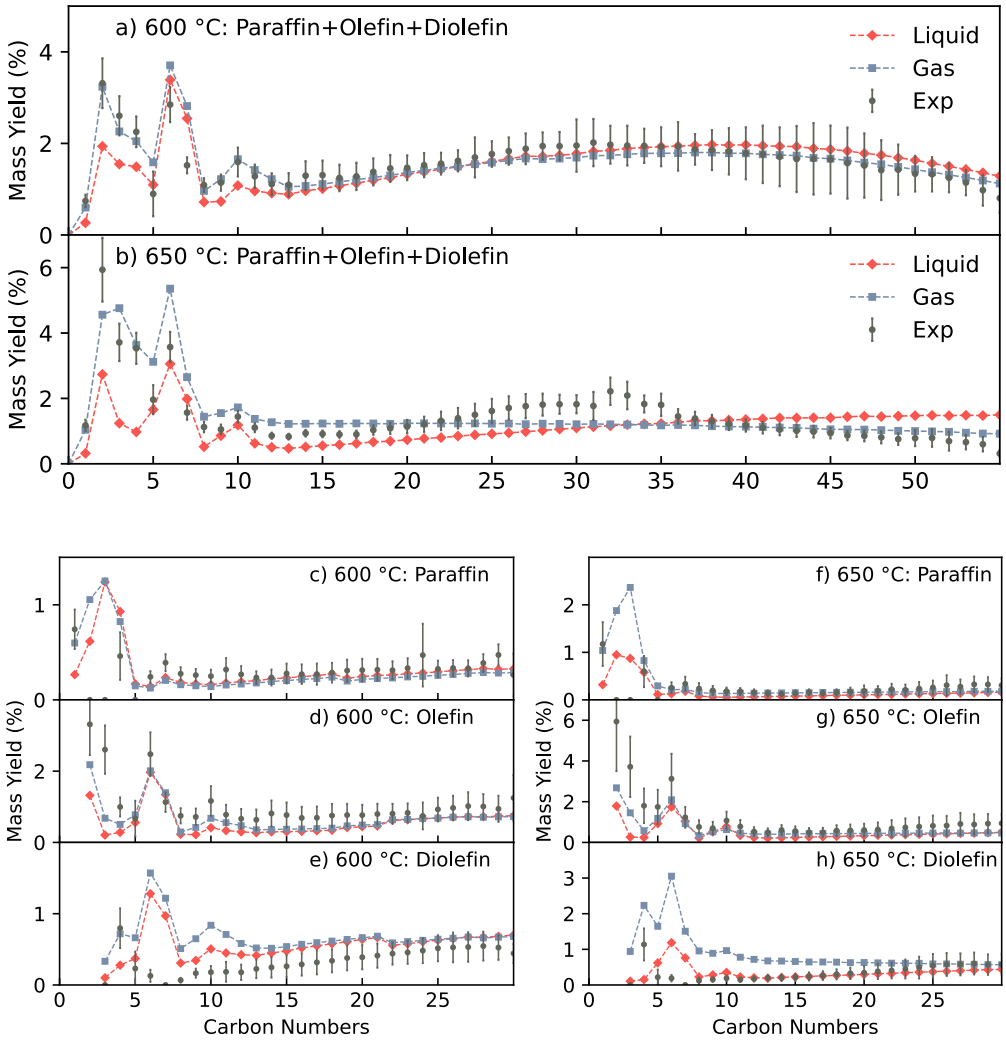

Figure 5.15: Experimental results (•, with vertical error) for HDPE pyrolysis at 600 °C (a, c-e) and 650 °C (b, f-h), compared with predictions: melt-phase pyrolysis (⧫) and melt + gas-phase pyrolysis (■).

The inclusion of secondary reactions in the gas-phase model increases light gas production while reducing the mass fraction of heavier hydrocarbons. A comparison with the melt-phase-only results (Figure 5.15) suggests that longer residence times reduce wax formation and favor the production of lighter hydrocarbons, aligning with observations from pyrolysis reactors with reflux. Similarly, an increase in scale is also expected to enhance the yield of lighter products for the same reason. However, it clear that extended residence times and intensified secondary reactions also leads to a higher yield of olefins and, specially, diolefins, which can subsequently promote the formation of naphthenes and aromatics.

Additionally, the model effectively captures the overall trend of product distribution across carbon numbers. However, as observed at 550 °C, it tends to overpredict diolefin yields, despite its good agreement with experimental data for paraffins and olefins. Furthermore, C_2, C_3 and C_5 hydrocarbons co-eluted, although were

classified as olefins. Overall, the model provides a robust representation of HDPE pyrolysis products, reinforcing its applicability for studying mixed plastic pyrolysis and optimizing the process.

5.3.4 Influence of the pressure

As demonstrated in previous sections, the model accurately predicts HDPE products, capturing key details such as reaction time, carbon chain length, and the distribution of hydrocarbon classes (paraffins, olefins, and diolefins). Since the experiments were conducted in a micro-pyrolyzer, the data was obtained with minimal influence from secondary effects, such as heat and mass transfer limitations. However, the pressure in the pyrolysis reactor operated at a fixed pressure of 2.7 bar, which could not be easily adjusted. Thus, to assess the impact of pressure on thermodynamic equilibrium, the model was tested at different pressures, aiming to simulate other pyrolysis systems such as those that utilize a back-pressure regulator.

Figure 5.16 presents the model results at 550 °C and pressures of 1.0, 2.7 and 5.0 bar. At higher pressure, heavier hydrocarbons – those in equilibrium between the melt and vapor phases (see Section 5.3.2) – face greater resistance to volatilization, resulting in lower mass fraction yields. This trend aligns with experimental observations reported in other studies [447, 448]. This occurs because the phase partitioning of species between the melt and gas phase is governed by their fugacities, which are pressure-dependent. Therefore, changes in system pressure alter the equilibrium condition. These findings suggest that pressure can be a key parameter for optimizing wax formation, reinforcing its importance in the design and optimization of plastic pyrolysis processes.

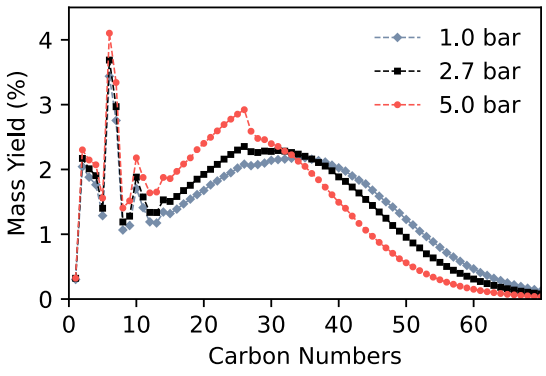

Figure 5.16: Modeled product distribution of HDPE pyrolysis at 550 °C under different pressures (1.0, 2.8 and 5.0 bar).

5.3.5 Influence of the initial molecular weight distribution

Since only a single HDPE grade was tested, all the experiments were conducted with the same molecular weight distribution. Therefore, to assess the influence of other $\overline{M}_n$ and $\overline{M}_w$, the initial polymer distribution was artificially constructed, as described in Section 5.2.2. Figure 5.17 presents the results for $\overline{M}_n$ values of 20, 35, and 90 kg/mol. As $\overline{M}_n$ increases, there is a corresponding increase in the production of light gases (C_1 to C_10). This can be attributed to enhanced hydrogen-transfer, mid-chain β-scission, or depropagation reactions occurring before the polymer becomes volatile.

However, the impact of the initial $\overline{M}_n$ on yield may not be as significant in a real industrial recycling context as variability exists in HDPE grades and other types of plastics. As a result, variations in pyrolysis yields are commonly observed. Furthermore, heat and mass transfer dynamics can also significantly influence outcomes. For instance, larger quantities of plastic or a larger reactor may prolong the time required to reach the optimal reaction temperature, leading to the initiation of reactions at lower temperatures, which tend to produce fewer light gases. Moreover, gas-phase reactions may also change the yields, as discussed earlier.

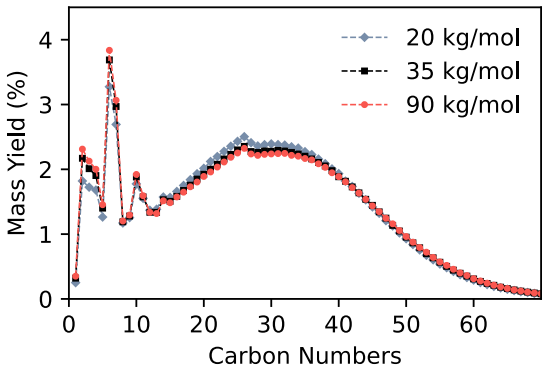

Figure 5.17: Modeled product distribution of HDPE pyrolysis at 550 °C and 2.7 bar for HDPE with different initial $\overline{M}_n$ values.

5.4 Conclusion

This work presents a mechanistic kinetic model for the thermal degradation of HDPE using kinetic Monte Carlo (kMC) simulations. kMC was chosen because it tracks all radical positions and chain lengths without relying on assumptions about product or melt-phase distributions, a limitation of other methods. While kMC offers high accuracy, it is computationally intensive and challenging to model certain reactor configurations. Despite this, it remains a valuable tool for understanding pyrolysis kinetics.

To improve model accuracy, the kMC was integrated to a thermodynamic equilibrium model using either the Peng-Robinson or PC-SAFT equation of states to account for pyrolysis product volatilization. This aspect is often overlooked in the literature, where volatilization is set arbitrarily without considering temperature and pressure effects. The findings, supported by experimental data, demonstrated that including vapor-liquid equilibrium (VLE) is crucial for accurately predicting product volatilization and optimizing pyrolysis processes.

The use of kMC to model semi-batch reactors, especially when integrated with thermodynamic models, is rare in the literature, making our approach a novel and more accurate method for predicting pyrolysis products based on system temperature and pressure. The model has been validated at 550-650 °C using established kinetic parameters, and time-resolved experiments at 450 and 500 °C further support its accuracy in predicting conversion trends. However, broader validation is needed under different conditions. Additionally, further refinement is required for the VLE model, particularly in EoS parameters such as binary interactions between polymers and pyrolysis products. The lack of validated parameters, especially for heavier compounds, may impact prediction accuracy. Future work should also address model simplifications, including the exclusion of ramifications and cyclization reactions, the simplified treatment of diffusion effects (e.g., initiation efficiency or gel effect), and the influence of factors such as mass transfer and long residence times (e.g., reflux or operation without carrier gas), which may affect reactions like Diels-Alder.

Chapter 6

Life Cycle Assessment of Plastic Pyrolysis: Challenges, Limitations, and Opportunities

6.1 Introduction

The previous chapters have detailed the development of models for polystyrene and polyethylene pyrolysis, illustrating the crucial role of process parameters such as temperature, pressure, and gas residence time as they directly affect product yields, which in turn influence the overall efficiency and sustainability of recycling processes. The development of the PS and PE models, however, are only the initial building blocks towards the final goal of truly simulating plastic waste, which, therefore, must consider a mixture of different plastics, impurities, moisture, biomass, and other materials.

Additionally, it is important to recognize that some technologies used commercially can be very different from those commonly used in scientific investigations, which can delay technological development. For instance, some technologies are based on the screw (or auger) reactor technology, such as the one developed by Agilyx, which can process 50 tons per day (TPD) in continuous mode, while other technologies are based on stirred tank reactors (STR) operated in semibatch mode (Plastic Energy – 20 TPD), rotary kiln (VadXX, 60 TPD), melting vessel (Nexus, 50 TPD), fluidized bed (Recycling Technologies, 20 TPD) [25, 143, 449]. Meanwhile, most scientific research studies are based on bench-scale reactors, usually operated in batch and semi-batch modes, and make use of thermogravimetric analysis (TGA), micropyrolysis, fluidized bed reactors, and closed stirred tank batch reactors [94, 145].

In parallel, important effects associated with the huge variety of distinct plas-

tic wastes (due to the spatio-regional-seasonal variations of municipal solid waste), impurities eventually present in the residues (that could be dangerous, corrosive to the pyrolysis process/cracker, or toxic to human health), reactor designs, and reactor performances (due to the inherent poor heat and mass transfer rates of plastic mixtures, presence of water and other impurities) have been mostly overlooked in the research studies.

Moreover, as discussed in the previous chapter, phenomenological descriptions of polymer degradation and the consequential integration with representative mathematical mechanistic models have been relatively scarce, making the development and implementation of optimization and control tasks more difficult [313, 314, 334].

Given these gaps, it is understandable (although not acceptable) how recycling technologies can be simultaneously marketable and misleading. A company may claim recycling activities without sharing yields, conditions, and environmental impacts, making independent evaluation of sustainability impossible. Conversely, based solely on a small collection of fundamental studies, one may equivocally claim that the technology is either unsustainable or sustainable, overlooking the holistic effects of recycling technologies on the chemical chain and neglecting the available degrees of freedom that can significantly affect the environmental impacts of actual large-scale activities, as recommended by consistent circular strategies.

To support more rigorous assessments, exergy (or entropy) analysis is a key tool for energy-intensive production processes [450, 451]. Few articles have been published focusing on post-consumer plastic pyrolysis and such work should certainly be encouraged [452, 453]. Another valuable method is life cycle assessment (LCA), which is among the most established methodological procedures [454]. Particularly, LCA analyses can quantitatively translate mass and heat balances into greenhouse gas (GHG) emissions, process toxicity to human health and ecosystems, and relative advantages of using either recycled or virgin raw materials such as naphtha or liquefied natural gas. They can also assess the benefits of using renewable hydrocarbon feed streams, including ethanol or succinic acid, among other valuable information [454–456].

However, LCAs are still frequently conducted using non-optimized data or based on fixed conditions and a fixed feedstock, often disregarding how the data was generated. As a consequence, biased conclusions about the sustainability of plastic recycling technologies can result.

This issue is compounded by the lack of industrial data and well-documented sets of experimental data, which makes it very difficult to prepare accurate life cycle inventories and evaluate corresponding LCA models [457, 458]. With inadequate information, results can be inconsistent, dubious, or unsatisfactory. In fact, pyrolysis results can be highly dependent on the experimental apparatus, which can wrongly

suggest reproducibility issues and help explain the apparent scatter in data reported by scientific studies [147, 459]. Consequently, when the LCA user does not fully understand the recycling process, the current dispersion of data and wide range of degrees of freedom may lead to inappropriate use of available data.

For example, when a researcher uses reference pyrolysis data collected at 800 °C - a common temperature in many scientific studies, yet far from the typical industrial range of 400–500 °C — the analysis will reflect unnecessary energy consumption, leading to misleading conclusions about environmental impacts. Furthermore, if the researcher overlooks that pyrolysis depends on numerous process variables that can synergistically influence product yields [147, 459], the resulting LCA inventory will likely be biased. Moreover, due to the significant differences in scale and conditions between industrial and academic setups, critical factors remain unclear. For instance, if a carrier gas (usually nitrogen) is accounted as a consumable, as done in experimental studies but not industrial processes, the predicted environmental impacts will be much higher due to the added burden of gas manufacture, purification, and recycling. On the other hand, the effects of carrier gas and hence residence time on heat and mass transfer, as well as product vaporization rates, have been largely overlooked [94, 129, 460]. As a matter of fact, no consensus exists about optimal conditions and reactor designs for plastic pyrolysis [138, 459]. While this can be considered tolerable due to the high sensitivity of the process to feed compositions and variables, better reporting and analytical practices are essential for both pyrolysis data and LCA analyses.

Another consideration is that typical LCA studies regarding chemical recycling often compare it to landfill disposal, plastic incineration, and mechanical recycling. While these are legitimate strategies, mechanical recycling is complementary to chemical recycling and should not be treated as a technological competitor. Furthermore, landfill disposal and incineration, known to be environmentally harmful and non-value-adding, should not be used as baselines in most fundamental studies. Including them often results in biased positive evaluations of the alternative technology under study, as it will almost always appear more favorable by comparison [461].

In summary, to highlight key points previously discussed, LCA studies focused on the chemical recycling of polyolefins via pyrolysis are briefly reviewed in the following section. The main objective is to illustrate the most commonly used approaches in published LCA studies and to identify opportunities to improve the consistency and representativeness of future investigations.

6.2 LCA analyses of polyolefins pyrolysis

Table 6.1 provides a brief overview of published LCA studies on the chemical recycling of polyolefins via pyrolysis. Other chemical recycling technologies, such as microwave pyrolysis, gasification, and hydrogenation, were considered out of scope due to their current technical limitations or lower technology readiness levels compared to pyrolysis [22, 103, 141, 144]. Similarly, solvolysis and enzymatic degradation were excluded because they are not suitable for polyolefins like polyethylene and polypropylene [90, 462]. Nevertheless, these processes would also benefit from the application of LCAs, and further research in this direction should be encouraged.

Among the 16 studies presented in Table 6.1, five reported the use of confidential information [323, 463–466], which hinders the possibility of independent and critical evaluation. Other studies relied on laboratory-scale data [467–469], without a clear connection to industrial-scale operations, raising concerns about the applicability of their findings to practical chemical recycling scenarios. While some researchers extrapolated lab-scale results using process simulators, pyrolysis units were often represented using simplified conversion, yield, or stoichiometric reactor models, without incorporating kinetic mechanisms.

For example, ZHAO e YOU [469] (2021) based their LCA on pyrolysis experiments performed with just 2 g of high-density polyethylene (HDPE). They then extrapolated the results to a 2 ton/h reactor, despite the significant uncertainty associated with scaling product yields and compositions due to mass and heat transfer limitations or differences in reactor configuration.

Additionally, key information regarding pyrolysis operating conditions is often missing. While most studies identified pyrolysis oil as the primary product, the reported yields varied widely, from 65 to 85 wt%, and in many cases, the operating conditions were not disclosed, making cross-study comparisons difficult. To accurately assess inputs, outputs, and related environmental impacts, it is essential that studies report at least the reactor type, operating temperature, and residence time, even if the residence time is inferred from the residual plastic left in the reactor, as these are among the most influential parameters [139]. It is also important to state whether the process involves pure thermolysis, catalysis, or catalytic upgrading of pyrolysis vapors. Although atmospheric pressure is commonly assumed, explicitly reporting the operating pressure is still recommended, as it can influence reaction kinetics and vapor–liquid equilibria.

Moreover, both upstream and downstream steps can significantly affect product quality and overall LCA outcomes [135, 470–473]. For instance, preheating plastic in an extruder can reduce energy demand and remove hydrochloric acid, while downstream catalytic upgrading of pyrolysis vapors can improve product specifications.

However, many studies fail to consider or even mention these steps.

Regarding the LCA methodology, most studies adopted the approach based on attributes combined with system expansion [454]. While useful for comparing technologies, this method is often applied to justify chemical recycling in contrast with mechanical recycling, incineration, or through "avoided impacts" such as reduced fossil fuel use. However, to fully understand the regional socio-environmental impacts of pyrolysis, impact categories should be geographically contextualized, a step that remains rare in the literature. By neglecting regional variability, this omission introduces a significant source of uncertainty, as it assumes equivalence among recycling systems that differ substantially in practice [474].

As previously discussed, assigning credits for avoiding incineration or landfill may not be appropriate in most cases, given that these practices are not aligned with circular economy principles and should generally be avoided, with the exception of cases involving genuinely unrecyclable materials.

Despite the importance of clarifying the LCA approach (e.g., consequential or attributional, with or without system expansion), many authors cite adherence to ISO standards without specifying the methodology used [467, 474–477]. This lack of transparency makes it difficult to interpret, compare, and build upon existing studies.

Table 6.1: LCA studies regarding polyolefins pyrolysis.

Year	Data	Type of ACV	Comparison	Impact Categories [1]	Feed	Reactor	T	P	Time	Carrier Gas	Cat	Product	Co-Products	Process Fuel	Circular Economy
2005 [475]	-	Attributional with system expansion	Landfill, incineration, mechanical recycling, pyrolysis, hydrocracking	WC, GW, energy and crude oil consumption, organic compounds air emission, waste production	PE, PET	Fluidized bed (BP cracking technology)	-	-	-	No	-	45 % Wax, 26.5 % Naphtha	14.7% gases (C_3 - C_4); 7.6% sand and coke; 5.7% CaO / $CaCl_2$	0.212 MJ/tonne Feed (electricity), 0.131 MJ/tonne Feed (naphtha)	No
2012 [478]	Fixed bed (5 g)	Attributional	Fossil-based gas, gasoline, and diesels products; incineration; and landfilling	CED, ADP, AP, EP, GWP, OOP, POFP	PE	-	450 °C	-	-	-	No	1 kg gasoline, 0.09 kg diesel, 1.50 kg gas fraction;	0.03 kg char	0.17 kWh/2.94 kg PE, 17.52 MJ/2.94 kg PE	No
2014 [463]	Pilot (50 kg/h)	Attributional with system expansion	Incineration, landfill, hydrogenation	GWP, AP, POCP, EP	PE + PP (83%), PVC (2%), PS (15%)	Fluidized bed (BP cracking technology)	500 °C	-	-	No	No	45 % Wax, 26.5 % Naphtha	14.7% gases (C_3 - C_4); 4% CaO, 1.7% $CaCl_2$	0.212 MJ/tonne Feed (electricity), 0.131 MJ/tonne Feed (naphtha)	Yes
2017 [323]	Industrial (24 - 265 t/day)	Attributional (without system expansion)	Conventional ultra-low sulfur diesel (ULSD) fuel	fossil energy consumption, WCP, GWP	LDPE (33 %), HDPE (25 %), PP (42 %)	-	-	-	-	No	No	67% condensable liquid (80% diesel, 20% naphtha)	21% gases (used for electricity/heat); 12% char (landfilled)	13% Natural Gas, 87% Electricity	No
2018 [464]	Laboratory (Recycling Technology)	Attributional with system expansion	Incineration, landfill, naphtha-based (BAU), crude-oil (refinery-feed)	GWP, ADP-fossil FAETP	Generic, dry plastic waste	Fluidized bed	-	-	-	N_2	-	Plaxx™	Gas product (used as heat generator)	-	No
2019 [324]	-	Attributional with system expansion	Landfill, incineration	AP, CCP, POP, EP	PE, PP, PS, PU and PET	-	600 °C	-	-	No	-	-	-	1.9 MJ natural gas per kg waste; 0.49 MJ syngas/kg for mixed plastic.	No
2019 [479]	-	Attributional (without system expansion)	Incineration, mechanical recycling, gasification, landfill	CC, TA, and particulate matter formation	40% PE, 17% PVC, 12% PP, 4% PS, 4.8% PET, and 22.2% others	-	-	-	-	No	-	65% Diesel	6.5% Solid waste	18.3 MJ natural gas/tonne of mixed plastic waste; 106 MJ electricity/tonne of mixed plastic waste	No
2019 [480]	-	Consequential	Mechanical recycling	GWP, human toxicity, POFP, TA, ET	PP (< 2% PVC)	-	-	-	-	No	No	77% Pyrolysis oil	12 % Gas ("steam", used as heat production); 8 % solid waste	40 kWh/858 kg PP (electricity mix); 1278 MJ/858 kg PP (natural gas)	Yes

Table 6.1: LCA studies reviewed focusing on polyolefins pyrolysis (continued).

Year	Data	Type of ACV	Comparison	Impact Categories	Feed	Reactor	T	P	Time	Carrier Gas	Cat	Product	Co-Products	Process Fuel	Circular Economy
2019 [481]	Laboratory (0.4-0.6 mg) (extrapolated using Aspen Hysys)	Attributional (without system expansion) (mass allocation)	Fossil-based ethylene, propylene, and aromatics	GWP	HDPE	Fluidized bed	650 °C	-	-	Helium (1 kg/h)	-	4.3% CH_4, 20.1% C_2H_4, 13.4% C_3H_6, 3.7% aromatics	52.6% low molecular weight hydrocarbons, 5.2% high molecular weight hydrocarbons	electricity: 333 kWh/ton HDPE, natural gas: 2.20 GJ/ton HDPE, self-sustained methane (purge combustion): 3.10 GJ/ton HDPE	Yes
2020 [326]	-	Attributional with system expansion	Mechanical recycling, incineration, energy recovery in cement kilns, refinery feedstock, fuel production, monomer production	GWP, ADP-fossil	HDPE, LDPE, PP, PS, PET	-	-	-	-	No.	-	0.846 kg ethylene/kg HDPE; 0.828 kg ethylene/kg LDPE; 0.846 kg propylene/kg PP	Waste residues (0.1 kg/kg HDPE, 0.1 kg/kg LDPE, 0.1 kg/kg PP)	2.3 - 2.8 MJ/kg plastic	Yes
2020 [468]	Laboratory (0.3 mg)	Attributional with system expansion	Naphtha-based (BAU); incineration and landfill	CC, TA, WC, FE, ME, FRE	PE	Flash gas pyrolyzer	1000 °C	1 bar	20 s	*He*	No	4.62 C_2H_4 (for 1 mol PE)	1.17 C_3H_6 + 0.07 C_3H_4 + 0.09 C_4H_8 + 0.59 C_4H_6 + 0.45 C_6H_6 + 1.66 CH_4	27.8 MW	Yes
2020 [465]	Industrial (7,5 kt/a pyrolysis oil) (BASF)	Attributional with system expansion	Incineration, mechanical recycling, naphtha-based (BAU)	GWP, AP, EP, HOFP, ADP-fossil, Human toxicity (BASF method)	Mixed plastic waste (33% PP, 51 % PE, 16 % PS)	-	-	-	-	-	-	70% Pyrolysis oil	Gas (used for internal energy recovery); char	-	Yes
2020 [482]	Pilot	Attributional with system expansion	Incineration, gasification, hydropyrolysis	CC	Mixed plastics	-	-	-	-	-	-	-	-	-	-
2020 [317]	Laboratory (extrapolated using Aspen)	Attributional without system expansion	Landfilling, incineration, mechanical recycling, gasification	CC, ODP, TA, FETP, ME, HT, POFP, PMFP, TETP, METP, IRP, etc (ReCiPe method)	PP	-	500 °C	1 atm	-	N_2	No	15.7 wt% gases, 82.8 wt% oil	1.6 wt% ash	-	Yes
2021 [466]	Industrial (5000 t/y) (Plastic Energy)	Attributional with system expansion	Incineration, mechanical recycling, naphtha-based (BAU)	GWP, AP, EP, HOFP, ADP-fossil, Human toxicity (BASF method)	Mixed plastic waste	Semi-batch reactor	-	-	-	No	-	71 % pyrolysis oil	7.8 % char (lignite substitute); impurities (incinerated); HVR (fossil HVR substitute)	10 kg/t pyrolysis oil (natural gas); 3260 MJ/t pyrolysis oil (electricity)	Yes

Table 6.1: LCA studies reviewed focusing on polyolefins pyrolysis (continued).

Year	Data	Type of ACV	Comparison	Impact Categories	Feed	Reactor	T	P	Time	Carrier Gas	Cat	Product	Co-Products	Process Fuel	Circular Economy
2021 [469]	Laboratory (2 g) (Extrapolated using Aspen)	Consequential	Effect on market dynamics	GWP, ADP-fossil,etc.	HDPE	Fluidized bed	600 °C	1 bar	-	N_2	HZSM5	Naphtha, aromatics, gasoline, diesel	Ethylene, propylene, propane, 1-butene, i-butene, butane	High temperature heating energy provided by natural gas	Yes
2021 [477]	-	Attributional with system expansion	Polymers, incineration, gasification, mechanical recycling, dissolution, hydrolysis	LOP, CC, HT, ME, ODP, PMFP, POP, TA, TETP, WC	PP, PE, PET, PS, etc.	-	700 °C	-	-	-	-	50% Paraffin, 10% lubricating oil, 40% gases/char	-	-	Yes
2021 [474]	Pilot (PS: 50 kt; polyolefins: 120 kt)	Attributional with system expansion	Mechanical recycling, incineration	Resource consumption, global warming impact	PE, PP, PS	-	350 °C	-	-	-	-	Naphtha, slack wax, styrene	-	-	Yes

"-" stands for information not reported.

[1]Impact categories: acidification potential (AP); aquatic toxicity (FAETP); climate change - global warming potential (GWP100); climate change (CC); climate change potential (CCP); eutrophication potential (EP); fossil resources scarcity (FRE); freshwater ecotoxicity (FETP); human toxicity (HT); ionizing radiation (IRP); land use (LOP); marine ecotoxicity (ME) or (METP); marine eutrophication (ME); metal depletion (MD); mineral resource scarcity (SOP); ozone depletion (ODP); particulate matter formation (PMFP); photochemical oxidation potential (POP); photochemical ozone formation (POFP); photochemical ozone formation, human health (HOFP); abiotic resource depletion fossil fuels (ADP-fossil); terrestrial acidification (TA) or (TAP); terrestrial ecotoxicity (TETP); terrestrial eutrophication (ET); water consumption (WC).

Additionally, in current practice, achieving commercial viability for chemical recycling has often come at the expense of mass balance efficiency. This occurs due to non-optimal process conditions, which result in the accumulation of high molecular weight plastic residues in the reactor, and also due to inadequate treatment of the gaseous product fraction, which is typically combusted to supply process heat, even though a less valuable energy source could be used for that purpose. Improving overall carbon mass balance and maximizing the yield of valuable products, such as naphtha, monomers, and fuel gases, can significantly enhance both the environmental performance and circularity of plastic pyrolysis.

As shown in Table 6.1, several studies report using by-products for internal energy recovery; however, comparative assessments with alternatives that employ combined renewable energy sources (e.g., solar energy) are lacking. Such comparisons are crucial to understanding the potential for greenhouse gas emission reductions and align with emerging trends in electricity-based steam crackers [483]. Furthermore, it has already been demonstrated that, instead of combusting the gas stream, it could be upgraded into high-value chemicals (HVCs).

If this strategy is implemented, carbon emissions as CO_2 could be limited to less than 5% of the total, potentially reducing overall emissions to approximately 0.2 t CO_2 per ton of plastic, compared to 2.3 t CO_2 per ton when using virgin fossil feedstock is used [484].

Despite the fact that all reviewed studies assessed greenhouse gas emissions, other relevant environmental impacts must also be quantified and mitigated [466]. Even when simpler tools such as systemic material flow analysis are used [484], it is essential for analysts and developers of chemical recycling technologies to evaluate whether specific interventions are justified, such as the use of catalysts to shift product distributions and reaction rates, or the use of carrier gases to alleviate mass and heat transfer limitations. These technological considerations are seldom addressed in published studies, raising doubts about whether the reported figures can realistically reflect full-scale industrial operations.

Finally, to the best of our knowledge, existing LCA studies have not yet incorporated the social dimensions of chemical recycling operations. These include the impact on the quality of life in low-income communities and the role of informal waste collectors. This omission is problematic, particularly given how discretely the social consequences of dumping grounds, landfilling, and toxic emissions from incinerators have been treated.

In addition to emissions and environmental performance, it is also crucial to assess end-of-life (EOL) consumer responsibilities, such as proper separation and disposal of plastics, along with community engagement, local job creation, value chain collaboration (e.g., among recyclers, refineries, and manufacturers), and re-

gional development. These aspects are central to effective EOL-related policies that aim to reduce the environmental burden.

Although there is no universally agreed-upon framework for social life cycle assessments (S-LCA), several early studies [485–490] and emerging guidelines [491–494] provide a solid foundation for integrating social aspects into future assessments.

6.3 Concluding Remarks and Recommendations

LCA studies focused on the chemical recycling of polyolefins via pyrolysis were reviewed, revealing significant gaps and highlighting key opportunities for improvement in this field. In the context of plastic pyrolysis, future LCA research should prioritize representativeness across temporal, geographical, and technological dimensions. In parallel, experimental studies should focus on improving carbon conversion efficiency and integrating renewable energy sources into chemical recycling strategies.

Rather than comparing chemical recycling to less relevant or outdated practices such as mechanical recycling, landfill disposal, or incineration, it is more constructive to compare different chemical recycling strategies among themselves. In this context, results from attributional LCA analyses should be evaluated against each other (preferably without system expansion - i.e. not including additional products within the system boundaries to account for environmental impacts that are not directly linked to pyrolysis process itself), considering scenarios that involve plastic production from recycled streams, fossil-based feedstocks, and renewable raw materials.

Furthermore, LCA can play a crucial role in guiding business model decisions for chemical recycling. For example, is it more sustainable to construct multiple small pyrolysis units distributed across a region? This approach could minimize the transport of bulky plastic waste with low density. Alternatively, would it be better to centralize operations in a large facility and transport the waste instead? Such considerations can have a major impact on the overall environmental performance of the system.

In terms of good LCA practices, it is strongly recommended that chemists, chemical engineers, and industrial engineers be directly involved in conducting LCA analyses or managing LCA inventories, as their deep understanding of the underlying processes enhances the credibility of the results. When industrial data is unavailable, which is often the case for emerging technologies with low Technological Readiness Levels (TRLs), uncertainty increases. In addition, academic data may be fragmented or influenced by multiple interacting variables. In such cases, life cycle assessments should explicitly reflect these sources of uncertainty. Including sensitivity or uncer-

tainty analyses can improve transparency, enrich the interpretation of results, and enhance the overall reliability of the conclusions.

Integrating LCA with process simulation tools is another promising strategy to ensure more accurate representations of large-scale processes. However, this approach must be undertaken with caution, as pyrolysis reactor outputs are highly sensitive to process parameters and reactor configurations, which can vary significantly.

Finally, improved documentation of LCAs is urgently needed, especially when system expansion is applied. Clear and comprehensive reporting allows independent reproduction of studies and ensures that assessments are not overly dependent on "avoided impact" assumptions. A more absolute and transparent evaluation of process performance is necessary to support optimization efforts and facilitate meaningful comparisons across studies. As discussed earlier, the current state of the literature makes it very difficult to verify published results or benchmark findings across different authors.

Chapter 7

Conclusions and Perspectives

The central motivation of this thesis was to revalidate and extend mathematical models of the thermal degradation of plastics, particularly polystyrene (PS) and polyethylene (HDPE), in light of their growing relevance for chemical recycling technologies. While several mechanistic and lumped models exist in the literature, they often are setup-specific (data-driven), lacking integration with vaporization phenomena or proper validation under a broad range of conditions. Many of these models were developed for closed systems or neglected transport phenomena such as heat and mass transfer, leaving gaps that this work sought to address.

Initially, the thesis builds upon the foundation of lumped kinetic models, which are especially useful for process understanding and optimization when time or experimental data are limited. A lumped model was proposed and applied to both catalytic and non-catalytic pyrolysis, demonstrating its utility for preliminary evaluations and quick decision-making scenarios.

To overcome the limitations of oversimplified kinetics, a detailed mechanistic model for PS pyrolysis was then developed. This model is based on the chemistry of small radical moieties and proved robust across different temperatures and scales without requiring parameter adjustments. However, due to limitations in experimental data and modeling scope, this study did not account for volatilization behavior or track the full conversion profile. These missing components were addressed in a subsequent model for HDPE.

The HDPE model introduces a pioneering integration of kinetic Monte Carlo (kMC) simulations with a thermodynamic module capable of performing vapor-liquid equilibrium (VLE) calculations using either the Peng-Robinson (PR) or PC-SAFT equations of state. This marks the first known attempt to couple a fundamental evaporation model with a detailed pyrolysis mechanism. The resulting framework successfully captures volatilization phenomena and offers a more realistic and predictive tool for pyrolysis modeling.

A critical evaluation of the current state of life cycle assessments (LCAs) for

pyrolysis was also done. It was shown that many LCAs fail to reflect the complexity of real systems due to oversights in feedstock composition, operational conditions, or reactor configurations. These simplifications can lead to inaccurate assessments of the environmental impact and economic feasibility of pyrolysis-based recycling.

Additionally, LCAs for plastic pyrolysis should be region-specific, as the environmental and economic impacts of the technology are highly dependent on local waste management infrastructures and regulatory frameworks. Furthermore, there is an urgent need to incorporate social life cycle assessments into the analysis. Social dimensions are critical, particularly because the collection and sorting of plastic waste may be related to an inadequate work environment, including informality, low wages, and long working hours.

Moreover, the development and deployment of plastic recycling technologies, including pyrolysis, are often limited by intellectual property barriers, and, consequently, their implementation may be restricted to regions with strong legislative incentives or where deployment results in profit or improved company public image.

Therefore, for chemical engineers, chemical recycling represents a rapidly evolving and highly active area of research and development. This momentum is driven by the urgent need to develop robust kinetic models capable of accurately capturing the behavior of complex, heterogeneous feedstocks, including mixed plastics, biomass residues, and various contaminants commonly found in real waste streams. The physical properties of these materials, particularly their high viscosity and low thermal conductivity, further complicate reactor design, heat transfer, and process optimization, making this a technically demanding field. At the same time, addressing the plastic waste crisis requires a multidisciplinary perspective that extends beyond technical innovation. Social and environmental dimensions must be considered in parallel, including issues such as equitable access to emerging technologies and the varying regional capacities for implementation. Only through a multidisciplinary approach that integrates engineering, environmental science, economics, and social equity can the full potential and impact of plastic pyrolysis pathways be properly assessed and realized.

7.0.1 Future Works

While the individual modeling efforts presented here provide valuable insights, real plastic waste is a complex mixture of polymers and non-polymeric components. Future research should focus on integrating the developed models for individual polymers to represent mixed plastic waste streams. However, experimental data for validating such multi-component models are currently scarce. A more extensive experimental effort is needed, particularly using reactors that allow the removal and

condensation of volatiles to accurately validate both kinetic and thermodynamic predictions.

Equally important is the development of detailed reactor models that account for heat and mass transfer, fluid dynamics, and scale-dependent effects. These models are essential for transitioning from lab-scale studies to industrial implementation. Additionally, the influence of impurities and biomass, frequently found in municipal waste, should be included in future models to enhance their applicability and realism.

Finally, the proposed framework integrating kMC and VLE offers an opportunity to explore advanced process configurations. Process variations such as longer residence times, staged condensation, or reflux strategies could be simulated to optimize product yields, especially of lighter hydrocarbons. These explorations will further bridge the gap between fundamental chemistry and applied process engineering, advancing the viability of pyrolysis as a circular economy solution for plastic waste.

References

[1] FOUNDATION, H. B. *Plastic Atlas 2019: Facts and figures about the world of synthetic polymers*. Heinrich Böll Foundation and Break Free From Plastic, 2019.

[2] EUROPE, P. *The Circular Economy for Plastics: A European View*. Plastics Europe, 2019. Available in: <https://plasticseurope.org/knowledge-hub/the-circular-economy-for-plastics-a-european-overview/>.

[3] OKAN, M., AYDIN, H. M., BARSBAY, M. "Current approaches to waste polymer utilization and minimization: a review", *Journal of Chemical Technology & Biotechnology*, v. 94, n. 1, pp. 8–21, 2019.

[4] CHENG, L., GU, J., WANG, Y., et al. "Polyethylene high-pressure pyrolysis: Better product distribution and process mechanism analysis", *Chemical Engineering Journal*, v. 385, pp. 123866, 2020.

[5] MOENS, E. K., DE SMIT, K., MARIEN, Y. W., et al. "Progress in reaction mechanisms and reactor technologies for thermochemical recycling of poly (methyl methacrylate)", *Polymers*, v. 12, n. 8, pp. 1667, 2020.

[6] SHEN, Y. "Fractionation of biomass and plastic wastes to value-added products via stepwise pyrolysis: a state-of-art review", *Reviews in Chemical Engineering*, v. 37, n. 5, pp. 643–661, 2021.

[7] SIMHA, R., WALL, L., BLATZ, P. "Depolymerization as a chain reaction", *Journal of Polymer Science*, v. 5, n. 5, pp. 615–632, 1950.

[8] CARNITI, P., BELTRAME, P. L., ARMADA, M., et al. "Polystyrene thermodegradation. 2. Kinetics of formation of volatile products", *Industrial & engineering chemistry research*, v. 30, n. 7, pp. 1624–1629, 1991.

[9] KOO, J.-K., KIM, S.-W. "Reaction kinetic model for optimal pyrolysis of plastic waste mixtures", *Waste management & research*, v. 11, n. 6, pp. 515–529, 1993.

[10] WU, C.-H., CHANG, C.-Y., HOR, J.-L., et al. "On the thermal treatment of plastic mixtures of MSW: pyrolysis kinetics", *Waste Management*, v. 13, n. 3, pp. 221–235, 1993.

[11] SONGIP, A. R., MASUDA, T., KUWAHARA, H., et al. "Kinetic studies for catalytic cracking of heavy oil from waste plastics over REY zeolite", *Energy & Fuels*, v. 8, n. 1, pp. 131–135, 1994.

[12] LIN, Y.-H., HWU, W.-H., GER, M.-D., et al. "A combined kinetic and mechanistic modelling of the catalytic degradation of polymers", *Journal of Molecular Catalysis A: Chemical*, v. 171, n. 1-2, pp. 143–151, 2001.

[13] CARDONA, S. C., CORMA, A. "Kinetic study of the catalytic cracking of polypropylene in a semibatch stirred reactor", *Catalysis today*, v. 75, n. 1-4, pp. 239–246, 2002.

[14] COSTA, P. A., PINTO, F. J., RAMOS, A. M., et al. "Kinetic evaluation of the pyrolysis of polyethylene waste", *Energy & Fuels*, v. 21, n. 5, pp. 2489–2498, 2007.

[15] OHMUKAI, Y., HASEGAWA, I., MAE, K. "Pyrolysis of the mixture of biomass and plastics in countercurrent flow reactor Part I: experimental analysis and modeling of kinetics", *Fuel*, v. 87, n. 13-14, pp. 3105–3111, 2008.

[16] ARTETXE, M., LOPEZ, G., AMUTIO, M., et al. "Kinetic modelling of the cracking of HDPE pyrolysis volatiles on a HZSM-5 zeolite based catalyst", *Chemical Engineering Science*, v. 116, pp. 635–644, 2014.

[17] TILL, Z., VARGA, T., SÓJA, J., et al. "Kinetic identification of plastic waste pyrolysis on zeolite-based catalysts", *Energy Conversion and Management*, v. 173, pp. 320–330, 2018.

[18] AL-SALEM, S. "Thermal pyrolysis of high density polyethylene (HDPE) in a novel fixed bed reactor system for the production of high value gasoline range hydrocarbons (HC)", *Process Safety and Environmental Protection*, v. 127, pp. 171–179, 2019.

[19] ELORDI, G., LOPEZ, G., OLAZAR, M., et al. "Product distribution modelling in the thermal pyrolysis of high density polyethylene", *Journal of Hazardous Materials*, v. 144, n. 3, pp. 708–714, 2007.

[20] VINU, R., BROADBELT, L. J. "Unraveling reaction pathways and specifying reaction kinetics for complex systems", *Annual review of chemical and biomolecular engineering*, v. 3, pp. 29–54, 2012.

[21] COATES, G. W., GETZLER, Y. D. "Chemical recycling to monomer for an ideal, circular polymer economy", *Nature Reviews Materials*, v. 5, n. 7, pp. 501–516, 2020.

[22] VOLLMER, I., JENKS, M. J., ROELANDS, M. C., et al. "Beyond Mechanical Recycling: Giving New Life to Plastic Waste", *Angewandte Chemie International Edition*, 2020.

[23] FARAVELLI, T., PINCIROLI, M., PISANO, F., et al. "Thermal degradation of polystyrene", *Journal of analytical and applied pyrolysis*, v. 60, n. 1, pp. 103–121, 2001.

[24] QIU, B., DENG, N., ZHANG, Y., et al. "Application of industrial solid wastes in catalytic pyrolysis", *Asia-Pacific Journal of Chemical Engineering*, v. 13, n. 1, pp. e2150, 2018.

[25] QURESHI, M. S., OASMAA, A., PIHKOLA, H., et al. "Pyrolysis of plastic waste: Opportunities and challenges", *Journal of Analytical and Applied Pyrolysis*, v. 152, pp. 104804, 2020. doi: 10.1016/j.jaap.2020.104804.

[26] BUEKENS, A., HUANG, H. "Catalytic plastics cracking for recovery of gasoline-range hydrocarbons from municipal plastic wastes", *Resources, Conservation and Recycling*, v. 23, n. 3, pp. 163–181, 1998.

[27] BRANDÃO, A. L., SOARES, J. B., PINTO, J. C., et al. "Comparison of different dynamic Monte Carlo methods for the simulation of olefin polymerization". In: *Macromolecular Symposia*, v. 360, pp. 160–178. Wiley Online Library, 2016.

[28] MAAFA, I. M., SOARES, J. B., ELKAMEL, A. "Prediction of chain length distribution of polystyrene made in batch reactors with bifunctional free-radical initiators using dynamic monte carlo simulation", *Macromolecular Reaction Engineering*, v. 1, n. 3, pp. 364–383, 2007.

[29] GEYER, R., JAMBECK, J. R., LAW, K. L. "Production, use, and fate of all plastics ever made", *Science advances*, v. 3, n. 7, pp. e1700782, 2017.

[30] BUCKNALL, D. "Plastics as a Materials System in a Circular Economy", *Philosophical Transactions of the Royal Society A: Mathematical, Physical and Engineering Sciences*, 2020.

[31] "The History of Plastic: The Invention of Throwaway Living". Available in: <`https://www.thedieline.com/blog/2020/3/10/the-history-of-plastic-the-invention-of-throwaway-living`>.

[32] EUROPE, P. *Plastics - the Facts 2019*. Plastics Europe, 2019. Available in: <https://www.plasticseurope.org/en/resources/publications/1804-plastics-facts-2019>.

[33] "'Throwaway Living': When Tossing Out Everything Was All the Rage". Available in: <https://time.com/3879873/throwaway-living-when-tossing-it-all-was-all-the-rage/>.

[34] ZAMAN, A., NEWMAN, P. "Plastics: are they part of the zero-waste agenda or the toxic-waste agenda?" *Sustainable Earth*, v. 4, pp. 1–16, 2021.

[35] LINO, F. A., ISMAIL, K. A., CASTAÑEDA-AYARZA, J. A. "Municipal solid waste treatment in Brazil: A comprehensive review", *Energy Nexus*, v. 11, pp. 100232, 2023.

[36] ASSOCIAÇÃO BRASILEIRA DE RESÍDUOS E MEIO AMBIENTE. "Panorama dos Resíduos Sólidos no Brasil 2024". 2024. Available in: <https://www.abrema.org.br/panorama/>. Acessado em 18 de maio de 2025.

[37] EUROSTAT. "Packaging waste by waste management operations". 2022. Available in: <https://ec.europa.eu/eurostat/databrowser/bookmark/7c9a8d23-41c1-4028-8528-7d50f50705a8?lang=en>. Acessado em 18 de maio de 2025.

[38] STATISTA. "Per capita plastic waste generation in the United States in 2019, with projections for 2030 and 2060". 2022. Available in: <https://www.statista.com/statistics/1339210/us-plastic-waste-generation-per-capita-outlook/>. Acessado em 18 de maio de 2025.

[39] U.S. ENVIRONMENTAL PROTECTION AGENCY. "National Overview: Facts and Figures on Materials, Wastes and Recycling". 2023. Available in: <https://www.epa.gov/facts-and-figures-about-materials-waste-and-recycling/national-overview-facts-and-figures-materials>. Acessado em 18 de maio de 2025.

[40] OECD. "Annual plastic waste by disposal method, World, 2000 to 2019". Our World in Data, 2023. Available in: <https://ourworldindata.org/grapher/plastic-fate>. Acessado em 18 de maio de 2025.

[41] ASSOCIAÇÃO BRASILEIRA DA INDÚSTRIA DO PLÁSTICO. "Reciclagem de plásticos no Brasil: estudo aponta índice de 24,3% para as embalagens em 2023". 2023. Available in: <https://www.abiplast.org.br/noticias/reciclagem-de-plasticos-no-brasil-estudo-aponta-indice-de-243-para-as-emba Acessado em 18 de maio de 2025.

[42] HEIDBREDER, L. M., BABLOK, I., DREWS, S., et al. "Tackling the plastic problem: A review on perceptions, behaviors, and interventions", *Science of the total environment*, v. 668, pp. 1077–1093, 2019.

[43] WINANS, K., KENDALL, A., DENG, H. "The history and current applications of the circular economy concept", *Renewable and Sustainable Energy Reviews*, v. 68, pp. 825–833, 2017.

[44] ÁVILA-GUTIÉRREZ, M. J., MARTÍN-GÓMEZ, A., AGUAYO-GONZÁLEZ, F., et al. "Standardization framework for sustainability from circular economy 4.0", *Sustainability*, v. 11, n. 22, pp. 6490, 2019.

[45] BROOKS, A. L., WANG, S., JAMBECK, J. R. "The Chinese import ban and its impact on global plastic waste trade", *Science advances*, v. 4, n. 6, pp. eaat0131, 2018.

[46] "Two dozen types of scrap imports banned by China in 2018". Available in: <https://www.recyclingtoday.com/article/plastic-scrap-china-import-ban-2018-mixed-paper/>.

[47] PEW CHARITABLE TRUSTS, S. L. *Breaking the Plastic Wave: A Comprehensive Assessment of Pathways Towards Stopping Ocean Plastic Pollution.* Report, Pew Charitable Trusts, SYSTEMIQ Ltd. Available in: <https://www.pewtrusts.org/-/media/assets/2020/07/breakingtheplasticwave_report.pdf>.

[48] KERSTEN-JOHNSTON, S. *The Bridge to Circularity: Putting the New Plastics Economy Into Practice in the U.S.* The Recycling Partnership.

[49] CRIPPA, M., DE WILDE, B., KOOPMANS, R., et al. *A circular economy for plastics : insights from research and innovation to inform policy and funding decisions.* : Directorate-General for Research and Innovation (European Commission). Available in: <http://op.europa.eu/en/publication-detail/-/publication/33251cf9-3b0b-11e9-8d04-01aa75ed71a1/

language-en/format-PDF>. ISBN: 9789279984297 Publisher: Publications Office of the European Union.

[50] ENVIRONMENT, U. N. *Legal Limits on Single-Use Plastics and Microplastics: A Global Review of National Laws and Regulations*. United Nations Environment Programme. Available in: <http://www.unenvironment.org/resources/publication/legal-limits-single-use-plastics-and-microplastics-global-review-national> Section: publications.

[51] *Mission Possible: Plastics*. Energy Transitions Commission (ETC).

[52] DE SMET, M. *The New Plastics Economy: Rethinking the future of plastics & catalysing action*. Ellen MacArthur Foundation. Available in: <https://www.ellenmacarthurfoundation.org/publications/the-new-plastics-economy-rethinking-the-future-of-plastics-catalysing-acti

[53] *Plastics Policy Playbook: Strategies for a Plastic-Free Ocean*. Ocean Conservancy and Trash Free Seas Alliance. Available in: <https://oursharedseas.com/oss_downloads/plastics-policy-playbook-strategies-for-a-plastic-free-oceans/>.

[54] *Single-Use Plastics: A Roadmap for Sustainability*. United Nations Environment Programme (UNEP).

[55] BOND, K., BENHAM, H., VAUGHAN, E., et al. *The Future's Not in Plastics: Why plastics demand won't rescue the oil sector*. Carbon Tracker.

[56] WILTS, H., SCHINKEL, J., FEDER, L. *Prevention of plastic waste in production and consumption by multi-actor partnerships*. PREVENT Waste Alliance, Wuppertal Institut.

[57] ADVISORS D, DE WIT W, H. A. S. R. S. T. A. S. *Solving Plastic Pollution Through Accountability | Publications | WWF*. WWF International. Available in: <https://www.worldwildlife.org/publications/solving-plastic-pollution-through-accountability>.

[58] BANU, J. R., SHARMILA, V. G., USHANI, U., et al. "Impervious and influence in the liquid fuel production from municipal plastic waste through thermochemical biomass conversion technologies-A review", *Science of The Total Environment*, v. 718, pp. 137287, 2020.

[59] CS3, C. S., SUMMIT, S. *Science to enable sustainable plastics - A white paper from the 8th Chemical Sciences and Society Summit (CS3)*. Chemical Sciences and Society Summit (CS3), 2020. Available in: <rsc.li/sustainable-plastics-report>.

[60] HONG, M., CHEN, E. Y.-X. "Chemically recyclable polymers: a circular economy approach to sustainability", *Green Chemistry*, v. 19, n. 16, pp. 3692–3706, 2017.

[61] REN, T., PATEL, M., BLOK, K. "Olefins from conventional and heavy feedstocks: Energy use in steam cracking and alternative processes", *Energy*, v. 31, n. 4, pp. 425–451, 2006.

[62] LEE, A., LIEW, M. S. "Tertiary recycling of plastics waste: an analysis of feedstock, chemical and biological degradation methods", *Journal of Material Cycles and Waste Management*, pp. 1–12, 2020.

[63] HAHLADAKIS, J. N., VELIS, C. A., WEBER, R., et al. "An overview of chemical additives present in plastics: migration, release, fate and environmental impact during their use, disposal and recycling", *Journal of hazardous materials*, v. 344, pp. 179–199, 2018.

[64] SCHYNS, Z. O., SHAVER, M. P. "Mechanical Recycling of Packaging Plastics: A Review", *Macromolecular Rapid Communications*, p. 2000415, 2020.

[65] ERIKSEN, M. K., CHRISTIANSEN, J., DAUGAARD, A. E., et al. "Closing the loop for PET, PE and PP waste from households: Influence of material properties and product design for plastic recycling", *Waste management*, v. 96, pp. 75–85, 2019.

[66] "Design for Recycling Guidelines – Recyclass". Available in: <https://recyclass.eu/recyclass/design-for-recycling-guidelines/>.

[67] SINGH, N., HUI, D., SINGH, R., et al. "Recycling of plastic solid waste: A state of art review and future applications", *Composites Part B: Engineering*, v. 115, pp. 409–422, 2017. doi: 10.1016/j.compositesb.2016.09.013.

[68] DATTA, J., KOPCZYŃSKA, P. "From polymer waste to potential main industrial products: Actual state of recycling and recovering", *Critical Reviews in Environmental Science and Technology*, v. 46, n. 10, pp. 905–946, 2016.

[69] RAHIMI, A., GARCÍA, J. M. "Chemical recycling of waste plastics for new materials production", *Nature Reviews Chemistry*, v. 1, n. 6, pp. 1–11, 2017.

[70] OLIVEIRA, J. A., BISCAIA, E. C., PINTO, J. C. "Analysis of Kinetic Models Proposed for the Controlled Degradation of Poly(propylene) – Presentation of a General and Analytical Solution", v. 12, n. 9, pp. 696–704. ISSN: 1521-3919. doi: https://doi.org/10.1002/mats.200350023. Available in: <https://onlinelibrary.wiley.com/doi/abs/10.1002/mats.200350023>. _eprint: https://onlinelibrary.wiley.com/doi/pdf/10.1002/mats.200350023.

[71] GONZÁLEZ-GONZÁLEZ, V. A., NEIRA-VELÁZQUEZ, G., ANGULO-SÁNCHEZ, J. L. "Polypropylene chain scissions and molecular weight changes in multiple extrusion", v. 60, n. 1, pp. 33–42. ISSN: 0141-3910. doi: 10.1016/S0141-3910(96)00233-9. Available in: <http://www.sciencedirect.com/science/article/pii/S0141391096002339>.

[72] QIAN, S., IGARASHI, T., NITTA, K.-H. "Thermal degradation behavior of polypropylene in the melt state: molecular weight distribution changes and chain scission mechanism", v. 67, n. 8, pp. 1661–1670. ISSN: 1436-2449. doi: 10.1007/s00289-011-0560-6. Available in: <https://doi.org/10.1007/s00289-011-0560-6>.

[73] PINHEIRO, L. A., CHINELATTO, M. A., CANEVAROLO, S. V. "The role of chain scission and chain branching in high density polyethylene during thermo-mechanical degradation", v. 86, n. 3, pp. 445–453. ISSN: 0141-3910. doi: 10.1016/j.polymdegradstab.2004.05.016. Available in: <http://www.sciencedirect.com/science/article/pii/S0141391004002058>.

[74] WHITLOCK, L. R., PORTER, R. S. "The source of degradation during extrusion of polystyrene", v. 17, n. 9, pp. 2761–2770. ISSN: 1097-4628. doi: https://doi.org/10.1002/app.1973.070170913. Available in: <https://onlinelibrary.wiley.com/doi/abs/10.1002/app.1973.070170913>. _eprint: https://onlinelibrary.wiley.com/doi/pdf/10.1002/app.1973.070170913.

[75] ARISAWA, K., PORTER, R. S. "The degradation of polystyrene during extrusion", v. 14, n. 4, pp. 879–896. ISSN: 1097-4628. doi: https://doi.org/10.1002/app.1970.070140402. Available in: <https://onlinelibrary.wiley.com/doi/abs/10.1002/app.1970.070140402>. _eprint: https://onlinelibrary.wiley.com/doi/pdf/10.1002/app.1970.070140402.

[76] FARAHANCHI, A., MALLOY, R., SOBKOWICZ, M. J. "Effects of ultrahigh speed twin screw extrusion on the thermal and mechanical

degradation of polystyrene", v. 56, n. 7, pp. 743–751. ISSN: 1548-2634. doi: https://doi.org/10.1002/pen.24301. Available in: <https://onlinelibrary.wiley.com/doi/abs/10.1002/pen.24301>. _eprint: https://onlinelibrary.wiley.com/doi/pdf/10.1002/pen.24301.

[77] NAIT-ALI, L. K., COLIN, X., BERGERET, A. "Kinetic analysis and modelling of PET macromolecular changes during its mechanical recycling by extrusion", v. 96, n. 2, pp. 236–246. ISSN: 0141-3910. doi: 10.1016/j.polymdegradstab.2010.11.004. Available in: <http://www.sciencedirect.com/science/article/pii/S0141391010004118>.

[78] FROUNCHI, M. "Studies on degradation of PET in mechanical recycling", v. 144, n. 1, pp. 465–469. ISSN: 1521-3900. doi: https://doi.org/10.1002/masy.19991440142. Available in: <https://onlinelibrary.wiley.com/doi/abs/10.1002/masy.19991440142>. _eprint: https://onlinelibrary.wiley.com/doi/pdf/10.1002/masy.19991440142.

[79] BRACHET, P., HØYDAL, L. T., HINRICHSEN, E. L., et al. "Modification of mechanical properties of recycled polypropylene from post-consumer containers", v. 28, n. 12, pp. 2456–2464. ISSN: 0956-053X. doi: 10.1016/j.wasman.2007.10.021. Available in: <http://www.sciencedirect.com/science/article/pii/S0956053X07004114>.

[80] WELLE, F. "Twenty years of PET bottle to bottle recycling—an overview", *Resources, Conservation and Recycling*, v. 55, n. 11, pp. 865–875, 2011.

[81] DA SILVA, D. J., WIEBECK, H. "Current options for characterizing, sorting, and recycling polymeric waste", *Progress in Rubber, Plastics and Recycling Technology*, p. 1477760620918603, 2020.

[82] VEOLIA. "A milk bottle with ten lives". Available in: <https://www.livingcircular.veolia.com/en/industry/milk-bottle-ten-lives>.

[83] ZHANG, X., FEVRE, M., JONES, G. O., et al. "Catalysis as an enabling science for sustainable polymers", *Chemical reviews*, v. 118, n. 2, pp. 839–885, 2018.

[84] FORTMAN, D. J., BRUTMAN, J. P., DE HOE, G. X., et al. "Approaches to sustainable and continually recyclable cross-linked polymers", *ACS Sustainable Chemistry & Engineering*, v. 6, n. 9, pp. 11145–11159, 2018.

[85] SHAH, A. A., HASAN, F., HAMEED, A., et al. "Biological degradation of plastics: a comprehensive review", *Biotechnology advances*, v. 26, n. 3, pp. 246–265, 2008.

[86] MUELLER, R.-J. "Biological degradation of synthetic polyesters—Enzymes as potential catalysts for polyester recycling", *Process Biochemistry*, v. 41, n. 10, pp. 2124–2128, 2006.

[87] AMMALA, A., BATEMAN, S., DEAN, K., et al. "An overview of degradable and biodegradable polyolefins", *Progress in Polymer Science*, v. 36, n. 8, pp. 1015–1049, 2011.

[88] WEI, R., ZIMMERMANN, W. "Microbial enzymes for the recycling of recalcitrant petroleum-based plastics: how far are we?" *Microbial biotechnology*, v. 10, n. 6, pp. 1308–1322, 2017.

[89] WEI, R., TISO, T., BERTLING, J., et al. "Possibilities and limitations of biotechnological plastic degradation and recycling", *Nature Catalysis*, v. 3, n. 11, pp. 867–871, 2020.

[90] CHEN, C.-C., DAI, L., MA, L., et al. "Enzymatic degradation of plant biomass and synthetic polymers", *Nature Reviews Chemistry*, v. 4, n. 3, pp. 114–126, 2020. doi: 10.1038/s41570-020-0163-6.

[91] KALE, S. K., DESHMUKH, A. G., DUDHARE, M. S., et al. "Microbial degradation of plastic: a review", *Journal of Biochemical Technology*, v. 6, n. 2, pp. 952–961, 2015.

[92] BLOCK, C., EPHRAIM, A., WEISS-HORTALA, E., et al. "Co-pyrogasification of plastics and biomass, a review", *Waste and biomass valorization*, v. 10, n. 3, pp. 483–509, 2019.

[93] KLEMEŠ, J. J., FAN, Y. V., JIANG, P. "Plastics: friends or foes? The circularity and plastic waste footprint", *Energy Sources, Part A: Recovery, Utilization, and Environmental Effects*, pp. 1–17, 2020.

[94] AL-SALEM, S., ANTELAVA, A., CONSTANTINOU, A., et al. "A review on thermal and catalytic pyrolysis of plastic solid waste (PSW)", *Journal of Environmental Management*, v. 197, pp. 177–198, 2017.

[95] "Polyester Renewal Technology | Eastman Circular Economy". . Available in: <https://www.eastman.com/Company/Circular-Economy/Solutions/Pages/Polyester-Renewal.aspx>.

[96] "BP's new technology to enable circularity for unrecyclable PET plastic waste". . Available in: <https://www.bp.com/en/global/corporate/news-and-insights/press-releases/bp-new-technology-to-enable-circularity-for-unrecyclable-pet-plastic-waste.html>.

[97] "Loop™ Industries - Infinite Loop". . Available in: <https://www.loopindustries.com/en/infinite_loop>.

[98] "Recycling | Indorama Ventures". . Available in: <https://sustainability.indoramaventures.com/en/environmental/recycling/at-a-glance>.

[99] KARASIAK, W., KARASIAK, D. "Procedimiento y dispositivo para el tratamiento de polímeros". Available in: <https://patents.google.com/patent/ES2755114T3/en?q=nylon&assignee=Aquafil>.

[100] SCHEIRS, J., KAMINSKY, W. *Feedstock recycling and pyrolysis of waste plastics*. John Wiley & Sons Chichester, UK:, 2006.

[101] TOKTAROVA, A., GÖRANSSON, L., THUNMAN, H., et al. "Thermochemical recycling of plastics–Modeling the implications for the electricity system", *Journal of Cleaner Production*, v. 374, pp. 133891, 2022.

[102] GUDDETI, R. R., KNIGHT, R., GROSSMANN, E. D. "Depolymerization of polypropylene in an induction-coupled plasma (ICP) reactor", *Industrial & engineering chemistry research*, v. 39, n. 5, pp. 1171–1176, 2000.

[103] THIOUNN, T., SMITH, R. C. "Advances and approaches for chemical recycling of plastic waste", *Journal of Polymer Science*, v. 58, n. 10, pp. 1347–1364, 2020.

[104] SOLIS, M., SILVEIRA, S. "Technologies for chemical recycling of household plastics–A technical review and TRL assessment", *Waste Management*, v. 105, pp. 128–138, 2020.

[105] LI, C., SUZUKI, K. "Tar property, analysis, reforming mechanism and model for biomass gasification—An overview", *Renewable and Sustainable Energy Reviews*, v. 13, n. 3, pp. 594–604, 2009.

[106] ARENA, U., ZACCARIELLO, L., MASTELLONE, M. L. "Tar removal during the fluidized bed gasification of plastic waste", *Waste Management*, v. 29, n. 2, pp. 783–791, 2009.

[107] XAYACHAK, T., HAQUE, N., LAU, D., et al. "Assessing the environmental footprint of plastic pyrolysis and gasification: a life cycle inventory study", *Process Safety and Environmental Protection*, v. 173, pp. 592–603, 2023.

[108] CHAUDHARI, U. S., KULAS, D. G., UMLOR, L., et al. "Liquid Fed Pyrolysis of Polyethylene Films: Environmental and Economic Assessments of Co-located and Remotely-Located US Facilities", *ACS Sustainable Resource Management*, v. 1, n. 3, pp. 493–503, 2024.

[109] HERNÁNDEZ, B., KOTS, P., SELVAM, E., et al. "Techno-economic and life cycle analyses of thermochemical upcycling technologies of low-density polyethylene waste", *ACS Sustainable Chemistry & Engineering*, v. 11, n. 18, pp. 7170–7181, 2023.

[110] TOMIĆ, T., SLATINA, I., SCHNEIDER, D. R. "Techno-economic review of pyrolysis and gasification plants for thermochemical recovery of plastic waste and economic viability assessment of small-scale implementation", *Clean technologies and environmental policy*, v. 26, n. 1, pp. 171–195, 2024.

[111] GHODRAT, M., ABASCALL ALONSO, J., HAGARE, D., et al. "Economic feasibility of energy recovery from waste plastic using pyrolysis technology: an Australian perspective", *International Journal of Environmental Science and Technology*, v. 16, pp. 3721–3734, 2019.

[112] JIANG, G., WANG, J., AL-SALEM, S. M., et al. "Molten solar salt pyrolysis of mixed plastic waste: process simulation and technoeconomic evaluation", *Energy & fuels*, v. 34, n. 6, pp. 7397–7409, 2020.

[113] RIEDEWALD, F., PATEL, Y., WILSON, E., et al. "Economic assessment of a 40,000 t/y mixed plastic waste pyrolysis plant using direct heat treatment with molten metal: A case study of a plant located in Belgium", *Waste Management*, v. 120, pp. 698–707, 2021.

[114] VOLK, R., STALLKAMP, C., STEINS, J. J., et al. "Techno-economic assessment and comparison of different plastic recycling pathways: A German case study", *Journal of industrial ecology*, v. 25, n. 5, pp. 1318–1337, 2021.

[115] LANGE, J.-P. "Fuels and chemicals manufacturing; guidelines for understanding and minimizing the production costs", *Cattech*, v. 5, n. 2, pp. 82–95, 2001.

[116] SINGH, A., AFZAL, S., NICHOLSON, S., et al. *Techno-economic analysis of waste plastic gasification to methanol process*. Report, National Renewable Energy Lab.(NREL), Golden, CO (United States), 2022.

[117] LAN, K., YAO, Y. "Feasibility of gasifying mixed plastic waste for hydrogen production and carbon capture and storage", *Communications Earth & Environment*, v. 3, n. 1, pp. 300, 2022.

[118] MUNIR, D., IRFAN, M. F., USMAN, M. R. "Hydrocracking of virgin and waste plastics: A detailed review", *Renewable and Sustainable Energy Reviews*, v. 90, pp. 490–515, 2018.

[119] LAREDO, G. C., REZA, J., RUIZ, E. M. "Hydrothermal liquefaction processes for plastics recycling: A review", *Cleaner Chemical Engineering*, v. 5, pp. 100094, 2023.

[120] KAMEEL, N. I. A., DAUD, W. M. A. W., PATAH, M. F. A., et al. "Influence of reaction parameters on thermal liquefaction of plastic wastes into oil: A review", *Energy Conversion and Management: X*, v. 14, pp. 100196, 2022.

[121] LACHOS-PEREZ, D., JAN, K., YU, E., et al. "Hydrothermal processing of polyethylene in superheated steam and supercritical water into fuels and chemicals", *Energy Conversion and Management*, v. 325, pp. 119355, 2025.

[122] POHJAKALLIO, M., VUORINEN, T., OASMAA, A. "Chemical routes for recycling—dissolving, catalytic, and thermochemical technologies". In: *Plastic Waste and Recycling*, Elsevier, pp. 359–384, 2020. doi: 10.1016/B978-0-12-817880-5.00013-X.

[123] THUNMAN, H., VILCHES, T. B., SEEMANN, M., et al. "Circular use of plastics-transformation of existing petrochemical clusters into thermochemical recycling plants with 100% plastics recovery", *Sustainable Materials and Technologies*, v. 22, pp. e00124, 2019.

[124] TUKKER, A., DE GROOT, H., SIMONS, L., et al. *Chemical Recycling of Plastics Waste (PVC and other resins)*. TNO Institute of Strategy, Technology and Policy.

[125] GRACIDA-ALVAREZ, U. R., BENAVIDES, P. T., LEE, U., et al. "Life-cycle analysis of recycling of post-use plastic to plastic via pyrolysis", *Journal of Cleaner Production*, v. 425, pp. 138867, 2023.

[126] BUTLER, E., DEVLIN, G., MCDONNELL, K. "Waste polyolefins to liquid fuels via pyrolysis: review of commercial state-of-the-art and recent laboratory research", *Waste and biomass valorization*, v. 2, n. 3, pp. 227–255, 2011. doi: 10.1007/s12649-011-9067-5.

[127] CHEN, D., YIN, L., WANG, H., et al. "Pyrolysis technologies for municipal solid waste: a review", *Waste management*, v. 34, n. 12, pp. 2466–2486, 2014. doi: 10.1016/j.wasman.2014.08.004.

[128] ALMEIDA, D., MARQUES, M. D. F. "Thermal and catalytic pyrolysis of plastic waste", *Polímeros*, v. 26, n. 1, pp. 44–51, 2016. doi: 10.1590/0104-1428.2100.

[129] SHARUDDIN, S. D. A., ABNISA, F., DAUD, W. M. A. W., et al. "A review on pyrolysis of plastic wastes", *Energy conversion and management*, v. 115, pp. 308–326, 2016. doi: 10.1016/j.enconman.2016.02.037.

[130] MIANDAD, R., BARAKAT, M., ABURIAZAIZA, A. S., et al. "Catalytic pyrolysis of plastic waste: A review", *Process Safety and Environmental Protection*, v. 102, pp. 822–838, 2016. doi: 0.1016/j.psep.2016.06.022.

[131] LOPEZ, G., ARTETXE, M., AMUTIO, M., et al. "Thermochemical routes for the valorization of waste polyolefinic plastics to produce fuels and chemicals. A review", *Renewable and Sustainable Energy Reviews*, v. 73, pp. 346–368, 2017. doi: 10.1016/j.rser.2017.01.142.

[132] RAGAERT, K., DELVA, L., VAN GEEM, K. "Mechanical and chemical recycling of solid plastic waste", *Waste management*, v. 69, pp. 24–58, 2017. ISSN: 0956-053X. doi: 10.1016/j.wasman.2017.07.044. Available in: <http://www.sciencedirect.com/science/article/pii/S0956053X17305354>.

[133] HORODYTSKA, O., VALDÉS, F. J., FULLANA, A. "Plastic flexible films waste management–A state of art review", *Waste management*, v. 77, pp. 413–425, 2018. doi: 10.1016/j.wasman.2018.04.023.

[134] VIJAYAKUMAR, A., SEBASTIAN, J. "Pyrolysis process to produce fuel from different types of plastic–a review". In: *IOP Conference Series: Materials Science and Engineering*, v. 396, p. 012062. IOP Publishing, 2018. doi: 10.1088/1757-899X/396/1/012062.

[135] DA SILVA, D. J., WIEBECK, H. "Current options for characterizing, sorting, and recycling polymeric waste", *Progress in Rubber, Plastics and*

Recycling Technology, v. 36, n. 4, pp. 284–303, 2020. doi: 10.1177/1477760620918603.

[136] JHA, K. K., KANNAN, T. "Recycling of plastic waste into fuel by pyrolysis-a review", *Materials Today: Proceedings*, v. 37, pp. 3718–3720, 2021. doi: 10.1016/j.matpr.2020.10.181.

[137] KOSLOSKI-OH, S. C., WOOD, Z. A., MANJARREZ, Y., et al. "Catalytic methods for chemical recycling or upcycling of commercial polymers", *Materials Horizons*, v. 8, n. 4, pp. 1084–1129, 2021. doi: 10.1039/D0MH01286F.

[138] KUMAGAI, S., NAKATANI, J., SAITO, Y., et al. "Latest trends and challenges in feedstock recycling of polyolefinic plastics", *Journal of the Japan Petroleum Institute*, v. 63, n. 6, pp. 345–364, 2020. doi: 10.1627/jpi.63.345.

[139] MURTHY, K., SHETTY, R. J., SHIVA, K. "Plastic waste conversion to fuel: a review on pyrolysis process and influence of operating parameters", *Energy Sources, Part A: Recovery, Utilization, and Environmental Effects*, pp. 1–21, 2020. doi: 10.1080/15567036.2020.1818892.

[140] NANDA, S., BERRUTI, F. "Thermochemical conversion of plastic waste to fuels: a review", *Environmental Chemistry Letters*, pp. 1–26, 2020. doi: 10.1007/s10311-020-01094-7.

[141] LEE, J., KWON, E. E., LAM, S. S., et al. "Chemical recycling of plastic waste via thermocatalytic routes", *Journal of Cleaner Production*, v. 321, pp. 128989, 2021. doi: 10.1016/j.jclepro.2021.128989.

[142] MAAFA, I. M. "Pyrolysis of Polystyrene Waste: A Review", *Polymers*, v. 13, n. 2, pp. 225, 2021. doi: 10.3390/polym13020225.

[143] SONI, V. K., SINGH, G., VIJAYAN, B. K., et al. "Thermochemical Recycling of Waste Plastics by Pyrolysis: A Review", *Energy & Fuels*, v. 35, n. 16, pp. 12763–12808, 2021. doi: 10.1021/acs.energyfuels.1c01292.

[144] SPREAFICO, C., RUSSO, D., SPREAFICO, M. "Investigating the evolution of pyrolysis technologies through bibliometric analysis of patents and papers", *Journal of Analytical and Applied Pyrolysis*, p. 105021, 2021. doi: 10.1016/j.jaap.2021.105021.

[145] ZHANG, F., ZHAO, Y., WANG, D., et al. "Current technologies for plastic waste treatment: A review", *Journal of Cleaner Production*, v. 282, pp. 124523, 2021. doi: 10.1016/j.jclepro.2020.124523.

[146] HUANG, J., VEKSHA, A., CHAN, W. P., et al. "Chemical recycling of plastic waste for sustainable material management: A prospective review on catalysts and processes", *Renewable and Sustainable Energy Reviews*, v. 154, pp. 111866, 2022. doi: 10.1016/j.rser.2021.111866.

[147] DOGU, O., PELUCCHI, M., VAN DE VIJVER, R., et al. "The chemistry of chemical recycling of solid plastic waste via pyrolysis and gasification: State-of-the-art, challenges, and future directions", *Progress in Energy and Combustion Science*, v. 84, pp. 100901, 2021. doi: 10.1016/j.pecs.2020.100901.

[148] CONESA, J., FONT, R., MARCILLA, A., et al. "Kinetic model for the continuous pyrolysis of two types of polyethylene in a fluidized bed reactor", *Journal of analytical and applied pyrolysis*, v. 40, pp. 419–431, 1997.

[149] MISKOLCZI, N., ATEŞ, F., BORSODI, N. "Comparison of real waste (MSW and MPW) pyrolysis in batch reactor over different catalysts. Part II: contaminants, char and pyrolysis oil properties", *Bioresource technology*, v. 144, pp. 370–379, 2013.

[150] OHNO, H., KUMAGAI, S., NAKATANI, J., et al. "Feedstock recycling of waste plastics in an oil refinery: Scenario development based on sorting and pyrolysis experiments", *Resources, Conservation and Recycling*, v. 208, pp. 107714, 2024.

[151] KUSENBERG, M., ROOSEN, M., DOKTOR, A., et al. "Contaminant removal from plastic waste pyrolysis oil via depth filtration and the impact on chemical recycling: A simple solution with significant impact", *Chemical Engineering Journal*, v. 473, pp. 145259, 2023.

[152] TORRES, D., JIANG, Y., MONSALVE, D. S., et al. "Chlorine removal from the pyrolysis of urban polyolefinic waste in a semi-batch reactor", *Journal of Environmental Chemical Engineering*, v. 9, n. 1, pp. 104920, 2021.

[153] EPHRAIM, A., PHAM MINH, D., LEBONNOIS, D., et al. "Co-pyrolysis of wood and plastics: Influence of plastic type and content on product yield, gas composition and quality", v. 231, pp. 110–117. ISSN: 0016-2361. doi: 10.1016/j.fuel.2018.04.140. Available in: <`http://www.sciencedirect.com/science/article/pii/S001623611830783X`>.

[154] GU, J., FAN, H., WANG, Y., et al. "Co-pyrolysis of xylan and high-density polyethylene: Product distribution and synergistic effects", v. 267, pp. 116896. ISSN: 0016-2361. doi: 10.1016/j.fuel.2019.116896. Available in: <http://www.sciencedirect.com/science/article/pii/S0016236119322860>.

[155] WU, J., CHEN, T., LUO, X., et al. "TG/FTIR analysis on co-pyrolysis behavior of PE, PVC and PS", v. 34, n. 3, pp. 676–682. ISSN: 0956-053X. doi: 10.1016/j.wasman.2013.12.005. Available in: <http://www.sciencedirect.com/science/article/pii/S0956053X13005722>.

[156] WONG, H.-W., BROADBELT, L. J. "Tertiary resource recovery from waste polymers via pyrolysis: neat and binary mixture reactions of polypropylene and polystyrene", *Industrial & engineering chemistry research*, v. 40, n. 22, pp. 4716–4723, 2001.

[157] MASTRAL, F., ESPERANZA, E., GARCIA, P., et al. "Pyrolysis of high-density polyethylene in a fluidised bed reactor. Influence of the temperature and residence time", *Journal of Analytical and Applied Pyrolysis*, v. 63, n. 1, pp. 1–15, 2002.

[158] CHEN, Z., ZHANG, X., CHE, L., et al. "Effect of volatile reactions on oil production and composition in thermal and catalytic pyrolysis of polyethylene", *Fuel*, v. 271, pp. 117308, 2020.

[159] MIANDAD, R., NIZAMI, A., REHAN, M., et al. "Influence of temperature and reaction time on the conversion of polystyrene waste to pyrolysis liquid oil", *Waste Management*, v. 58, pp. 250–259, 2016.

[160] ARTETXE, M., LOPEZ, G., AMUTIO, M., et al. "Styrene recovery from polystyrene by flash pyrolysis in a conical spouted bed reactor", v. 45, pp. 126–133. ISSN: 0956-053X. doi: 10.1016/j.wasman.2015.05.034. Available in: <http://www.sciencedirect.com/science/article/pii/S0956053X15004092>.

[161] YAN, G., JING, X., WEN, H., et al. "Thermal cracking of virgin and waste plastics of PP and LDPE in a semibatch reactor under atmospheric pressure", *Energy & Fuels*, v. 29, n. 4, pp. 2289–2298, 2015.

[162] GRACIDA-ALVAREZ, U. R., MITCHELL, M. K., SACRAMENTO-RIVERO, J. C., et al. "Effect of temperature and vapor residence time on

the micropyrolysis products of waste high density polyethylene", *Industrial Engineering Chemistry Research*, v. 57, n. 6, pp. 1912–1923, 2018. ISSN: 0888-5885.

[163] JIN, Z., CHEN, D., YIN, L., et al. "Molten waste plastic pyrolysis in a vertical falling film reactor and the influence of temperature on the pyrolysis products", *Chinese journal of chemical engineering*, v. 26, n. 2, pp. 400–406, 2018.

[164] ONWUDILI, J. A., INSURA, N., WILLIAMS, P. T. "Composition of products from the pyrolysis of polyethylene and polystyrene in a closed batch reactor: Effects of temperature and residence time", *Journal of Analytical and Applied Pyrolysis*, v. 86, n. 2, pp. 293–303, 2009.

[165] MARCILLA, A., BELTRAN, M., NAVARRO, R. "Evolution with the Temperature of the Compounds Obtained in the Catalytic Pyrolysis of Polyethylene over HUSY", *Industrial & engineering chemistry research*, v. 47, n. 18, pp. 6896–6903, 2008.

[166] SINGH, R., RUJ, B., SADHUKHAN, A., et al. "Thermal degradation of waste plastics under non-sweeping atmosphere: Part 1: Effect of temperature, product optimization, and degradation mechanism", *Journal of environmental management*, v. 239, pp. 395–406, 2019.

[167] SINGH, R. K., RUJ, B., SADHUKHAN, A. K., et al. "Thermal degradation of waste plastics under non-sweeping atmosphere: Part 2: Effect of process temperature on product characteristics and their future applications", *Journal of Environmental Management*, v. 261, pp. 110112, 2020.

[168] GUO, Z., LAN, X., XUE, P. "High-Precision Monitoring of Average Molecular Weight of Polyethylene Wax from Waste High-Density Polyethylene", *Polymers*, v. 12, n. 1, pp. 188, 2020.

[169] WANG, J., JIANG, J., SUN, Y., et al. "Recycling benzene and ethylbenzene from in-situ catalytic fast pyrolysis of plastic wastes", *Energy Conversion and Management*, v. 200, pp. 112088, 2019.

[170] ZHAO, D., WANG, X., MILLER, J. B., et al. "The Chemistry and Kinetics of Polyethylene Pyrolysis: A Feedstock to Produce Fuels and Chemicals", *ChemSusChem*, 2019.

[171] SOGANCIOGLU, M., AHMETLI, G., YEL, E. "A comparative study on waste plastics pyrolysis liquid products quantity and energy recovery potential", *Energy Procedia*, v. 118, pp. 221–226, 2017.

[172] PASSAMONTI, F. J., SEDRAN, U. "Recycling of waste plastics into fuels. LDPE conversion in FCC", *Applied Catalysis B: Environmental*, v. 125, pp. 499–506, 2012.

[173] AYDINLI, B., CAGLAR, A. "The investigation of the effects of two different polymers and three catalysts on pyrolysis of hazelnut shell", *Fuel processing technology*, v. 93, n. 1, pp. 1–7, 2012.

[174] MIRANDA, M., PINTO, F., GULYURTLU, I., et al. "Response surface methodology optimization applied to rubber tyre and plastic wastes thermal conversion", *Fuel*, v. 89, n. 9, pp. 2217–2229, 2010.

[175] WEI, T.-T., WU, K.-J., LEE, S.-L., et al. "Chemical recycling of post-consumer polymer waste over fluidizing cracking catalysts for producing chemicals and hydrocarbon fuels", *Resources, Conservation and Recycling*, v. 54, n. 11, pp. 952–961, 2010.

[176] LIN, Y.-H., YANG, M.-H. "Tertiary recycling of polyethylene waste by fluidised-bed reactions in the presence of various cracking catalysts", *Journal of Analytical and Applied Pyrolysis*, v. 83, n. 1, pp. 101–109, 2008.

[177] DEL REMEDIO HERNÁNDEZ, M., GÓMEZ, A., GARCÍA, Á. N., et al. "Effect of the temperature in the nature and extension of the primary and secondary reactions in the thermal and HZSM-5 catalytic pyrolysis of HDPE", *Applied Catalysis A: General*, v. 317, n. 2, pp. 183–194, 2007.

[178] MISKOLCZI, N., BARTHA, L., DEÁK, G., et al. "Thermal and thermocatalytic degradation of high-density polyethylene waste", *Journal of Analytical and Applied Pyrolysis*, v. 72, n. 2, pp. 235–242, 2004.

[179] MISKOLCZI, N., BARTHA, L., DEAK, G., et al. "Thermal degradation of municipal plastic waste for production of fuel-like hydrocarbons", *Polymer Degradation and Stability*, v. 86, n. 2, pp. 357–366, 2004.

[180] AYLÓN, E., FERNÁNDEZ-COLINO, A., NAVARRO, M., et al. "Waste tire pyrolysis: comparison between fixed bed reactor and moving bed reactor", *Industrial & engineering chemistry research*, v. 47, n. 12, pp. 4029–4033, 2008.

[181] PARKU, G. K., COLLARD, F.-X., GÖRGENS, J. F. "Pyrolysis of waste polypropylene plastics for energy recovery: Influence of heating rate and vacuum conditions on composition of fuel product", *Fuel Processing Technology*, v. 209, pp. 106522, 2020.

[182] COSTA, P., PINTO, F., RAMOS, A., et al. "Study of the pyrolysis kinetics of a mixture of polyethylene, polypropylene, and polystyrene", *Energy & Fuels*, v. 24, n. 12, pp. 6239–6247, 2010.

[183] KANNAN, P., AL SHOAIBI, A., SRINIVASAKANNAN, C. "Temperature effects on the yield of gaseous olefins from waste polyethylene via flash pyrolysis", *Energy & fuels*, v. 28, n. 5, pp. 3363–3366, 2014.

[184] HASSIBI, N., QUIRING, Y., CARRÉ, V., et al. "Analysis and control of products obtained from pyrolysis of polypropylene using a reflux semi-batch reactor and GC-MS/FID and FT-ICR MS", *Journal of Analytical and Applied Pyrolysis*, v. 169, pp. 105826, 2023.

[185] SETH, D., SARKAR, A. "Thermal pyrolysis of polypropylene: effect of reflux-condenser on the molecular weight distribution of products", *Chemical engineering science*, v. 59, n. 12, pp. 2433–2445, 2004. ISSN: 0009-2509.

[186] HASSIBI, N., VEGA-BUSTOS, Y. A., AISSAOUI, M. H., et al. "Thermochemical Recycling of Polystyrene by Pyrolysis: Importance of the Reflux to Maximize the Production of Styrene and BTEX", *Industrial & Engineering Chemistry Research*, v. 62, n. 34, pp. 13432–13439, 2023.

[187] SINGH, R. K., RUJ, B. "Time and temperature depended fuel gas generation from pyrolysis of real world municipal plastic waste", *Fuel*, v. 174, pp. 164–171, 2016.

[188] LIN, Y.-H., YANG, M.-H. "Catalytic reactions of post-consumer polymer waste over fluidised cracking catalysts for producing hydrocarbons", *Journal of Molecular Catalysis A: Chemical*, v. 231, n. 1-2, pp. 113–122, 2005.

[189] ATASHI, F., GHOLIZADEH, M., ATAEI, F. "Pyrolysis analysis of polyethylene terephthalate: effects of carrier gases (N2, He, and Ar) and zeolite catalyst (A4) on yield", *Journal of Chemical Technology & Biotechnology*, v. 97, n. 12, pp. 3395–3405, 2022.

[190] ABBAS-ABADI, M. S., HAGHIGHI, M. N., YEGANEH, H. "The effect of temperature, catalyst, different carrier gases and stirrer on the produced transportation hydrocarbons of LLDPE degradation in a stirred reactor", *Journal of Analytical and Applied Pyrolysis*, v. 95, pp. 198–204, 2012.

[191] BARBARIAS, I., LOPEZ, G., ARTETXE, M., et al. "Kinetic Modeling of the Catalytic Steam Reforming of High-Density Polyethylene Pyrolysis Volatiles", *Energy & Fuels*, v. 31, n. 11, pp. 12645–12653, 2017.

[192] DUFAUD, V., BASSET, J.-M. "Catalytic hydrogenolysis at low temperature and pressure of polyethylene and polypropylene to diesels or lower alkanes by a zirconium hydride supported on silica-alumina: a step toward polyolefin degradation by the microscopic reverse of ziegler–natta polymerization", *Angewandte Chemie International Edition*, v. 37, n. 6, pp. 806–810, 1998.

[193] DE WITT, M. J., BROADBELT, L. J. "Binary interactions between high-density polyethylene and 4-(1-naphthylmethyl) bibenzyl during low-pressure pyrolysis", *Energy & fuels*, v. 14, n. 2, pp. 448–458, 2000.

[194] KUMARI, A., KUMAR, S. "Pyrolytic degradation of polyethylene in autoclave under high pressure to obtain fuel", *Journal of Analytical and Applied Pyrolysis*, v. 124, pp. 298–302, 2017.

[195] JING, X., YAN, G., ZHAO, Y., et al. "Study on mild cracking of polyolefins to liquid hydrocarbons in a closed batch reactor for subsequent olefin recovery", *Polymer degradation and stability*, v. 109, pp. 79–91, 2014.

[196] KUMAR, P. S., BHARATHIKUMAR, M., PRABHAKARAN, C., et al. "Conversion of waste plastics into low-emissive hydrocarbon fuels through catalytic depolymerization in a new laboratory scale batch reactor", *International Journal of Energy and Environmental Engineering*, v. 8, n. 2, pp. 167–173, 2017.

[197] KARADUMAN, A., KOÇAK, M. Ç., BILGESÜ, A. Y. "Flash vacuum pyrolysis of low density polyethylene in a free-fall reactor", *Polymer-Plastics Technology and Engineering*, v. 42, n. 2, pp. 181–191, 2003.

[198] LOPEZ, G., OLAZAR, M., AGUADO, R., et al. "Vacuum pyrolysis of waste tires by continuously feeding into a conical spouted bed reactor", *Industrial & engineering chemistry research*, v. 49, n. 19, pp. 8990–8997, 2010.

[199] SCHUBERT, T., LEHNER, M., KARNER, T., et al. "Influence of reaction pressure on co-pyrolysis of LDPE and a heavy petroleum fraction", *Fuel Processing Technology*, v. 193, pp. 204–211, 2019.

[200] ABBAS-ABADI, M. S., KUSENBERG, M., ZAYOUD, A., et al. "Thermal pyrolysis of waste versus virgin polyolefin feedstocks: The role of pressure, temperature and waste composition", *Waste Management*, v. 165, pp. 108–118, 2023.

[201] DE MIRANDA, D. M. V. *Reciclagem Química Avançada de Poliolefinas Pós-Consumo via Pirólise*. Tese de doutorado, Programa de Pós-graduação em Engenharia Química, COPPE, Universidade Federal do Rio de Janeiro, 2024. Available in: <https://www.peq.coppe.ufrj.br/images/16_01_2024_DSc_D%C3%A9bora_Micheline_compressed.pdf>. Disponível online.

[202] BOCKHORN, H., HENTSCHEL, J., HORNUNG, A., et al. "Environmental engineering: stepwise pyrolysis of plastic waste", *Chemical engineering science*, v. 54, n. 15-16, pp. 3043–3051, 1999.

[203] FUKUSHIMA, M., WU, B., IBE, H., et al. "Study on dechlorination technology for municipal waste plastics containing polyvinyl chloride and polyethylene terephthalate", v. 12, n. 2, pp. 108–122, 2010. ISSN: 1611-8227. doi: 10.1007/s10163-010-0279-8. Available in: <https://doi.org/10.1007/s10163-010-0279-8>.

[204] LEI, J., YUAN, G., WEERACHANCHAI, P., et al. "Investigation on thermal dechlorination and catalytic pyrolysis in a continuous process for liquid fuel recovery from mixed plastic wastes", v. 20, n. 1, pp. 137–146, 2018. ISSN: 1611-8227. doi: 10.1007/s10163-016-0555-3. Available in: <https://doi.org/10.1007/s10163-016-0555-3>.

[205] WANG, Y., WU, K., LIU, Q., et al. "Low chlorine oil production through fast pyrolysis of mixed plastics combined with hydrothermal dechlorination pretreatment", *Process Safety and Environmental Protection*, v. 149, pp. 105–114, 2021. doi: 10.1016/j.psep.2020.10.023.

[206] LU, P., HUANG, Q., BOURTSALAS, A. T., et al. "Review on fate of chlorine during thermal processing of solid wastes", *Journal of Environmental Sciences*, v. 78, pp. 13–28, 2019.

[207] BHASKAR, T., MATSUI, T., KANEKO, J., et al. "Novel calcium based sorbent (Ca-C) for the dehalogenation (Br, Cl) process during halogenated mixed plastic (PP/PE/PS/PVC and HIPS-Br) pyrolysis", *Green chemistry*, v. 4, n. 4, pp. 372–375, 2002.

[208] TANG, Y., SONG, M., DONG, J., et al. "Synergetic effect of in-situ CaO on PVC plastic pyrolysis characteristics: TG and Py GC/MS analysis", *Polymer Degradation and Stability*, p. 111205, 2025.

[209] XUE, Y., JOHNSTON, P., BAI, X. "Effect of catalyst contact mode and gas atmosphere during catalytic pyrolysis of waste plastics", v. 142, pp. 441

– 451, 2017. ISSN: 0196-8904. doi: https://doi.org/10.1016/j.enconman.2017.03.071. Available in: <http://www.sciencedirect.com/science/article/pii/S0196890417302820>.

[210] PENG, Y., WANG, Y., KE, L., et al. "A review on catalytic pyrolysis of plastic wastes to high-value products", *Energy Conversion and Management*, v. 254, pp. 115243, 2022.

[211] OCHOA, A., BILBAO, J., GAYUBO, A. G., et al. "Coke formation and deactivation during catalytic reforming of biomass and waste pyrolysis products: A review", v. 119, pp. 109600, 2020. ISSN: 1364-0321. doi: https://doi.org/10.1016/j.rser.2019.109600. Available in: <http://www.sciencedirect.com/science/article/pii/S1364032119308081>.

[212] MONTROLL, E. W., SIMHA, R. "Theory of depolymerization of long chain molecules", *The Journal of Chemical Physics*, v. 8, n. 9, pp. 721–726, 1940.

[213] MARK, H., SIMHA, R. "Degradation of long chain molecules", *Transactions of the Faraday Society*, v. 35, pp. 611–618, 1940.

[214] TUCKETT, R. "The degradation of high polymers", *Transactions of the Faraday Society*, v. 41, pp. 351–359, 1945.

[215] NANDA, V., PATHRIA, R. "Polymers and Theory of Numbers. I. The Single-Chain Theory of Degradation", *The Journal of Chemical Physics*, v. 30, n. 1, pp. 27–30, 1959.

[216] SIMHA, R. "Kinetics of degradation and size distribution of long chain polymers", *Journal of Applied Physics*, v. 12, n. 7, pp. 569–578, 1941.

[217] CHARLESBY, A. "Molecular-weight changes in the degradation of long-chain polymers", *Proceedings of the Royal Society of London. Series A. Mathematical and Physical Sciences*, v. 224, n. 1156, pp. 120–128, 1954.

[218] JELLINEK, H. G. "On the degradation of long chain molecules. Part I", *Transactions of the Faraday Society*, v. 40, pp. 266–273, 1944.

[219] JELLINEK, H. "On the degradation of long-chain molecules. Part II", *Transactions of the Faraday Society*, v. 44, pp. 345–349, 1948.

[220] OAKES, W., RICHARDS, R. "The thermal degradation of ethylene polymers", *Journal of the Chemical Society (Resumed)*, pp. 2929–2935, 1949.

[221] JELLINEK, H. "Thermal degradation of polystyrene. Part I", *Journal of Polymer Science*, v. 3, n. 6, pp. 850–865, 1948.

[222] JELLINEK, H. "Thermal degradation of polystyrene. Part II", *Journal of Polymer Science*, v. 4, n. 1, pp. 1–12, 1949.

[223] JELLINEK, H. "Thermal degradation of polystyrene and polyethylene. Part III", *Journal of Polymer Science*, v. 4, n. 1, pp. 13–36, 1949.

[224] MADORSKY, S. L. "Rates of thermal degradation of polystyrene and polyethylene in a vacuum", *Journal of Polymer Science*, v. 9, n. 2, pp. 133–156, 1952.

[225] RICE, F. "The Decomposition of Organic Compounds from the Standpoint of Free Radicals." *Chemical Reviews*, v. 17, n. 1, pp. 53–63, 1935.

[226] SIMHA, R., WALL, L. "Some aspects of depolymerization kinetics", *Journal of Polymer Science*, v. 6, n. 1, pp. 39–44, 1951. ISSN: 0022-3832.

[227] SIMHA, R., WALL, L. "Kinetics of chain depolymerization", *The Journal of Physical Chemistry*, v. 56, n. 6, pp. 707–715, 1952.

[228] WALL, L., MADORSKY, S., BROWN, D., et al. "The depolymerization of polymethylene and polyethylene", *Journal of the American chemical Society*, v. 76, n. 13, pp. 3430–3437, 1954.

[229] TSUCHIYA, Y., SUMI, K. "Thermal decomposition products of polyethylene", *Journal of Polymer Science Part A-1: Polymer Chemistry*, v. 6, n. 2, pp. 415–424, 1968.

[230] TSUCHIYA, Y., SUMI, K. "Thermal decomposition products of polypropylene", *Journal of Polymer Science Part A-1: Polymer Chemistry*, v. 7, n. 7, pp. 1599–1607, 1969.

[231] KIRAN, E., GILLHAM, J. "Pyrolysis-molecular weight chromatography: A new on-line system for analysis of polymers. II. Thermal decomposition of polyolefins: Polyethylene, polypropylene, polyisobutylene", *Journal of Applied Polymer Science*, v. 20, n. 8, pp. 2045–2068, 1976.

[232] SEEGER, M., CANTOW, H.-J. "Thermische spaltungsmechanismen in homo- und copolymeren aus α-olefinen, 1. Grundlegende mechanismen und pyrolyse von linearem polyäthylen", *Die Makromolekulare Chemie: Macromolecular Chemistry and Physics*, v. 176, n. 5, pp. 1411–1425, 1975.

[233] SEEGER, M., BARRALL, E. M. "Pyrolysis–gas chromatographic analysis of chain branching in polyethylene", *Journal of Polymer Science: Polymer Chemistry Edition*, v. 13, n. 7, pp. 1515–1529, 1975.

[234] MCNEILL, I., ZULFIQAR, M., KOUSAR, T. "A detailed investigation of the products of the thermal degradation of polystyrene", *Polymer degradation and stability*, v. 28, n. 2, pp. 131–151, 1990.

[235] COSTA, L., CAMINO, G., GUYOT, A., et al. "The role of chain ends in the thermal degradation of anionic polystyrene", *Polymer Degradation and Stability*, v. 4, n. 4, pp. 245–260, 1982.

[236] AUDISIO, G., BERTINI, F., BELTRAME, P. L., et al. "Catalytic degradation of polymers: Part III—Degradation of polystyrene", *Polymer degradation and stability*, v. 29, n. 2, pp. 191–200, 1990.

[237] GUYOT, A. "Recent developments in the thermal degradation of polystyrene—A review", *Polymer degradation and stability*, v. 15, n. 3, pp. 219–235, 1986.

[238] MADORSKY, S., MCINTYRE, D., O'MARA, J., et al. "Thermal degradation of fractionated high and low molecular weight polystyrenes", *J Res Natl Bur Stand. A*, v. 66, pp. 307–11, 1962.

[239] RICHARDS, D., SALTER, D. "Thermal degradation of vinyl polymers I—Thermal degradation of polystyrene-poly (α-methylstyrene) mixtures", *Polymer*, v. 8, pp. 127–138, 1967.

[240] CAMERON, G., KERR, G. "Thermal degradation of polystyrene—I. Chain scission at low temperatures", *European Polymer Journal*, v. 4, n. 6, pp. 709–717, 1968.

[241] REICH, L. "Kinetic parameters in polypropylene degradation from DTA traces", *Journal of Applied Polymer Science*, v. 10, n. 3, pp. 465–472, 1966.

[242] KANNAN, P., IBRAHIM, S., SURESH KUMAR REDDY, K., et al. "A comparative analysis of the kinetic experiments in polyethylene pyrolysis", *Journal of Energy Resources Technology*, v. 136, n. 2, 2014.

[243] ALBANO, C., DE FREITAS, E. "Thermogravimetric evaluation of the kinetics of decomposition of polyolefin blends", *Polymer degradation and stability*, v. 61, n. 2, pp. 289–295, 1998.

[244] ABOULKAS, A., EL BOUADILI, A., OTHERS. "Thermal degradation behaviors of polyethylene and polypropylene. Part I: Pyrolysis kinetics and mechanisms", *Energy Conversion and Management*, v. 51, n. 7, pp. 1363–1369, 2010.

[245] ŠIMON, P. "Isoconversional methods", *Journal of Thermal Analysis and Calorimetry*, v. 76, n. 1, pp. 123, 2004.

[246] XU, F., WANG, B., YANG, D., et al. "Thermal degradation of typical plastics under high heating rate conditions by TG-FTIR: Pyrolysis behaviors and kinetic analysis", *Energy Conversion and Management*, v. 171, pp. 1106–1115, 2018.

[247] ALI, G., NISAR, J., IQBAL, M., et al. "Thermo-catalytic decomposition of polystyrene waste: Comparative analysis using different kinetic models", *Waste Management & Research*, v. 38, n. 2, pp. 202–212, 2020.

[248] OYEDUN, A. O., TEE, C. Z., HANSON, S., et al. "Thermogravimetric analysis of the pyrolysis characteristics and kinetics of plastics and biomass blends", *Fuel processing technology*, v. 128, pp. 471–481, 2014.

[249] KAYACAN, I., DOĞAN, Ö. "Pyrolysis of low and high density polyethylene. Part I: non-isothermal pyrolysis kinetics", *Energy Sources, Part A: Recovery, Utilization, and Environmental Effects*, v. 30, n. 5, pp. 385–391, 2008.

[250] ENCINAR, J., GONZÁLEZ, J. "Pyrolysis of synthetic polymers and plastic wastes. Kinetic study", *Fuel Processing Technology*, v. 89, n. 7, pp. 678–686, 2008.

[251] SÁNCHEZ-JIMÉNEZ, P. E., PÉREZ-MAQUEDA, L. A., PEREJÓN, A., et al. "Limitations of model-fitting methods for kinetic analysis: Polystyrene thermal degradation", *Resources, conservation and recycling*, v. 74, pp. 75–81, 2013.

[252] WESTERHOUT, R., WAANDERS, J., KUIPERS, J., et al. "Kinetics of the low-temperature pyrolysis of polyethene, polypropene, and polystyrene modeling, experimental determination, and comparison with literature models and data", *Industrial & Engineering Chemistry Research*, v. 36, n. 6, pp. 1955–1964, 1997.

[253] CONESA, J. A., MARCILLA, A., FONT, R., et al. "Thermogravimetric studies on the thermal decomposition of polyethylene", *Journal of analytical and applied pyrolysis*, v. 36, n. 1, pp. 1–15, 1996.

[254] MARCILLA, A., GÓMEZ, A., REYES-LABARTA, J. "MCM-41 catalytic pyrolysis of ethylene–vinyl acetate copolymers: kinetic model", *Polymer*, v. 42, n. 19, pp. 8103–8111, 2001.

[255] MARCILLA, A., GÓMEZ, A., GARCIA, Á. N., et al. "Kinetic study of the catalytic decomposition of different commercial polyethylenes over an MCM-41 catalyst", *Journal of Analytical and Applied Pyrolysis*, v. 64, n. 1, pp. 85–101, 2002.

[256] MARCILLA, A., GOMEZ, A., REYES-LABARTA, J., et al. "Catalytic pyrolysis of polypropylene using MCM-41: kinetic model", *Polymer degradation and stability*, v. 80, n. 2, pp. 233–240, 2003.

[257] MARCILLA, A., GÓMEZ-SIURANA, A., VALDES, F. "Catalytic cracking of low-density polyethylene over H-Beta and HZSM-5 zeolites: Influence of the external surface. Kinetic model", *Polymer degradation and stability*, v. 92, n. 2, pp. 197–204, 2007.

[258] LIN, Y.-H., YANG, M.-H. "Kinetic and mechanistic modeling of acid-catalyzed degradation of polymers with various cracking catalysts", *Journal of applied polymer science*, v. 114, n. 5, pp. 2591–2599, 2009.

[259] OYEDUN, A. O., GEBREEGZIABHER, T., NG, D. K., et al. "Mixed-waste pyrolysis of biomass and plastics waste–a modelling approach to reduce energy usage", *Energy*, v. 75, pp. 127–135, 2014.

[260] YOUNAN, Y., VAN GOETHEM, M. W., STEFANIDIS, G. D. "A particle scale model for municipal solid waste and refuse-derived fuels pyrolysis", *Computers & Chemical Engineering*, v. 86, pp. 148–159, 2016.

[261] TONDL, G., BONELL, L., PFEIFER, C. "Thermogravimetric analysis and kinetic study of marine plastic litter", *Marine pollution bulletin*, v. 133, pp. 472–477, 2018.

[262] DENTE, M., BOZZANO, G., FARAVELLI, T., et al. "Kinetic modelling of pyrolysis processes in gas and condensed phase", *Advances in chemical engineering*, v. 32, pp. 51–166, 2007. doi: 10.1016/S0065-2377(07)32002-4. Available in: <`http://www.sciencedirect.com/science/article/pii/S0065237707320024`>. ISSN: 0065-2377.

[263] POUTSMA, M. L. "Reexamination of the pyrolysis of polyethylene: data needs, free-radical mechanistic considerations, and thermochemical kinetic simulation of initial product-forming pathways", *Macromolecules*, v. 36, n. 24, pp. 8931–8957, 2003. ISSN: 0024-9297.

[264] SAWADA, H. "Depolymerization", *Encyclopedia of Polymer Science and Technology*, 2002.

[265] NISHIDA, H. "Development of materials and technologies for control of polymer recycling", *Polymer journal*, v. 43, n. 5, pp. 435–447, 2011.

[266] MCCOY, B. J. "Continuous-mixture kinetics and equilibrium for reversible oligomerization reactions", v. 39, n. 11, pp. 1827–1833. ISSN: 1547-5905. doi: https://doi.org/10.1002/aic.690391110. Available in: <https://aiche.onlinelibrary.wiley.com/doi/abs/10.1002/aic.690391110>. _eprint: https://aiche.onlinelibrary.wiley.com/doi/pdf/10.1002/aic.690391110.

[267] WANG, M., SMITH, J. M., MCCOY, B. J. "Continuous kinetics for thermal degradation of polymer in solution", v. 41, n. 6, pp. 1521–1533. ISSN: 1547-5905. doi: https://doi.org/10.1002/aic.690410616. Available in: <https://aiche.onlinelibrary.wiley.com/doi/abs/10.1002/aic.690410616>.

[268] MADRAS, G., SMITH, J. M., MCCOY, B. J. "Effect of Tetralin on the Degradation of Polymer in Solution", v. 34, n. 12, pp. 4222–4228, .

[269] MCCOY, B. J. "Continuous kinetics of cracking reactions: Thermolysis and pyrolysis", v. 51, n. 11, pp. 2903–2908. ISSN: 0009-2509. doi: 10.1016/0009-2509(96)00172-8. Available in: <http://www.sciencedirect.com/science/article/pii/0009250996001728>.

[270] MADRAS, G., SMITH, J. M., MCCOY, B. J. "Degradation of Poly(methyl methacrylate) in Solution", v. 35, n. 6, pp. 1795–1800, . ISSN: 0888-5885. doi: 10.1021/ie960018b. Available in: <https://doi.org/10.1021/ie960018b>. Publisher: American Chemical Society.

[271] KODERA, Y., MCCOY, B. J. "Distribution kinetics of radical mechanisms: Reversible polymer decomposition", v. 43, n. 12, pp. 3205–3214, . ISSN: 1547-5905. doi: https://doi.org/10.1002/aic.690431208. Available in: <https://aiche.onlinelibrary.wiley.com/doi/abs/10.1002/aic.690431208>. _eprint: https://aiche.onlinelibrary.wiley.com/doi/pdf/10.1002/aic.690431208.

[272] MADRAS, G., CHUNG, G. Y., SMITH, J. M., et al. "Molecular Weight Effect on the Dynamics of Polystyrene Degradation", v. 36, n. 6, pp. 2019–2024, . ISSN: 0888-5885. doi: 10.1021/ie9607513. Available in: <https://doi.org/10.1021/ie9607513>. Publisher: American Chemical Society.

[273] MCCOY, B. J., MADRAS, G. "Degradation kinetics of polymers in solution: Dynamics of molecular weight distributions", v. 43, n. 3,

pp. 802–810, . ISSN: 1547-5905. doi: https://doi.org/10.1002/aic.690430325. Available in: <https://aiche.onlinelibrary.wiley.com/doi/abs/10.1002/aic.690430325>. _eprint: https://aiche.onlinelibrary.wiley.com/doi/pdf/10.1002/aic.690430325.

[274] MADRAS, G., MCCOY, B. J. "Effect of hydrogen donors on polymer degradation", v. 40, n. 4, pp. 321–332, . ISSN: 0920-5861. doi: 10.1016/S0920-5861(98)00061-3. Available in: <http://www.sciencedirect.com/science/article/pii/S0920586198000613>.

[275] MADRAS, G., MCCOY, B. J. "Time evolution to similarity solutions for polymer degradation", v. 44, n. 3, pp. 647–655, . ISSN: 1547-5905. doi: https://doi.org/10.1002/aic.690440313. Available in: <https://aiche.onlinelibrary.wiley.com/doi/abs/10.1002/aic.690440313>. _eprint: https://aiche.onlinelibrary.wiley.com/doi/pdf/10.1002/aic.690440313.

[276] MCCOY, B. J., MADRAS, G. "Evolution to similarity solutions for fragmentation and aggregation", *Journal of Colloid and Interface Science*, v. 201, n. 2, pp. 200–209, 1998.

[277] SEZGI, N. A., CHA, W. S., SMITH, J., et al. "Polyethylene pyrolysis: Theory and experiments for molecular-weight-distribution kinetics", *Industrial engineering chemistry research*, v. 37, n. 7, pp. 2582–2591, 1998. ISSN: 0888-5885. doi: 10.1021/ie980106r. Available in: <https://doi.org/10.1021/ie980106r>. Publisher: American Chemical Society.

[278] MADRAS, G., MCCOY, B. J. "Distribution Kinetics for Polymer Mixture Degradation", v. 38, n. 2, pp. 352–357, . ISSN: 0888-5885. doi: 10.1021/ie9805335. Available in: <https://doi.org/10.1021/ie9805335>. Publisher: American Chemical Society.

[279] MCCOY, B. J. "Distribution Kinetics for Temperature-Programmed Pyrolysis", v. 38, n. 12, pp. 4531–4537. ISSN: 0888-5885. doi: 10.1021/ie990462p. Available in: <https://doi.org/10.1021/ie990462p>. Publisher: American Chemical Society.

[280] J. MCCOY, B. "Polymer thermogravimetric analysis: effects of chain-end and reversible random scission", v. 56, n. 4, pp. 1525–1529. ISSN: 0009-2509. doi: 10.1016/S0009-2509(00)00379-1. Available in: <http://www.sciencedirect.com/science/article/pii/S0009250900003791>.

[281] MCCOY, B. J., MADRAS, G. "Discrete and continuous models for polymerization and depolymerization", v. 56, n. 8, pp. 2831–2836, . ISSN: 0009-2509. doi: 10.1016/S0009-2509(00)00516-9. Available in: <http://www.sciencedirect.com/science/article/pii/S0009250900005169>.

[282] STERLING, W. J., MCCOY, B. J. "Distribution kinetics of thermolytic macromolecular reactions", v. 47, n. 10, pp. 2289–2303. ISSN: 1547-5905. doi: https://doi.org/10.1002/aic.690471014. Available in: <https://aiche.onlinelibrary.wiley.com/doi/abs/10.1002/aic.690471014>. _eprint: https://aiche.onlinelibrary.wiley.com/doi/pdf/10.1002/aic.690471014.

[283] CHA, W. S., KIM, S. B., MCCOY, B. J. "Study of polystyrene degradation using continuous distribution kinetics in a bubbling reactor", *Korean Journal of Chemical Engineering*, v. 19, n. 2, pp. 239–245, 2002.

[284] KODERA, Y., MCCOY, B. J. "Distribution Kinetics of Polymer Thermogravimetric Analysis: A Model for Chain-End and Random Scission", v. 16, n. 1, pp. 119–126, . ISSN: 0887-0624. doi: 10.1021/ef0100855. Available in: <https://doi.org/10.1021/ef0100855>. Publisher: American Chemical Society.

[285] MADRAS, G., MCCOY, B. J. "Numerical and Similarity Solutions for Reversible Population Balance Equations with Size-Dependent Rates", v. 246, n. 2, pp. 356–365, . ISSN: 0021-9797. doi: 10.1006/jcis.2001.8073. Available in: <http://www.sciencedirect.com/science/article/pii/S0021979701980737>.

[286] SMAGALA, T. G., MCCOY, B. J. "Mechanisms and Approximations in Macromolecular Reactions: Reversible Initiation, Chain Scission, and Hydrogen Abstraction", v. 42, n. 12, pp. 2461–2469. ISSN: 0888-5885. doi: 10.1021/ie0205750. Available in: <https://doi.org/10.1021/ie0205750>. Publisher: American Chemical Society.

[287] KRUSE, T. M., LEVINE, S. E., WONG, H.-W., et al. "Binary mixture pyrolysis of polypropylene and polystyrene: A modeling and experimental study", *Journal of analytical and applied pyrolysis*, v. 73, n. 2, pp. 342–354, 2005.

[288] POUTSMA, M. L. "Fundamental reactions of free radicals relevant to pyrolysis reactions", *Journal of Analytical and Applied Pyrolysis*, v. 54, n. 1-2, pp. 5–35, 2000. ISSN: 0165-2370.

[289] POUTSMA, M. L. "Comparison of literature models for volatile product formation from the pyrolysis of polyisobutylene at mild conditions: Data analysis, free-radical mechanistic considerations, and simulation of initial product-forming pathways", *Journal of analytical and applied pyrolysis*, v. 73, n. 2, pp. 159–203, 2005.

[290] POUTSMA, M. L. "Mechanistic analysis and thermochemical kinetic simulation of the pathways for volatile product formation from pyrolysis of polystyrene, especially for the dimer", *Polymer degradation and stability*, v. 91, n. 12, pp. 2979–3009, 2006.

[291] POUTSMA, M. L. "Mechanistic analysis and thermochemical kinetic simulation of the products from pyrolysis of poly (α-methylstyrene), especially the unrecognized role of phenyl shift", *Journal of Analytical and Applied Pyrolysis*, v. 80, n. 2, pp. 439–452, 2007.

[292] POUTSMA, M. L. "Further considerations of the sources of the volatiles from pyrolysis of polystyrene", *Polymer degradation and stability*, v. 94, n. 11, pp. 2055–2064, 2009. ISSN: 0141-3910.

[293] KRUSE, T. M., WOO, O. S., BROADBELT, L. J. "Detailed mechanistic modeling of polymer degradation: application to polystyrene", *Chemical engineering science*, v. 56, n. 3, pp. 971–979, 2001.

[294] KRUSE, T. M., WOO, O. S., WONG, H.-W., et al. "Mechanistic modeling of polymer degradation: a comprehensive study of polystyrene", *Macromolecules*, v. 35, n. 20, pp. 7830–7844, 2002. ISSN: 0024-9297.

[295] KRUSE, T. M., WONG, H.-W., BROADBELT, L. J. "Modeling the evolution of the full polystyrene molecular weight distribution during polystyrene pyrolysis", *Industrial & engineering chemistry research*, v. 42, n. 12, pp. 2722–2735, 2003.

[296] LEVINE, S. E., BROADBELT, L. J. "Reaction pathways to dimer in polystyrene pyrolysis: a mechanistic modeling study", *Polymer degradation and stability*, v. 93, n. 5, pp. 941–951, 2008.

[297] LEVINE, S. E., BROADBELT, L. J. "Detailed mechanistic modeling of high-density polyethylene pyrolysis: Low molecular weight product evolution", *Polymer Degradation and Stability*, v. 94, n. 5, pp. 810–822, 2009. ISSN: 0141-3910.

[298] VINU, R., LEVINE, S. E., WANG, L., et al. "Detailed mechanistic modeling of poly (styrene peroxide) pyrolysis using kinetic Monte Carlo simulation", *Chemical engineering science*, v. 69, n. 1, pp. 456–471, 2012.

[299] RANZI, E., DENTE, M., FARAVELLI, T., et al. "Kinetic modeling of polyethylene and polypropylene thermal degradation", v. 40-41, pp. 305 – 319. ISSN: 0165-2370. doi: https://doi.org/10.1016/S0165-2370(97)00032-6. Available in: <http://www.sciencedirect.com/science/article/pii/S0165237097000326>.

[300] FARAVELLI, T., BOZZANO, G., SCASSA, C., et al. "Gas product distribution from polyethylene pyrolysis", *Journal of Analytical and Applied Pyrolysis*, v. 52, n. 1, pp. 87–103, 1999. ISSN: 0165-2370. doi: https://doi.org/10.1016/S0165-2370(99)00032-7. Available in: <http://www.sciencedirect.com/science/article/pii/S0165237099000327>.

[301] RANZI, E., DENTE, M., GOLDANIGA, A., et al. "Lumping procedures in detailed kinetic modeling of gasification, pyrolysis, partial oxidation and combustion of hydrocarbon mixtures", *Progress in Energy and Combustion Science*, v. 27, n. 1, pp. 99–139, 2001. ISSN: 0360-1285. doi: 10.1016/S0360-1285(00)00013-7.

[302] FARAVELLI, T., BOZZANO, G., COLOMBO, M., et al. "Kinetic modeling of the thermal degradation of polyethylene and polystyrene mixtures", v. 70, n. 2, pp. 761 – 777, 2003. ISSN: 0165-2370. doi: https://doi.org/10.1016/S0165-2370(03)00058-5. Available in: <http://www.sciencedirect.com/science/article/pii/S0165237003000585>.

[303] MARONGIU, A., FARAVELLI, T., BOZZANO, G., et al. "Thermal degradation of poly(vinyl chloride)", v. 70, n. 2, pp. 519 – 553, 2003. ISSN: 0165-2370. doi: https://doi.org/10.1016/S0165-2370(03)00024-X. Available in: <http://www.sciencedirect.com/science/article/pii/S016523700300024X>.

[304] MEHL, M., MARONGIU, A., FARAVELLI, T., et al. "A kinetic modeling study of the thermal degradation of halogenated polymers", v. 72, n. 2, pp. 253 – 272, 2004. ISSN: 0165-2370. doi: https://doi.org/10.1016/j.jaap.2004.07.007. Available in: <http://www.sciencedirect.com/science/article/pii/S016523700400066X>.

[305] MARONGIU, A., FARAVELLI, T., RANZI, E. "Detailed kinetic modeling of the thermal degradation of vinyl polymers", v. 78, n. 2, pp. 343

– 362, 2007. ISSN: 0165-2370. doi: https://doi.org/10.1016/j.jaap.2006.09.008. Available in: <http://www.sciencedirect.com/science/article/pii/S0165237006001240>.

[306] MASTRAL, J., BERRUECO, C., CEAMANOS, J. "Modelling of the pyrolysis of high density polyethylene: product distribution in a fluidized bed reactor", *Journal of analytical and applied pyrolysis*, v. 79, n. 1-2, pp. 313–322, 2007.

[307] MASTRAL, J., BERRUECO, C., CEAMANOS, J. "Theoretical prediction of product distribution of the pyrolysis of high density polyethylene", *Journal of Analytical and Applied Pyrolysis*, v. 80, n. 2, pp. 427–438, 2007.

[308] PANTANO, I. A. G., DÍAZ, M. F., BRANDOLIN, A., et al. "Mathematical modeling of the catalytic degradation of polystyrene in the presence of aluminum chloride", *Polymer degradation and stability*, v. 94, n. 4, pp. 566–574, 2009.

[309] GIANOGLIO PANTANO, I. A., ASTEASUAIN, M., DÍAZ, M. F., et al. "Catalytic Degradation of Polystyrene: Modeling of Molecular Weight Distribution", *Macromolecular Reaction Engineering*, v. 5, n. 5-6, pp. 243–253, 2011.

[310] PANTANO, I. A. G., BRANDOLIN, A., SARMORIA, C. "Mathematical modeling of the graft reaction between polystyrene and polyethylene", *Polymer degradation and stability*, v. 96, n. 4, pp. 416–425, 2011.

[311] ZAVALA-GUTIÉRREZ, J., PEREZ-CAMACHO, O., VILLARREAL-CARDENAS, L., et al. "Mathematical modeling of the catalytic pyrolysis of high-density polyethylene in a plug-flow tubular reactor", *Industrial & Engineering Chemistry Research*, v. 58, n. 41, pp. 19050–19060, 2019.

[312] ORDAZ-QUINTERO, A., MONROY-ALONSO, A., SALDÍVAR-GUERRA, E. "Thermal Pyrolysis of Polystyrene Aided by a Nitroxide End-Functionality. Experiments and Modeling", *Processes*, v. 8, n. 4, pp. 432, 2020.

[313] SMIT, K. D., MARIEN, Y. W., GEEM, K. M. V., et al. "Connecting polymer synthesis and chemical recycling on a chain-by-chain basis: a unified matrix-based kinetic Monte Carlo strategy", *Reaction Chemistry & Engineering*, v. 5, n. 10, pp. 1909–1928, 2020. ISSN: 2058-9883. doi: 10.1039/D0RE00266F. Available in: <https://pubs.rsc.org/

en/content/articlelanding/2020/re/d0re00266f>. Publisher: The Royal Society of Chemistry.

[314] DOGU, O., PLEHIERS, P. P., VAN DE VIJVER, R., et al. "Distribution changes during thermal degradation of poly (styrene peroxide) by pairing tree-based kinetic Monte Carlo and artificial intelligence tools", *Industrial Engineering Chemistry Research*, v. 60, n. 8, pp. 3334–3353, 2021. ISSN: 0888-5885. doi: 10.1021/acs.iecr.0c05414.

[315] GUILLÉN-GOSÁLBEZ, G., YOU, F., GALÁN-MARTÍN, Á., et al. "Process systems engineering thinking and tools applied to sustainability problems: current landscape and future opportunities", *Current Opinion in Chemical Engineering*, v. 26, pp. 170–179, 2019.

[316] GU, F., GUO, J., ZHANG, W., et al. "From waste plastics to industrial raw materials: A life cycle assessment of mechanical plastic recycling practice based on a real-world case study", *Science of the total environment*, v. 601, pp. 1192–1207, 2017.

[317] BORA, R. R., WANG, R., YOU, F. "Waste Polypropylene Plastic Recycling toward Climate Change Mitigation and Circular Economy: Energy, Environmental, and Technoeconomic Perspectives", *ACS Sustainable Chemistry & Engineering*, v. 8, n. 43, pp. 16350–16363, 2020. doi: 10.1021/acssuschemeng.0c06311.

[318] RAMESH, P., VINODH, S. "State of art review on Life Cycle Assessment of polymers", *International Journal of Sustainable Engineering*, v. 13, n. 6, pp. 411–422, 2020.

[319] HUYSVELD, S., HUBO, S., RAGAERT, K., et al. "Advancing circular economy benefit indicators and application on open-loop recycling of mixed and contaminated plastic waste fractions", *Journal of Cleaner Production*, v. 211, pp. 1–13, 2019.

[320] HOU, P., XU, Y., TAIEBAT, M., et al. "Life cycle assessment of end-of-life treatments for plastic film waste", *Journal of Cleaner Production*, v. 201, pp. 1052–1060, 2018.

[321] *Exploration chemical recycling – Extended summary: What is the potential contribution of chemical recycling to Dutch climate policy?* CE Delft, 2020. Available in: <https://ce.nl/en/publications/2173/exploratory-study-on-chemical-recycling-update-2019>. Acesso em: 17/01/2021.

[322] *Life cycle assessment (LCA) for ChemCycling*. BASF, 2020. Available in: <https://www.basf.com/global/en/who-we-are/sustainability/we-drive-sustainable-solutions/circular-economy/mass-balance-approach/chemcycling/lca-for-chemcycling.html>. Acesso em: 17/01/2021.

[323] BENAVIDES, P. T., SUN, P., HAN, J., et al. "Life-cycle analysis of fuels from post-use non-recycled plastics", *Fuel*, v. 203, pp. 11–22, 2017. doi: 10.1016/j.fuel.2017.04.070.

[324] DEMETRIOUS, A., CROSSIN, E. "Life cycle assessment of paper and plastic packaging waste in landfill, incineration, and gasification-pyrolysis", *Journal of Material Cycles and Waste Management*, v. 21, n. 4, pp. 850–860, 2019. doi: 10.1007/s10163-019-00842-4.

[325] KELLER, F., LEE, R. P., MEYER, B. "Life cycle assessment of global warming potential, resource depletion and acidification potential of fossil, renewable and secondary feedstock for olefin production in Germany", *Journal of Cleaner Production*, v. 250, pp. 119484, 2020.

[326] MEYS, R., FRICK, F., WESTHUES, S., et al. "Towards a circular economy for plastic packaging wastes–the environmental potential of chemical recycling", *Resources, Conservation and Recycling*, v. 162, pp. 105010, 2020. doi: 10.1016/j.resconrec.2020.105010.

[327] ANTELAVA, A., DAMILOS, S., HAFEEZ, S., et al. "Plastic Solid Waste (PSW) in the Context of Life Cycle Assessment (LCA) and Sustainable Management", *Environmental management*, v. 64, n. 2, pp. 230–244, 2019.

[328] EUROPE, Z. W. *El Dorado of Chemical Recycling: State of play and policy challenges*. Zero Waste Europe, 2019. Available in: <https://zerowasteeurope.eu/wp-content/uploads/2019/08/zero_waste_europe_study_chemical_recycling_updated_en.pdf>. Acesso em: 17/01/2021.

[329] MERY, Y., TIRUTA-BARNA, L., BENETTO, E., et al. "An integrated "process modelling-life cycle assessment" tool for the assessment and design of water treatment processes", *The International Journal of Life Cycle Assessment*, v. 18, n. 5, pp. 1062–1070, 2013.

[330] GUILLÉN-GOSÁLBEZ, G., GONZÁLEZ-GARAY, A., LIMLEAMTHONG, P., et al. "Systematic MultiObjective Life Cycle Optimization Tools Ap-

plied to the Design of Sustainable Chemical Processes". In: *Sustainable Nanoscale Engineering*, Elsevier, pp. 435–449, 2020.

[331] COSTA, L. P. D. M., DE MIRANDA, D. M. V., CARDOSO, C., et al. "A short-cut method for analysis of catalyst performances in pyrolytic reactor", *Journal of Analytical and Applied Pyrolysis*, v. 174, pp. 106121, 2023.

[332] "Refining: High-impact challenges in today's global refining market". 2016. Available in: <https://www.hydrocarbonprocessing.com/magazine/2016/november-2016/columns/refining-high-impact-challenges-in-today-s-global-refining-market>.

[333] WILLIAMS, C. L., WESTOVER, T. L., EMERSON, R. M., et al. "Sources of biomass feedstock variability and the potential impact on biofuels production", *BioEnergy Research*, v. 9, n. 1, pp. 1–14, 2016.

[334] HARMON, R. E., SRIBALA, G., BROADBELT, L. J., et al. "Insight into Polyethylene and Polypropylene Pyrolysis: Global and Mechanistic Models", *Energy & Fuels*, v. 35, n. 8, pp. 6765–6775, 2021. ISSN: 0887-0624. doi: 10.1021/acs.energyfuels.1c00342. Available in: <https://doi.org/10.1021/acs.energyfuels.1c00342>. Publisher: American Chemical Society.

[335] MUHAMMAD, C., ONWUDILI, J. A., WILLIAMS, P. T. "Thermal degradation of real-world waste plastics and simulated mixed plastics in a two-stage pyrolysis–catalysis reactor for fuel production", *Energy & Fuels*, v. 29, n. 4, pp. 2601–2609, 2015.

[336] ONWUDILI, J. A., MUHAMMAD, C., WILLIAMS, P. T. "Influence of catalyst bed temperature and properties of zeolite catalysts on pyrolysis-catalysis of a simulated mixed plastics sample for the production of upgraded fuels and chemicals", *Journal of the Energy Institute*, v. 92, n. 5, pp. 1337–1347, 2019.

[337] SERRANO, D., AGUADO, J., ESCOLA, J. "Developing advanced catalysts for the conversion of polyolefinic waste plastics into fuels and chemicals", *ACS Catalysis*, v. 2, n. 9, pp. 1924–1941, 2012.

[338] MARCILLA, A., GÓMEZ, A., REYES-LABARTA, J. A., et al. "Kinetic study of polypropylene pyrolysis using ZSM-5 and an equilibrium fluid

catalytic cracking catalyst", v. 68-69, pp. 467–480, 2003. ISSN: 0165-2370. doi: 10.1016/S0165-2370(03)00036-6. Available in: <https://www.sciencedirect.com/science/article/pii/S0165237003000366>.

[339] LIN, Y.-H., SHARRATT, P. N., GARFORTH, A. A., et al. "Catalytic Conversion of Polyolefins to Chemicals and Fuels over Various Cracking Catalysts", v. 12, n. 4, pp. 767–774, 1998. ISSN: 0887-0624. doi: 10.1021/ef970233k. Available in: <https://doi.org/10.1021/ef970233k>. Publisher: American Chemical Society.

[340] LIN, Y. H., HWU, W. H., GER, M. D., et al. "A combined kinetic and mechanistic modelling of the catalytic degradation of polymers", v. 171, n. 1, pp. 143–151, 2001. ISSN: 1381-1169. doi: 10.1016/S1381-1169(01)00079-6. Available in: <https://www.sciencedirect.com/science/article/pii/S1381116901000796>.

[341] LIN, Y. H., YANG, M. H., WEI, T. T., et al. "Acid-catalyzed conversion of chlorinated plastic waste into valuable hydrocarbons over post-use commercial FCC catalysts", v. 87, n. 1, pp. 154–162, 2010. ISSN: 0165-2370. doi: 10.1016/j.jaap.2009.11.006. Available in: <https://www.sciencedirect.com/science/article/pii/S0165237009001624>.

[342] HUANG, W.-C., HUANG, M.-S., HUANG, C.-F., et al. "Thermochemical conversion of polymer wastes into hydrocarbon fuels over various fluidizing cracking catalysts", v. 89, n. 9, pp. 2305–2316, 2010. ISSN: 0016-2361. doi: 10.1016/j.fuel.2010.04.013. Available in: <https://www.sciencedirect.com/science/article/pii/S0016236110001857>.

[343] CARDONA, S. C., CORMA, A. "Kinetic study of the catalytic cracking of polypropylene in a semibatch stirred reactor", v. 75, n. 1, pp. 239–246, 2002. ISSN: 0920-5861. doi: 10.1016/S0920-5861(02)00075-5. Available in: <https://www.sciencedirect.com/science/article/pii/S0920586102000755>.

[344] TILL, Z., VARGA, T., SÓJA, J., et al. "Structural assessment of lumped reaction networks with correlating parameters", v. 209, pp. 112632, 2020. ISSN: 0196-8904. doi: 10.1016/j.enconman.2020.112632. Available in: <https://www.sciencedirect.com/science/article/pii/S0196890420301709>.

[345] BOLLAS, G., LAPPAS, A., IATRIDIS, D., et al. "Five-lump kinetic model with selective catalyst deactivation for the prediction of the product se-

lectivity in the fluid catalytic cracking process", *Catalysis Today*, v. 127, n. 1-4, pp. 31–43, 2007.

[346] ELORDI, G., OLAZAR, M., LOPEZ, G., et al. "Role of pore structure in the deactivation of zeolites (HZSM-5, Hβ and HY) by coke in the pyrolysis of polyethylene in a conical spouted bed reactor", *Applied Catalysis B: Environmental*, v. 102, n. 1-2, pp. 224–231, 2011.

[347] CASTANO, P., ELORDI, G., OLAZAR, M., et al. "Insights into the coke deposited on HZSM-5, Hβ and HY zeolites during the cracking of polyethylene", *Applied Catalysis B: Environmental*, v. 104, n. 1-2, pp. 91–100, 2011.

[348] CHEN, Z., ZHANG, X., YANG, F., et al. "Deactivation of a Y-zeolite based catalyst with coke evolution during the catalytic pyrolysis of polyethylene for fuel oil", *Applied Catalysis A: General*, v. 609, pp. 117873, 2021.

[349] VIRTANEN, P., GOMMERS, R., OLIPHANT, T. E., et al. "SciPy 1.0: Fundamental Algorithms for Scientific Computing in Python", *Nature Methods*, v. 17, pp. 261–272, 2020. doi: 10.1038/s41592-019-0686-2.

[350] PAN, R., MARTINS, M. F., DEBENEST, G. "Pyrolysis of waste polyethylene in a semi-batch reactor to produce liquid fuel: Optimization of operating conditions", *Energy Conversion and Management*, v. 237, pp. 114114, 2021.

[351] DA MATA COSTA, L. P., BRANDÃO, A. L., PINTO, J. C. "Modeling of polystyrene degradation using kinetic Monte Carlo", *Journal of Analytical and Applied Pyrolysis*, v. 167, pp. 105683, 2022. ISSN: 0165-2370.

[352] EUROPE, P. *Plastics - the Facts 2020*. Report, Plastics Europe, 2021. Available in: <`https://www.plasticseurope.org/en/resources/publications/4312-plastics-facts-2020`>.

[353] COSTA, L., CAMINO, G. "Thermal degradation of polymer-fire retardant mixtures: Part VII—Products of degradation and mechanism of fire retardance in polystyrene-chloroparaffin mixtures", *Polymer degradation and stability*, v. 12, n. 4, pp. 287–296, 1985.

[354] BOUSTER, C., VERMANDE, P., VERON, J. "Evolution of the product yield with temperature and molecular weight in the pyrolysis of polystyrene", *Journal of Analytical and Applied Pyrolysis*, v. 15, pp. 249–259, 1989.

[355] TSUGE, S., OKUMOTO, T., TAKEUCHI, T. "Study of thermal degradation of fractionated polystyrenes by pyrolysis gas chromatography", *Journal of Chromatographic Science*, v. 7, n. 4, pp. 250–252, 1969.

[356] OHTANI, H., TSUGE, S., MATSUSHITA, Y., et al. "Pyrolysis Gas Chromatographic Characterization of Block Copolymers of Ordinary and Deuterated Styrenes", *Polymer Journal*, v. 14, n. 6, pp. 495–499, 1982.

[357] SUGIMURA, Y., NAGAYA, T., TSUGE, S. "Pyrolysis-gas chromatographic studies on head-to-head polystyrene", *Macromolecules*, v. 14, n. 3, pp. 520–523, 1981.

[358] LEHRLE, R. S., PEAKMAN, R. E., ROBB, J. C. "Pyrolysis-gas-liquid-chromatography utilised for a kinetic study of the mechanisms of initiation and termination in the thermal degradation of polystyrene", *European Polymer Journal*, v. 18, n. 6, pp. 517–529, 1982.

[359] CASCAVAL, C., STRAUS, S., BROWN, D., et al. "Thermal degradation of polystyrene: Effect of end groups derived from azobisisobutyronitrile". In: *Journal of Polymer Science: Polymer Symposia*, v. 57, pp. 81–88. Wiley Online Library, 1976.

[360] LEHRLE, R., ATKINSON, D., COOK, S., et al. "Polymer degradation mechanisms: new approaches", *Polymer degradation and stability*, v. 42, n. 3, pp. 281–291, 1993.

[361] SAWAGUCHI, T., SENO, M. "Controlled thermal degradation of polystyrene leading to selective formation of end-reactive oligomers", *Journal of Polymer Science Part A: Polymer Chemistry*, v. 36, n. 1, pp. 209–213, 1998.

[362] REGO, A. S., BRANDÃO, A. L. "General Method for Speeding Up Kinetic Monte Carlo Simulations", *Industrial & Engineering Chemistry Research*, v. 59, n. 19, pp. 9034–9042, 2020.

[363] NONOBE, T., OHTANI, H., USAMI, T., et al. "Characterization of stereoregular polystyrenes by pyrolysis-gas chromatography", *Journal of analytical and applied pyrolysis*, v. 33, pp. 121–138, 1995. ISSN: 0165-2370.

[364] DEAN, L., GROVES, S., HANCOX, R., et al. "Pyrolysis-GC and MS applied to study oligomer formation in the degradation of polystyrene and styrene copolymers", *Polymer degradation and stability*, v. 25, n. 2-4, pp. 143–160, 1989.

[365] GARDNER, P., LEHRLE, R. "Polystyrene pyrolysis mechanisms—I. As deduced from the dependence of product yields on film thickness", *European polymer journal*, v. 29, n. 2-3, pp. 425–435, 1993.

[366] AHMED, I., GUPTA, A. "Hydrogen production from polystyrene pyrolysis and gasification: characteristics and kinetics", *International journal of hydrogen energy*, v. 34, n. 15, pp. 6253–6264, 2009.

[367] LEHMANN, F. A., BRAUER, G. M. "Analysis of pyrolyzates of polystyrene and poly (methyl methacrylate) by gas chromatography", *Analytical Chemistry*, v. 33, n. 6, pp. 673–676, 1961.

[368] ACHILIAS, D. S., KANELLOPOULOU, I., MEGALOKONOMOS, P., et al. "Chemical recycling of polystyrene by pyrolysis: potential use of the liquid product for the reproduction of polymer", *Macromolecular Materials and Engineering*, v. 292, n. 8, pp. 923–934, 2007.

[369] PARK, K.-B., JEONG, Y.-S., GUZELCIFTCI, B., et al. "Two-stage pyrolysis of polystyrene: Pyrolysis oil as a source of fuels or benzene, toluene, ethylbenzene, and xylenes", *Applied Energy*, v. 259, pp. 114240, 2020.

[370] SAKAKIBARA, Y., TAKATORI, H., YAMADA, I., et al. "Mutual diffusivity of volatile materials in molten polystyrene", *Journal of chemical engineering of Japan*, v. 23, n. 2, pp. 170–174, 1990.

[371] KHUONG, K. S., JONES, W. H., PRYOR, W. A., et al. "The mechanism of the self-initiated thermal polymerization of styrene. Theoretical solution of a classic problem", *Journal of the American Chemical Society*, v. 127, n. 4, pp. 1265–1277, 2005.

[372] KIM, K., CHOI, K. "Modeling of free radical polymerization of styrene catalyzed by unsymmetrical bifunctional initiators", *Chemical engineering science*, v. 44, n. 2, pp. 297–312, 1989.

[373] HUI, A. W., HAMIELEC, A. E. "Thermal polymerization of styrene at high conversions and temperatures. An experimental study", *Journal of Applied Polymer Science*, v. 16, n. 3, pp. 749–769, 1972.

[374] COSTA, L. P., AKIN, O., GARCIA, J. A., et al. "High Density Polyethylene Thermal Pyrolysis: Kinetic and Volatilization Modeling", *Journal of Analytical and Applied Pyrolysis*, p. 107168, 2025.

[375] EUROPE, P. *Plastics – the Facts 2022*. Report, Plastic Europe, 2022. Available in: <https://plasticseurope.org/knowledge-hub/plastics-the-facts-2022/>.

[376] ZOLGHADR, A., KULAS, D., SHONNARD, D. "Evaluation of pyrolysis wax as a solvent in polyolefin pyrolysis processing", *Industrial Engineering Chemistry Research*, v. 61, n. 30, pp. 11080–11088, 2022. ISSN: 0888-5885.

[377] YARIN, A., LASTOCHKIN, D., TALMON, Y., et al. "Bubble nucleation during devolatilization of polymer melts", *AIChE journal*, v. 45, n. 12, pp. 2590–2605, 1999. ISSN: 0001-1541.

[378] POPOV, K. V., KNYAZEV, V. D. "Initial stages of the pyrolysis of polyethylene", *The Journal of Physical Chemistry A*, v. 119, n. 49, pp. 11737–11760, 2015. ISSN: 1089-5639.

[379] MASTALSKI, I., SIDHU, N., ZOLGHADR, A., et al. "Intrinsic Millisecond Kinetics of Polyethylene Pyrolysis via Pulse-Heated Analysis of Solid Reactions", *Chemistry of Materials*, v. 35, n. 9, pp. 3628–3639, 2023. ISSN: 0897-4756.

[380] PIRES COSTA, L., VAZ DE MIRANDA, D. M., PINTO, J. C. "Critical evaluation of life cycle assessment analyses of plastic waste pyrolysis", *ACS Sustainable Chemistry Engineering*, v. 10, n. 12, pp. 3799–3807, 2022. ISSN: 2168-0485.

[381] DOGU, O., ESCHENBACHER, A., VARGHESE, R. J., et al. "Bayesian tuned kinetic Monte Carlo modeling of polystyrene pyrolysis: Unraveling the pathways to its monomer, dimers, and trimers formation", *Chemical Engineering Journal*, v. 455, pp. 140708, 2023. ISSN: 1385-8947.

[382] JAYARAMA KRISHNA, J., PEREZ, B. A., TORAMAN, H. E. "Parametric Study of Polyethylene Primary Decomposition Using a Micropyrolyzer Coupled with Two-Dimensional Gas Chromatography", *ACS Sustainable Chemistry Engineering*, 2024. ISSN: 2168-0485.

[383] PEREZ, B. A., TORAMAN, H. E. "Investigating primary decomposition of polypropylene through detailed compositional analysis using two-dimensional gas chromatography and principal component analysis", *Journal of Analytical and Applied Pyrolysis*, v. 177, pp. 106376, 2024. ISSN: 0165-2370.

[384] ALVAREZ-MAJMUTOV, A., CHEN, J., GIELECIAK, R. "Molecular-level modeling and simulation of vacuum gas oil hydrocracking", *Energy Fuels*, v. 30, n. 1, pp. 138–148, 2016. ISSN: 0887-0624.

[385] LOCASPI, A., PELUCCHI, M., MEHL, M., et al. "Towards a lumped approach for solid plastic waste gasification: Polyethylene and polypropylene pyrolysis", *Waste Management*, v. 156, pp. 107–117, 2023. ISSN: 0956-053X.

[386] GAO, Z., AMASAKI, I., NAKADA, M. "A thermogravimetric study on thermal degradation of polyethylene", *Journal of Analytical and Applied Pyrolysis*, v. 67, n. 1, pp. 1–9, 2003. ISSN: 0165-2370.

[387] STAGGS, J. "Modelling random scission of linear polymers", *Polymer Degradation and Stability*, v. 76, n. 1, pp. 37–44, 2002. ISSN: 0141-3910.

[388] STAGGS, J. "A continuous model for vapourisation of linear polymers by random scission and recombination", *Fire safety journal*, v. 40, n. 7, pp. 610–627, 2005. ISSN: 0379-7112.

[389] MOENS, E. K., MARIEN, Y. W., FIGUEIRA, F. L., et al. "Coupled matrix-based Monte Carlo modeling for a mechanistic understanding of poly (methyl methacrylate) thermochemical recycling kinetics", *Chemical Engineering Journal*, v. 475, pp. 146105, 2023. ISSN: 1385-8947.

[390] ZHOU, J., QIAO, Y., WANG, W., et al. "Formation of styrene monomer, dimer and trimer in the primary volatiles produced from polystyrene pyrolysis in a wire-mesh reactor", *Fuel*, v. 182, pp. 333–339, 2016. ISSN: 0016-2361.

[391] ZAYOUD, A., THI, H. D., KUSENBERG, M., et al. "Pyrolysis of end-of-life polystyrene in a pilot-scale reactor: Maximizing styrene production", *Waste Management*, v. 139, pp. 85–95, 2022. ISSN: 0956-053X.

[392] LIN, X., KONG, L., CAI, H., et al. "Effects of alkali and alkaline earth metals on the co-pyrolysis of cellulose and high density polyethylene using TGA and Py-GC/MS", *Fuel processing technology*, v. 191, pp. 71–78, 2019. ISSN: 0378-3820.

[393] FU, Z., HUA, F., YANG, S., et al. "Evolution of light olefins during the pyrolysis of polyethylene in a two-stage process", *Journal of Analytical and Applied Pyrolysis*, v. 169, pp. 105877, 2023. ISSN: 0165-2370.

[394] ALVAREZ-MAJMUTOV, A., CHEN, J. "Stochastic modeling and simulation approach for industrial fixed-bed hydrocrackers", *Industrial Engineering Chemistry Research*, v. 56, n. 24, pp. 6926–6938, 2017. ISSN: 0888-5885.

[395] KELLY, B., SMITH, W. R. "Molecular simulation of chemical reaction equilibria by Kinetic Monte Carlo", *Molecular Physics*, v. 117, n. 20, pp. 2778–2785, 2019. ISSN: 0026-8976.

[396] AKIN, O., VARGHESE, R. J., ESCHENBACHER, A., et al. "Chemical recycling of plastic waste to monomers: Effect of catalyst contact time, acidity and pore size on olefin recovery in ex-situ catalytic pyrolysis of polyolefin waste", *Journal of Analytical and Applied Pyrolysis*, v. 172, pp. 106036, 2023. ISSN: 0165-2370.

[397] UREEL, Y., DOBBELAERE, M. R., AKIN, O., et al. "Active learning-based exploration of the catalytic pyrolysis of plastic waste", *Fuel*, v. 328, pp. 125340, 2022. ISSN: 0016-2361.

[398] ESCHENBACHER, A., GOODARZI, F., VARGHESE, R. J., et al. "Boron-modified mesoporous ZSM-5 for the conversion of pyrolysis vapors from LDPE and mixed polyolefins: Maximizing the C2–C4 olefin yield with minimal carbon footprint", *ACS Sustainable Chemistry Engineering*, v. 9, n. 43, pp. 14618–14630, 2021. ISSN: 2168-0485.

[399] DE RAS, K., KUSENBERG, M., VANHOVE, G., et al. "A detailed experimental and kinetic modeling study on pyrolysis and oxidation of oxymethylene ether-2 (OME-2)", *Combustion and Flame*, v. 238, pp. 111914, 2022. ISSN: 0010-2180.

[400] ESCHENBACHER, A., VARGHESE, R. J., DELIKONSTANTIS, E., et al. "Highly selective conversion of mixed polyolefins to valuable base chemicals using phosphorus-modified and steam-treated mesoporous HZSM-5 zeolite with minimal carbon footprint", *Applied Catalysis B: Environmental*, v. 309, pp. 121251, 2022. ISSN: 0926-3373.

[401] MIKAIA, A., EI, P. E. W. V., EI, V. Z., et al. "NIST standard reference database 1A", *Standard Reference Data, NIST, Gaithersburg, MD, USA*, 2014.

[402] `CHRÉTIEN, J. R., DUBOIS, J.- "New perspectives in the prediction of kováts indices", *Journal of Chromatography A*, v. 126, pp. 171–189, 1976. ISSN: 0021-9673.

[403] DE SAINT LAUMER, J.-Y., CICCHETTI, E., MERLE, P., et al. "Quantification in gas chromatography: prediction of flame ionization detector response factors from combustion enthalpies and molecular structures", *Analytical chemistry*, v. 82, n. 15, pp. 6457–6462, 2010. ISSN: 0003-2700.

[404] AKIN, O., HE, Q., YAZDANI, P., et al. "Tailored HZSM-5 catalyst modification via phosphorus impregnation and mesopore introduction for selective catalytic conversion of polypropylene into light olefins", *Journal of Analytical and Applied Pyrolysis*, v. 181, pp. 106592, 2024. ISSN: 0165-2370.

[405] SRIBALA, G., VAN DE VIJVER, R., LI, L., et al. "On the primary thermal decomposition pathways of hydroxycinnamic acids", *Proceedings of the Combustion Institute*, v. 38, n. 3, pp. 4207–4214, 2021. ISSN: 1540-7489.

[406] PYL, S. P., SCHIETEKAT, C. M., VAN GEEM, K. M., et al. "Rapeseed oil methyl ester pyrolysis: On-line product analysis using comprehensive two-dimensional gas chromatography", *Journal of Chromatography A*, v. 1218, n. 21, pp. 3217–3223, 2011. ISSN: 0021-9673.

[407] ESCHENBACHER, A., SARAEIAN, A., SHANKS, B. H., et al. "Counteracting rapid catalyst deactivation by concomitant temperature increase during catalytic upgrading of biomass pyrolysis vapors using solid acid catalysts", *Catalysts*, v. 10, n. 7, pp. 748, 2020. ISSN: 2073-4344.

[408] ESCHENBACHER, A., GOODARZI, F., SARAEIAN, A., et al. "Performance of mesoporous HZSM-5 and Silicalite-1 coated mesoporous HZSM-5 catalysts for deoxygenation of straw fast pyrolysis vapors", *Journal of analytical and applied pyrolysis*, v. 145, pp. 104712, 2020. ISSN: 0165-2370.

[409] ESCHENBACHER, A., SARAEIAN, A., SHANKS, B. H., et al. "Performance-screening of metal-impregnated industrial HZSM-5/-Al2O3 extrudates for deoxygenation and hydrodeoxygenation of fast pyrolysis vapors", *Journal of Analytical and Applied Pyrolysis*, v. 150, pp. 104892, 2020. ISSN: 0165-2370.

[410] FLORY, P. J. *Principles of polymer chemistry*. Cornell university press, 1953. ISBN: 0801401348.

[411] MATTHIESEN, K., PLESSING, L., LUINSTRA, G. A. "Fast Pyrolysis Product Analysis of Commercial Polyethylenes", *Energy Fuels*, v. 38, n. 16, pp. 15543–15559, 2024. ISSN: 0887-0624.

[412] VINU, R., BROADBELT, L. J. "Unraveling reaction pathways and specifying reaction kinetics for complex systems", *Annual review of chemical and biomolecular engineering*, v. 3, n. 1, pp. 29–54, 2012. ISSN: 1947-5438.

[413] ACHILIAS, D. S. "A review of modeling of diffusion controlled polymerization reactions", *Macromolecular theory and simulations*, v. 16, n. 4, pp. 319–347, 2007. ISSN: 1022-1344.

[414] VAN DE VIJVER, R., SABBE, M. K., REYNIERS, M.-F., et al. "Ab initio derived group additivity model for intramolecular hydrogen abstraction reactions", *Physical Chemistry Chemical Physics*, v. 20, n. 16, pp. 10877–10894, 2018.

[415] DESTRO, F., FOURNET, R., BOUNACEUR, R., et al. "Automatization of theoretical kinetic data generation for tabulated TS models building-Part II: 1, 2 to 1, 5-H-shift reactions in alkyl radicals", *Combustion and Flame*, p. 113732, 2024. ISSN: 0010-2180.

[416] KLAMT, A., ECKERT, F., ARLT, W. "COSMO-RS: an alternative to simulation for calculating thermodynamic properties of liquid mixtures", *Annual review of chemical and biomolecular engineering*, v. 1, n. 1, pp. 101–122, 2010. ISSN: 1947-5438.

[417] KLAMT, A. *COSMO-RS: from quantum chemistry to fluid phase thermodynamics and drug design*. Elsevier, 2005. ISBN: 0080455530.

[418] WARNATZ, J. "Rate coefficients in the C/H/O system", *Combustion chemistry*, pp. 197–360, 1984. ISSN: 1468401882.

[419] POWER, J., SOMERS, K. P., ZHOU, C.-W., et al. "Theoretical, experimental, and modeling study of the reaction of hydrogen atoms with 1-and 2-pentene", *The Journal of Physical Chemistry A*, v. 123, n. 40, pp. 8506–8526, 2019. ISSN: 1089-5639.

[420] RANDAZZO, J. B., SIVARAMAKRISHNAN, R., JASPER, A. W., et al. "An experimental and theoretical study of the high temperature reactions of the four butyl radical isomers", *Physical Chemistry Chemical Physics*, v. 22, n. 33, pp. 18304–18319, 2020.

[421] TSANG, W., HAMPSON, R. "Chemical kinetic data base for combustion chemistry. Part I. Methane and related compounds", *Journal of physical and chemical reference data*, v. 15, n. 3, pp. 1087–1279, 1986. ISSN: 0047-2689.

[422] ROBERTSON, S., PILLING, M., BAULCH, D., et al. "Fitting of pressure-dependent kinetic rate data by master equation/inverse Laplace transform analysis", *The Journal of Physical Chemistry*, v. 99, n. 36, pp. 13452–13460, 1995. ISSN: 0022-3654.

[423] TSANG, W. "Chemical kinetic data base for combustion chemistry part V. Propene", *Journal of Physical and Chemical Reference Data*, v. 20, n. 2, pp. 221–273, 1991. ISSN: 0047-2689.

[424] TSANG, W. "Chemical kinetic data base for combustion chemistry. Part 3: Propane", *Journal of physical and chemical reference data*, v. 17, n. 2, pp. 887–951, 1988. ISSN: 0047-2689.

[425] CURRAN, H. J. "Rate constant estimation for C1 to C4 alkyl and alkoxyl radical decomposition", *International journal of chemical kinetics*, v. 38, n. 4, pp. 250–275, 2006. ISSN: 0538-8066.

[426] WANG, K., VILLANO, S. M., DEAN, A. M. "Ab initio study of the influence of resonance stabilization on intramolecular ring closure reactions of hydrocarbon radicals", *Physical Chemistry Chemical Physics*, v. 18, n. 12, pp. 8437–8452, 2016.

[427] VIDAL, A., KOUKOUVINIS, P., GAVAISES, M. "Vapor-liquid equilibrium calculations at specified composition, density and temperature with the perturbed chain statistical associating fluid theory (PC-SAFT) equation of state", *Fluid Phase Equilibria*, v. 521, pp. 112661, 2020. ISSN: 0378-3812.

[428] FRENKEL, M., CHIRICO, R. D., DIKY, V., et al. "ThermoData Engine (TDE): software implementation of the dynamic data evaluation concept", *Journal of chemical information and modeling*, v. 45, n. 4, pp. 816–838, 2005. ISSN: 1549-9596.

[429] PETERS, F. T., LAUBE, F. S., SADOWSKI, G. "Development of a group contribution method for polymers within the PC-SAFT model", *Fluid phase equilibria*, v. 324, pp. 70–79, 2012. ISSN: 0378-3812.

[430] NGUYENHUYNH, D. "A modified group-contribution PC-SAFT equation of state for prediction of phase equilibria", *Fluid Phase Equilibria*, v. 430, pp. 33–46, 2016. ISSN: 0378-3812.

[431] NGUYENHUYNH, D., NGUYENHUYNH, D. "Application of the modified group-contribution perturbed-chain SAFT to branched alkanes, n-olefins

and their mixtures", *Fluid Phase Equilibria*, v. 434, pp. 176–192, 2017. ISSN: 0378-3812.

[432] PÀMIES, J. C., VEGA, L. F. "Vapor liquid equilibria and critical behavior of heavy n-alkanes using transferable parameters from the soft-SAFT equation of state", *Industrial engineering chemistry research*, v. 40, n. 11, pp. 2532–2543, 2001. ISSN: 0888-5885.

[433] TIHIC, A., KONTOGEORGIS, G. M., VON SOLMS, N., et al. "Applications of the simplified perturbed-chain SAFT equation of state using an extended parameter table", *Fluid phase equilibria*, v. 248, n. 1, pp. 29–43, 2006. ISSN: 0378-3812.

[434] KULAS, D. G., ZOLGHADR, A., SHONNARD, D. "Micropyrolysis of polyethylene and polypropylene prior to bioconversion: the effect of reactor temperature and vapor residence time on product distribution", *ACS Sustainable Chemistry Engineering*, v. 9, n. 43, pp. 14443–14450, 2021. ISSN: 2168-0485.

[435] TING, P. D., JOYCE, P. C., JOG, P. K., et al. "Phase equilibrium modeling of mixtures of long-chain and short-chain alkanes using Peng–Robinson and SAFT", *Fluid phase equilibria*, v. 206, n. 1-2, pp. 267–286, 2003. ISSN: 0378-3812.

[436] ALFRADIQUE, M. F., CASTIER, M. "Critical points of hydrocarbon mixtures with the Peng–Robinson, SAFT, and PC-SAFT equations of state", *Fluid phase equilibria*, v. 257, n. 1, pp. 78–101, 2007. ISSN: 0378-3812.

[437] CEAMANOS, J., MASTRAL, J., MILLERA, A., et al. "Kinetics of pyrolysis of high density polyethylene. Comparison of isothermal and dynamic experiments", *Journal of Analytical and Applied Pyrolysis*, v. 65, n. 2, pp. 93–110, 2002. ISSN: 0165-2370.

[438] KPLE, M., GIRODS, P., FAGLA, B., et al. "Kinetic study of low density polyethylene using thermogravimetric analysis, Part 2: Isothermal study", *Waste and Biomass valorization*, v. 8, pp. 707–719, 2017. ISSN: 1877-2641.

[439] BUDRUGEAC, P. "Theory and practice in the thermoanalytical kinetics of complex processes: Application for the isothermal and non-isothermal thermal degradation of HDPE", *Thermochimica Acta*, v. 500, n. 1-2, pp. 30–37, 2010. ISSN: 0040-6031.

[440] AL-SALEM, S., LETTIERI, P. "Kinetic study of high density polyethylene (HDPE) pyrolysis", *Chemical engineering research and design*, v. 88, n. 12, pp. 1599–1606, 2010. ISSN: 0263-8762.

[441] KHEDRI, S., ELYASI, S. "Kinetic analysis for thermal cracking of HDPE: A new isoconversional approach", *Polymer Degradation and Stability*, v. 129, pp. 306–318, 2016. ISSN: 0141-3910.

[442] LANE, J. M. D., MOORE, N. W. "Molecular and kinetic models for high-rate thermal degradation of polyethylene", *The Journal of Physical Chemistry A*, v. 122, n. 16, pp. 3962–3970, 2018. ISSN: 1089-5639.

[443] STRAZNICKY, J. I., IEDEMA, P. D., REMERIE, K., et al. "A Deterministic Model to Predict Tacticity Changes During Controlled Degradation of Polypropylene", *Chemical Engineering Science*, v. 293, pp. 120064, 2024. ISSN: 0009-2509.

[444] TSANG, W. "Thermal decomposition of cyclopentane and related compounds", *International Journal of Chemical Kinetics*, v. 10, n. 6, pp. 599–617, 1978. ISSN: 0538-8066.

[445] MEHL, M., PITZ, W. J., WESTBROOK, C. K., et al. "Kinetic modeling of gasoline surrogate components and mixtures under engine conditions", *Proceedings of the Combustion Institute*, v. 33, n. 1, pp. 193–200, 2011. ISSN: 1540-7489.

[446] ZHOU, C.-W., LI, Y., BURKE, U., et al. "An experimental and chemical kinetic modeling study of 1, 3-butadiene combustion: Ignition delay time and laminar flame speed measurements", *Combustion and Flame*, v. 197, pp. 423–438, 2018. ISSN: 0010-2180.

[447] MURATA, K., SATO, K., SAKATA, Y. "Effect of pressure on thermal degradation of polyethylene", *Journal of Analytical and Applied Pyrolysis*, v. 71, n. 2, pp. 569–589, 2004. ISSN: 0165-2370.

[448] ABBAS-ABADI, M. S., ZAYOUD, A., KUSENBERG, M., et al. "Thermochemical recycling of end-of-life and virgin HDPE: A pilot-scale study", *Journal of Analytical and Applied Pyrolysis*, v. 166, pp. 105614, 2022. ISSN: 0165-2370.

[449] BAYTEKIN, B., BAYTEKIN, H. T., GRZYBOWSKI, B. A. "Retrieving and converting energy from polymers: deployable technologies and emerging concepts", *Energy & Environmental Science*, v. 6, n. 12, pp. 3467–3482, 2013. doi: 10.1039/C3EE41360H.

[450] LUIS, P. "Exergy as a tool for measuring process intensification in chemical engineering", *Journal of Chemical Technology & Biotechnology*, v. 88, n. 11, pp. 1951–1958, 2013. doi: 10.1002/jctb.4176.

[451] LUIS, P., VAN DER BRUGGEN, B. "Exergy analysis of energy-intensive production processes: advancing towards a sustainable chemical industry", *Journal of Chemical Technology & Biotechnology*, v. 89, n. 9, pp. 1288–1303, 2014. doi: 10.1002/jctb.4422.

[452] ZHANG, Y., JI, G., MA, D., et al. "Exergy and energy analysis of pyrolysis of plastic wastes in rotary kiln with heat carrier", *Process Safety and Environmental Protection*, v. 142, pp. 203–211, 2020. doi: 10.1016/j.psep.2020.06.021.

[453] NIMMEGEERS, P., PARCHOMENKO, A., DE MEULENAERE, P., et al. "Extending multilevel statistical entropy analysis towards plastic recyclability prediction", *Sustainability*, v. 13, n. 6, pp. 3553, 2021. doi: 10.3390/su13063553.

[454] KLÖPFFER, W. *Background and future prospects in life cycle assessment*. Springer Science & Business Media, 2014.

[455] PATEL, M. K., BECHU, A., VILLEGAS, J. D., et al. "Second-generation biobased plastics are becoming a reality–Non-renewable energy and greenhouse gas (GHG) balance of succinic acid-based plastic end products made from lignocellulosic biomass", *Biofuels, Bioproducts and Biorefining*, v. 12, n. 3, pp. 426–441, 2018. doi: 10.1002/bbb.1849.

[456] BISHOP, G., STYLES, D., LENS, P. N. "Environmental performance comparison of bioplastics and petrochemical plastics: A review of life cycle assessment (LCA) methodological decisions", *Resources, Conservation and Recycling*, v. 168, pp. 105451, 2021. doi: 10.1016/j.resconrec.2021.105451.

[457] REAP, J., ROMAN, F., DUNCAN, S., et al. "A survey of unresolved problems in life cycle assessment", *The International Journal of Life Cycle Assessment*, v. 13, n. 5, pp. 374–388, 2008. doi: 0.1007/s11367-008-0008-x.

[458] AGOSTINI, A., GIUNTOLI, J., MARELLI, L., et al. "Flaws in the interpretation phase of bioenergy LCA fuel the debate and mislead policymakers", *The International Journal of Life Cycle Assessment*, v. 25, n. 1, pp. 17–35, 2020. doi: 10.1007/s11367-019-01654-2.

[459] HASAN, M., RASUL, M., KHAN, M., et al. "Energy recovery from municipal solid waste using pyrolysis technology: A review on current status and developments", *Renewable and Sustainable Energy Reviews*, v. 145, pp. 111073, 2021. doi: /10.1016/j.rser.2021.111073.

[460] PAPARI, S., BAMDAD, H., BERRUTI, F. "Pyrolytic conversion of plastic waste to value-added products and fuels: A Review", *Materials*, v. 14, n. 10, pp. 2586, 2021. doi: 10.3390/ma14102586.

[461] ALHAZMI, H., ALMANSOUR, F. H., ALDHAFEERI, Z. "Plastic Waste Management: A Review of Existing Life Cycle Assessment Studies", *Sustainability*, v. 13, n. 10, pp. 5340, 2021. doi: 10.3390/su13105340.

[462] ÜGDÜLER, S., VAN GEEM, K. M., ROOSEN, M., et al. "Challenges and opportunities of solvent-based additive extraction methods for plastic recycling", *Waste Management*, v. 104, pp. 148–182, 2020. ISSN: 0956-053X. doi: 10.1016/j.wasman.2020.01.003. Available in: <http://www.sciencedirect.com/science/article/pii/S0956053X20300040>.

[463] AL-SALEM, S., EVANGELISTI, S., LETTIERI, P. "Life cycle assessment of alternative technologies for municipal solid waste and plastic solid waste management in the Greater London area", *Chemical Engineering Journal*, v. 244, pp. 391–402, 2014. doi: 10.1016/j.cej.2014.01.066.

[464] GEAR, M., SADHUKHAN, J., THORPE, R., et al. "A life cycle assessment data analysis toolkit for the design of novel processes–A case study for a thermal cracking process for mixed plastic waste", *Journal of cleaner production*, v. 180, pp. 735–747, 2018. doi: 10.1016/j.jclepro.2018.01.015.

[465] "Life cycle assessment (LCA) for ChemCycling™. BASF." Available in: <https://www.basf.com/global/en/who-we-are/sustainability/we-drive-sustainable-solutions/circular-economy/mass-balance-approach/chemcycling/lca-for-chemcycling.html>. accessed 2021-08-24.

[466] JESWANI, H., KRÜGER, C., RUSS, M., et al. "Life cycle environmental impacts of chemical recycling via pyrolysis of mixed plastic waste in comparison with mechanical recycling and energy recovery", *Science of The Total Environment*, v. 769, pp. 144483, 2021. doi: 10.1016/j.scitotenv.2020.144483.

[467] AHAMED, A., VEKSHA, A., YIN, K., et al. "Environmental impact assessment of converting flexible packaging plastic waste to pyrolysis oil and

multi-walled carbon nanotubes", *Journal of hazardous materials*, v. 390, pp. 121449, 2020. doi: 10.1016/j.jhazmat.2019.121449.

[468] SOMOZA-TORNOS, A., GONZALEZ-GARAY, A., POZO, C., et al. "Realizing the potential high benefits of circular economy in the chemical industry: ethylene monomer recovery via polyethylene pyrolysis", *ACS Sustainable Chemistry & Engineering*, v. 8, n. 9, pp. 3561–3572, 2020. doi: 10.1021/acssuschemeng.9b04835.

[469] ZHAO, X., YOU, F. "Consequential Life Cycle Assessment and Optimization of High-Density Polyethylene Plastic Waste Chemical Recycling", *ACS Sustainable Chemistry & Engineering*, v. 9, n. 36, pp. 12167–12184, 2021. doi: 10.1021/acssuschemeng.1c03587.

[470] HEYDARIARAGHI, M., GHORBANIAN, S., HALLAJISANI, A., et al. "Fuel properties of the oils produced from the pyrolysis of commonly-used polymers: Effect of fractionating column", *Journal of Analytical and Applied Pyrolysis*, v. 121, pp. 307–317, 2016. doi: 10.1016/j.jaap.2016.08.010.

[471] JIANG, G., SANCHEZ MONSALVE, D., CLOUGH, P., et al. "Understanding the Dechlorination of Chlorinated Hydrocarbons in the Pyrolysis of Mixed Plastics", *ACS Sustainable Chemistry & Engineering*, v. 9, n. 4, pp. 1576–1589, 2021. doi: 10.1021/acssuschemeng.0c06461.

[472] KOL, R., ROOSEN, M., ÜGDÜLER, S., et al. "Recent Advances in Pre-Treatment of Plastic Packaging Waste", 2021. doi: 10.5772/intechopen.99385.

[473] KUSENBERG, M., ZAYOUD, A., ROOSEN, M., et al. "A comprehensive experimental investigation of plastic waste pyrolysis oil quality and its dependence on the plastic waste composition", *Fuel Processing Technology*, v. 227, pp. 107090, 2022. doi: 10.1016/j.fuproc.2021.107090.

[474] CIVANCIK-USLU, D., NHU, T. T., VAN GORP, B., et al. "Moving from linear to circular household plastic packaging in Belgium: Prospective life cycle assessment of mechanical and thermochemical recycling", *Resources, Conservation and Recycling*, v. 171, pp. 105633, 2021. doi: 10.1016/j.resconrec.2021.105633.

[475] PERUGINI, F., MASTELLONE, M. L., ARENA, U. "A life cycle assessment of mechanical and feedstock recycling options for management of plastic packaging wastes", *Environmental Progress*, v. 24, n. 2, pp. 137–154, 2005. doi: 10.1002/ep.10078.

[476] VEKSHA, A., AHAMED, A., WU, X. Y., et al. "Technical and environmental assessment of laboratory scale approach for sustainable management of marine plastic litter", *Journal of Hazardous Materials*, v. 421, pp. 126717, 2022. doi: 10.1016/j.jhazmat.2021.126717.

[477] SCHWARZ, A., LIGTHART, T., BIZARRO, D. G., et al. "Plastic recycling in a circular economy; determining environmental performance through an LCA matrix model approach", *Waste Management*, v. 121, pp. 331–342, 2021. doi: 10.1016/j.wasman.2020.12.020.

[478] IRIBARREN, D., DUFOUR, J., SERRANO, D. P. "Preliminary assessment of plastic waste valorization via sequential pyrolysis and catalytic reforming", *Journal of Material Cycles and Waste Management*, v. 14, n. 4, pp. 301–307, 2012. doi: 10.1007/s10163-012-0069-6.

[479] KHOO, H. H. "LCA of plastic waste recovery into recycled materials, energy and fuels in Singapore", *Resources, Conservation and Recycling*, v. 145, pp. 67–77, 2019. doi: 10.1016/j.resconrec.2019.02.010.

[480] FARACA, G., MARTINEZ-SANCHEZ, V., ASTRUP, T. F. "Environmental life cycle cost assessment: Recycling of hard plastic waste collected at Danish recycling centres", *Resources, Conservation and Recycling*, v. 143, pp. 299–309, 2019. doi: 10.1016/j.resconrec.2019.01.014.

[481] GRACIDA-ALVAREZ, U. R., WINJOBI, O., SACRAMENTO-RIVERO, J. C., et al. "System analyses of high-value chemicals and fuels from a waste high-density polyethylene refinery. Part 2: carbon footprint analysis and regional electricity effects", *ACS Sustainable Chemistry & Engineering*, v. 7, n. 22, pp. 18267–18278, 2019. doi: 10.1021/acssuschemeng.9b04763.

[482] "Exploration chemical recycling - Extended summary. CE Delft." 2020. Available in: <`https://cedelft.eu/wp-content/uploads/sites/2/2021/03/CE_Delft_2P22_Exploration_chemical_recycling_Extended_summary.pdf`>. accessed 2021-08-24.

[483] PIRES DA MATA COSTA, L., MICHELINE VAZ DE MIRANDA, D., COUTO DE OLIVEIRA, A. C., et al. "Capture and Reuse of Carbon Dioxide (CO2) for a Plastics Circular Economy: A Review", *Processes*, v. 9, n. 5, pp. 759, 2021. doi: 10.3390/pr9050759.

[484] "Industrial Transformation 2050 - Pathways to Net-Zero Emissions from EU Heavy Industry - Material Economics". 2019. Avail-

able in: <https://materialeconomics.com/publications/industrial-transformation-2050>. accessed 2021-08-24.

[485] REINALES, D., ZAMBRANA-VASQUEZ, D., SAEZ-DE-GUINOA, A. "Social Life Cycle Assessment of Product Value Chains Under a Circular Economy Approach: A Case Study in the Plastic Packaging Sector", *Sustainability*, v. 12, n. 16, pp. 6671, 2020. doi: 10.3390/su12166671.

[486] EKENER-PETERSEN, E., FINNVEDEN, G. "Potential hotspots identified by social LCA—part 1: a case study of a laptop computer", *The International Journal of Life Cycle Assessment*, v. 18, n. 1, pp. 127–143, 2013. doi: 10.1007/s11367-012-0442-7.

[487] SPIERLING, S., KNÜPFFER, E., BEHNSEN, H., et al. "Bio-based plastics-A review of environmental, social and economic impact assessments", *Journal of Cleaner Production*, v. 185, pp. 476–491, 2018. doi: 10.1016/j.jclepro.2018.03.014.

[488] ARENA, U., ARDOLINO, F., DI GREGORIO, F. "Technological, environmental and social aspects of a recycling process of post-consumer absorbent hygiene products", *Journal of Cleaner Production*, v. 127, pp. 289–301, 2016. doi: 10.1016/j.jclepro.2016.03.164.

[489] VALENTE, C., BREKKE, A., MODAHL, I. S. "Testing environmental and social indicators for biorefineries: bioethanol and biochemical production", *The International Journal of Life Cycle Assessment*, v. 23, n. 3, pp. 581–596, 2018. doi: 10.1007/s11367-017-1331-x.

[490] IBÁÑEZ-FORÉS, V., BOVEA, M. D., COUTINHO-NÓBREGA, C., et al. "Assessing the social performance of municipal solid waste management systems in developing countries: Proposal of indicators and a case study", *Ecological indicators*, v. 98, pp. 164–178, 2019. doi: 10.1016/j.ecolind.2018.10.031.

[491] HUARACHI, D. A. R., PIEKARSKI, C. M., PUGLIERI, F. N., et al. "Past and future of Social Life Cycle Assessment: Historical evolution and research trends", *Journal of Cleaner Production*, v. 264, pp. 121506, 2020. doi: 10.1016/j.jclepro.2020.121506.

[492] KÜHNEN, M., HAHN, R. "Indicators in social life cycle assessment: a review of frameworks, theories, and empirical experience", *Journal of Industrial Ecology*, v. 21, n. 6, pp. 1547–1565, 2017. doi: 10.1111/jiec.12663.

[493] PETTI, L., SERRELI, M., DI CESARE, S. "Systematic literature review in social life cycle assessment", *The International Journal of Life Cycle Assessment*, v. 23, n. 3, pp. 422–431, 2018. doi: 10.1007/s11367-016-1135-4.

[494] BONILLA-ALICEA, R. J., FU, K. "Evaluation of a challenge-derived social life cycle assessment (S-LCA) framework", *International Journal of Sustainable Engineering*, pp. 1–18, 2021. doi: 10.1080/19397038.2021.2004258.

Appendix A

Polyethylene Experimental Data

Table A.1 Mass fraction results of HDPE pyrolysis at 550, 600, and 650 °C (non-normalized). Unavailable values are denoted as n.a.

Name			**Class**	**550 °C**	**600 °C**	**650 °C**
n-paraffins (sum)				**8.69**	**8.95**	**7.19**
Methane	1	C_1H_4	Paraffin	0.39 ± 0.27	0.74 ± 0.21	1.18 ± 0.46
Ethane	2	C_2H_6	Paraffin	n.a.	n.a.	n.a.
Propane	3	C_3H_8	Paraffin	0.01 ± 0.01	n.a.	n.a.
Butane	4	C_4H_{10}	Paraffin	0.44 ± 0.38	0.46 ± 0.25	0.60 ± 0.33
Pentane	5	C_5H_{12}	Paraffin	0.48 ± 0.59	n.a.	n.a.
Hexane	6	C_6H_{14}	Paraffin	0.61 ± 0.70	0.24 ± 0.06	0.25 ± 0.12
Heptane	7	C_7H_{16}	Paraffin	0.42 ± 0.30	0.39 ± 0.09	0.34 ± 0.15
Octane	8	C_8H_{18}	Paraffin	0.30 ± 0.21	0.28 ± 0.07	0.24 ± 0.11
Nonane	9	C_9H_{20}	Paraffin	0.24 ± 0.15	0.26 ± 0.06	0.20 ± 0.09
Decane	10	$C_{10}H_{22}$	Paraffin	0.17 ± 0.14	0.25 ± 0.07	0.18 ± 0.08
Undecane	11	$C_{11}H_{24}$	Paraffin	0.16 ± 0.21	0.32 ± 0.12	0.18 ± 0.07
Dodecane	12	$C_{12}H_{26}$	Paraffin	0.11 ± 0.17	0.27 ± 0.09	0.15 ± 0.07
Tridecane	13	$C_{13}H_{28}$	Paraffin	0.09 ± 0.15	0.23 ± 0.07	0.14 ± 0.06
Tetradecane	14	$C_{14}H_{30}$	Paraffin	0.21 ± 0.19	0.23 ± 0.08	0.12 ± 0.05
Pentadecane	15	$C_{15}H_{32}$	Paraffin	0.24 ± 0.23	0.28 ± 0.10	0.14 ± 0.06
Hexadecane	16	$C_{16}H_{34}$	Paraffin	0.24 ± 0.21	0.27 ± 0.10	0.16 ± 0.06
Heptadecane	17	$C_{17}H_{36}$	Paraffin	0.25 ± 0.21	0.27 ± 0.11	0.14 ± 0.06
Octadecane	18	$C_{18}H_{38}$	Paraffin	0.26 ± 0.21	0.29 ± 0.10	0.15 ± 0.07
Nonadecane	19	$C_{19}H_{40}$	Paraffin	0.26 ± 0.20	0.31 ± 0.12	0.17 ± 0.09
Eicosane	20	$C_{20}H_{42}$	Paraffin	0.28 ± 0.21	0.31 ± 0.12	0.19 ± 0.12
Henicosane	21	$C_{21}H_{44}$	Paraffin	0.28 ± 0.19	0.32 ± 0.11	0.19 ± 0.10
Docosane	22	$C_{22}H_{46}$	Paraffin	0.30 ± 0.19	0.31 ± 0.09	0.22 ± 0.12
Tricosane	23	$C_{23}H_{48}$	Paraffin	0.31 ± 0.19	0.33 ± 0.10	0.21 ± 0.11
Tetracosane	24	$C_{24}H_{50}$	Paraffin	0.32 ± 0.18	0.47 ± 0.33	0.24 ± 0.14
Pentacosane	25	$C_{25}H_{52}$	Paraffin	0.34 ± 0.19	0.33 ± 0.09	0.26 ± 0.14
Hexacosane	26	$C_{26}H_{54}$	Paraffin	0.38 ± 0.22	0.34 ± 0.08	0.31 ± 0.21
Heptacosane	27	$C_{27}H_{56}$	Paraffin	0.41 ± 0.23	0.33 ± 0.08	0.28 ± 0.15
Octacosane	28	$C_{28}H_{58}$	Paraffin	0.43 ± 0.25	0.39 ± 0.09	0.33 ± 0.17
Nonacosane	29	$C_{29}H_{60}$	Paraffin	0.35 ± 0.25	0.47 ± 0.11	0.32 ± 0.15
Triacontane	30	$C_{30}H_{62}$	Paraffin	0.42 ± 0.27	0.26 ± 0.23	0.31 ± 0.14
α-olefins (sum)				**24.38**	**30.43**	**33.96**
Ethylene	2	C_2H_4	Olefin	1.88 ± 1.12	3.31 ± 0.86	5.94 ± 2.43
Propylene	3	C_3H_6	Olefin	1.84 ± 1.04	2.60 ± 0.68	3.71 ± 1.48
1-Butene	4	C_4H_8	Olefin	0.88 ± 0.58	1.00 ± 0.27	1.80 ± 0.85
1-Pentene	5	C_5H_{10}	Olefin	0.65 ± 0.55	0.67 ± 0.50	1.74 ± 0.84
1-Hexene	6	C_6H_{12}	Olefin	1.71 ± 0.92	2.48 ± 0.61	3.13 ± 1.23

Name			Class	550 °C	600 °C	650 °C
1-Heptene	7	C_7H_{14}	Olefin	0.81 ± 0.46	1.13 ± 0.27	1.23 ± 0.51
1-Octene	8	C_8H_{16}	Olefin	0.59 ± 0.39	0.75 ± 0.21	0.76 ± 0.32
1-Nonene	9	C_9H_{18}	Olefin	0.57 ± 0.40	0.72 ± 0.23	0.70 ± 0.31
1-Decene	10	$C_{10}H_{20}$	Olefin	1.07 ± 1.03	1.16 ± 0.42	1.07 ± 0.44
1-Undecene	11	$C_{11}H_{22}$	Olefin	0.93 ± 0.85	0.78 ± 0.28	0.78 ± 0.32
1-Dodecene	12	$C_{12}H_{24}$	Olefin	0.54 ± 0.70	0.66 ± 0.27	0.53 ± 0.21
1-Tridecene	13	$C_{13}H_{26}$	Olefin	0.67 ± 0.88	0.64 ± 0.29	0.49 ± 0.19
1-Tetradecene	14	$C_{14}H_{28}$	Olefin	0.63 ± 0.58	0.81 ± 0.36	0.61 ± 0.24
1-Pentadecene	15	$C_{15}H_{30}$	Olefin	0.60 ± 0.53	0.77 ± 0.35	0.56 ± 0.23
1-Hexadecene	16	$C_{16}H_{32}$	Olefin	0.56 ± 0.48	0.69 ± 0.31	0.50 ± 0.20
1-Heptadecene	17	$C_{17}H_{34}$	Olefin	0.55 ± 0.44	0.69 ± 0.32	0.50 ± 0.22
Octadecene	18	$C_{18}H_{36}$	Olefin	0.61 ± 0.46	0.75 ± 0.33	0.58 ± 0.27
1-Nonadecene	19	$C_{19}H_{38}$	Olefin	0.63 ± 0.45	0.77 ± 0.32	0.59 ± 0.29
Eicosene	20	$C_{20}H_{40}$	Olefin	0.63 ± 0.42	0.77 ± 0.29	0.61 ± 0.31
Heneicosene	21	$C_{21}H_{42}$	Olefin	0.64 ± 0.39	0.80 ± 0.29	0.63 ± 0.34
Docosene	22	$C_{22}H_{44}$	Olefin	0.68 ± 0.39	0.81 ± 0.28	0.68 ± 0.41
Tricosene	23	$C_{23}H_{46}$	Olefin	0.71 ± 0.41	0.83 ± 0.27	0.74 ± 0.44
Tetracosene	24	$C_{24}H_{48}$	Olefin	0.75 ± 0.43	0.74 ± 0.38	0.77 ± 0.46
Pentacosene	25	$C_{25}H_{50}$	Olefin	0.76 ± 0.45	0.93 ± 0.33	0.81 ± 0.50
Hexacosene	26	$C_{26}H_{52}$	Olefin	0.82 ± 0.49	0.97 ± 0.34	0.83 ± 0.48
Heptacosene	27	$C_{27}H_{54}$	Olefin	0.86 ± 0.54	1.02 ± 0.39	0.91 ± 0.54
Octacosene	28	$C_{28}H_{56}$	Olefin	0.86 ± 0.57	1.01 ± 0.35	0.88 ± 0.50
Nonacosene	29	$C_{29}H_{58}$	Olefin	0.96 ± 0.60	0.94 ± 0.37	0.93 ± 0.47
Triacontene	30	$C_{30}H_{60}$	Olefin	0.98 ± 0.61	1.25 ± 0.65	0.94 ± 0.45
Dienes (sum)				**6.81**	**9.26**	**9.59**
1,3-Butadiene	4	C_4H_6	Diolefin	0.33 ± 0.24	0.80 ± 0.28	1.14 ± 0.45
Pentadiene	5	C_5H_8	Diolefin	0.09 ± 0.08	0.23 ± 0.24	0.22 ± 0.21
Hexadiene	6	C_6H_{10}	Diolefin	0.08 ± 0.11	0.13 ± 0.08	0.19 ± 0.09
Heptadiene	7	C_7H_{12}	Diolefin	0.45 ± 0.30	0.00 ± 0.00	0.00 ± 0.00
Octadiene	8	C_8H_{14}	Diolefin	0.03 ± 0.03	0.07 ± 0.03	0.12 ± 0.09
Nonadiene	9	C_9H_{16}	Diolefin	0.08 ± 0.06	0.17 ± 0.06	0.15 ± 0.06
Decadiene	10	$C_{10}H_{18}$	Diolefin	0.10 ± 0.09	0.18 ± 0.09	0.19 ± 0.07
Undecadiene	11	$C_{11}H_{20}$	Diolefin	0.10 ± 0.09	0.18 ± 0.14	0.15 ± 0.06
Dodecadiene	12	$C_{12}H_{22}$	Diolefin	0.09 ± 0.11	0.18 ± 0.11	0.17 ± 0.07
Tridecadiene	13	$C_{13}H_{24}$	Diolefin	0.12 ± 0.13	0.23 ± 0.13	0.20 ± 0.08
Tetradecadiene	14	$C_{14}H_{26}$	Diolefin	0.35 ± 0.54	0.25 ± 0.14	0.20 ± 0.08
Pentadecadiene	15	$C_{15}H_{28}$	Diolefin	0.17 ± 0.17	0.26 ± 0.15	0.22 ± 0.09
Hexadecadiene	16	$C_{16}H_{30}$	Diolefin	0.19 ± 0.20	0.29 ± 0.16	0.24 ± 0.11
Heptadecadiene	17	$C_{17}H_{32}$	Diolefin	0.22 ± 0.20	0.32 ± 0.17	0.26 ± 0.12
Octadecadiene	18	$C_{18}H_{34}$	Diolefin	0.24 ± 0.20	0.34 ± 0.16	0.30 ± 0.14
Nonadecadiene	19	$C_{19}H_{36}$	Diolefin	0.25 ± 0.20	0.38 ± 0.17	0.33 ± 0.16
Eicosadiene	20	$C_{20}H_{38}$	Diolefin	0.26 ± 0.19	0.39 ± 0.17	0.34 ± 0.18
Heneicosadiene	21	$C_{21}H_{40}$	Diolefin	0.29 ± 0.20	0.41 ± 0.17	0.38 ± 0.22
Docosadiene	22	$C_{22}H_{42}$	Diolefin	0.30 ± 0.19	0.44 ± 0.15	0.41 ± 0.22
Tricosadiene	23	$C_{23}H_{44}$	Diolefin	0.31 ± 0.18	0.46 ± 0.16	0.45 ± 0.26
Tetracosadiene	24	$C_{24}H_{46}$	Diolefin	0.34 ± 0.19	0.48 ± 0.17	0.49 ± 0.31
Pentacosadiene	25	$C_{25}H_{48}$	Diolefin	0.35 ± 0.20	0.52 ± 0.18	0.54 ± 0.33
Hexacosadiene	26	$C_{26}H_{50}$	Diolefin	0.37 ± 0.23	0.53 ± 0.21	0.58 ± 0.32
Heptacosadiene	27	$C_{27}H_{52}$	Diolefin	0.38 ± 0.25	0.53 ± 0.21	0.58 ± 0.31
Octacosadiene	28	$C_{28}H_{54}$	Diolefin	0.41 ± 0.24	0.55 ± 0.20	0.60 ± 0.31
Nonacosadiene	29	$C_{29}H_{56}$	Diolefin	0.42 ± 0.25	0.52 ± 0.17	0.57 ± 0.29
Triacontadiene	30	$C_{30}H_{58}$	Diolefin	0.48 ± 0.29	0.44 ± 0.13	0.58 ± 0.29
Lump of Paraffin, Olefins and Diolefins (sum)				**36.05**	**42.57**	**29.54**
-	31	-	-	1.90 ± 1.18	2.02 ± 0.93	1.77 ± 1.03
-	32	-	-	1.83 ± 1.37	1.97 ± 0.68	2.22 ± 1.09
-	33	-	-	1.92 ± 1.26	1.95 ± 0.69	2.09 ± 1.05
-	34	-	-	2.08 ± 1.44	1.95 ± 0.67	1.83 ± 0.77
-	35	-	-	1.97 ± 1.28	1.93 ± 0.64	1.80 ± 0.85

Name			Class	550 °C	600 °C	650 °C
-	36	-	-	2.03 ± 1.35	1.93 ± 0.75	1.45 ± 0.58
-	37	-	-	1.78 ± 1.11	1.87 ± 0.51	1.39 ± 0.54
-	38	-	-	1.75 ± 1.09	1.85 ± 0.61	1.30 ± 0.51
-	39	-	-	1.72 ± 1.11	1.83 ± 0.68	1.22 ± 0.48
-	40	-	-	1.67 ± 1.08	1.78 ± 0.74	1.17 ± 0.47
-	41	-	-	1.60 ± 1.07	1.76 ± 0.80	1.10 ± 0.44
-	42	-	-	1.55 ± 1.06	1.71 ± 0.81	1.05 ± 0.43
-	43	-	-	1.48 ± 1.04	1.66 ± 0.88	1.01 ± 0.44
-	44	-	-	1.41 ± 1.03	1.66 ± 0.94	0.98 ± 0.42
-	45	-	-	1.35 ± 1.04	1.65 ± 0.9	0.94 ± 0.39
-	46	-	-	1.28 ± 1.00	1.57 ± 0.93	0.87 ± 0.36
-	47	-	-	1.18 ± 0.95	1.52 ± 0.85	0.86 ± 0.38
-	48	-	-	1.14 ± 0.92	1.42 ± 0.79	0.81 ± 0.38
-	49	-	-	1.03 ± 0.82	1.43 ± 0.68	0.76 ± 0.36
-	50	-	-	0.94 ± 0.71	1.34 ± 0.52	0.78 ± 0.43
-	51	-	-	0.81 ± 0.63	1.32 ± 0.50	0.79 ± 0.46
-	52	-	-	0.74 ± 0.57	1.25 ± 0.43	0.69 ± 0.46
-	53	-	-	0.60 ± 0.44	1.14 ± 0.39	0.66 ± 0.38
-	54	-	-	0.51 ± 0.33	0.98 ± 0.43	0.60 ± 0.36
-	55	-	-	0.43 ± 0.31	0.80 ± 0.40	0.31 ± 0.19
-	56	-	-	0.36 ± 0.23	0.85 ± 0.51	0.30 ± 0.16
-	57	-	-	0.24 ± 0.16	0.49 ± 0.23	0.20 ± 0.14
-	58	-	-	0.22 ± 0.21	0.28 ± 0.21	0.17 ± 0.09
-	59	-	-	0.20 ± 0.18	0.30 ± 0.30	0.14 ± 0.06
-	60	-	-	0.13 ± 0.07	0.16 ± 0.10	0.09 ± 0.05
-	61	-	-	0.15 ± 0.15	0.13 ± 0.11	0.12 ± 0.05
-	62	-	-	0.07 ± 0.04	0.06 ± 0.06	0.07 ± 0.03
Others (sum)				**1.52**	**1.98**	**1.96**
Propyne	3	C_3H_4	Alkyne	0.01 ± 0.01	n.a.	n.a.
Isobutane	4	C_4H_{10}	Iso-paraffin	0.01 ± 0.01	0.01 ± 0.005	n.a.
1-Butene, 3-methyl-	5	C_5H_{10}	Iso-olefin	0.02 ± 0.02	0.06 ± 0.03	0.02 ± 0.004
Butane, 2-methyl-	5	C_5H_{12}	Iso-paraffin	0.38 ± 0.37	0.75 ± 0.44	0.10 ± 0.04
2-Methyl-1-butene	5	C_5H_{10}	Iso-olefin	0.12 ± 0.11	0.08 ± 0.05	0.18 ± 0.10
2-Butene, 2-methyl-	5	C_5H_{10}	Iso-olefin	0.04 ± 0.03	0.06 ± 0.02	0.12 ± 0.03
1,3-Cyclopentadiene	5	C_5H_6	Naphthene	0.02 ± 0.01	0.01 ± 0.02	0.09 ± 0.02
Cyclopentane	5	C_5H_{10}	Naphthene	0.02 ± 0.01	0.02 ± 0.05	0.17 ± 0.03
Pentane, 2-methyl-	6	C_6H_{14}	Iso-paraffin	0.01 ± 0.01	0.02 ± 0.01	0.04 ± 0.01
1,3-Pentadiene, 2-methyl-	6	C_6H_{10}	Iso-olefin	0.17 ± 0.15	0.11 ± 0.02	0.20 ± 0.03
Cyclopentane, methyl-	6	C_6H_{12}	Naphthene	0.06 ± 0.04	0.02 ± 0.01	0.09 ± 0.08
1,3-Cyclohexadiene	6	C_6H_8	Naphthene	0.08 ± 0.06	0.15 ± 0.05	0.12 ± 0.05
Benzene	6	C_6H_6	Aromatic	0.11 ± 0.04	0.16 ± 0.03	0.19 ± 0.03
1,3-Cyclopentadiene, 5-methyl-	6	C_6H_8	Naphthene	0.02 ± 0.02	0.02 ± 0.02	0.11 ± 0.01
Cyclopentane, 1,2-dimethyl-	7	C_7H_{14}	Naphthene	0.08 ± 0.05	0.11 ± 0.02	0.09 ± 0.08
1,4-Hexadiene, 2-methyl-	7	C_7H_{12}	Iso-olefin	0.11 ± 0.07	0.12 ± 0.08	0.06 ± 0.01
Cyclohexane, methyl-	7	C_7H_{14}	Naphthene	0.13 ± 0.05	0.07 ± 0.04	0.18 ± 0.04
Toluene	7	C_7H_8	Aromatic	0.05 ± 0.02	0.07 ± 0.02	0.08 ± 0.02
Cyclohexene, 2-Methyl	7	C_7H_{12}	Naphthene	0.06 ± 0.05	0.07 ± 0.02	n.a.
3-Methylenecyclohexene	7	C_7H_{10}	Naphthene	0.02 ± 0.01	0.04 ± 0.02	0.06 ± 0.01
Cyclopentane, 1-ethyl-2-methyl-	8	C_8H_{16}	Naphthene	0.01 ± 0.01	0.05 ± 0.02	0.06 ± 0.01

Appendix B

Specific Gas-phase Backbiting Kinetic Constants used for Polyethylene

Table B.1: Arrhenius parameters for reactions k_{12} to k_{x6}.

Rate	**Pre-exponential Factor** A **(s or L/(mol·s))**	E_a **(kcal/mol)**	**Ref.**
k_{12}	$\frac{1.56}{2} \cdot 10^{5.0} \cdot T^{2.34}$	34.00	
k_{13}	$\frac{5.60}{2} \cdot 10^{1.0} \cdot T^{3.13}$	32.00	
k_{14}	$\frac{3.48}{2} \cdot 10^{3.0} \cdot T^{2.36}$	16.60	
k_{15}	$\frac{1.60}{2} \cdot 10^{3.0} \cdot T^{2.16}$	9.90	
k_{16}	$\frac{1.29}{2} \cdot 10^{4.0} \cdot T^{1.67}$	10.20	
k_{17}	$\frac{5.31}{2} \cdot 10^{2.0} \cdot T^{1.81}$	13.20	[162]
k_{x2}	$\frac{2.60}{2} \cdot 10^{4.0} \cdot T^{2.54}$	35.70	
k_{x3}	$\frac{1.45}{2} \cdot 10^{1.0} \cdot T^{3.28}$	33.20	
k_{x4}	$\frac{1.09}{2} \cdot 10^{3.0} \cdot T^{2.44}$	17.80	
k_{x5}	$\frac{2.26}{2} \cdot 10^{2.0} \cdot T^{2.31}$	10.80	
k_{x6}	$\frac{6.71}{2} \cdot 10^{3.0} \cdot T^{1.75}$	10.70	